PANIC05

XVII Particles and Nuclei International Conference

October 24 – 28, 2005

Santa Fe, New Mexico

Book of Abstracts

XVII Particles and Nuclei International Conference

October 24 – 28, 2005

Book of Abstracts

Sante Fe, New Mexico, USA

October 7, 2005

Conference Program

Monday, October 24th **5**
9:00 AM–12:15 PM, Plenary Session #1 . . . 5
2:30–4:00 PM, Parallel Session #1 . . . 6
I.1 Quarks and Gluons in Hot/Cold and Dense Matter: *Quarkonia* . . . 6
I.2 Quarks and Gluons in Hot/Cold and Dense Matter: *High-pt and High-pt Correlations I* . . . 11
II.1 Quantum Chromodynamics: *Gluon Saturation* . . . 17
III.1 Nucleon Structure: *Strangeness Content and Form Factors I* . . . 20
III.2 Nucleon Structure: *PDFs from Small to Large x I* . . . 24
IV.1 Hadrons, Nuclei, Hypernuclei - Light Quarks: *Hypernuclei and Bound Kaons* . . . 28
IV.2 Hadrons, Nuclei, Hypernuclei - Light Quarks: *Nuclei* . . . 33
V.1 Heavy Flavor Physics - Search for New Particles: *Bottom Physics* . . . 39
VI.1 Fundamental Symmetries: *Symmetry Tests from Kaon Decay I* . . . 41
VIII.1 Neutrino Physics: *Short Baseline Oscillations* . . . 44
XI.1 Nuclear and Particle Astrophysics and Cosmology: *Neutrinos* . . . 47
XII.1 Facilities and Instrumentation: *New Accelerator Facilities I* . . . 49
4:30–6:00 PM, Parallel Session #2 . . . 53
I.3 Quarks and Gluons in Hot/Cold and Dense Matter: *Heavy Flavor* . . . 53
I.4 Quarks and Gluons in Hot/Cold and Dense Matter: *Hadronization, Forward Physics and Future Facilities* . . . 58
II.2 Quantum Chromodynamics: *Confinement/Chiral Symmetry* . . . 64
III.3 Nucleon Structure: *Form Factors II* . . . 68
III.4 Nucleon Structure: *PDFs from Small to Large x II* . . . 72
IV.3 Hadrons, Nuclei, Hypernuclei - Light Quarks: *Exotics/ Spectroscopy* . . . 76
IV.4 Hadrons, Nuclei, Hypernuclei - Light Quarks: *Pentaquarks* . . . 82
V.2 Heavy Flavor Physics - Search for New Particles: *Charm Physics* . . . 87
VI.2 Fundamental Symmetries: *Symmetry Tests from Kaon Decays II and Higgs Sector* . 90
VIII.2 Neutrino Physics: *Double Beta Decay and Underground Laboratories* . . . 95
XI.2 Nuclear and Particle Astrophysics and Cosmology: *Dark Matter and Cosmology* . . . 99
XII.2 Facilities and Instrumentation: *New Accelerator Facilities II* . . . 105

Tuesday, October 25th **109**
9:00 AM–12:30 PM, Plenary Session #2 . . . 109
2:30–4:00 PM, Parallel Session #3 . . . 111
I.5 Quarks and Gluons in Hot/Cold and Dense Matter: *QGP Thermodynamics and Dense Quark Matter* . . . 111
I.6 Quarks and Gluons in Hot/Cold and Dense Matter: *High-pt and High-pt Correlations II* . . . 116
II.3 Quantum Chromodynamics: *Lattice Calculations* . . . 120
III.5 Nucleon Structure: *Flavor Decomposition and GPDs* . . . 126
IV.5 Hadrons, Nuclei, Hypernuclei - Light Quarks: *Strange Quarks* . . . 132
V.3 Heavy Flavor Physics - Search for New Particles: *Quarkonium Physics* . . . 137
VI.3 Fundamental Symmetries: *Charm Mixing, Bs Mixing, and Lepton Flavor Violation* . 139
VII.1 Fundamental Interactions in Atomic and Neutron Physics: *EDM of Electrons, Muons, Neutrons, Atoms* . . . 142
VIII.3 Neutrino Physics: *Accelerator and High Energy Neutrinos* . . . 146
IX.1 Muon Physics: *Overview and Muon Decay Parameters* . . . 152
XI.3 Nuclear and Particle Astrophysics and Cosmology: *Gamma Rays I* . . . 154
XII.3 Facilities and Instrumentation: *New Detector Systems - Silicon Detectors* . . . 157
4:00–6:30 PM, Poster Session . . . 163
Quarks and Gluons in Hot/Cold and Dense Matter . . . 163

Quantum Chromodynamics . . . 176
Nucleon Structure . . . 177
Hadrons, Nuclei, Hypernuclei - Light Quarks . . . 188
Heavy Flavor Physics - Search for New Particles . . . 216
Fundamental Symmetries . . . 224
Fundamental Interactions in Atomic and Neutron Physics . . . 234
Nuclear and Particle Astrophysics and Cosmology . . . 241
Facilities and Instrumentation . . . 249
Miscellaneous . . . 254
Student Posters . . . 258
Public Science Lecture . . . 265

Wednesday, October 26th **266**
9:00 AM–12:10 PM, Plenary Session #3 . . . 266

Thursday, October 27th **268**
9:00 AM–12:10 PM, Plenary Session #4 . . . 268
2:30–4:00 PM, Parallel Session #4 . . . 269
I.7 Quarks and Gluons in Hot/Cold and Dense Matter: *Collision Dynamics, Correlations and Fluctuations* . . . 269
I.8 Quarks and Gluons in Hot/Cold and Dense Matter: *Collision Dynamics, Particle Spectra and Strangeness* . . . 273
II.4 Quantum Chromodynamics: *Experimental Results I* . . . 278
III.6 Nucleon Structure: *Transverse Spin I* . . . 282
IV.6 Hadrons, Nuclei, Hypernuclei - Light Quarks: *Miscellaneous Talks I* . . . 285
V.4 Heavy Flavor Physics - Search for New Particles: *Top Physics* . . . 291
VI.4 Fundamental Symmetries: *Rare B Decays* . . . 294
VII.2 Fundamental Interactions in Atomic and Neutron Physics: *Fundamental Measurements in Atomic and Molecular Physics* . . . 297
VIII.4 Neutrino Physics: *Neutrino Theoretical Developments* . . . 303
IX.2 Muon Physics: *Muon Lifetime and Capture* . . . 309
XI.4 Nuclear and Particle Astrophysics and Cosmology: *Gamma Rays II* . . . 314
XII.4 Facilities and Instrumentation: *New Detector Systems - Particle ID & Trigger Detectors* . . . 316
4:30–6:00 PM, Parallel Session #5 . . . 322
I.9 Quarks and Gluons in Hot/Cold and Dense Matter: *Electromagnetic Probes* . . . 322
II.5 Quantum Chromodynamics: *Experimental Results II* . . . 328
III.7 Nucleon Structure: *Fragmentation and Transverse Spin II* . . . 331
IV.7 Hadrons, Nuclei, Hypernuclei - Light Quarks: *Miscellaneous Talks II* . . . 335
V.5 Heavy Flavor Physics - Search for New Particles: *SUSY/New Physics* . . . 341
VI.5 Fundamental Symmetries: *CP Violation in B Decays and Constraints on New Physics* . . . 344
VII.3 Fundamental Interactions in Atomic and Neutron Physics: *Neutron Lifetime and Beta Decay* . . . 347
VIII.5 Neutrino Physics: *Solar, Reactor, and Other Neutrinos* . . . 354
IX.3 Muon Physics: *Lepton Flavor Violation* . . . 357
X.1 Theoretical Topics . . . 359
XI.5 Nuclear and Particle Astrophysics and Cosmology: *Ultra-High-Energy Cosmic Rays* 362
XII.5 Facilities and Instrumentation: *New Detector Systems - Underground Systems* . . . 364

Friday, October 28th **367**
9:00 AM–11:45 PM, Plenary Session #5 . . . 367
1:30–4:30 PM, Plenary Session #6 . . . 369

Index of First Authors **370**

Monday, October 24th

9:00 AM–12:15 PM, Plenary Session #1

Electroweak Physics: Status and Outlook

William Marciano
Brookhaven National Laboratory

Quantum Chromodynamics: Status and Challenges

Martin Savage
University of Washington

The mystery of ultra-high energy cosmic rays

Angela V Olinto
The University of Chicago

The origin of the highest energy particles ever to be observed are a mystery. They are messengers of an extreme universe and they test the limits of physical laws. The largest cosmic ray experiments are starting to probe the extremely high-energy region where pointing to cosmic ray sources is feasible and a long awaited Greisen-Zatsepin-Kuzmin feature in the spectrum is expected. Past experiments have claimed opposing results: AGASA reports an intriguing excess of cosmic rays above 10^{20} eV that challenges most theoretical models while HiRes does not confirm the excess. The mystery of ultra-high energy cosmic rays will be reviewed in light of the first results from the Pierre Auger Observatory.

QCD at the Dawn of the LHC Era

David A Kosower
CEA - Saclay

Precision computations of QCD and QCD+electroweak emission scattering processes will play an important role in understanding experimental data from the LHC, and thereby in uncovering new physics beyond the Standard Model. Recent years have seen substantial progress in expanding our ability to perform and implement such calculations. In this review, I will focus on a sampling of new ideas in three different topics. I'll discuss the ongoing program of next-to-next-to-leading order calculations, and also progress in merging the parton-shower and matrix-element calculations. I will also outline some of the techniques emerging from twistor-space string theory and its intellectual progeny, and give examples of applications to QCD loop amplitudes.

2:30–4:00 PM, Parallel Session #1

I.1 Quarks and Gluons in Hot/Cold and Dense Matter: *Quarkonia*

Results from NA60 experiment

Gianluca Usai
Physics Department and INFN

on behalf of the NA60 collaboration.

NA60 has greatly improved the quality of dimuon measurements in proton-nucleus and heavy-ion collisions with respect to previous experiments, such as NA38 and NA50. The most important improvements are due to a radiation-tolerant silicon vertex telescope, placed immediately downstream of the target, which tracks the produced charged particles and allows to select the two muons which gave the trigger. This matching procedure improves the dimuon mass resolution from $\sim$ 80 MeV to $\sim$ 20 MeV at the ω mass. Furthermore, the dipole field in the target region significantly increases the acceptance of low p_T and low mass dimuons. This allowed NA60 to do a high quality measurement even at rather low dimuon masses. This talk will present results obtained in In-In collisions at 158 GeV per nucleon from the 2003 running period. In particular, the following points will be addressed.

Low mass dimuon production (below the ϕ mass)
The data for p-A and peripheral In-In compare very well to the cocktail of neutral meson decays, with production yields in agreement with previous measurements. In more central In-In collisions, however, a significant excess is seen over the expected reference, which increases with event multiplicity and is highest for low p_T pairs. We compare our data to the superposition of meson decays and theoretical results on thermal radiation from pion annihilation in the hot fireball, including or not medium modifications of the intermediate ρ meson. The very high quality of our measurements allows to discriminate among the two standard medium effects. The broadening of the ρ spectral function due to interactions in a dense medium (Rapp-Wambach model) provides a good description of our results while the mass shift scenario (Brown-Rho model) fails to reproduce the data.

Intermediate mass dimuon production
The measurement of the impact parameter of each muon track with respect to the collision vertex, thanks to very good vertexing capabilities, allows to measure the open charm contribution to the dimuon spectrum, given the long lifetime of D mesons. This allows to identify the origin of the excess dimuons previously observed in this mass window. We see that, in In-In collisions, there are two times more intermediate mass prompt dimuons than expected from the Drell-Yan calculations.

J/ψ anomalous production
We have seen that the J/ψ is already anomalously suppressed in In-In collisions and we have investigated the suppression pattern as a function of several centrality variables, as L, N_{part}, the density of participants, etc, in order to identify the physics mechanism driving the suppression.

Lattice results on behavior of quarkonia in a gluonic plasma

Saumen Datta, et al.
Brookhaven National Laboratory

on behalf of the RBRC-Bielefeld Collab. collaboration.

Lattice studies for quenched QCD have found that while the 1P charmonium states $\chi_{c_{0,1}}$ are seriously modified, possibly dissolved, by the deconfining transition in a gluonic matter, the 1S states η_c, J/ψ survive the transition with very little changes and exist as bound states till quite high temperatures. We will present here results from our ongoing study into the modification of the properties of these bound states in the gluonic plasma. In particular, we find that when the states are moving with respect to the heatbath, they show much stronger modifications of their behavior, and examine the appearance of a possible thermal width of the states. We will also present initial results on the properties of 1S and 1P bottomonia in a gluonic plasma at temperatures of 1-3 T_c.

Charmonium in Medium and at RHIC

David B Blaschke
GSI Darmstadt

The production of charmonia in relativistic heavy-ion collisions is formulated within the framework of a quantum kinetic theory simultaneously accounting for breakup and recombination processes [1,2]. The survival probability of J/ψ mesons is evaluated for different systems including a Mott-Hagedorn resonance gas [3], a quark-meson gas [4] and a pure gluon gas [5]. It is demonstrated that the pattern of anomalous J/ψ suppression can be explained by a strong coupling to open-charm states and their in-medium modification. Recent data for charmonium suppression in In-In and Pb-Pb experiments at CERN, as well as from Au-Au collisions at RHIC, are discussed.

[1] G. Burau, D. Blaschke and Yu.L. Kalinovsky, Phys. Lett. **B 506** (2001) 297
[2] L. Grandchamp, R. Rapp and G. E. Brown, J. Phys. G **30** (2004) S1355
[3] D. Blaschke and K.A. Bugaev, Prog. Part. Nucl. Phys. **53** (2004) 197
[4] D. Blaschke, G. Burau, Y. L. Kalinovsky and V. L. Yudichev, Prog. Theor. Phys. Suppl. **149** (2003) 182
[5] D. Blaschke, O. Kaczmarek, E. Laermann and V. Yudichev, Eur. J. Phys. C **43** (2005) 81; [arXiv:hep-ph/0505053]

J/ψ Production in p+p, d+Au and Cu+Cu Collisions at RHIC

Vince Cianciolo
Oak Ridge National Lab[*]

on behalf of the PHENIX collaboration.

The J/ψ is an interesting probe of the extremely hot and dense matter produced in heavy ion collisions at RHIC. Suppression of J/ψ production, relative to expected binary collision scaling from p+p production, was predicted by Matsui and Satz to be an unambiguous signature for the formation of the quark-gluon plasma due to Debye screening by free color charges. Such a suppression was indeed observed by the NA50 experiment at CERN. However, interpretation has been made difficult by subsequent theoretical work which has demonstrated that there are numerous mechanisms that can suppress J/ψ formation, including initial parton energy loss, shadowing, cold nuclear matter absorption and co-mover absorption. In addition to these effects the produced charm quark density at RHIC may allow for J/ψ production via recombination, thus countering suppression of prompt production. The observation of final-state charm-quark energy loss at RHIC will presumably also modify J/ψ production. Unraveling this rich structure will likely require measurement of J/ψ production as a function of numerous independent variables, and in this talk we present current PHENIX results for J/ψ production versus transverse momentum, rapidity and system size for light systems p+p, d+Au and Cu+Cu).

---

[*]Managed by UT-Battelle, LLC, for the U.S. Department of Energy under contract DE-AC05-00OR22725.

Measurements of J/ψ yields at forward rapidity and mid-rapidity in Au+Au collisions at $\sqrt{s_{NN}}$ = 200 GeV by PHENIX at RHIC

Taku Gunji

Center for Nuclear Study, University of Tokyo

on behalf of the PHENIX collaboration.

Measurements of the J/ψ yield in heavy ion collisions are expected to be one of the most promising probes of deconfined matter, since theoretical models predict that the J/ψ yield could be strongly suppressed due to the color Debye screening effect in Quark Gluon Plasma. Recently, many theoretical efforts have been made to investigate the behavior of J/ψ production at RHIC energy. One of the interesting predictions that has emerged, is that the J/ψ yield could be enhanced due to the recombination of uncorrelated $c\bar{c}$ pairs.

The PHENIX experiment measured the J/ψ yield in Au+Au collisions at $\sqrt{s_{NN}} = 200$ GeV by using the $\mu^+\mu^-$ decay mode at forward-rapidities (1.2$\leq |\eta| \leq$2.2) and the e^+e^- decay mode at mid-rapidity ($|\eta| \leq$0.35).

We present the centrality, rapidity and p_T dependence of the production of J/ψ to both $\mu^+\mu^-$ and e^+e^- in Au+Au collisions at $\sqrt{s_{NN}}$= 200 GeV and compare to theoretical models to show how various models may or may not be supported by the data.

I.2 Quarks and Gluons in Hot/Cold and Dense Matter:
High-pt and High-pt Correlations I

Systematic Study of Particle Production at High p_T with the PHENIX Experiment at RHIC

Henner Buesching

Brookhaven National Laboratory

on behalf of the PHENIX collaboration.

Previous measurements of the nuclear modification factor R_{AA} at RHIC have shown both a strong suppression of π^0 and charged hadron yields in central Au+Au collisions for $p_T > 5$ GeV/c independent of p_T and particle species, and an enhanced proton yield (relative to pions) at intermediate p_T (2-5 GeV/c). The dependence on p_T and on the particle species reflects the detailed interplay between jet quenching and other effects such as flow and recombination.

The PHENIX experiment at RHIC has analyzed a wealth of data for different particle species, collision energies ($\sqrt{s_{NN}}$ = 62.4, 130, 200 GeV) and collision systems (p+p, d+Au, Cu+Cu, Au+Au) allowing a detailed study of particle production at high p_T. Recently the p_T reach of identified particles could be extended by a high statistics run and the introduction of an aerogel detector.

We will present a systematic comparison of p_T spectra for different particle species, collision energies and systems to discuss the influence of various mechanisms on the particle production.

What do Azimuthal Angular Correlation Measurements tell us about sQGP production at RHIC?

Wolf G Holzmann

Department of Chemistry SUNY Stony Brook

on behalf of the PHENIX collaboration.

Recent measurements at RHIC suggest that a fireball of strongly interacting matter having an energy density in excess of the value required for the creation of a deconfined phase, is produced in Au+Au collisions at $\sqrt{s_{NN}}$=200 GeV. Azimuthal angular correlation measurements provide a powerful probe for the properties and the dynamical evolution of this matter. In recent experiments, the PHENIX collaboration has made detailed measurements of two- and three-particle azimuthal angular correlations for several particle species at several bombarding energies and for different colliding systems. These measurements allow simultaneous and systematic studies of elliptic flow and modifications to (di-)jet fragmentation. The former provides invaluable insights on reaction dynamics and the equation of state. The latter affords tomographic information about the high energy density matter. Results from these measurements will be presented and discussed with an eye toward what can be inferred about the strongly interacting matter produced in energetic Au+Au collisions at RHIC.

Azimuthal correlations of high-p_T neutral strange baryons and mesons at RHIC

Jana Bielcikova

Yale University

on behalf of the STAR collaboration.

Partonic energy loss is predicted to be a sensitive probe of the matter created in high energy heavy-ion collisions because its magnitude depends strongly on the color charge density of the medium traversed. Partons originating from hard scattering of quarks or gluons from the colliding nuclei fragment into jets. As a direct measurement of jets in nuclear collisions is difficult due to the high multiplicities of emitted particles, azimuthal correlations of particles with large transverse momentum (p_T) are commonly used to study jet related processes.

In order to gain more insight into particle production and jet quenching mechanisms a detailed study of identified azimuthal correlations is needed. We present studies of correlations of high-p_T neutral strange baryons (Λ,$\bar{\Lambda}$) and mesons (K^0_S) associated with non-identified charged particles in p+p, d+Au, and Au+Au collisions at $\sqrt{s_{NN}}$ = 200 GeV measured by the STAR experiment. In all three systems the data exhibit clear near-side and away-side correlation patterns typical for hard scattering. While the near-side correlation is present for all centralities, we observe a suppression of the away-side peak in central Au+Au collisions with respect to the measurement in p+p and d+Au collisions. This observation is similar to the previous measurement of correlations triggered on non-identified charged particles. We investigate in detail possible flavor, baryon/meson and particle/antiparticle differences by studying the associated yield of charged particles as a function centrality of the collision and trigger particle transverse momentum. We compare our results to the proton and pion triggered correlations as well as to fragmentation and recombination models.

Measurements of high-pT neutral mesons in $\sqrt{s_{NN}}$ = 200 GeV Au+Au and Cu+Cu Collisions at RHIC-PHENIX

Tadaaki Isobe

CNS, University of Tokyo

on behalf of the PHENIX collaboration.

Measurements from the RHIC experiments show strong suppression in the yield of high-p_T single hadrons and a clear reduction in strength of the di-jet signal in two-hadron azimuthal-angle correlation functions in central Au+Au collisions at RHIC. In previous measurements of the nuclear modification factor R_{AA}, the PHENIX experiment has observed a strong suppression of π^0 and charged hadron yields in central Au+Au collisions for $p_T > 5$ GeV/c independent of p_T and particle species. The observed suppression is interpreted as a consequence of the energy loss of initially hard-scattered partons traversing the hot and dense matter produced in central Au+Au collisions.

The PHENIX Year-4 Au+Au measurements have extended the p_T reach of the π^0 spectra to 20 GeV/c and v2 to 10 GeV/c. And the PHENIX Year-5 Cu+Cu measurements allow studying the particle production in a lighter system and can provide the system-size dependence of the suppression. The suppression pattern of π^0 and η production at high p_T will be presented as a function of the collision system (Cu+Cu/Au+Au). We will use the results to discuss various mechanisms for particle production at high p_T.

High P_t suppression in CuCu Collsions at $\sqrt{s_{NN}} = 200$ GeV at RHIC

Selemon Bekele
The University of Kansas

on behalf of the BRAHMS collaboration.

Collisions between hadronic systems at relativistic energies provide a window on the small-x gluon distributions of fast moving nuclei. It has been predicted that gluon saturation effects will manifest themselves as a suppression in the transverse momentum (P_t) distribution at a scale which is connected with the rapidity of the measured particles. Saturation effects are most evident at large (pseudo)-rapidity, i.e at small angles relative to the beam direction. BRAHMS has already studied the rapidity dependence of the nuclear modification factor as a function of rapidity in dAu and AuAu collisions. While the absence of high P_t suppression around midrapidity rules out initial state effects, a marked high P_t suppression with increasing (pseudo)-rapidity may be related to the initial conditions of the colliding deutron and gold nuclei, in particular to the possible existence of the color glass condensate(CGC)[1,2]. For AuAu collisions, we do see a suppression at (pseudo)-rapidity ~ 3. This may be due to final state effects such as parton recombination, energy loss, or initial state effects such as CGC. The dependence of the nuclear modification factors on the number of participants also provides an additional constraint on the mechanism underlying the observed suppression. This was the motivation for studying CuCu collisions. We will present results for the nuclear modification factor Rcp at forward rapidities for CuCu collsions at $\sqrt{s_{NN}} = 200$ GeV. The results will be compared to previous results in AuAu and dAu collisions at the same energy.

[1] L.V. Girbov, E.M. Levin, M.G.Ryskin, Phys. Rep. 100(1983)1.

[2] D. Kharzeev, E. Levin, L. McLerran, Phys. Lett. B 561(2003)93.

Identified particle transverse momentum distributions upto 12 GeV/c from Au+Au and Cu+Cu collisions at $\sqrt{s_{NN}} = 200$ GeV

Lijuan Ruan

Lawrence Berkerly National Laboratory

on behalf of the STAR collaboration.

Extended particle identification enables to probe different regimes of particle production. In Au+Au collisions at $\sqrt{s_{NN}} = 200$ GeV at RHIC, meson and baryon production at intermediate p_T region (2< p_T <5 GeV/c) shows distinct dependence on collision centrality and exhibits a meson-baryon scaling. This observation can be explained by coalescence of constituent quarks at hadronization from a collective partonic system. At high p_T (p_T >6 GeV/c), the particle composition was believed to be dominated by fragmentation mechanism. We recently developed a particle identification technique for charged pions, proton and anti-proton upto p_T ∼12 GeV/c at STAR to further study the particle production mechanism. Particle identification at low, intermediate and high p_T is achieved from Time Projection Chamber and Time-of-Flight system at STAR. In this talk, charged pions, proton and anti-proton mid-rapidity spectra and their nuclear modification factors up to p_T ∼12 GeV/c from 200 GeV Au+Au and Cu+Cu collisions will be reported. Comparisons with models will be made.

II.1 Quantum Chromodynamics: *Gluon Saturation*

Of Colored Glass and saturation scales

Heribert Weigert
University of Regensburg/Ohio State University

The Color Glass Condensate or CGC has become a buzzword in the context on small x physics in the context of RHIC and LHC experiments. I will provide an introductory overview of ideas and concepts and will try to delineate the borderline between established results and desired pheomenology.

High-energy effective action from scattering of QCD shock waves

Ian Balitsky
JLab/ODU

At high energies, the relevant degrees of freedom are Wilson lines - infinite gauge links ordered along straight lines collinear to the velocities of colliding particles. The effective action for these Wilson lines is determined by the scattering of QCD shock waves. I develop the symmetric expansion of the effective action in powers of strength of one of the shock waves and calculate the leading term of the series. The corresponding first-order effective action, symmetric with respect to projectile and target, includes both up and down fan diagrams and pomeron loops.

Effective Hamiltonian for QCD evolution at high energy

Yoshitaka Hatta, et al.
RIKEN BNL Research Center

We construct the effective Hamiltonian which governs the renormalization group flow of the gluon distribution with increasing energy and in the leading logarithmic approximation. This Hamiltonian defines a two-dimensional field theory which involves two types of Wilson lines: longitudinal Wilson lines which describe gluon recombination (or merging) and temporal Wilson lines which account for gluon bremsstrahlung (or splitting). The Hamiltonian is self-dual, i.e., it is invariant under the exchange of the two types of Wilson lines. In the high density regime where one can neglect gluon number fluctuations, the general Hamiltonian reduces to that for the JIMWLK evolution. In the dilute regime where gluon recombination becomes unimportant, it reduces to the dual partner of the JIMWLK Hamiltonian, which describes bremsstrahlung.

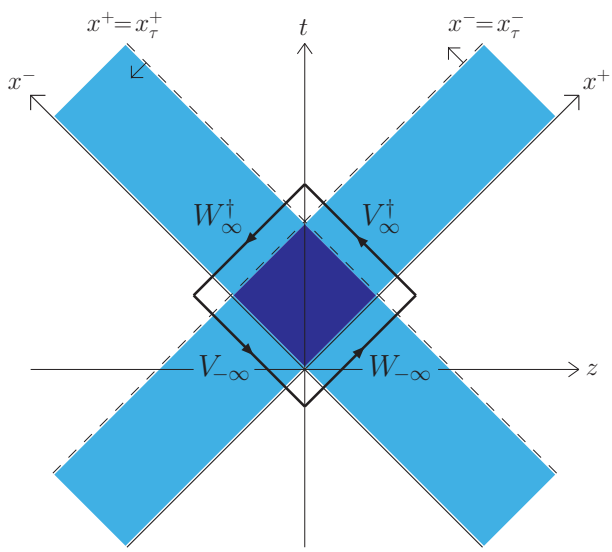

Fig. 1. The effective action is constructed from the four Wison lines which delimit the interaction region in the $x^+ - x^-$ plane.

Two-scale transverse structure of the nucleon and central pp collisions at LHC

Mark Strikman

Penn State University

We consider proton-proton and proton-nucleus interactions at the LHC energies. We use unitarity considerations to estimate up to what virtualities the interaction of leading partons of the nucleon ($x \geq 0.1$) with the proton (nucleus) remains black at the LHC energies[1,2]. We find that the black regime holds for the central pp and central pA collisions up to transverse momenta of few GeV/c. Presence of two scales in the transverse parton structure of the nucleon leads to a strong enhancement of the high gluon density effects for the processes with dijet, heavy particle, Higgs production at central rapidities. The discussed effects include a strong suppression of the leading hadron production, presence of the long range correlations in rapidity between fragmentation regions, an enhancement of the soft hadron production at central rapidities. Implications for the elastic pp scattering and onset of the Froissart limit also discussed[3].

References:

[1] L. Frankfurt, M. Strikman and C. Weiss, Phys. Rev. D **69**, 114010 (2004)

[2] L. Frankfurt, M. Strikman and C. Weiss, "Small-x physics: From HERA to LHC and beyond," arXiv:hep-ph/0507286, Ann.Rev. Nucl.Part.Sci. in press.

[3] L. Frankfurt, M. Strikman and M. Zhalov, Phys. Lett. B **616**, 59 (2005) [arXiv:hep-ph/0412052].

Transverse parton structure of the nucleon and the black-disk limit in high-energy scattering

Christian Weiss

Jefferson Lab

The transverse spatial distribution of partons in the nucleon (generalized parton distributions) is a crucial ingredient in the description of high–energy ep and pp scattering with hard QCD processes. Experimental information about the transverse spatial distribution of gluons comes from measurements of the t–dependence of J/ψ production at HERA and other processes. We discuss the physical mechanisms leading to a growth of the nucleon's transverse size at small x. Based on this information, we study the interaction of small–size color dipoles with the proton in the leading $\log Q^2$ approximation. We find that at small x and central impact parameters the dipole–nucleon interaction approaches the unitarity, or black–disk (BDL) limit. We argue that this new regime of strong interactions can be probed in central pp collisions at LHC.

III.1 Nucleon Structure: *Strangeness Content and Form Factors I*

The $s\bar{s}$ component of the proton and the strangeness magnetic moment

Dan O Riska[1], B. S. Zou[2]

[1]*Helsinki Institute of Physics*
[2]*Institute of High Energy Physics, CAS, Beijing, China*

A complete analysis of all $uuds\bar{s}$ configurations in the P-shell, and which may be admixed in the proton, reveals that in the $s\bar{s}$ configuration, where the uuds subsystem is orbitally excited with $[4]_{FS}[22]_F[22]_S$ flavor-spin symmetry, which is likely to have the lowest energy, the strangeness magnetic moment μ_s is positive. This is consistent with the results of all 4 experiments that measure μ_s [1-4]. The configurations, in which the $\bar{s}$ is orbitally excited, which include the $K^+\Lambda^0$ loop fluctuation, with exception of the energetically disfavored one, in which the uuds component has spin 2, yield negative values for μ_s. The hidden strangeness analogues of recently proposed quark cluster models for the θ^+ [5-7] give differing signs for for μ_s.

Research supported in part by the Academy of Finland and the National Natural Science Foundation of China.

[1] D. T. Spayde et al., Phys. Lett. **B583**, 79 (2004), [2] K. Aniol et al., Phys. Rev. **C69**, 065501 (2004), [3] F. Maas et al., Phys. Rev. Lett. **94**, 152001 (2005), [4] D. S. Armstrong et al., nucl-ex/0506021

[5] R. Jaffe and F. Wilczek, Phys. Rev. Lett. **91**, 232003 (2003), [6] E. Shuryak and I. Zahed, Phys. Lett. **589**, 21 (2004), [7] M. Karliner and H. Lipkin, Phys. Lett. **B75**, 249 (2003)

Results from the G^0 Forward Angle Measurement

Jianglai Liu

Dept. of Physics, Univ. of Maryland

on behalf of the G^0 collaboration.

The strange electric and magnetic form factors of the nucleon, G_E^s and G_M^s, give the contributions of strange quarks to the charge and magnetization distributions of the nucleon, which solely arise from the sea of $s\bar{s}$. G_E^s and G_M^s can be determined by combining the well-known electromagnetic form factors of the proton and the neutron, $G_{E,M}^{\gamma,p}$ and $G_{E,M}^{\gamma,n}$, with the less-measured neutral weak form factors of the proton, $G_{E,M}^{Z,p}$.

Elastic electron-proton scattering carries a small parity-violating (PV) asymmetry (typically a few ppm), arising from the interference between the electromagnetic and neutral weak interactions, which gives direct access to $G_{E,M}^{Z,p}$. G^0 [1] is an experiment at Jefferson lab making precise measurements of this PV effect. Its forward angle measurement was concluded last spring, during which the longitudinally polarized electrons were scattered from an unpolarized liquid hydrogen target. The recoiling protons were detected by a toroidal spectrometer, covering the four-momentum transfer (Q^2) range of $0.12 - 1.0$ GeV$^2/c^2$. This measurement, combined with $G_{E,M}^{\gamma,p}$ and $G_{E,M}^{\gamma,n}$, yields linear combinations of G_E^s and G_M^s in 18 different Q^2 bins [1]. The G^0 results, combined with measurements from other experiments [2−7], indicate that G_E^s and G_M^s are both likely non-zero.

In this talk I will give a brief overview of the forward angle measurement, and present the data analysis and the results. The physics implications of the measurement will also be discussed.

[1] D. S. Armstrong *et al.* (G^0), nucl-ex/0506021.

[2] D. T. Spayde *et al.* (SAMPLE), Phys. Letter. B 583, 79 (2004).

[3] F. E. Mass *et al.* (PVA4), Phys. Rev. Letter. 93, 022002 (2004).

[4] F. E. Mass *et al.* (PVA4), Phys. Rev. Letter. 94, 152001 (2005).

[5] K. A. Aniol *et al.* (HAPPEX), Phys. Rev. C 69, 065501 (2004).

[6] K. A. Aniol *et al.* (HAPPEX), nucl-ex/0506010.

[7] K. A. Aniol *et al.* (HAPPEX), nucl-ex/0506011.

[1] JLab Experiment E00-006, D. H. Beck, spokesperson. A list of the collaborators and information about the experiment can be found at http://www.npl.uiuc.edu/exp/G0/Forward/.

Strangeness Contribution to the Electromagnetic and Axial Form Factors of the Nucleon: Combined Analysis of G0, HAPPEx and Brookhaven E734 Data

Stephen F. Pate, Glen A. MacLachlan, David W. McKee, Vassili Papavassiliou
New Mexico State University

The strangeness contribution to the electromagnetic and axial form factors of the nucleon has been determined for momentum transfers in the range $0.45 < Q^2 < 1.0$ GeV^2. The results are obtained via a combined analysis of forward-scattering, parity-violating elastic $\vec{e}$p asymmetry data from the G^0 and HAPPEx experiments at Jefferson Lab, and elastic νp and $\bar{\nu}$p scattering data from Experiment 734 at Brookhaven National Laboratory. The parity-violating asymmetries measured in elastic $\vec{e}$p scattering at forward angles establish a relationship between the strange electromagnetic form factors G_E^s and G_M^s, with little sensitivity to the strange axial form factor G_A^s. On the other hand, elastic neutrino scattering at low Q^2 is dominated by the axial form factor, with some significant sensitivity to the electromagnetic form factors as well. Combination of the two data sets allows the simultaneous extraction of G_E^s, G_M^s, and G_A^s over a significant range of Q^2 for the very first time.

Physical Nucleon Form Factors from Lattice QCD

Hrayr H. Matevosyan[1], Anthony W. Thomas [2], Gerald A. Miller [3]
[1]*Louisiana State University / Thomas Jefferson National Accelerator Facility*
[2]*Thomas Jefferson National Accelerator Facility*
[3]*University of Washington*

We explore the possibility of extrapolating state of the art lattice QCD calculations of nucleon form factors to the physical regime. We find that the lattice results can be reproduced using the Light Front Cloudy Bag Model and the Extended Gari-Krmpelmann Model by letting their parameters be analytic functions of the quark mass. We then use the models to extend the lattice calculations to large values of Q^2 of interest to current and planned experiments. These functions for the first model are also used to define extrapolations to the physical value of the pion mass, thereby allowing us to study how the predicted zero in $G_E(Q^2)/G_M(Q^2)$ varies as a function of quark mass.

The Charge Form Factor of the Neutron at Low Q^2

Ricardo Alarcon
Arizona State University

Measurement of the charge form factor of the neutron G_E^n presents a sensitive test of nucleon models and QCD-inspired theories. In particular, the pion cloud is expected to play a dominant role in the low-Q^2 region of G_E^n. At the MIT-Bates Linear Accelerator Center, G_E^n has been measured by means of quasielastic scattering of polarized electrons from vector-polarized deuterium, $^2\vec{H}(\vec{e},e'n)$. The experiment uses the longitudinally polarized stored electron beam of the MIT-Bates South Hall Ring along with an isotopically pure, highly vector-polarized internal atomic deuterium target provided by an atomic beam source. The measurements have been carried out with the symmetric Bates Large Acceptance Spectrometer Toroid (BLAST) with enhanced neutron detection capability. From the spin-perpendicular vector-polarized beam-target spin asymmetry A_{ed}^V the form factor ratio G_E^n/G_M^n is extracted over a range of momentum transfer Q^2 between 0.12 and 0.80 $(GeV/c)^2$ with minimized model dependencies. Details of the BLAST experiment will be presented together with preliminary results for G_E^n in the context of the present world data.

III.2 Nucleon Structure: *PDFs from Small to Large x I*

The relevance of gluon polarization to our understanding of nucleon structure

Werner Vogelsang

RIKEN BNL Research Center & Brookhaven National Laboratory

A measurement of the polarization of gluons in the nucleon is the key focus of several experiments that are now underway, in particular at BNL's polarized proton-proton collider, RHIC. The talk discusses the role gluon polarization plays in QCD and for our understanding of the structure of the nucleon. It describes the theoretical background, addressing also some model calculations of gluon polarization. The talk also gives an introduction into the subsequent talks that present the experimental aspects of gluon polarization.

The overview of the spin physics at RHIC-PHENIX experiment.

Yoshinori Fukao
Kyoto University

on behalf of the PHENIX collaboration.

In Spring 2005, Relativistic Heavy Ion Collider (RHIC) at the Brookhaven National Laboratory successfully completed its first long data collection run with polarized proton beam (the 2005 run). The center of mass energy was $\sqrt{s}$=200 GeV and the beam polarization was about 50%. The PHENIX experiment accumulated an integrated luminosity of $\sim$3 pb^{-1} with longitudinal polarization and $\sim$0.1 pb^{-1} with vertical polarization.

One of the major goals of the PHENIX spin program is to experimentally study the origin of the proton spin. Past measurements in polarized deep inelastic scattering have led to the so called "spin crisis": quarks and anti-quarks carry only $\sim$30% of the nucleon spin. Contributions from gluon spin and orbital angular momentum remain unknown. In the past we have reported the double helicity asymmetries in inclusive π^0 production. Vogelsang and collaborators have shown that this observable provides good sensitivity to the polarized gluon distribution. The 2005 run with it's ten fold larger statistics and higher polarization than the previous spin physics run in 2003 will lead to significant constraints for the spin dependent gluon distribution in the proton.

In addition to the measurement of the π^0, the greatly improved RHIC performance allows a wide-range of measurements using different probes including pions, single electrons and muons, prompt photons and jets. Analysis in multiple channels will lead to good control of systematic uncertainties and robust results on the gluon polarization.

For transverse spin, a short run in 2005 will give a much larger figure of merit for single spin asymmetries than for the previous transverse spin run in 2001/2. Studies in progress include spin transfer to the anti-lambda, J/psi polarization, and method of probing the parton transverse momentum in the proton. Finally a short test in RHIC, accelerating and colliding beams at $\sqrt{s}$=410 GeV, has produced preliminary results for very forward neutron asymmetry.

In this talk, we report current status and results from the PHENIX experiment and discuss future plans for the PHENIX spin program.

Nucleon Spin and Structure Studies with COMPASS

Stephane Platchkov

CEA Saclay DSM/DAPNIA & CERN

on behalf of the COMPASS collaboration.

The COMPASS experiment at CERN investigates the nucleon structure and spectroscopy with high–intensity muon and hadron beams. The COMPASS set–up features a two–stage, large–acceptance spectrometer that includes several type of trackers, RICH particle identification and both hadron and electromagnetic calorimeters. Between 2002 and 2004 COMPASS has mainly concentrated on the spin structure of the nucleon via deep–inelastic scattering of polarized muons on polarized nucleons. Data were taken with either longitudinally or transversely polarized ^{6}LiD target. The first results include measurements of the gluon contribution to the nucleon spin via charm production and high–p_t pairs, Λ polarization, vector–meson production, transverse Collins and Sivers asymmetries, inclusive and semi–inclusive deep–inelastic scattering asymmetries. In addition to the studies with muons, a first run with a pion beam was also performed. The data collected should allow precise measurement of the pion electric and magnetic polarizabilities.

Measurement of the double longitudinal spin asymmetry in inclusive jet production in polarized p+p collisions at sqrt(s)=200 GeV

Joanna Kiryluk

MIT

on behalf of the STAR collaboration.

One of the main objectives of the STAR spin physics program at RHIC is the precise determination of the polarized gluon distribution in the nucleon over a wide kinematic range, $0.01 < x_g < 0.3$, by measurements of double longitudinal spin asymmetries in collisions of polarized protons at $\sqrt{s} = 200\,\mathrm{GeV}$ and $\sqrt{s} = 500\,\mathrm{GeV}$.

This contribution reports on first results for the double longitudinal spin asymmetry A_{LL} in inclusive jet production at mid-rapidity in polarized proton proton collsions at $\sqrt{s} = 200\,\mathrm{GeV}$. The data amount to ~ 0.5 pb^{-1} and the jet transverse energies are in the range of $5 < E_T < 20\,\mathrm{GeV}$. The measurements will be compared with evaluations based on polarized deep-inelastic scattering data. The status of the STAR measurements with higher integrated luminosity of ~ 3 pb^{-1} collected in the year 2005 will be presented, as well as an outlook for future measurements.

IV.1 Hadrons, Nuclei, Hypernuclei - Light Quarks: *Hypernuclei and Bound Kaons*

Three body weak interaction process in the Decay of Lambda Hypernuclei

Hyoung C. Bhang

Department of Physics, Seoul National University

on behalf of the KEK-PS E462 and E508 collaboration.

The emitted pair nucleons in the nonmesonic weak decay (NMWD) of ${}^{5}_{\Lambda}$He and ${}^{12}_{\Lambda}$C have been measured in coincidence method in the KEK-PS E462 and E508 experiments. The angular correlations of np pair from the decay showed the predominant back-to-back kinematic events for both hypernuclei which is the signature of the two-body final state. This is the first experimental verification of the long-believed mechanism of nonmesonic weak decay, namely LN $\rightarrow$ NN two body process.

However, those of nn pairs showed significant non-back-to-back kinematic events, in addition to those of back-to-back, which is considered a signature of two-nucleon induced nonmesonic weak decay, namely the three-body interaction process in the weak decay of Lambda hypernuclei. We also see the signatures in other observables as the the degraded energy sum spectra of nn coincidence pair nucleons, the quenching of singles yields and that of pair yields.

Surprising thing is that the signature of the three body weak interaction process can be found rather abundantly in many places, which indicate its sizable contribution. This is a contrasting result to the situation of strongly interacting systems like ^{3}H and ^{3}He where three body intercation contributes only about a percent of the total binding energy. Details on the experimental signatures of the three body weak interaction process in the decay of Λ hypernuclei will be presented.

A lattice framework for hypernuclear physics

Assumpta Parreno[1], S.R. Beane[2], P.F. Bedaque[3], M.J. Savage[4]

[1]*University of Barcelona*
[2]*University of New Hampshire and Jefferson Laboratory*
[3]*Lawrence-Berkeley Laboratory*
[4]*University of Washington*

We outline a program for lattice QCD simulations of the strong and weak interactions of baryons with valence strange quarks. The study of hypernuclear physics has provided a significant amount of information regarding the structure and weak decays of light nuclei containing one or two Λ's, and Σ's. From a theoretical standpoint, little is known about the hyperon-nucleon and hyperon-hyperon interaction required to perform systematic calculations of the hypernuclear structure. Furthermore, the long-standing discrepancies in the P-wave amplitudes for nonleptonic hyperon decays remains to be understood, and is central to a better understanding of the weak decays of hypernuclei. We present a framework that utilizes Lüscher's finite volume techniques in lattice QCD to extract the scattering length and effective range for ΛN scattering in both QCD and PQQCD. The effective theory describing the nonleptonic decays of hyperons using isospin symmetry alone, appropriate for lattice calculations, is constructed.

Spectroscopy of light to medium mass Λ hypernuclei

Joerg Reinhold

Florida International University

on behalf of the Jefferson Lab E01-011 collaboration.

The production of Λ hypernuclei in the (e,e'K$^+$) reaction has been studied in Hall C at Jefferson Lab in Virginia. Electron beams of up to 30 μA were incident on thin ^{12}C and enriched ^{28}Si targets. The scattered electrons and electroproduced kaons were momentum analyzed in a new spectrometer system consisting of a splitter magnet, a tilted ENGE spectrometer and high resolution kaon spectrometer (HKS). This system is expected to achieve unprecedented accuracy as good as 300 keV (FWHM) for hypernuclear spectroscopy with yields increased by more than an order of magnitude compared to Jefferson Lab experiment E89-009 (HNSS). Thus, the current experiment is expected to be the start of a vibrant hypernuclear spectroscopy program at Jefferson Lab that will provide spectroscopic data, initially, up to the mass 100 region. The collaboration wishes that this will stimulate further interest from the theoretical community.

The experiment took data in Summer 2005. This talk will present the experimental technique and preliminary results from the current status of the analysis.

Non-mesonic and Mesonic Weak Decay of ${}^{5}_{\Lambda}$He

Haruhiko Outa

Advanced Meson Science Lab., DRI, RIKEN

on behalf of the KEK-PS E462/E508 collaboration.

We performed a coincidence measurement of two nucleons emitted from the non-mesonic weak decay (NMWD) of ${}^{5}_{\Lambda}\mathrm{He}$ and ${}^{12}_{\Lambda}$C hypernuclei formed via the (π^+,K$^+$) reaction. In both of n+p and n+n pair coincidence spectra, we observed clean back-to-back correlation coming from the two-body decay of Λp $\rightarrow$ np and Λn $\rightarrow$ nn, respectively.

We obtained the ratio of the nucleon pair numbers, $N_{nn}/N_{hp}({}^{5}_{\Lambda}\mathrm{He})$ = 0.45 $\pm$ 0.11(stat) $\pm$ 0.03(syst) at the kinematic region of cosθ_{NN} $<$ -0.8. Since each decay mode was exclusively detected, the measured ratio must be close to the ratio of $\Gamma(\Lambda n \rightarrow nn)/\Gamma(\Lambda p \rightarrow np)$. The Γ_n/Γ_p ratio was measured also for the NMWD of ${}^{12}_{\Lambda}$C. It is also close to 0.5 [1].

Those ratios are consistent with recent theoretical calculations based on the heavy meson/direct quark exchange picture. However, the asymmetry parameter for a proton emitted from the Λp $\rightarrow$ np NMWD decay of polarized ${}^{5}_{\Lambda}$He (0.11$\pm$0.08$\pm$0.04) shows large contradiction to the prediction (~ -0.6) of those theoretical calculations. This seems to suggest the importance of a scalar-type meson exchange mechanism [2].

We also measured the lifetimes and π^- and π^0 mesonic decay branching ratios of ${}^{5}_{\Lambda}$He and ${}^{12}_{\Lambda}$C. Present accurate measurement of the π-mesonic decay widths(5$-$6 % accuracy) opened the door to investigate the hypernuclear structure. The errors of π^-/π^0 decay widths are small enough to distinguish the difference of the Λ-α potentials. Comparison with most recent theoretical calculation suggests the existence of inner repulsive core in the Λ-α potential. The ratio os π^0 to π^- decay rate of ${}^{12}_{\Lambda}$C 1.25$\pm$0.16$\pm$0.06 is in good agreement with the theoretical calculation [3] assuming that the ${}^{12}_{\Lambda}$C ground state as 1^-.

[1] M. Kim, Abstract for this PCNIA05 conference

[2] K. Sasaki et al., Phys. Rev. C71 (2005) 035502

[3] T. Motoba et al., Nucl. Phys. A489 (1988) 683

The FINUDA experiment: A new powerful laboratory for studies on strangeness in nuclear matter

Maurizio Palomba

INFN & Dipartimento di Fisica, Universit¤ di Bari

on behalf of the FINUDA collaboration.

The FINUDA experiment, performed at the $e^+ e^-$ machine DAΦNE of the Laboratori Nazionali di Frascati, Italy, is the first fixed–target experiment carried on at a collider. The experiment is able to perform a wide physics program, mainly focused onto Λ–hypernuclei production and decays, but also, owing to its design, onto further relevant items, related to the investigation on strange nuclear matter (such as neutron–rich Λ–hypernuclei, deeply bound kaonic nuclei, exotic decays). In fact, the detector is able to reconstruct complex multi–particles events with very good momentum resolution, large solid angle acceptance and good charged and neutral particles detection efficiency. Λ–hypernuclei are produced through the (K^-_{stop}, π^-) reactions, induced by stopping in thin targets of different materials the monochromatic K^- mesons (kinetic energy = 16 MeV) coming out from the reactions $e^+ + e^-$ à $\phi(1020)$ à $K^+ + K^-$ occurring at DAΦNE.

After the first months of data taking, FINUDA has already produced some very interesting results. Among the more relevant ones, the analysis on $^{12}{}_{\Lambda}C$ spectroscopy, implementing the recent experimental data from KEK, with an improvement in energy resolution; the evidence of a kaon–bound state K^-pp, that has been observed through the analysis of its decays in Λ+p on various targets; some new hints that have been obtained on the existence of low–Z neutron–rich Λ–hypernuclei; finally, new data on nucleon spectra from non–mesonic decay.

For these items, the main results of the present status of the analysis will be shown, and the analysis in progress will be discussed, together with suggestions for future developments.

Recent theoretical progress in hypernuclear decay

Gianni Garbarino[1], W. M. Alberico[1], A. Parreno[2], A. Ramos[2]

[1]*University of Torino*
[2]*University of Barcelona*

Recent important progress has been experienced in the field of hypernuclear weak decay [1]. Various measurements have been carried out with accuracies largely improved with respect to the ones at disposal in previous experiments. Both single– and double–coincidence nucleon spectra from the non–mesonic weak decay of Λ–hypernuclei have been reported, by KEK [2], in forms that suggest suitable comparison with theory. Thanks to these experiments as well as to recent theoretical analyses [3] of the measured spectra, strong evidences have been found for a solution of the long–standing puzzle on the ratio Γ_n/Γ_p between the neutron– ($\Lambda n \to nn$) and the proton–induced ($\Lambda p \to np$) decay rates. Confirmation of this conclusion is awaited from forthcoming experiments at DAPHNE, HypHI and J–PARC.

Despite this recent progress, the reaction mechanism for the hypernuclear non–mesonic weak decay seems to be not fully understood. Indeed, an intriguing problem, of more recent origin, is open: it concerns the asymmetry of the angular emission of non–mesonic weak decay protons from polarized hypernuclei. While theoretical models predict negative asymmetries [4], with a moderate dependence on the hypernucleus, the experiments seem to favor negative values for ${}^{12}_{\Lambda}\vec{C}$ hypernuclei but positive values for ${}^{5}_{\Lambda}\vec{H}e$ hypernuclei.

In this talk, the recent developments in the calculation of single and double–coincidence nucleon spectra and the (weak interaction model independent) extraction from experimental data of the Γ_n/Γ_p ratio are discussed. The results of a very recent evaluation of the asymmetry parameters and the comparison with available data are also presented. The important role played by final state interactions and two–nucleon induced decay channels ($\Lambda NN \to nNN$) in the determination of both Γ_n/Γ_p and the decay asymmetries is analyzed in detail.

References

[1] W. M. Alberico and G. Garbarino, Phys. Rep. **369**, 1 (2002), and references therein.

[2] J. H. Kim et al., Phys Rev. **C 68**, 065201 (2003); S. Okada et al., Phys. Lett. **B 597**, 249 (2004); Y. Sato et al., Phys Rev. **C 71**, 025203 (2005); H. Outa et al., Nucl. Phys. **A 754**, 157c (2005);

[3] G. Garbarino, A. Parreño and A. Ramos, Phys. Rev. Lett. **91**, 112501 (2003); Phys. Rev. **C 69**, 054603 (2004).

[4] W. M. Alberico, G. Garbarino, A. Parreño and A. Ramos, Phys. Rev. Lett. **94**, 082501 (2005).

IV.2 Hadrons, Nuclei, Hypernuclei - Light Quarks: *Nuclei*

A comprehensive study of the reaction $\gamma d \rightarrow \pi^0 d$ above 500 MeV

Yordanka Y Ilieva
The George Washington University

on behalf of the CLAS collaboration.

The reaction $\gamma d \rightarrow \pi^0 d$ was measured with the CLAS detector at the Thomas Jefferson National Accelerator Facility at photon energies between 0.5 and 2.0 GeV and pion CM scattering angles between 50° and 150°. For photon energies between 0.6 and 0.8 GeV and pion angles above 130° the excitation functions show well pronounced enhancement, which can be related to the opening of the η photoproduction channel and intermediate η formation and rescattering via the excitation of the $S_{11}(1535)$ resonance [1].
At photon energies above 0.9 GeV and CM angles above 130° our data are in agreement with the predictions of the Reduced Nuclear Amplitudes (RNA) approach [2]. This would mean that the relative contribution of two-step processes, such as intermediate meson rescattering, to the reaction cross section becomes small at high momentum tranfer above 0.9 GeV. Our scaled invariant cross sections $s^{13}\frac{d\sigma}{dt}$ vary about a constant value as a function of s. Fits to the dependence of $\frac{d\sigma}{dt}$ on s at fixed θ^{π}_{CM} show that for $\theta^{\pi}_{CM} > 100°$ our data are generally consistent with the predictions of the Constituent Counting Rules (CCR) [3]. This is surprising, since scaling is expected to happen only at higher energies. Traditional meson-nucleon theoretical models are able to explain well the forward differential cross sections, but they fail to do so for the backward cross sections above 0.7 GeV. Comparisons with other exclusive processes and theoretical models will be discussed.

1. A.E. Kudryavtsev *et al.*, Phys. Rev. C **71**, 035202 (2005)
2. S.J. Brodsky and G.P. Lepage, Perturbative Quantum Chromodynamics, SLAC-R-224, 133 (1979)
3. S.J. Brodsky, J.R. Hiller, Chueng-Ryong Ji and G.A. Miller, Phys. Rev. C **64**, 055204 (2001)

Time and space-like pion form factor and Fock state components

Giovanni Salme'[1], J. P. B. C. de Melo[2], T. Frederico[3], E. Pace [4]

[1]*Istituto Nazionale di Fisica Nucleare*
[2]*CCET, Univ. Cruzeiro do Sul and IFT, Univ. Estadual Paulista, Sp, Brazil*
[3] *Dep. de Fi sica, ITA-CTA, 12.228-900 S. Jose' dosCampos, SP, Brazil*
[4]*U. di Tor Vergata and INFN*

A unified description of space-like (SL) and time-like (TL) pion electromagnetic form factors within the front-form dynamics [1] will be presented, which takes into account contributions of pion and photon wave functions beyond the valence components. The dressed photon vertex where a photon decays in a quark-antiquark pair is described through the vector meson dominance ansatz at the level of the photon vertex function, by means of the vector meson (VM) vertex functions. The momentum components of VM and pion vertex functions, in the valence sector, are related to the corresponding front-form wave functions as given by a QCD-inspired model that describes the meson spectrum in both the light- and heavy-quark sector [2]. The virtual processes where a constituent quark radiates or absorbs a pion are described through the model of Ref. [3] by a pseudoscalar coupling multiplied by a constant, fixed by the charge normalization. In this contribution, as a first step, we use a vanishing mass for the pion. Only very few parameters define our approach: i) the oscillator strength ($\omega = 1.539$ GeV^2) and the constituent quark mass ($m_q = .265$ GeV), constrained by the meson spectrum [2], and ii) a single vector meson width (equal to 0.15 GeV) for the vector mesons with $M_n \geq 2.150$ GeV, while experimental widths are used in the other cases. The calculated form factor of the pion, from -10 $(\mathrm{GeV}/c)^2$ to 10 $(\mathrm{GeV}/c)^2$ (see Fig. 1), shows a nice, overall agreement with the time-like data, while in the space-like region the model works very well [1].

We are presently using the same approach to evaluate the SL and TL nucleon form factors.

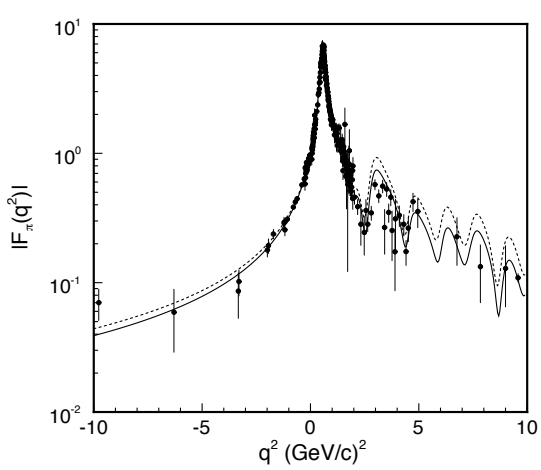

Pion electromagnetic form factor vs. the square momentum transfer q^2. Dashed and solid lines are the results with the asymptotic and the full pion wave function, respectively. (After Ref. [1])

References

1. J. de Melo, T. Frederico, E. Pace, G. Salmè, Phys. Lett. **B 581**, 75 (2004) and hep-ph/0507331. 2. T. Frederico, H.-C. Pauli, S.-G. Zhou, Phys. Rev. **D 66**, 116011 (2002). 3. C.-R. Ji and H.-M. Choi, Phys. Lett. **B 513**, 330 (2001).

Measurement of 2- and 3-Nucleon Short Range Correlation Probabilities in Nuclei

Kim Egiyan

Yerevan Physics Institute,Yerevan, Armenia and Jefferson Lab, Newport News VA, USA

on behalf of the CLAS collaboration.

Calculations of nuclear wave functions using a realistic NN interactions suggest a substantial probability for the nucleon in a nucleus to have a momentum above the Fermi-momentum. The dominant mechanism for generating such a high momenta is the two nucleon interaction at distances less than the average internucleon distance (corresponding to nuclear densities several times higher than the average nuclear density),producing a short-range nucleon correlations (SRC) with characteristic feature: the momentum of a high-momentum nucleon is balanced not by the rest of the nucleus, but by the other nucleons in the correlation, resulting in the universal shape of the nuclear wave function for allnuclei at momentum $k > k_F$. Based on this shape-universality we studied the probabilities of 2- and 3-Nucleon SRC in nuclei ^{4}He, ^{12}C and ^{56}Fe using the inclusive A(e,e′) scattering at $1<x_B<3$. If one measure the ratios r(A,^{3}He) of this reaction cross sections

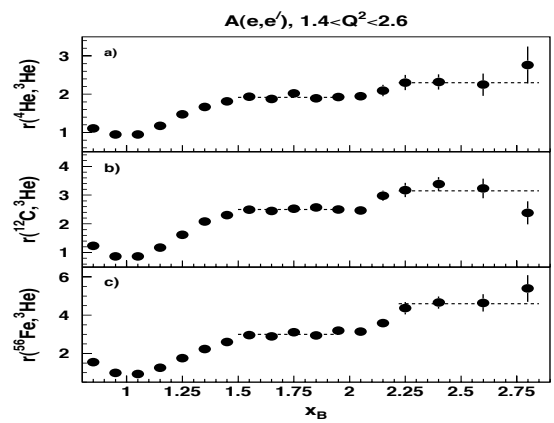

Fig. 1. Cross section ratios of ^{4}He, ^{12}C and ^{56}Fe to ^{3}He as a function of x_B.

for nucleus A and ^{3}He one can expect the scaling (independence) of this ratio to the scattered electron variables Q^2 and x_B in the kinematic regions where (2-, 3- nucleon) SRC have a dominant contribution, and scaling factor will identify the ratios of SRC probabilities in nucleus A relative to ^{3}He. We measure these ratios with CLAS detector, and the obtained results are shown in Fig.1. Using the measured scaling factors we obtain that the probabilities of 2-nucleon SRC in nuclei ^{4}He, ^{12}C, ^{56}Fe are, respectively, 1.93, 2.49, 4.98 times larger than in ^{3}He, while probabilities of 3-nucleon SRC in the same nuclei are, respectively, 2.33, 3.18, 4.63 times larger than in ^{3}He.Using the measured onset values of nucleon momenta in nuclei and the well known wave functions of ^{3}He and deuterium, the absolute values of SRC probabilities were extracted. For 2-nucleon SRC they are: 0.15, 0.2 and 0.25 for ^{4}He, ^{12}C and ^{56}Fe respectively, while for 3-nucleon SRC they are: 0.0042, 0.0056 and 0.0083 respectively, i.e., more than one order of magnitude smaller.

Elastic scattering of low energy pions by nuclei and the in-medium isovector pi N amplitude

Eli Friedman

Racah Institute of Physics

on behalf of the LEPS at PSI collaboration.

Measurements of elastic scattering of 21.5 MeV $\pi^{\pm}$ by Si, Ca, Ni and Zr were made using a single arm magnetic spectrometer and absolute calibration was made by parallel measurements of Coulomb scattering of muons [PRL 93 122303 (2004); nucl-ex/0507008]. Parameters of a pion-nucleus optical potential were obtained from fits to all eight angular distributions put together and examples are shown in fig.1.

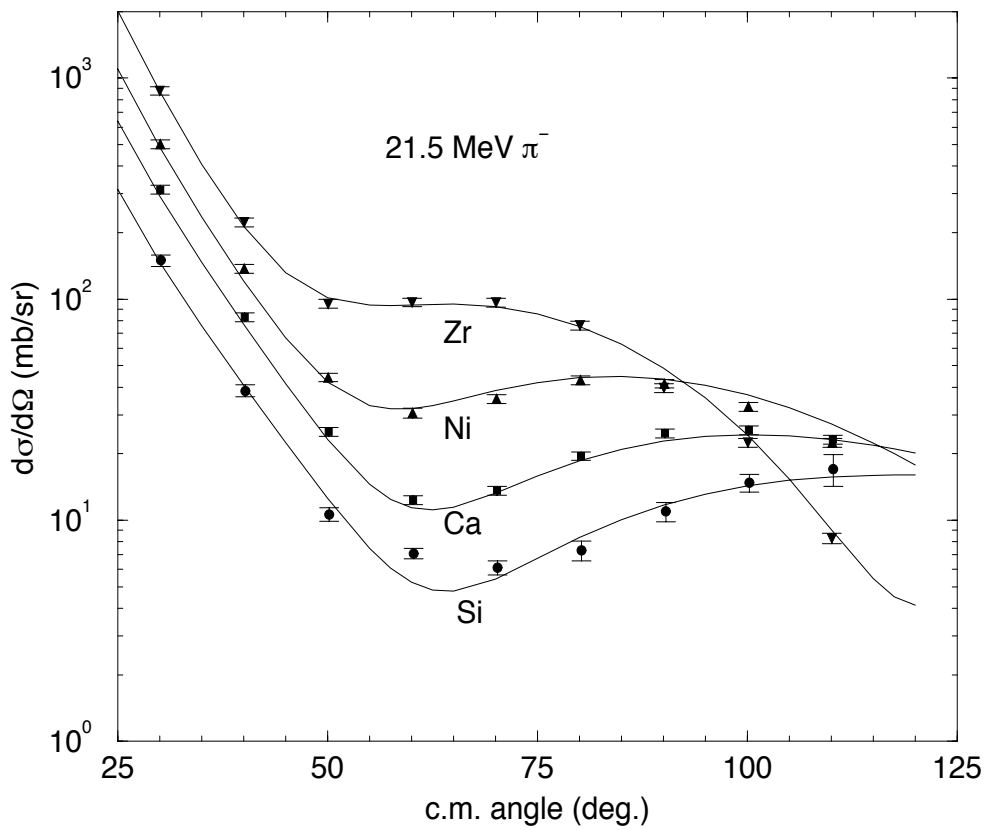

Fig. 1. Experimental results for π^- compared to predictions. Potential parameters were obtained from fits to the combined data for π^+ and π^-

The 'anomalous' s-wave repulsion known from pionic atoms is clearly observed and could be removed by introducing a chiral-motivated density dependence of the isovector scattering amplitude, which also greatly improved the fits to the data. The empirical energy dependence of the isoscalar amplitude also improves the fits to the data but, contrary to what is found with pionic atoms, on its own is incapable of removing the anomaly.

Precise Measurement of the EMC Effect in Light Nuclei

David Gaskell
Jefferson Lab

on behalf of the E03-103 collaboration.

While the modification of structure functions in nuclei (the EMC effect) has been the focus of intense experimental and theoretical study since the original discovery in 1983, the experimental emphasis has been on heavy or medium-heavy nuclei. The theoretical interpretation of the EMC effect is far from clear; it remains difficult to disentangle the "conventional" nuclear physics effects of binding and Fermi motion from more exotic effects.

I will present preliminary results from Jefferson Lab Experiment 03-103, a high precision measurement of the EMC effect with emphasis on the large x_{Bj} region and few-body nuclei (^{3}He and ^{4}He). The large x_{Bj} data are particularly sensitive to conventional nuclear physics effects such as binding and Fermi motion and will help to constrain calculations of these effects. The data on ^{3}He and ^{4}He will allow the unambiguous determination of whether the EMC effect depends on the number of nucleons in the nucleus or the nuclear density. In addition, since there is much less uncertainty in the structure of few-body nuclei, ^{3}He and ^{4}He are an excellent testing ground for calculations of the EMC effect.

Large σ-channel low-mass enhancement in exclusively measured double pionic fusion to He

Mikhail Bashkanov, et al.

Physikalisches Institut - Univ. Tübingen

on behalf of the CELSIUS-WASA collaboration.

Some time ago the Abashian, Booth and Crowe discovered a very peculiar enhancement (lateron called ABC effect) in the ^{3}He missing mass spectrum close to the $\pi\pi$ threshold in the reaction pd $\rightarrow^3$ HeX. Follow-up measurements at Saclay and other places confirmed this finding both in the above reaction as well as on other systems. Originally interpretated as a very strong $\pi\pi$ interaction effect or an σ like resonance ,later attempts tried to describe the effect by $\Delta\Delta$ two-step calculations with varying success.

In order to shed more light onto this unsolved phenomenon,the pd $\rightarrow^3$ He$\pi\pi$ reaction at $T_p = 0.9$ GeV has been measured exclusively at CELSIUS using the WASA 4π detector setup with pellet target system. For the channels ^{3}He$\pi^+\pi^-$ and ^{3}He$\pi^0\pi^0$ all ejectiles were detected leading to 4-6 overconstraints in the data reconstruction.

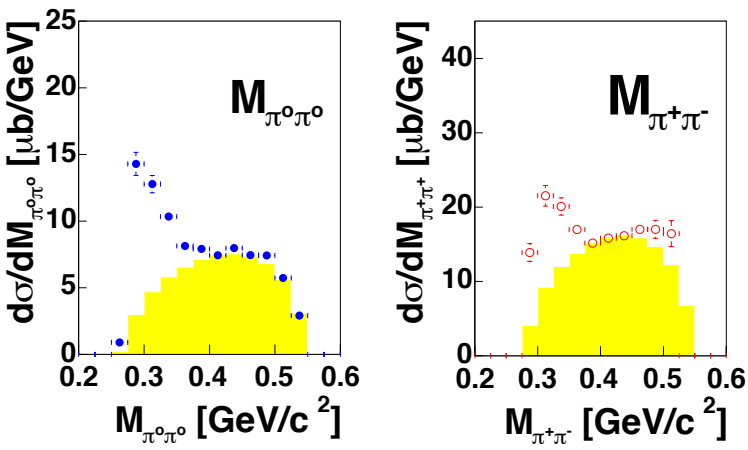

Fig. 1. $\pi\pi$ invariant-mass distributions from the pd $\rightarrow$ ^{3}He $\pi^0\pi^0$ (left) and pd $\rightarrow$ ^{3}He $\pi^+\pi^-$ (right) reactions. The shaded areas show the phase-space distributions.

The new measurements reveal a very pronounced low-mass enhancement close to $\pi\pi$ threshold, in $\pi^0\pi^0$ even much stronger than in $\pi^+\pi^-$, posing the question of isospin breaking at threshold, which due to the different $\pi^\pm$ and π^0 masses is different for both channels. Since ^{3}He acts as an isospin filter, only isoscalar and isovector terms can contribute to the $\pi\pi$ system, the isosvector term moreover only in $\pi^+\pi^-$ at large invariant masses. Comparison of the measurements in both channels shows the isovector contribution to be very small. Since the angular distribution in the $\pi\pi$ subsystem is flat, the observed low-mass enhancement is of scalar-isoscalar origin. Possible interpretations will be discussed.

V.1 Heavy Flavor Physics - Search for New Particles: *Bottom Physics*

Factorization in exclusive semileptonic radiative B decays

Vincenzo Cirigliano[1], Dan Pirjol [2]

[1]*California Institute of Technology*
[2]*MIT, Center For Theoretical Physics*

We derive a new factorization relation for the semileptonic radiative decay $B \to \pi \ell \nu \gamma$ in the kinematical region of a slow pion $|\vec{p}_\pi| \sim \Lambda$ and an energetic photon $E_\gamma \gg \Lambda$ (in the B meson rest frame), working at leading order in Λ/m_b. In the limit of a soft pion, the nonperturbative matrix element appearing in this relation can be computed using chiral perturbation theory. We present a phenomenological study of this decay, which may be important for a precise determination of the exclusive nonradiative decay.

Studies of Orbitally Excited B^{**} abd D^{**}s Mesons at CDF and D0

Jennifer M. Pursley

Johns Hopkins University

Properties of the B_c Meson

Dmitri Tsybychev

SUNY, Stony Brook

on behalf of the DZero collaboration.

The B_c meson is an interesting system since it is comprised of two heavy, different quarks. Experimental measurements of its properties such as mass and lifetime provide stringent tests of theoretical predictions. Using data collected with the DØ detector from $p\bar{p}$ collisions at 1.96 TeV in Run II of the Tevatron, we study the B_c^+ meson in the $J/\psi\mu^+\nu$. final state. We use these events to make a measurement of the mass and the lifetime of the B_c. We also present studies of fully exclusive modes such as $B_c \to J/\psi\pi$.

Rare B Meson Decays at Collider Experiments

Tulay Donszelmann

on behalf of the BaBar Collaboration.

Hadronic B Decays at Belle and Babar

Chung-Hsiang Wang
National United U., Taiwan

on behalf of the Belle collaboration.

Y(5S) Results from CLEO

Victor Pavlunin

on behalf of the CLEO Collaboration.

VI.1 Fundamental Symmetries: *Symmetry Tests from Kaon Decay I*

Edoardo Mazzucato

CEA Saclay

on behalf of the NA48 collaboration.

The NA48/2 experiment has collected an unprecedented statistics of charged kaon decays of both sign, including more than $4x10^9$ pi+-/pi+pi- and $2x10^8$ pi+/-pi0pi0 decays. The data is being analyzed to search for direct CP violating asymmetries in the Dalitz plot slopes. The preliminary results on CP violation in the former decay mode are presented and discussed, as well as the progress in the analysis of the latter mode, which is complementary and has some comparative advantages; a preliminary result for this mode should be available at the time of the conference. The prospects for the experiment and for these measurements are also discussed.

NA48 extraction of Vus from kaon decays and SM test from Km3/Ke3

Michal Szleper

Northwestern University

on behalf of the NA48 collaboration.

First, we present precise measurements of Gamma(Kl3)/ Gamma(K2π), where l=μ or e, and Gamma(Kμ3)/Gamma(Ke3) for charged kaon decays. These measurements are based on K decays collected in a dedicated run in 2003 by the NA48/2 experiment at CERN. We find values that imply higher branching fractions for the corresponding semileptonic decays, than the current world average given in the PDG. As a consequence, the Vus value will increase accordingly. In addition, our more precise value of Gamma(Kμ3)/Gamma(Ke3) is found to be consistent with the theoretical prediction, but points to inconsistencies between the form factor measurements made from neutral and charged kaon decays. Second, the corresponding measurements for the semileptonic decays for neutral kaon decays made by NA48 will also be discussed. Therefore, a complete picture of the experimental and theoretical picture of Vus will be given.

Probing the structure of light mesons from direct measurements of rare electromagnetic Kaon and Pion decays

Rune Niclasen

University of Colorado at Boulder

on behalf of the KTeV collaboration.

Measurements of the kaon and pion decay branching ratios : $K_L \to e^+e^-\gamma$, $\pi^0 \to e^+e^-e^+e^-$ and $\pi^0 \to e^+e^-$ made with the KTeV experiment at Fermilab will be presented. The first two modes are also directly sensitive to the $K\gamma^*\gamma$ and $\pi^0\gamma^*\gamma^*$ vertex form factors. From $K_L \to e^+e^-\gamma$ parameters from two form factor models have been extracted. Both the momentum dependence and the CP properties of the $\pi^0\gamma^*\gamma^*$ vertex are extracted from the $\pi^0 \to e^+e^-e^+e^-$ final state phase space distribution. A new high precision measurement of the very rare decay $\pi^0 \to e^+e^-$ has been done giving valuable information about the meson to two leptons vertex. In particular it serves as an important input to chiral perturbation models of meson decavs.

New Results from BNL E949 on ultra-rare Kaon and Pion decays

Peter S Cooper, et al.

Fermi National Accelertor Laboratory

on behalf of the E949 collaboration.

The E949 experiment is an ultra-rare charged kaon decay experiment whose primary goal is the measurement of the branching ratio of the ultra-rare standard model decay $K^+ \to \pi^+\nu\overline{\nu}$ in order to cleanly measure the magnitude of the CKM matrix element $|V_{td}|$. I will report on the results of this measurement and new results on searches for $K^+ \to \pi^+\gamma\gamma$ and $\pi^0 \to \nu\overline{\nu}$.

Rare Kaon meson decays on the Lattice

Paolo Turchetti[1], Gino Isidori[2], Guido Martinelli[1]
[1]*University of Rome "La Sapienza"*
[2]*Laboratori Nazionali di Frascati*

The experimental evidence of the $K^+ \to \pi^+\nu\bar{\nu}$ decay and the recent new proposals to reach high-precision measurements of this mode, spurred a new interest in rare kaon meson decays. The theoretical determination of various measurable observables relevant to those decays can be made very accurately. This is the major reason why these decays represent an excellent testing ground of Standard Model physics.

In this talk we discuss the recent theoretical progress in estimating long-distance effects in $K \to \pi\nu\bar{\nu}$ and $K \to \pi\ell^+\ell^-$ decays. In particular, we will show the role of Lattice QCD of reducing present theoretical uncertainties on these model.

Kaon semileptonic decay form factors from lattice QCD

Naoto Tsutsui
KEK

on behalf of the JLQCD collaboration.

The Kaon semileptonic decay form factors are defined as

$$\langle\pi(p)|\bar{s}\gamma^\mu u|K(k)\rangle = f_+(q^2)(k+p)^\mu + f_-(q^2)(k-p)^\mu, \tag{1}$$

where $q^2 = (k-p)^2$ is the momentum transfer squared.

One of the most important quantities in the low energy Kaon physics is the form factor f_+ at zero momentum transfer, which provides a theoretical input for the determination of the CKM matrix element $|V_{us}|$ through the K_{l3} decay.

For this form factor it is known that

(1) The leading contribution is unity, which is exact in the SU(3) limit,
(2) There is no contribution of $O(m_s - \bar{m})$ due to the Ademollo-Gatto theorem.

In 1984, Leutwyler and Roos calculated it and their result $f_+(0) = 0.961 \pm 0.008$ has been used as the standard in the phenomenological analysis. Though the leading correction was determined unambiguously using the chiral perturbation theory, the next-to-leading order correction was estimated from a model of the wave function of the pseudoscalar meson,

VIII.1 Neutrino Physics: *Short Baseline Oscillations*

Neutrino Cross Section Studies at MiniBooNE

Janet M. Conrad
Columbia University

on behalf of the MiniBooNE collaboration.

The MiniBooNE neutrino oscillation experiment has the world's largest data sample of charged current quasi-elastic, charged current π^+, and neutral current π^0 events in the 100 MeV to few GeV region. These data are used to measure neutrino cross sections on carbon (mineral oil). The results are intrinsically interesting as well as crucial to understanding rates and backgrounds for the oscillation analysis. This talk will report the recent results on neutrino cross sections from MiniBooNE.

Study of the backgrounds to neutrino appearance signal at MiniBooNE

Zelimir Djurcic
Columbia University

on behalf of the MiniBooNE collaboration.

The MiniBooNE (Booster Neutrino Experiment) experiment is very precise search for neutrino oscillation but is crucially sensitive to background processes that would mimic an oscillation signal. The background sources include intrinsic ν_es from kaon and muon decays, mis-identified π^0, and gammas from radiative delta decays. A summary of efforts to constrain these backgrounds will be presented.

Antineutrino Running at MiniBooNE

Morgan O. Wascko
Louisiana State University

on behalf of the MiniBooNE collaboration.

MiniBooNE is a neutrino oscillation experiment at Fermilab designed to confirm or refute the LSND antineutrino oscillation signal. While currently running with a beam of muon neutrinos, it has the capability to run with an antineutrino beam. Expectations for antineutrino cross section measurements, and oscillation sensitivities, from a one year antineutrino run will be presented.

Constraining the Kaon Content in the MiniBoone Secondary Beam with the Little Muon Counter

Robert H Nelson

University of Colorado, Boulder

on behalf of the MiniBooNE collaboration.

K^+ and K^0_L decays are sources of intrinsic ν_e background to the MiniBooNE (Mini-Booster Neutrino Experiment) neutrino oscillation experiment. In order to constrain this background, MiniBooNE uses a novel technique of measuring the momentum spectrum of off-axis muons from the secondary beam. Muons from kaon decays are kinematically distinguishable from those from pion decays at large angles because of the K/π mass difference. A momentum spectrometer, the Little Muon Counter (LMC), is set at 7° off-axis from the MiniBooNE beamline to perform this measurement. The concept, experimental setup, physics reach, and preliminary results will be presented.

Neutrinos from the NuMI beamline in MiniBooNE

Alexis A Aguilar-Arevalo

Columbia University

on behalf of the MiniBooNE collaboration.

With the startup of the NuMI beamline earlier this year, the MiniBooNE detector has the unique opportunity to be the first user of an off-axis neutrino beam (110 mrad off axis). MiniBooNE has observed neutrinos comming from this source and is assembling a rich sample of neutrino interactions. Some of the applications of this new sample to MiniBooNE are discussed.

Results from the HARP Experiment

Silvia Borghi
Geneva University

on behalf of the HARP Collaboration collaboration.

The HARP experiment at CERN is performing extensive measurements of cross sections and secondary particle yields in the energy range 2-15 GeV as close as possible to full angular coverage, and full particle identification.
The hadron production in this region is a relevant ingredient in several branches of neutrino physics like characterization of neutrino beams, precise prediction of atmospheric neutrino fluxes and quantification of pion production and capture for neutrino factory design.
Harp have successfully collected 30 TB of data in 2 years.
We will report about the double differential production cross section for pions of positive charge. The incident particle are protons of 12.9 GeV/C momentum hitting an aluminum target of 5% nuclear interaction length.
The measurement of this cross section has a direct application to the calculation of the neutrino flux of K2K experiment and in particular on the far/near ratio. These data were fitted with a Sanford-Wang parametrization and the results are given in the momentum range from 0.5 GeV/C to 6.5 GeV/C and angular range 30-210 mrad.
The first results of the production cross section for positive pions for incident protons of 8.9 GeV/C hitting a Berillium target 5% nuclear interaction length will also be shown. This has an immediate interest for the MiniBoone experiment.
Finally we present a preliminary analysis of the differential cross-section in the angular range -30 - 45 degrees using an incident beam of 3 GeV/C protons impinging a 5% nuclear interaction length Tantalum target. These data are decisive for a quantitative design of a proton driver of a future neutrino factory, being at the moment the CERN scenario based on a 3 GeV/C proton linac with an heavy target.

XI.1 Nuclear and Particle Astrophysics and Cosmology: *Neutrinos*

First Results from IceCube

Spencer R. Klein

Lawrence Berkeley National Laboratory

on behalf of the IceCube collaboration.

IceCube is a 1 km^3 neutrino observatory being built to search for neutrino production in active galactic nuclei, gamma–ray bursts, supernova remnants, and a host of other astrophysical sources. High–energy neutrinos may signal the sources of ultra–high energy cosmic rays. In addition, IceCube will study many particle–physics topics: search for WIMP annihilation in the earth or the sun, search for signatures of supersymmetry in neutrino interactions, study neutrino properties, including searches for extra dimensions, and search for exotica such as magnetic monopoles or Q–balls. IceCube will also study the cosmic–ray composition.

IceCube completed its first deployment in the South Pole icecap in January, 2005. Sixty digital optical modules (DOMs) were deployed at depths ranging from 1450 to 2450 meters, and 8 ice–tanks, each containing 2 DOMs were deployed as a surface air–shower array. All 76 DOMs are functioning correctly.

After discussing the IceCube physics program, I will present some initial results with the first IceCube string.

Initial Results and Status of the ANITA Cosmogenic Neutrino Discovery Experiment

Peter W. Gorham

University of Hawaii

on behalf of the ANITA collaboration.

We report on the status of the Antarctic Impulsive Transient Antenna (ANITA) experiment. ANITA will fly a balloon-borne UHF antenna array over Antarctica to detect cosmogenic EeV neutrinos via the Askaryan effect, in an effective detector volume of order 1M cubic km of the Antarctic ice sheet from 40km balloon altitudes. We include results from the ANITA-lite prototype flight completed in 2004. ANITA-lite has effectively ruled out any possibility that the Z-burst model or its variants can account for the ultra-high energy cosmic rays. At the time of this abstract submission, the full ANITA payload was preparing for its engineering test flight in late August. Plans for a first launch in December 2006 are still on track.

SalSA: A Teraton UHE Neutrino Detector

Kevin Reil
Stanford Linear Accelerator Center (SLAC)

on behalf of the SalSA collaboration.

The observed spectrum of ultra-high energy cosmic rays virtually guarantees the presence of ultra-high energy neutrinos due to their interaction with the cosmic microwave background. Unlike cosmic rays, each of these neutrinos will point back directly to its source and will arrive at the Earth unattenuated, from sources perhaps as distant as z $= 20$. The neutrino telescopes currently under construction, should discover a handful of these events, probably too few for detailed study.

In this talk I will describe how an array of VHF and UHF antennas embedded in a large salt dome, SalSA (Saltdome Shower Array) promises to yield a teraton detector (> 500 km$^3 -$ sr) for contained neutrino events with energies above 10^{17}eV. Our simulations show that such a detector may observe several hundreds of these neutrinos over its lifetime. Our simulations also show how such interactions will provide high energy physicists with an energy frontier for weak interactions an order-of-magnitude larger than that of the LHC. The flavor ID capalities of SALSA, combined with the extreme L/E (distance over energy) of these neutrinos, will provide a window on neutrino oscillations and decay times eight orders of magnitude higher than laboratory experiments. In addition to the latest simulation results, I will show progress on detectors and site selection.

Neutrino Astronomy at the South Pole : Latest Results from the AMANDA-II Neutrino Telescope

Paolo Desiati
University of Wisconsin - Madison

on behalf of the IceCube collaboration.

AMANDA-II is the largest neutrino telescope collecting data at the moment, and its main goal is to search for sources of high energy extraterrestrial neutrinos. The detection of such sources could give incontrovertible evidence for the acceleration of charged hadrons in cosmic objects like Supernova Remnants, Microquasars, Active Galactic Nuclei or Gamma Ray Bursts. The talk will provide the most recent results on the search for diffuse and point-like fluxes of high energy neutrinos as well as results on the measurements of the atmospheric neutrino energy spectrum above 1 TeV. It will also address the search for Supernova explosions in our Galaxy using low-energy neutrinos and results on the search for dark matter candidates in the form of MSSM neutralinos. AMANDA-II has significantly improved its sensitivity for the search of high energy neutrinos and it is approaching the Waxman-Bahcall bound level. A further significant improvement in sensitivity is expected with the kilometer cube successor IceCube.

XII.1 Facilities and Instrumentation: *New Accelerator Facilities I*

Upgrading the CEBAF Accelerator to 12 GeV

Leigh Harwood

Jefferson Lab

Jefferson Lab is preparing to upgrade its 6 GeV Continuous Electron Beam Accelerator Facility (CEBAF) to 12 GeV reach in energy. The energy doubling will significantly extend the three existing experimental Halls A, B and C, and the upgrade will add the capability, with a newly constructed hall, Hall D. Areas of special initial interest are reactions at high $x_{Bjorken}$, GPD's and exotic hybrid mesons. The present linacs will their acceleration roughly doubled through the addition of 10 new cryomodules which will perform at >5-times the original specification for CEBAF. The cryogenics plant will be roughly doubled and new rf systems installed for the new cryomodules. The beam transport system will strongly leverage existing hardware but must be enhanced with new power supplies, one new recirculation arc, a beamline to the new Hall D. A brief description of the scope for the various subsystems will be given as well as the status of the project as a whole.

RHIC Upgrades for Heavy Ions and Polarized Protons*

Wolfram Fischer

Brookhaven National Laboratory

The Relativistic Heavy Ion Collider (RHIC), in operation since 2000, has exceeded its design parameters. We describe the performance evolution to the Enhanced Design parameters, to be reached in 2008. The Enhanced Design parameters call for a 4–fold increase over the heavy ion design luminosity, and a 16–fold increase over the proton design luminosity, the latter with an average polarization of 70%. Next we will outline the expected performance of RHIC–II. RHIC–II is based on electron cooling and aims to increase the average heavy ion luminosities by an order of magnitude, and the polarized proton luminosity by a factor 2–5. We will mention ways to further increase the polarized proton luminosity.

*Work supported by U.S. DOE under contract No DE–AC02–98CH10886

eRHIC - Future Electron–Ion Collider at BNL

Vadim I Ptitsyn

Brookhaven National Laboratory, C−AD

on behalf of the eRHIC Accelerator collaboration.

The work on the detailed design of electron–ion collider, eRHIC, on the basis of existing RHIC machine is underway. eRHIC aims to be an instrument for the exploration of important QCD aspects using collisions of polarized electrons and positrons on ions and polarized protons in the center of mass energy range of 30–100 GeV, with a luminosity of 10^{32}–10^{34} $cm^{-2}s^{-1}$ for e–p and 10^{30}–10^{32} $cm^{-2}s^{-1}$ for e–Au collisions. An electron accelerator, which delivers about 0.5A polarized electron beam current in the electron energy range of 5 to 10 GeV, would be constructed at BNL, near the existing RHIC complex and would intersect an ion ring in at least one of the available ion ring interaction regions. One design option considers the circular electron machine based on the accelerator technology similar to that of storage rings at the e^+–e^- B–factories. Another pursued design option employs an energy recovery linac for electron acceleration. This option paves way to higher luminosities but meets challenges of developments of high current electron polarized source and high beam power ERL technologies. To maximize the collider luminosity certain upgrades are considered for RHIC ion rings.

*Work supported by U.S. DOE under contract No DE–AC02–98CH10886

A Conceptual Detector Design for eRHIC

Renee Fatemi
Massachusetts Institute of Technology

An electron-proton/ion collider facility (eRHIC) is under consideration at Brookhaven National Laboratory (BNL). This high energy, high intensity polarized electron/positron beam ($5-10$ GeV/10 GeV) facility is designed to provide collisions with the existing RHIC heavy ion (100GeV per nucleon) and polarized proton beams (50-250GeV). Primary physics motivations include a substantial extention in x and Q^2 of current polarized structure function measurements, allowing for a more precise polarized gluon extraction, as well as the continuation of the unpolarized DIS program, with emphasis on measuring the unpolarized gluon density in nucleons and nuclei.

A detailed report on the accelerator and interaction region design of this new collider facility has been completed based on studies performed jointly by BNL and MIT-Bates in collaboration with BINP and DESY. Such a new facility will require the design and construction of a detector, optimized for the reconstruction of the underlying ep event kinematics and naturally profiting from the world's first ep collider facility HERA at DESY. The detector and interaction region designs are closely coupled, and in turn influence machine development as well.

The main physics questions to be addressed by eRHIC will be briefly reviewed, followed by a discussion of the conceptual detector design. Design and simulation results will be presented along with the constraints placed on the accelerator design at the interaction region. Finally, the outlook for this unique opportunity to continue the collider based DIS program beyond HERA will be discussed.

The FAIR Project: Status and New Developments

Lars Schmitt

GSI, Darmstadt

Detailed planning and R & D for both, the accelerator and the experimental systems of the future international Facility for Antiproton and Ion Research (FAIR) is in progress on many fronts. It involves a range of activities, both at laboratories in partner countries participating in the preparatory activities as well as at GSI.

The present report summarizes the current situation, with emphasis on recent important developments. This includes new performance aspects of FAIR, in particular also the plans towards QCD spin physics with polarized antiprotons. The presentation will conclude with an outlook on facility development and construction and on the key research opportunities, in particular those of interest to the present conference.

4:30–6:00 PM, Parallel Session #2

I.3 Quarks and Gluons in Hot/Cold and Dense Matter: *Heavy Flavor*

QCD Predictions for Charm and Bottom Production at RHIC

Ramona Vogt
LBNL and UC Davis

We make up-to-date QCD predictions for open charm and bottom quark and heavy flavor meson production in nucleon-nucleon collisions at $\sqrt{S} = 200$ and 500 GeV at RHIC. We also calculate the electron p_T spectra from these decays. A rigorous benchmark, including theoretical uncertainties, is established against which nuclear collision data can be compared to obtain evidence for nuclear effects.

Open Heavy Flavor Production as a Probe of Nuclear Effects and High Density matter in pp, dAu and AA collisions at $\sqrt{s_{NN}}$ =200 GeV

Xiaorong Wang
New Mexico State University

on behalf of the PHENIX collaboration.

Heavy flavor production in hadron collisions is dominated by gluonic processes and is a sensitive probe of the gluon structure function in the nucleon and its modification in nuclei. A study of heavy flavor production in different collision systems in various kinematic regions presents an opportunity to probe cold nuclear medium and hot dense matter effects. In pp and dAu collisions, parton shadowing, color glass condensate, initial state energy loss, and coherent multiple scattering in final state interactions can be studied. Nuclear modification in hot dense matter can also be studied by looking at open charm flow and energy loss in nucleus-nucleus collisions.

The PHENIX detector can measure the semi-leptonic decays of open charm and open bottom through the single electron and single muon channels. Single electrons can be measured at mid-rapidity ($|y| < 0.35$) with the PHENIX central arms and single muons can be measured at forward and backward rapidity in the range $1.2 < |\eta| < 2.4$ with the muon spectrometers. We investigate nuclear medium effects on heavy flavor production via single muons and single electrons in pp dAu and AA collisions over wide kinematic ranges. Preliminary PHENIX results and the current status of these analyses will be presented.

Open Charm Production in $\sqrt{s_{NN}}$=200 GeV Au+Au Collisions

Zhangbu Xu
BNL

on behalf of the the STAR Collaboration collaboration.

Charm quarks are produced in the early stage of high-energy collisions and thus provide a unique tool to probe the partonic matter created in relativistic heavy-ion collisions at RHIC energies. The direct measurement of D mesons with low p_T coverage allows to extract important information on the scaling properties of the charm production

cross-section and their transport properties in the medium.

We will report the first results of directly reconstructed D mesons via their hadronic decay products in Au+Au collisions at $\sqrt{s_{NN}}$=200 GeV up to $p_T \simeq$3 GeV/c. Single electron spectra from the charm semi-leptonic decays are also analyzed from the same data set using the STAR TPC, TOF and BEMC detectors. The total cross-sections and the nuclear modification factor R_{AA} of open charm hadrons are presented. The spectra from Au+Au collisions are compared to that in d+Au collisions [PRL 94 (2005) 062301] to infer information of the level of radial flow of charmed mesons. Implications and future related measurements will be discussed.

Heavy-quark energy loss at RHIC and LHC

Andrea Dainese
Padova - University and INFN

High-p_T partons, produced in heavy-ion collisions, are expected to suffer a significant additional medium-induced energy degradation prior to hadronization in the vacuum. Models based on this picture account for the main modifications of high-p_T hadron production in nucleus–nucleus collisions at RHIC. Studying the nuclear modification of heavy-flavor particles allows to further test the microscopic dynamics of medium-induced parton energy loss and, in particular, its predicted dependence on the identity of the parent parton. In fact, hard gluons (from which most of the light-flavored hadrons are expected to originate at LHC energy) lose more energy than hard quarks due to the stronger coupling to the medium, and the energy loss of massive quarks is further reduced due to the mass-dependent restriction of the phase space into which medium-induced gluon radiation can take place.

Parton energy loss effects in heavy-ion collisions will be discussed within a model constructed using the BDMPS quenching weights and a realistic collision geometry [1]. After tuning the only free parameter to the nuclear modification factor suppression measured in central Au–Au collisions at top RHIC energy, the model is consistently applied to other quenching observables: the centrality evolution of the nuclear modification factor, the suppression of the away-side jet-like correlations, and the azimuthal anisotropies for these observables. Extending the model to charm and beauty quarks, the ratios of nuclear modification factors of high-p_T heavy-flavored mesons to light-flavored hadrons (”heavy-to-light ratios”) will be shown to be sensitive to the mass and color-charge dependences of parton energy loss [2]. The potential for identifying these two effects in D and B meson production at RHIC and at LHC will be assessed, and the predictions will be compared to the most recent data from RHIC on the nuclear modification factor of electrons from heavy-quark decays.

[1] A. Dainese, C. Loizides and G. Paic, Eur. Phys. J. C 38 (2005) 461 [arXiv:hep-ph/040620

[2] N. Armesto, A. Dainese, C.A. Salgado and U.A. Wiedemann, Phys. Rev. D 71 (2005) 054027 [arXiv:hep-ph/0501225].

Thermalization and Flow of Heavy Quarks in the Quark Gluon Plasma

Hendrik van Hees[1], Vincenzo Greco[2], Ralf Rapp[1]

[1]*Cyclotron Institute, Texas A&M University, College Station, Texas 77843-3366, USA*

[2]*Laboratori Nazionali del Sud INFN, via S. Sofia 62, I-95123 Catania, Italy*

We address the thermalization and flow of c- and b-quarks in a Quark-Gluon Plasma (QGP), as believed to be produced in ultra-relativistic heavy-ion collisions (URHIC's), within a Fokker-Planck-Langevin approach. We evaluate resonant c- and b-quark rescattering as a non-perturbative mechanism for the thermalization of heavy quarks with the QGP to address recent experimental results on the transverse-momentum (p_T) spectra and elliptic flow, v_2, of non-photonic single electrons at the Relativistic Heavy Ion Collider (RHIC).

We describe the interactions of heavy quarks with light quarks within a field theory with light and heavy quarks as well as heavy-light meson resonances as effective degrees of freedom within the QGP. The model is based on chiral and heavy-quark symmetry, taking into account pseudo-scalar D (B) and vector D^* (B^*) mesons and their chiral partners.

Within this model, we evaluate drag and diffusion coefficients to assess the flow properties of c- and b-quarks within the QGP, as produced in URHIC's, using a relativistic Langevin simulation. We find that the survival of the resonances at temperatures $T \lesssim 2T_c$ ($T_c \simeq 180\ \mathrm{MeV}$: critical temperature for the deconfinement transition) accelerates the equilibration of c- and (to less extent) b- quarks significantly compared to the use of perturbative-QCD elastic scattering processes only. Using the such obtained heavy-quark p_T-spectra and elliptic flow, v_2, we employ a coalescence model for hadronization to D- and B mesons for the pertinent non-photonic electron observables and compare to the data from the PHENIX and STAR collaborations at RHIC.

A Complete Onium Program with R2D at RHIC II

Richard A Witt

Yale University

on behalf of the Exploratory Physics Working Group on a New Detector for RHIC-II (R2D) collaboration.

Following on the discovery of a strongly interacting quark-gluon plasma at RHIC, a program of detailed quarkonia measurements is crucial to understanding the nature of deconfinement. Lattice QCD calculations suggest a sequential melting of the quarkonia states in the deconfined medium. Such a melting would lead to a suppression in the measured charmonium and bottomonium yields. However, distinguishing a true suppression from shadowing, absorption, and recombination effects requires detailed measurements of all quarkonia species including the charmonium states (J/ψ, ψ', and χ_c) and bottomonium states (Υ(1S), Υ(2S), and Υ(3S)). For example, the χ_c feeds down to the J/ψ through its J/ψ+γ decay channel, but the χ_c also melts before the J/ψ. Therefore, a precise measurement of the χ_c yield is needed to distinguish actual J/ψ suppression from suppression of the χ_c.

To fully realize the program outlined above a new detector will be required at RHIC-II. Separation of the Υ(2S) and Υ(3S) states will only be possible with excellent energy and momentum resolution and the ability to handle high rates. Large acceptance is needed for acquiring precise yields out to large Feynman x. Also, since measurements are needed not only in A+A but also in p+p for determining primary yields, and in p+A for evaluating absorption, the detector should perform well in all collision environments. We present a proposal for a complete quarkonia program as well as simulations highlighting the abilities of a new detector, R2D, to meet the stated requirements. Comparisons will be made with proposed upgrades to existing RHIC detectors and with the upcoming LHC program.

I.4 Quarks and Gluons in Hot/Cold and Dense Matter:
Hadronization, Forward Physics and Future Facilities

Hadronization in nuclear deep inelastic scattering and ultra-relativistic heavy-ion collsions

Thomas Falter[1], Kai Gallmeister[2], Ulrich Mosel[2]

[1]*Physics Department, Brookhaven National Laboratory, USA*
[2]*Institut fuer Theoretische Physik, Universitaet Giessen, Germany*

Hadron production in deep inelastic lepton scattering (DIS) off complex nuclei provides an ideal tool to investigate the space-time evolution of hadron formation. The nuclear target can be viewed as a kind of 'micro-detector' that is located directly behind the virtual photon-nucleon interaction vertex. It allows us to study the interactions of the reaction products with the surrounding nuclear environment on a length scale that is set by the size of the target nucleus. By comparison with hadron production on a deuterium target one can draw conclusions about the space-time picture of hadronization. The latter information is crucial for the interpretation of jet quenching in ultra-relativistic heavy ion-collisions at RHIC as a possible signature for the creation of a deconfined quark-gluon plasma phase.

In the recent past the HERMES collaboration at DESY has started an extensive experimental investigation of hadron attenuation in DIS on various gas targets and a similar experiment is currently performed at Jefferson Lab. Furthermore, hadron attenuation in nuclear DIS will be subject to investigation after the 12 GeV upgrade at Jefferson Lab and at a possible future electron ion collider. In Refs. [1] the observed attenuation of high energy hadrons at HERMES has been interpreted as being due to a partonic energy loss of the quark that was struck by the virtual photon. The colored quark undergoes rescattering inside the nucleus giving rise to induced gluon radiation. However, the authors of Refs. [2,3] achieve a very good agreement with experiment by assuming that the struck quark forms a color neutral prehadron early after the virtual photon-nucleon interaction. This prehadron than scatters off the surrounding nucleons on its way out of the nucleus.

In Ref. [3] and references therein we have developed a method to incorporate coherence length effects in a semi-classical BUU-transport model that uses the Lund string models PYTHIA and FRITIOF for the simulation of the elementary DIS process and the (pre)hadronic interactions respectively. This allows for a complete probabilistic coupled-channel description of high-energy photo- and electroproduction off complex nuclei. Our simulation works on an event-by-event basis and can be directly compared to experiment accounting for all sorts of kinematic cuts and detector acceptances. Our theoretical results are in perfect agreement with the experimental findings at HERMES. However, similar transport studies [4] show that the prehadronic final state interactions cannot explain the jet quenching observed in most central heavy-ion collisions at RHIC. This indicates the presence of an additional source of jet suppression in the hot and dense fire ball, e.g. a partonic energy loss in a deconfined phase.

[1] E. Wang, X.-N. Wang, PRL **89**, 162301 (2002); F. Arleo, EPJ C**30**, 213 (2003).
[2] A. Accardi *et al.*, NPA **720**, 131 (2003); B. Z. Kopeliovich *et al.*, NPA **740**, 211 (2004).
[3] T. Falter *et al.*, PLB **594**, 61 (2004); PRC **70**, 054609 (2004); nucl-th/0502015.
[4] W. Cassing *et al.*, NPA **735**, 277 (2004).

Particle suppression at large x_F at RHIC

J.H. Lee

Brookhaven National Laboratory

on behalf of the BRAHMS collaboration.

The available kinematic phase-space at large Feynman-x (x_F) in high-energy nuclear collisions demands the probability of particle production to be constrained. In the nuclear medium, the effect is expected to be enhanced by multiple interactions given to the projectile partons. This nuclear-induced effect, referred to as the Sudakov suppression [1] , has been shown to scale with x_F. To understand the dynamic nature of nuclear collisions, it is necessary to distinguish such kinematically dominated effects from dynamically driven processes, such as parton energy loss in the hot nuclear medium and gluon saturation in the initial state.

The BRAHMS experiment has measured the centrality dependent particle production over wide kinematic ranges ($0 < p_T < 4$ GeV/c, $0 < x_F < 0.5$) in d+Au, Au+Au, and Cu+Cu collisions at RHIC. The x_F-dependent nuclear modification factors of charged hadrons will be presented in the context of parton energy loss [2] and energy conservation in the medium. Comparisons with lower-energy measurements and theoretical models will be also discussed.

[1] B.Z. Kopeliovich *et al.*, arXiv:hep-ph/0501260, and references therein.
[2] M. Gyulassy *et al.*, arXiv:nucl-th/0302077, and references therein.

Global Observables from Au+Au, Cu+Cu, d+Au and p+p Collisions at RHIC Energies

Rachid Nouicer

Brookhaven National Laboratory (BNL)

on behalf of the PHOBOS collaboration.

Quantum ChromoDynamics (QCD) predicts a phase transition from a state of hadronic constituents to a Plasma of deconfined Quarks and Gluons (QGP) at sufficiently high energy densities. Creation and study of the QGP is the main goal of the Relativistic Heavy Ion Collider (RHIC). The investigation of QGP properties is expected to provide new insights into the strong interaction and QCD.

The latest results obtained by the PHOBOS experiment at RHIC will be presented, including charged particle multiplicities, transverse momentum spectra, collective flow observables, and anti-particle to particle production ratios from Au+Au, Cu+Cu, d+Au and p+p collisions at RHIC energies. The results will be discussed in terms of their implications for the characterization of the hot and dense matter formed in Au+Au collisions at RHIC energies.

Study nuclear modification at forward rapidity via two particle correlations in $\sqrt{s_{NN}}$ = 200GeV

Chun Zhang

Ork Ridge National Lab.

on behalf of the PHENIX collaboration.

The PHENIX experiment has observed a suppression relative to binary collision scaling on hadron production at forward rapidity in deuteron gold collisions at $\sqrt{s_{NN}} = 200$GeV. Several theoretic models were proposed to interpret this phenomenon, such as CGC, power correction, and recombination model, etc. Although CGC seems to give the most accurate calculation results compared to experimental data, there are still ambiguities to really tell which model is more correct by only looking single particle production. In the mean time, CGC and power correction also predict a modification of away side jet when there is a rapidity gap between the near side jet and far side jet. Here, we report on two particle azimuthal correlation between charged hadrons at forward/ backward rapidity and charged hadrons at middle rapidity in deuteron-gold and proton proton reactions at $\sqrt{s_{NN}} = 200$ GeV. Our measurements covers $1.4 < \eta < 2.2$ at forward rapidity (Deuteron direction),$-2.2 < \eta < -1/4$ at backward rapidity (gold direction) and $-0.35 < \eta < 0.35$ at middle rapidity.

Quark-gluon densities in the nuclear fragmentation region in heavy ion collisions at LHC

Mark Strikman

Penn State University

We consider the initial state formed in the nuclear fragmentation region in the central heavy ion collisions at LHC. We estimate the range of virtualities of partons for which interactions remains black (Black Disk Limit - BDL) and find that it extends to much larger virtualities than for the central rapidities. As a result we find that for $x \geq 0.2$ the average transverse momenta of leading quarks and gluons should exceed $\geq 4\mathrm{GeV}/c$. As a result in generic central AA collisions all leading partons of the nucleons are stripped off "soft" partons and fragment into a collection of leading quarks and gluons with large p_t. In the rest frame of the fragmenting ion the incoming nucleus is a pancake shape with the longitudinal length ~ 1fm for the soft interactions and the longitudinal length $r_N(m_N/p_N)(x_V/x)$ for hard interactions (Here $x_V \sim 0.2$ is the average x for the valence quarks). Hence, the nucleons at different locations along the collision axis are hit one after another. In the BDL no spectators are left. The hit partons are produced with practically the same x that they had in the nucleus (because the fractional energy losses are small), $\left\langle p_t \sim p_t^{BDL} \right\rangle$, and virtuality, $\mu^2 \leq (p_t^{BDL})^2$. The partons move in the direction of the projectile nucleus. Because they are emitted at finite angles their longitudinal velocity is smaller than the speed of light. Hence, they are left behind the projectile wave. However, because the emission angles are small, the shock wave is formed compressing the produced system in the nucleus rest frame. In the reference frame co-moving with the shock wave valence quarks and gluons are streaming in the opposite directions. The resulting pattern of the fragmentation of the colliding nuclei leads to an implosion of the quark and gluon constituents of the nuclei. The non-equilibrium state produced at the initial stage in the nucleus fragmentation region is estimated to have densities $\propto p^2_{BDL}$ and it is ≥ 100 GeV/fm^3 at the LHC energies and probably ≥ 10 GeV/fm^3 at BNL RHIC. It appears likely that the partons will rescatter strongly at the second stage, though much more detailed modeling is required to find out whether the system may reach thermal equilibrium. The large angle rescatterings of partons will lead to production of partons at higher rapidities and re-population of the cool region. In particular, two gluons from the pancake have the right energies to produce near threshold $c\bar{c}$ pairs and in particular χ_c-mesons with rather small transverse momenta and $x_F(c\bar{c}) \sim 2x_g \sim 0.1$.

ATLAS detector heavy ion physics program

Helio Takai

Brookhaven National Laboratory

on behalf of the ATLAS collaboration.

The ATLAS detector is one of the two large detectors being built to carry on high pT physics at the Large Hadron Collider. The detector is designed to perform optimally at the challenging nominal machine luminosity of 10^34 cm-2s-1. ATLAS has a finely segmented electromagnetic and hadronic calorimeters covering 10 units of rapidity. The inner tracking system is composed of sicilicon pixel detector, silicon central tracker, transition radiation tracker and a 2T solenoidal magnet, covering 5 units of rapidity. The muon spectrometer is located outside the calorimeter volume. Muon chambers and air core toroids are used to track muons of momentum larger than 4 GeV. Results from RHIC on jet quenching observed in Au+Au collisions have stimulated the ATLAS collaboration to pursue a program centered around jet physics and upsilon suppression. Jets can be studied well with the ATLAS detector due to the quality of the calorimetric measurement and inner detector information. Preliminary studies also indicate that it will be possible to tag b-jets in the heavy ion environment. Upsilon and J/Psi can be reconstructed through the di-muon decay channel. The detector is ideal for the study of global variables, namely total energy flow and particle production multiplicity. We will discuss the current status of simulation studies and plans of the heavy ion physics program with the ATLAS detector during the AA and pA runs.

II.2 Quantum Chromodynamics: *Confinement/Chiral Symmetry*

Confinement of color: open problems and perspectives.

Adriano Di Giacomo
PISA UNIVERSITY and INFN

Some basic features of confinement are reviewed , in particular the symmetry pattern of the dual dynamics. Open problems and possible directions of progress are discussed.

Approaching continuum monopoles

Alex Kovner[1], Arsen Khvedelidze[2], David McMullan[2]
[1]*University of Connecticut*
[2]*University of Plymouth*

I present a recent approach to calculating expectation value of the monopole creation operator in continuum nonabelian gauge theory. The interst in this quantity stems from its possible relevance for the mechanism of confinement. However some serious questions about it's importance remain. We set up the calculation directly in the continuum limit, and find that int he confining phase the expectation value os dominated by a semiclassical field configuration. The configuration surprisingly turns out to be not spherically symmetric, but rather posesses only axial symmetry. We find that pertrubatively VEV valishes as a power of volume. This sugeests that nonperturbative effects wich should provide IR cutoff at the scale of order Λ_{QCD}, will stabilize the VEV at some finite value.

Analysis of full-QCD and quenched-QCD lattice propagators

Mandar S Bhagwat, Peter C Tandy
Kent State University

Recent lattice-QCD results for the dressed-gluon propagator are used within the quark Dyson-Schwinger equation to determine the phenomenological accounting of gluon-quark vertex dressing necessary to reproduce the lattice-QCD results for the dressed-quark propagator. Landau gauge is used throughout. Both quenched and full QCD lattice simulations are analyzed and contrasted for the amount of infrared vertex enhancement found necessary. Particular attention is paid to the current m_q dependence.

This analysis represents a mapping of lattice-QCD simulations onto a Dyson-Schwinger equation kernel. This provides a vehicle for a chiral extrapolation that allows the non-linearities from Dyson-Schwinger dynamics to enter as needed, it permits an analysis of whether positivity is violated (a sufficient condition for confinement), and it provides an unambiguous link to the chiral quark condensate $\langle\bar{q}q\rangle$ and meson observables. Chiral and physical pion observables are materially underestimated in the quenched theory: $|\langle\bar{q}q\rangle|$ by a factor of two and f_π by 30%. The correspondng results from full-QCD will be presented. Fig. 1 provides an illustration of some of the results.

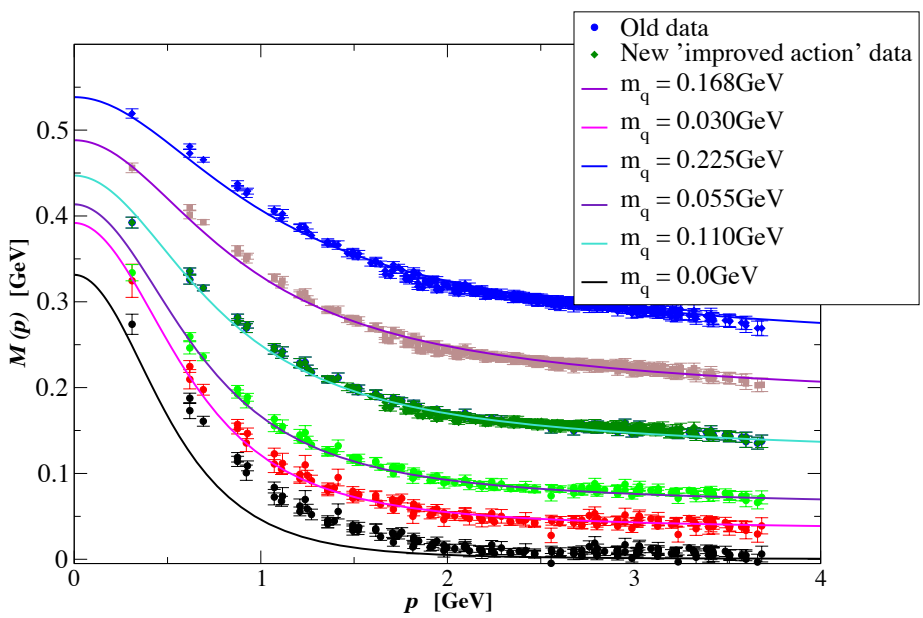

Fig. 1. Quenched lattice-QCD results for the Landau gauge quark mass function, for a variety of current masses, as reproduced by the Dyson-Schwinger equation kernel determined from the corresponding lattice gluon propagator and the effective quark-gluon vertex. The chiral limit extrapolation via the DSE provides dynamical non-linearities; the linear extrapolation of lattice data is shown for comparison.

η'-mesic nuclei formation and $U_A(1)$ anomaly at finite density

Hideko Nagahiro[1], Makoto Takizawa[2], Satoru Hirenzaki[3]

[1]*Research Center for Nuclear Physics, Osaka University*
[2]*Showa Pharmaceutical University*
[3]*Depertment of Physics, Nara Women's University*

The huge mass of the $\eta'(958)$ meson is believed to have close connection with the breaking of the axial $U(1)$ symmetry at the quantum level referred as *the* $U_A(1)$ *anomaly*. There are many theoretical studies for the effects of the $U_A(1)$ anomaly on the η' meson, not only in vacuum, but also at finite temperature and finite density, which suggest the possible character changes of η' at finite temperature and/or finite density. At the present time, however, there exists no experimental information on the property and behavior of the $U_A(1)$ anomaly at finite density.

In this presentation, we propose the formation reaction of the η'-mesic nuclei in order to investigate the η' properties, especially its mass shift, at finite density. We apply the NJL model to describe η' properties in nuclear medium, and show the clear relations between NJL parameters and expected reaction spectra, which should be the first step to get deeper insights on $U_A(1)$ anomaly at finite density from experimental data. The η' mass in the medium should provide us important information on the properties of the $U_A(1)$ anomaly in the nuclear medium.

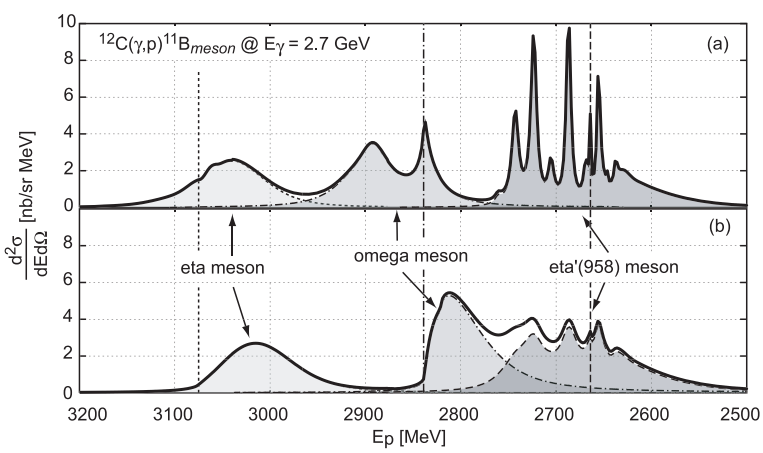

Fig. 1. The calculated spectra of the $^{12}C(\gamma,p)^{11}B$ reactions at $E_\gamma = 2.7$ GeV as functions of the emitted proton energy E_p. The contributions from the η-, ω-, and η'-mesic nuclei are shown by dotted lines, dash-dotted lines, and dashed lines, respectively. Some theoretical models are used to obtain the optical potential for each mesic-nucleus, (a) an attractive potential for η, attractive for ω, and attractive for η' with narrow widths, (b) a repulsive potential for η, repulsive for ω, and attractive for η' with broader widths.

References

1. H. Nagahiro and S. Hirenzaki, Phys. Rev. Lett. **94**, 232503 (2005).
2. H. Nagahiro, D. Jido, S. Hirenzaki, Nucl. Phys. A in press, nucl-th/0504081.
3. H. Nagahiro, D. Jido, S. Hirenzaki, Phys. Rev. **C68**, 035205 (2003).

Multi-Quarks and Two-Baryon Interaction in Lattice QCD

Hideo Suganuma[1], Takumi Doi[2], Fumiko Okiharu[3], Toru T. Takahashi[4]

[1]*Department of Physics, Kyoto University*
[2]*RIKEN-BNL Research Center, BNL*
[3]*Department of Physics, Nihon University*
[4]*Yukawa Institute for Theoretical Physics, Kyoto University*

We perform the detailed studies of the three-quark (3Q) potential [1,2], the tetra-quark (4Q) potential [3] and the penta-quark (5Q) potential [4] in SU(3) lattice QCD. The 3Q potential is found to be well described by the Y Ansatz [1,2]: the sum of the Coulomb term and the Y-type linear term based on the flux-tube picture. Actually, the 3Q potential subtracted by the Coulomb part is proportional to Y-shaped flux-tube length L_{min} as shown in Fig.1 [3].

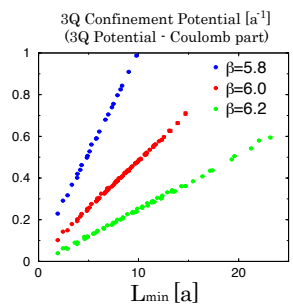

Fig. 1. 3Q confinement potential V_{3Q}^{conf}, i.e., 3Q potential subtracted by the Coulomb part, plotted against Y-shaped flux-tube length L_{min} in lattice unit.

We perform the first study of the multi-quark potential in lattice QCD [3,4] to clarify the inter-quark interaction in multi-quark systems. The 5Q potential V_{5Q} for the QQ-$\bar{Q}$-QQ system is found to be well described by the "OGE Coulomb plus multi-Y Ansatz" [4]: the sum of the one-gluon-exchange (OGE) Coulomb term and the multi-Y-type linear term based on the flux-tube picture. The 4Q potential V_{4Q} for the QQ-$\bar{Q}\bar{Q}$ system is also described by the OGE Coulomb plus multi-Y Ansatz [3], when QQ and $\bar{Q}\bar{Q}$ are well separated. We observe a lattice-QCD evidence for the "flip-flop", i.e., the flux-tube recombination between the connected 4Q state and the "two-meson" state [3].

We study also the nuclear force, i.e., the interaction between two nucleons, in SU(3) lattice QCD at the quenched level. These lattice-QCD studies give an important bridge between elementary particle physics and nuclear physics.

1. T.T. Takahashi, H. Matsufuru, Y. Nemoto and H. Suganuma, *Phys. Rev. Lett.* **86** (2001) 18; *Phys. Rev.* **D65** (2002) 114509.
2. T.T. Takahashi and H. Suganuma, *Phys. Rev. Lett.* **90** (2003) 182001; *Phys. Rev.* **D70** (2004) 074506.
3. F. Okiharu, H. Suganuma, T.T. Takahashi, *Phys. Rev.* **D72** (2005) 014505.
4. F.Okiharu, H.Suganuma, T.T.Takahashi, *Phys. Rev. Lett.* **94** (2005) 192001.

III.3 Nucleon Structure: *Form Factors II*

The Proton Electric to Magnetic Form Factor Ratio at Low Q^2

Michael Kohl, et al.

MIT-Bates Linear Accelerator Center

on behalf of the BLAST collaboration.

Measurements of nucleon form factors at low $Q^2 < 1$ (GeV/c)^2, where the pion cloud is expected to play a significant role, present a sensitive test of nucleon models and QCD-inspired theories.

At the MIT-Bates Linear Accelerator Center, the ratio G_E^p/G_M^p has been measured by means of elastic scattering of polarized electrons from polarized hydrogen, $^1\vec{H}(\vec{e}$,e'p). The experiment used the longitudinally polarized stored electron beam of the MIT-Bates South Hall Ring along with an isotopically pure, highly polarized internal atomic hydrogen target provided by an atomic beam source. The measurements have been carried out with the symmetric Bates Large Acceptance Spectrometer Toroid (BLAST).

For values of Q^2 between 0.15 and 0.85 (GeV/c)^2, the combination of the two simultaneously measured spin-dependent asymmetries in the left and right sectors of BLAST provides the form factor ratio G_E^p/G_M^p with high precision and minimized systematic errors. Preliminary results will be presented.

Two-photon Exchange Contribution to the Elastic e-p Scattering at Large Momentum Transfer

Yu-Chun Chen[1], Marc Vanderhaeghen[2], Carl E. Carlson[2], Andrei V. Afanasev[3]

[1]*Department of Physics,National Taiwan University*
[2]*Department of Physics, College of William and Mary,*
[3]*Thomas Jefferson National Accelerator Facility*

The electromagnetic form factors G_E and G_M are very important quantities in our knowledge of the structure of the nucleon. However the experiment for unpolarized scattering using Rosenbluth method and the polarization extractions give different result of R = G_E/G_M at large Q^2. This apparent discrepancy between the Rosenbluth and the polarization transfer methods for the ratio of the electric to magnetic proton form factors can be explained by a two-photon exchange correction. We estimate the two-photon exchange contribution to elastic electron-proton scattering at large momentum transfer by using a quark-parton representation of virtual Compton scattering. We thus can relate the two-photon exchange amplitude to the generalized parton distributions. We find that the interference of one- and two-photon exchange contribution is able to substantially resolve the difference between electric form factor measurements from Rosenbluth and polarization transfer experiments.

Two-photon exchange in elastic and inelastic electron-proton scattering

Sergey Kondratyuk[1], P. G. Blunden[1], W. Melnitchouk[2], J. A. Tjon[3]

[1]*Department of Physics and Astronomy, University of Manitoba*
[2]*Jefferson Lab*
[3]*Jefferson Lab and University of Maryland*

We present an explicit quantum field theoretical calculation of two-photon exchange contribution to elastic electron-proton scattering and to Δ resonance production in electron-proton collisions.

This work is motivated in part by the apparent disagreement between the Rosenbluth and polarisation transfer methods of measuring the nucleon form factors in elastic electron-proton scattering. Our results show that the two-photon exchange contribution, which is traditionally omitted in analyses of the data, can resolve the bulk of the discrepancy.

We include the nucleon and the Δ resonance as hadronic degrees of freedom in the two-photon exchange diagrams. We stress that it is essential to treat the nucleon and the Δ on the same footing since their contributions have opposite signs. The obtained two-photon exchange contribution to the elastic electron-proton scattering cross section varies from $\approx -3\%$ at backward angles to $\approx 1\%$ at forward angles, for the momentum-transfer squared Q^2 up to ≈ 6 GeV^2. We show that to make the Rosenbluth and polarisation transfer experimental methods compatible, the theoretical explanation of the data must include the additional two-photon exchange contribution.

The two-photon exchange effects are also quite important in the production of the Δ resonance in electron-proton collisions. The angular dependence of the two-photon contribution to the differential cross section for this process is shown in the figure below (at fixed Q^2, $\epsilon \to 0$ and $\epsilon \to 1$ correspond to the backward and forward scattering angles, respectively). The the two-photon exchange effects in Δ production are relatively large even at low Q^2.

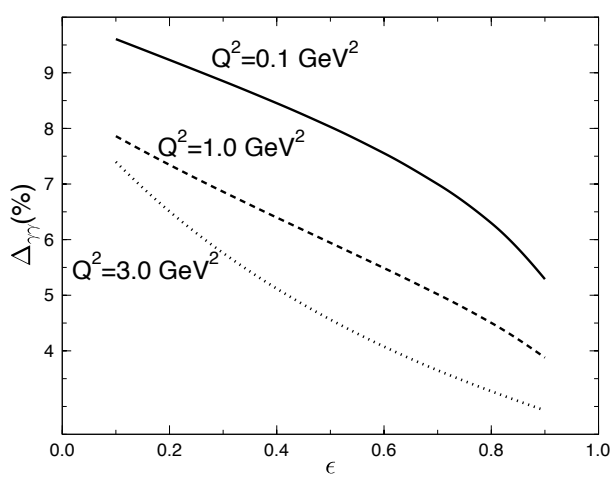

Fig. 1. Two-photon exchange contribution to the cross section for Δ production in electron-proton collisions

Nucleon resonance studies in phenomenological analysis of recent CLAS data on double charged pion photo- and electroproduction off proton.

Victor Ivanovich Mokeev[1], Volker D. Burkert[2]

[1]*Jefferson Lab & Moscow State university*
[2]*Jefferson Lab*

on behalf of the CLAS collaboration.

First comprehensive data on evolution of N* photocouplings in a wide range of photon virtualites ($0.<Q^2<1.5$ GeV^2) were obtained from analysis of recent CLAS experiments [1,2] on double charged pion photo- and electroproduction. Photocouplings were extracted for most nucleon excitations with masses <2.0 GeV. The analysis was carried out within the framework of most complete phenomenological model for description of double charged pion photo- and electroproduction in N* excitation region. Quality of recent CLAS data allowed to account for all relevant mechanisms in this exclusive channel at W<2.0 GeV and $Q^2<1.5$ GeV^2, implementing particular meson-baryon diagrams. Good description of all observables in recent CLAS data [1,2] was achieved without any need for remaining processes of unknown dynamic. Several new non-resonant mechanisms were established for the first time. Reliability of non-resonant mechanisms treatment and N*/background separation was confirmed in combined analysis of CLAS single and double pion electroproduction data [3]. Reasonable description of all observables in these two major exclusive channels was achieved with common N* photocouplings.

Our analysis provided first data on Q^2-evolution of the photocouplings for high lying N*'s (M>1.6 GeV) with major hadronic decays to the multi- pion final states. We found further evidences for possible new $3/2^+(1720)$ state, previously reported by CLAS Collaboration [2]. Combined analysis of double charged pion photo- and electroproduction at several photon virtualities enable us to improve considerably the knowledge of hadronic N* decays to $\pi\Delta$ and ρp final states.

References.

1. M.Bellis, et. al. in: Proc. of the Workshop on the Physics of Excited Nucleons, Grenoble, France 24-27 March 2004, World Scientific, ed. by J.-P. Bocquet, V.Kuznetsov, D.Rebreyend., 139.
2. M.Ripani, et. al., Phys. Rev. Lett. 91, 022002 (2003).
3. I.G.Aznauryan, et. al., Submitted to Phys. Rev. C.

Electromagnetic Form Factors of the Pion, Kaon, and Proton at Q^2 = 13.48 GeV^2

Peter Zweber
Northwestern University

on behalf of the CLEO collaboration.

We report on the measurement of the timelike electromagnetic form factors of the pion, kaon, and proton at Q^2 = 13.48 GeV^2 using 20.7 pb^{-1} of e^+e^- data accumulated at $\sqrt{s} = 3.67$ GeV at CLEO.

Measurements of Real Compton Scattering Cross Sections at Jefferson Lab

Areg Danagoulian
University of Illinois

on behalf of the E99-114 collaboration.

Similar to elastic electron scattering, Compton Scattering on the proton at high momentum transfers(and high $p_\perp$) can be an effective method to study its short-distance structure. An experiment has been carried out to measure the cross sections for Real Compton Scattering (RCS) on the proton for 3-6 GeV electron beam energies and a wide distribution of large scattering angles. The 25 kinematic settings sampled a domain of $s = 5-11(\mathrm{GeV/c})^2$, $-t = 2-7(\mathrm{GeV/c})^2$ and $-u = 0.5-6.5(\mathrm{GeV/c})^2$. In addition, a measurement of longitudinal and transverse polarization transfer asymmetries was made at a 3.48 GeV beam energy and a scattering angle of $\theta_{cm} = 120^o$. These measurements were performed to test the existing theoretical mechanisms for this process as well as to determine RCS form factors, which are the first moments of the Generalized Parton Distributions (GPD). The experiment was conducted in Hall A of Thomas Jefferson National Accelerator Facility(Jefferson Lab). It used a polarized and unpolarized electron beam, a 6% copper radiator (to produce a bremsstrahlung photon beam), the Hall A liquid hydrogen target, a high resolution spectrometer with a focal plane polarimeter, and a photon hodoscope calorimeter. Results of the cross sections and polarization transfer measurements will be presented.

III.4 Nucleon Structure: *PDFs from Small to Large x II*

Recent results on the polarisation of gluons from COMPASS experiment

Jan Nassalski

Soltan Institute for Nuclear Studies, Warsaw

on behalf of the COMPASS collaboration.

COMPASS experiment at CERN is using 160 GeV beam of polarised muons and longitudinaly polarised deuterium in a ^{6}LiD double-cell target. The gluon polarisation, $\Delta g/g$, is determined from the double-spin cross section asymmetries for the events selected by tagging the photon-gluon fusion process. Two methods of tagging are used: by requiring $D^{*\pm}$ or $D^0(\overline{D}^0)$ in the final state and by having two hadrons of large p_t. We obtain three independent preliminary results on $\Delta g/g$ at $\eta_g \simeq 0.12$: (1) from open charm production, (2) from large p_t hadrons using events with $Q^2 > 1\,\mathrm{GeV}^2$ and (3) from large p_t hadrons with $Q^2 < 1\,\mathrm{GeV}^2$. The respective values based on 2002 and 2003 data are: -1.08 ± 0.73(stat.), 0.06 ± 0.31(stat.)± 0.06(syst.) and 0.024 ± 0.089(stat.)± 0.057(syst.). A first analysis of 2004 data has been done, and it is very likely that more precise values will be shown.

Neutral Pion Double Longitudinal Spin Asymmetry in Proton-Proton Collisions at $\sqrt{s_{NN}} = 200$ GeV Using the PHENIX Detector

Kieran Boyle

Stony Brook University

on behalf of the PHENIX collaboration.

In the past 15 years, polarized DIS fixed target experiments have established that the quarks carry 20%-30% of the nucleon spin. Since in deep inelastic scattering the virtual photons, and gluons do not directly interact, the contribution of the proton's spin due to gluons is poorly measured. In the PHENIX Detector at the Relativistic Heavy Ion Collider (RHIC), we study longitudinally polarized proton collisions at $\sqrt{s_{NN}} = 200$ GeV. Measurement of double spin asymmetries in pp collisions allows us to measure the polarized gluon distribution through lowest order interactions. In the 2005 RHIC run, both the proton beam polarization and the luminosity were higher than previous years, our new measurement will give the first significant constraint on the gluon contribution. We present the latest PHENIX results from π^0 A_{LL}.

Probing the gluon polarization with the helicity asymmetry in J/Psi production in longitudinally polarized p+p collisions at sqrt(s) = 200 GeV/c

Ming X Liu[1], Imran Younus[2]

[1]*Los Alamos National Lab*
[2]*Univ. of New Mexico*

on behalf of the PHENIX collaboration.

Understanding the contribution of the polarized gluons to the protons total spin is one of the key steps toward resolving the nucleon spin crisis. At RHIC energy, heavy quark production is dominated by gluon-gluon interaction, thus measurements of A_{LL} of heavy flavor production in the polarized p-p collisions will allow us to directly access the polarized gluon distribution.

During the recent polarized p-p run, the PHENIX experiment has collected about 3.8^{-1}pb data with longitudinal beam polarization of 50%. The forward muon spectrometers can measure JPsi production through the mu+mu- decay mode at forward rapidities ($1.2 < |\eta| < 2.2$). In this talk we present the current status of the analysis of the double longitudinal spin asymmetry A_{LL} in the J/Ψ production in the polarized p+p collisions at $\sqrt{s} = 200$GeV. Probing the gluon polarization with the helicity asymmetry in J/Psi production in longitudinally polarized p+p collisions at $\sqrt{s} = 200$GeV.

Measurements of Separated Structure Functions and Moments on Nucleons and Nuclei

Cynthia E. Keppel

Hampton University / Jefferson Lab

on behalf of the E94110, E99118, E00116, E02109, E04001 collaborations.

The ratio R of longitudinal (L) to transverse (T) electron scattering off nucleons and nuclei is a fundamental quantity which has been at the center of a program in Hall C at Jefferson Lab. Data from experiments in this program have measured precision inclusive elastic, quasi-elastic, resonance, and deep inelastic cross sections from nucleons and nuclei over the four-momentum transfer range $0.01 < Q^2 < 7.0$ GeV^2. This new data has been used to accurately perform already over 200 Rosenbluth-type L/T separations. These separations have allowed for the longitudinal component of the electron-nucleon(us) cross section to be extracted, for the first time in many cases, and for the inelastic structure functions F_1, F_2, and F_L to be obtained.

Many physics issues are addressed by the new data, including: the nuclear dependence of the longitudinal structure function; quark-hadron duality; precision target mass corrections; improved measurements of F_2 at low Q^2; longitudinal resonance behavior; modeling the vector contribution to neutrino cross sections; and structure function moment extractions. An overview of the data and results will be presented, with some focus on the latter topic. Of particular interest in this case is the ability to extract gluon distributions.

Structure Function Measurements at the LHC

Ian Dawson

University of Sheffield

on behalf of the ATLAS Collaboration.

The large cross-sections and luminosity expected at the LHC promises the production of very large samples of W, Z and jet events. The potential for improvement in the determination of the proton structure functions, in particular the gluon distribution at low x, is presented. Implications on precision measurements and on discovery physics are discussed.

A Unified Model for inelastic $e - N$ and $\nu - N$ cross sections

Arie Bodek[1], Un-Ki Yang[2]

[1]*Dept. of Physics and Astronomy, Univ. of Rochester*
[2]*Enrico Fermi Institute, University of Chicago*

We present results using a new scaling variable, ξ_w in modeling electron- and neutrino-nucleon scattering cross sections with effective leading order PDFs. Our model uses all inelastic charged lepton F_2 data (SLAC/BCDMS/NMC/HERA), and photoproduction data on hydrogen and deuterium. We find that our model describes all inelastic scattering charged lepton data, the average of JLAB resonance data, and neutrino data at all Q^2. This model is currently used by current neutrino oscillation experiments in the few GeV region.

IV.3 Hadrons, Nuclei, Hypernuclei - Light Quarks: *Exotics/ Spectroscopy*

Partial Wave Analysis of the $\pi^+\pi^+\pi^-$ system in photo-production at CLAS

Mina Nozar
TRIUMF

on behalf of the CLAS collaboration.

A partial Wave Analysis (PWA) has been performed on a sample of $84,000$ $\pi^+\pi^+\pi^-$ events produced in the reaction γ p $\rightarrow \pi^+\pi^+\pi^-$ n with a tagged photon beam in the $4.8 - 5.4$ GeV energy range. The first high statistics photo-produced 3π data were collected during the $\mathrm{E01-017}$ (g6c) running of CLAS at Jefferson Lab. Numerous PWA fits varying the number of input partial waves, choosing random sets of initial parameters, and up to rank2 fits have been tried. The results indicate that the main contribution to the intensity distribution in the low mass ($1.2 - 1.4$ GeV) region is due to the well known $a_2(1320)$ state, while around the 1600 MeV mass region most of the strength is absorbed by the $\pi_2(1670)$. We have estimated an upper limit for the $\pi_1(1600)$ photo-production cross section in the $\pi^+\pi^+\pi^-$ final state.

The observation of the $\pi_1(1600)$ state, the lowest lying exotic meson with $J^{PC} = 1^{-+}$ quantum numbers, by the E852 collaboration [1] provided the main motivation behind this study. The production of this state in the reaction π^-p $\rightarrow \rho\pi^-$p , $\rho \rightarrow \pi^+\pi^-$, was seen to proceed through natural parity (most likely a ρ) exchange. Within the framework of the Vector Dominance Model (VDM), with the photon turning into a vector meson, i.e. ρ, ω, ϕ, and by reversing the role of the exchanged particle and the beam, this state should also be produced in a photon beam [2].

Earlier low statistics photo-produced charged 3π experiments [3–5] reported the observation of a peak in the $1.7 - 1.85$ GeV region. We now believe this observation is consistent with production of the $\pi_2(1670)$.

References

[1] S. U. Chung et al., *Phys. Rev.* **D65**, (2002).

[2] A. V. Afanasev, A. P. Szczepaniak, *Phys. Rev.* **D61**, (2000).

[3] Condo et al., *Phys. Rev.* **D48**, 3045 (1993), *Phys. Rev.* **D43**, 2787 (1991).

[4] Aston et al., *Nucl. Phys.* **B189**, 15 (1981).

[5] Eisenberg et al., *Phys. Rev. Lett.* **23**, 1322 (1969).

Nuclear response functions for the N-N*(1440) transition

Luis Alvarez Ruso[1], M. B. Barbaro[2], T. W. Donnelly[3], A. Molinari[2]

[1]*Institut fur Theoretische Physik, Universitat Giessen*
[2]*University of Turin and INFN*
[3]*Lab for Nuclear Science and Center for Theoretical Physics, MIT*

Using the relativistic Fermi gas model of nuclear matter, we have computed parity-conservin (PC) and -violating (PV) response functions for the inclusive electroexcitation of the $N^*(1440$ (Roper) resonance.

Being one of the most puzzling states found just above the Delta, the Roper is usually viewed as a radial excitation of a three-quark nucleon state. However, the standard non-relativistic constituent quark model fails to describe all of its properties, Further studies describe it as Skyrme soliton, a hybrid state with a large gluonic component, a nucleon-sigma molecule, or point at the relevance of relativistic corrections, configuration mixing and meson clouds.

Using various empirical parameterizations and theoretical models of the $N - N^*(1440)$ transition form factors, the sensitivity of the response functions to details of the structure of the Roper resonance is investigated. In particular, the non-relativistic quark model and the hybrid model with a large gluon component predict a quite different PC longitudinal response. The possibility of disentangling this resonance from the contribution of Delta electroproduction in nuclei is also addressed. The longitudinal response associated with the Roper can be large compared with the contribution from the Delta near the light-cone, although it might be hard to extract this information from data due to the suppression of the longitudinal response. Our results show that values of the momentum transfer around 500 MeV/c are the most favorable for studies of $N - N^*(1440)$ transitions because here the Roper signal is already relatively large due to its considerable width, while heavier resonances are not likely to be too disruptive.

We have explored as well the contributions of the Roper resonance to the Coulomb sum rule. Given a longitudinal/transverse separation, the impact of the Roper on sum rule can be significant (up to 20 % at 1 GeV/c of transfered momentum).

In the PV sector we obtain that the longitudinal response shows some interesting features in spite of its smallness, namely how it mixes the information about the $N - N^*$ transition on protons and neutrons in a non trivial way. Finally, we have computed the asymmetry, finding that the contribution from the Roper changes it appreciably above the quasielastic peak at high momentum transfer (1 GeV). It is however not relevant around 0.5 GeV, which implies that any deviation from flatness in the measured asymmetry could be safely used to extract the $N - \Delta$ axial response function.

Chiral unitary approach for the $\gamma p \to \pi^0 \eta p$ and $\pi^0 K^0 \Sigma^+$ reactions

M. Döring, E. Oset, D. Strottman
IFIC, University of Valencia

It is known that in the chiral unitary model, several low-lying resonances appear automatically as dynamically generated objects, examples of which are the $\Lambda^*(1405)$ and the $N^*(1535)$. In this model the essential dynamics are derived from the meson-baryon chiral Lagrangian which is then implemented via a non-perturbative scheme by unitarizing the amplitudes by the solution of the Bethe-Salpeter equation in a coupled channel approach.

Using this model with additions as described below, we have studied the reactions $\gamma p \to \pi^0 \eta p$ and $\gamma p \to \pi^0 K^0 \Sigma^+$ at photon energies for which the final states are produced close to threshold. In addition to the processes included via the lowest-order chiral Lagrangian, we have included other reactions which we find to be important. Motivated by the work of [1], we have included intermediate states arising from excitation of baryons from the decuplet, specifically the Δ and the Σ^*. In particular the interaction of the meson octet with the baryon decuplet dyanamically generates resonances, one of which can be identified with the $\Delta^*(1700)$ [1] and provides the dominant contributions.

The $\gamma p \to \pi^0 \eta p$ is shown to lead to sizable cross sections and the $N^*(1535)$ resonance shape is seen clearly in the ηp invariant mass distribution. The ηp invariant mass spectrum at higher energies shows a second maximum that is energy dependent which reflects the $\Delta(1232)$ intermediate state in one of the processes.

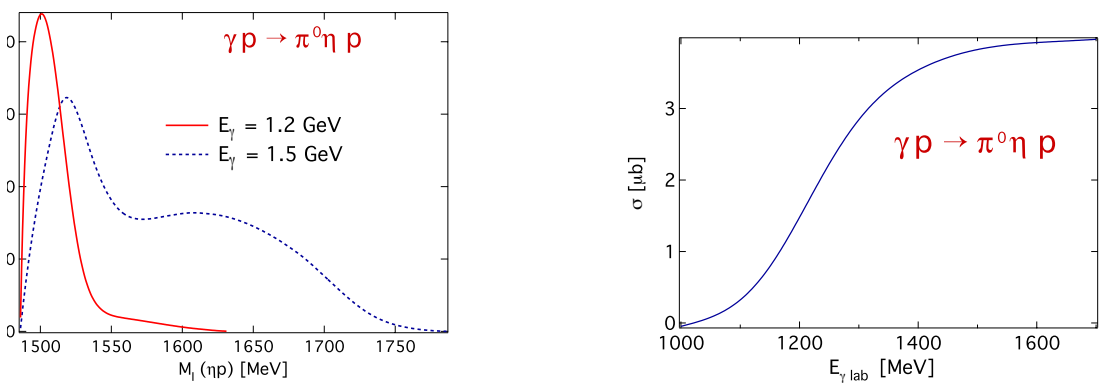

Fig. 1. Invariant mass spectra for two incident photon lab energies E_γ (left side) and total cross section (right side).

The same model leads to much smaller cross sections at low energies in the $\gamma p \to \pi^0 K^0 \Sigma^+$ reaction. Predictions are made for cross sections and invariant mass distributions which can be compared with forthcoming experiments at ELSA.

References

[1] J. C. Nacher, E. Oset, M. J. Vicente and L. Roca, Nucl. Phys. A **695**, 295 (2001);
S. Sarkar, E. Oset and M. J. Vicente Vacas, Nucl. Phys. A **750** (2005) 294.

Study of the Decay $\Omega^- \to \Xi^-\pi^+\pi^-$ in the HyperCP Experiment

Oleg Kamaev
Illinois Institute of Technology

on behalf of the HyperCP collaboration.

The HyperCP (E871) experiment collected $\sim 10^{10}$ hyperon decays during the 1997 and 1999 Fermilab fixed-target running periods, including $\sim 10^7$ Omega decays. A signal of ~ 100 events has been observed in the rare decay modes $\Omega^\pm \to \Xi^\pm\pi^+\pi^-$. We extract limits on the contribution of $\Omega^- \to \Xi^{*0}(1530)\pi^-$ to this process.

Evidence for two states of the $\Lambda(1405)$ resonance

Eulogio Oset[1], A. Ramos[2], V. Magas, University of Valencia[1]

[1]*University of Valencia*
[2]*University of Barcelona*

We study the $K^-p \to \pi^0\pi^0\Sigma^0$ reaction with the $\pi^0\Sigma^0$ forming the $\Lambda(1405)$ state and find a peak at 1420 MeV, with a relatively narrow width of $\Gamma = 38$ MeV, both in agreement with experiment [1]. The mechanism for the reaction is largely dominated by the emission of a π^0 prior to the K^-p interaction leading to the $\Lambda(1405)$. Thus one ensures the coupling of the $\Lambda(1405)$ to the K^-p channel and maximizes the contribution of the second pole found in chiral unitary theories, which is narrow and of higher energy than the nominal $\Lambda(1405)$ [2,3].

This is unlike the $\pi^-p \to K^0\pi\Sigma$ reaction, which gives more weight to the pole at lower energy and with a larger width [4]. In ref. [5] we give details of the present work. In fig. 3 of this reference we show the $\pi\Sigma$ invariant mass distribution that we find for the $\pi^-p \to K^0\pi\Sigma$ reaction compared to experiment, showing a good agreement, and in fig. 5 we show the experimental shape of the the $\pi\Sigma$ mass distribution in the two reactions $\pi^-p \to K^0\pi\Sigma$ and $K^-p \to \pi^0\pi^0\Sigma^0$. The data of these two experiments, together with the theoretical analysis, provides a strong support for the two pole structure of the $\Lambda(1405)$ resonance.

References

[1] S. Prakhov *et al.* [Crystall Ball Collaboration], Phys. Rev. C **70** (2004) 034605.

[2] D. Jido, J. A. Oller, E. Oset, A. Ramos and U. G. Meissner, Nucl. Phys. A **725** (2003) 181 [arXiv:nucl-th/0303062].

[3] C. Garcia-Recio, M. F. M. Lutz and J. Nieves, Phys. Lett. B **582** (2004) 49 [arXiv:nucl-th/0305100].

[4] T. Hyodo, A. Hosaka, E. Oset, A. Ramos and M. J. Vicente Vacas, Phys. Rev. C **68** (2003) 065203 [arXiv:nucl-th/0307005].

[5] V. K. Magas, E. Oset and A. Ramos, arXiv:hep-ph/0503043, Phys. Rev. Lett., in print.

$\Lambda(1405)$ in a hybrid quark model

Choki Nakamoto[1], Hidekatsu NEMURA[2]

[1]*Suzuka National College of Technology*
[2]*Advanced Meson Science Laboratory, DRI, RIKEN*

In spite of much effort for the description of the baryon spectrum, nobody has been able to explain the $\Lambda(1405)$ mass in the 3-valence-quark model. It may be rather a 3q-state than a $\bar{K}N$ bound state, namely a $q^4\bar{q}$-state, or a mixed state of them. In the flavor-SU(3) limit, the $\Lambda(1405)$ mass evaluated by a one-gluon exchange mechanism is lower in a $q^4\bar{q}$-system than in a 3q-system[1]. This means that it may give a favorable description of $\Lambda(1405)$ as $q^4\bar{q}$-state to treat the flavor-symmetry breaking through the mass difference between the ud- and s-quarks appropriately.

A constituent quark mass is free parameter and should be fixed in the suitable value not only for one baryon system but also for two baryon system, namely, also for baryon spectrum as well as baryon-baryon interactions. It is known that one needs to take into account not only the gluon-exchange effect but also the meson-exchange effect between quarks in order to describe nuclear force[2]. We have the following quark Hamiltonian;

$$H = K - K_{CM} + \sum_{i<j}^{n} (U_{ij}^{conf} + U_{ij}^{OGEP} + U_{ij}^{\pi} + U_{ij}^{K} + U_{ij}^{\sigma}) \ ,$$

where K denotes the kinetic-energy term, U_{ij}^{conf} a confinement potential, U_{ij}^{OGEP} a one-gluon exchange potential, U_{ij}^{π} one-pion exchange potential, U_{ij}^{K} K-meson exchange potential, and U_{ij}^{σ} σ-meson exchange potential. The model-parameters are fixed by reproducing the ground states of the octet-baryons.

We will discuss the $\Lambda(1405)$ as $q^4\bar{q}$-state described by precisely solving the five-body Schrüdinger equation with the stochastic variational method in the present quark model.

References

[1] H. Nemura and C. Nakamoto, Abstract in this conference.

[2] Y. Fujiwara, Y. Fujita, M. Kohno, C. Nakamoto and Y. Suzuki, Phys. Rev. **C65** (2002) 014002.

IV.4 Hadrons, Nuclei, Hypernuclei - Light Quarks: *Pentaquarks*

Hadron spectroscopy in photo- and hadroproduction at COMPASS

Jan M Friedrich

Technische Universität München

on behalf of the COMPASS collaboration.

COMPASS at CERN uses a 160 GeV/c muon beam on a polarised ^{6}LiD target to measure spin-dependent nucleon structure functions. These high-statistics data on photoproduction offer additionally information on hadron spectroscopy. We present results on the search for the $\Phi(1860)$ pentaquark which had been observed by the NA49 experiment at CERN.
COMPASS has also taken a first data sample using a pion beam, aiming to improve the pion polarisability measurement via scattering off a photon in the Coulomb field of a heavy nucleus, as well as meson spectroscopy in the diffractive scattering regime. Preliminary results of the ongoing analysis will be presented.

Search for the Pentaquark Partners: Θ^{++}, Σ^0 and N^0

Yi Qiang
Massachusetts Instititue of Technology

on behalf of the Jefferson Lab E04-012 collaboration.

In 1997, D. Diakonov *et al.* using a soliton model predicted a $SU(3)_F$ flavor antidecuplet[1)] of pentaquarks. The most striking prediction using this symmetry group is a narrow exotic state, $\Theta^+(1540)$, which has quark component $uudd\bar{s}$. Many observations[2)] have shown indications of its existence. If such a state exists, other members of the antidecuplet could be expected to have sufficiently narrow widths to be observed as well. The Jefferson Laboratory experiment E04-012 focused on the search for Σ^0 and N^0 partner states in the missing mass spectra of the $H(e, e'K^+)X$ and $H(e, e'\pi^+)X$ channels. In addition, if the Θ^+ has non-zero isospin then a hypothetical isospin partner[3)], Θ^{++}, might be expected in the $H(e, e'K^-)X$ channel which was also studied. The experiment was performed in Hall A at Jefferson Lab using a 5 GeV CW electron beam incident on a liquid hydrogen target. The two high resolution magnetic spectrometers were coupled to septum magnets to allow measurement of scattered electrons and outgoing hadrons at angles as small as 6 degrees. Kaons were identified using a combination of a ring-imaging and two aerogel Cherenkov counters. The missing mass resolution was determined to be 3.5 MeV FWHM using neutron, $\Lambda(1116)$ and $\Sigma(1193)$ production and provided a high sensitivity to narrow resonances. A precise measurement of the $\Lambda(1520)$ resonance has also been conducted for a cross-section comparison. We will present final results of the experiment, including upper limits on production cross sections for the three pentaquark partner states.

[1] D. Diakonov, V. Petrov, and M. Polyakov, Z. Phys. A **359** (1997) 305
[2] see, for example, S. Stepanyan *et al.* [CLAS collaboration], Phys. Rev. Lett. **91** (2003) 252001
[3] S. Capstick *et al.*, Phys. Lett. **B570** (2003) 185

Serach for exotic hadrons, H-dibaryon resonance and pentaquark

Kenichi Imai

Kyoto University

on behalf of the KEK-E522 collaboration.

Exotic hadrons such as the pentaquark, Θ^+, have recently attracted much attention as well as an H-dibaryon and others. Existence of exotic hadrons is one of the most important questions to understand the confinement aspect of QCD. We have performed an experiment (KEK-PS E522) primarily to search for the H-dibaryon resonance by $^{12}C(K^-,K^+\Lambda\Lambda)$ reactions with a 1.67GeV/c K^- beam. The (K^-,K^+) reactions from a scintillating fiber active target (Scifi) were identified with a K^+-spectrometer consisting of a magnet, tracking detectors, Cherenkov and TOF counters. The Scifi itself consists of 300 μm square fibers and the total volume is 10x10x20cm^3. It was viewed by 4 stage image intensifiers. Visual data of reaction vertices of the (K^-,K^+) reactions were studied in detail in the Scifi detector. We have obtained about 45000 events of the (K^-,K^+) reactions which is 6 times more than those obtained by the previous experiment (KEK-E224). We have completed the computer-aided scanning of all the visual data.

We have obtained about 200 events which have two Λ emitted from the reaction vertices. The invariant mass spectrum of the two Λ shows a peak structure at 2242 MeV/c^2 which is near the $\Lambda\Lambda$ threshold. The peak structure is statistically significant (~7) compared to the phase space and a “combinatorial background”. This peak can be an evidence of the H-dibaryon resonance. However, a peak at the threshold can be also interpreted as a final state interaction of the two Λ. We will present the results of the analysis of the $\Lambda\Lambda$ invariant mass spectrum with two assumptions, namely the H-resonance and the $\Lambda\Lambda$ final-state interaction where the $\Lambda\Lambda$ interaction is already limited by the recent precise determination of the binding energy of $^6He_{\Lambda\Lambda}$.

As a byproduct experiment of E522, we searched for the pentaquark, Θ^+, by π-p ->$K^-\Theta^+$ reaction at 1.9 GeV/c with the same experimental apparatus. Since the most of the positive results of Θ^+ were obtained by photon beams, hadronic productions of the pentaquark at low energy are important to confirm its existence. We will present the final result comparing with theoretical calculations of the production cross sections.

Hadron spectroscopy and pentaquark searches at Babar

Xin Chen
University of Wisconson, Madison

on behalf of the Babar Collaboration.

The Babar experiment at the high luminosity e^+e^- storage ring PEP-II offers excellent opportunities in hadron spectroscopy.

We present results of the search for charmonium states in two body B decays $b \to c\bar{c}K$. Results of the study of the state X(3872) are presented.

We also study initial-state radiation events, $e^+e^- \to \gamma(\mathrm{ISR})\pi^+\pi^- J/\psi$, and observe an accumulation of events near 4.26 GeV/c^2 in the invariant-mass spectrum of $\pi^+\pi^- J/\psi$. Fits of the mass spectrum indicate that a broad resonance with a mass of about 4.26 GeV/c^2 is required to describe the observed structure. The presence of additional narrow resonances cannot be excluded. The fitted width of the broad resonance is 50 to 90 MeV/c^2, depending on the fit hypothesis.

In addition we present results for the search for pentaquark states $\Theta(1540)^+$, $\Xi_5(1860)^0$ and $\Xi_5(1860)^{++}$ observed by other experiments.

Variational Monte Carlo study of pentaquark states

Mark W Paris
Jefferson Lab

Accurate numerical solution of the five-body Schroedinger equation is effected via variational Monte Carlo. The spectrum is assumed to exhibit a narrow resonance with strangenes S=+1. A fully antisymmetrized and pair-correlated five-quark wave function is obtained for the assumed non-relativistic Hamiltonian which has spin, isospin, and color dependent pair interactions and many-body confining terms which are fixed by the non-exotic spectra. Gauge field dynamics are modeled via flux tube exchange factors. The energy determined for the ground states with J=1/2 and negative (positive) parity is 2.22 GeV (2.50 GeV). A lower energy negative parity state is consistent with recent lattice results. The short-range structure of the state is analyzed via its diquark content.

Production and decay of pentaquarks

Atsushi Hosaka

Research Center for nuclear Physics (RCNP), Osaka Univ.

In the first part we discuss the fall-apart decay of Theta$^+$ within a non-relativistic quark model. Assuming J^P of Theta$^+$ are $1/2^{pm}$, matrix elements and decay rates are computed in such way that the role of the overlap functions langleKN|Theta$^+$rangle for spin, flavor, color and orbital wave functions (spectroscopic factor) can be studied. We find that for $1/2^-$ of $(0s)^5$, the width becomes too large for the state to be identified with a narrow resonance, while it is about a several tens MeV for $1/2^+$. The too broad width of the $1/2^-$ state is a natural consequence that the quark model state of $(0s)^5$ is nothing but the KN scattering state. For $J^P = 1/2^+$, by assuming strong diquark correlations, the width is reduced to be of order 10 MeV. It is also pointed out that within a quark model, $(0s)^5$ configuration can accommodate the $J^P = 3/2^-$ state which leads to a strong suppression of the decay into d-wave KN states.

Based on these observations, we study more on the possibility $J^P = 3/2^-$. We take a brief look at an analysis based on flavor SU(3), where we find that the presently available data favor $J^P = 3/2^-$. Then we reconsider photo-productions of Theta$^+$ from the proton and neutron again but this time for $J = 3/2$. It is found that there is a large asymmetry between the production rates of the two targets; production from the proton is very much suppressed as compared with that from the neutron. The contact term of the Kroll-Ruderman type is playing a crucial role for the suppression. The resulting cross section is only a few nb, which does not contradict the new CLAS result.

Finally, production of K^* ($J^P = 1^-$) is briefly discussed. The K^* production allows kappa(0^-)$\cdot$ exchange which was not possible in the K-production. We propose a method to isolate an exchanged particle in the t-channel using polarizations of gamma and K^*. This will be useful to get more information on the reaction mechanism for the Theta$^+$ production.

V.2 Heavy Flavor Physics - Search for New Particles: *Charm Physics*

Strong one-pion decay of ground state charmed baryons

Conrado Albertus[1], Eliecer Hernandez[2], Juan Nieves[1], Jose M. Verde-Velasco[2]

[1]*Departamento de Fisica Moderna, Universidad de Granada*
[2]*Grupo de Fisica Nuclear,Universidad de Salamanca*

We evaluate the widths for the charmed-baryon $\Sigma_c^* \to \Lambda_c\pi$, $\Sigma_c \to \Lambda_c\pi$ and $\Xi_c^* \to \Xi_c\pi$ strong decays within the framework of a nonrelativistic quark model. To our knowledge, this is the first fully dynamical calculation within a nonrelativistic approach. We use wave functions constrained by heavy quark symmetry (HQS) and that were obtained with the help of a simple variational ansazt[1)]. For that purpose we take five different nonrelativistic quark–quark interactions[2−3)] that include a confining term, plus Coulomb and hyperfine terms coming from one-gluon exchange. To evaluate the pion emission amplitude we use a spectator or one-quark pion emission model. The amplitude is obtained with the use of PCAC from the analysis of weak current matrix elements. Our results are rather stable against the quark–quark interaction, with variations in the decay widths at the level of 6–8%. As seen in the Table, we find an overall good agreement with experiment for the three reactions in their different charge configurations.

	$\Gamma(\Sigma_c^{++} \to \Lambda_c^+\pi^+)$ [MeV]	$\Gamma(\Sigma_c^+ \to \Lambda_c^+\pi^0)$ [MeV]	$\Gamma(\Sigma_c^0 \to \Lambda_c^+\pi^-)$ [MeV]
This work	$2.43 \pm 0.07 \pm 0.04$	$2.80 \pm 0.08 \pm 0.05$	$2.39 \pm 0.06 \pm 0.04$
Exp.	$2.3 \pm 0.2 \pm 0.3$ [4)]	< 4.6 (CL=90%) [5)]	$2.5 \pm 0.2 \pm 0.3$ [4)]
	$2.05^{+0.41}_{-0.38} \pm 0.38$ [6)]		$1.55^{+0.41}_{-0.37} \pm 0.38$ [6)]
	$\Gamma(\Sigma_c^{*++} \to \Lambda_c^+\pi^+)$ [MeV]	$\Gamma(\Sigma_c^{*+} \to \Lambda_c^+\pi^0)$ [MeV]	$\Gamma(\Sigma_c^{*0} \to \Lambda_c^+\pi^-)$ [MeV]
This work	$17.7 \pm 0.7 \pm 0.3$	$17.5 \pm 0.7 \pm 0.3$	$17.1 \pm 0.7 \pm 0.2$
Exp.	$14.1^{+1.6}_{-1.5} \pm 1.4$ [7)]	< 17 (CL=90%) [5)]	$16.6^{+1.9}_{-1.7} \pm 1.4$ [7)]
	$\Gamma(\Xi_c^{*+} \to \Xi_c^0\pi^+ + \Xi_c^+\pi^0)$ [MeV]	$\Gamma(\Xi_c^{*+} \to \Xi_c^0\pi^+ + \Xi_c^+\pi^0)$ [MeV]	
This work	$3.19 \pm 0.09 \pm 0.05$	$3.03 \pm 0.10 \pm 0.04$	
Exp.	< 3.1 (CL=90%) [8)]	< 5.5 (CL=90%) [9)]	

[1] C. Albertus, J. E. Amaro, E. Hernández and J. Nieves, Nucl. Phys. A 740 (2004) 333

[2] R. K. Bhaduri, L. E. Cohler and Y. Nogami, Nuovo Cimento A 65 (1981) 376.

[3] B. Silvestre-Brac, Few-Body Systems 20 (1996) 1.

[4] M. Artuso *et al.* (CLEO Collaboration), Phys. Rev. D 65 (2002) 071101.

[5] R. Ammar *et al.* (CLEO Collaboration), Phys. Rev. Lett. 86 (2001) 1167.

[6] J. M. Link *et al.* (FOCUS Collaboration), Phys. Lett. B 525 (2002) 205.

[7] S. B. Athar *et al.* (CLEO Collaboration), Phys. Rev. D 71 (2005) 051101.

[8] L. Gibbons *et al.* (CLEO Collaboration), Phys. Rev. Lett. 77 (1996) 810.

[9] P. Avery *et al.* (CLEO Collaboration), Phys. Rev. Lett. 75 (1995) 4364.

Genetic Programming search for doubly Cabibbo suppressed decays of Λ_c^+ and D_s^+

Eric Vaandering
Vanderbilt University

on behalf of the FOCUS collaboration.

Genetic programming is a machine learning technique, popularized by Koza in 1992, in which computer programs which solve user-posed problems are automatically discovered. Populations of programs are evaluated for their fitness of solving a particular problem. New populations of ever increasing fitness are generated by mimicking the biological processes underlying evolution. These processes are principally genetic recombination, mutation, and survival of the fittest.

We will review the principles of genetic programming and show its successful application to a search for the DCS decays $\Lambda_c^+ \to pK^+\pi^-$ and $D_s^+ \to K^+K^+\pi^-$. We are able, using this technique, to acheive greater sensitivity than standard cut-based analyses.

New charm spectroscopy

Maurizio Lo Vetere
Università di Genova & INFN

D hadronic branching fractions

Werner Sun
Cornell

X(3872): Hadronic Molecules in Effective Field Theory

Alexey A Petrov
Wayne State University

We consider the implications from the possibility that the recently observed state $X(3872)$ is a $D^{*0} - \overline{D}^0$ meson-antimeson molecule. We write an effective Lagrangian consistent with the heavy-quark and chiral symmetries needed to describe the properties of $X(3872)$ and discuss implications for the existence of a similar molecular bound state in the B^{*0} and $\overline{B}^0$ system. We also consider production features of this state in $p\bar{p}$ collisions.

Measurement of the Dipion Mass Spectrum in the Decay $X(3872) \to J/\psi\, \pi^+\pi^-$

Alexander Y Rakitin
Lancaster University, Lancaster, UK

We investigate the puzzling nature of the state $X(3872)$ using data obtained with the CDF II detector at the Fermilab Tevatron Collider. The shape of the dipion mass spectrum in $X(3872) \to J/\psi\, \pi^+\pi^-$ decay is compared to theoretical predictions for the dipion spin-parity 0^{++} and 1^{--}. For 0^{++} case, the QCD multipole expansion for charmonium is used, and only $^3S_1$ state is found to be compatible with data.There is, however, no $^3S_1$ charmonium state available for assignment to the $X(3872)$. For the 1^{--} case the hypothesis $X(3872) \to J/\psi\rho^0$ is tested and found to be compatible with the data.

VI.2 Fundamental Symmetries: *Symmetry Tests from Kaon Decays II and Higgs Sector*

Search for T-Violation in Stopped Kaon Decay

Michael D Hasinoff, et al.

University of British Columbia

on behalf of the KEK-E246 collaboration.

The transverse muon polarization (P_T) in K^+ decay is an excellent CP- or T- violating observable to study since any non-zero value > 10^{-5} would imply new physics beyond the Standard Model. Furthermore, since P_T involves phases between both the quark-quark and lepton-lepton couplings it probes a different region of parameter space than the neutron dipole moment or the K^0 decay experiments. We have measured P_T by means of the T-violating triple product correlation between the μ^+ spin and the π^0 and μ^+ momenta in stopped K^+ decays at the 12 GeV PS at the National Laboratory for High Energy Physics (KEK) in Japan. An analysis of our complete data set (11.8 million good K^+ decays) indicates no evidence for any T-violation ($P_T < 0.0051$ at the 90 % confidence level). The details of our experiment and the various systematic errors will be presented along with our plans for an improved experiment at J-PARC.

Search for CP Violation in Hyperon Decays with the HyperCP Spectrometer at Fermilab

Edmond C. Dukes

University of Virginia

on behalf of the HyperCP collaboration.

The HyperCP collaboration at Fermilab is making high-precision searches for CP violation in charged hyperon decays. With data samples up to a thousand times larger than any previously taken, sensitive searches for CP violation have been made by comparing the proton and antiproton angular decay distributions in $\Xi^- \to \Lambda\pi^- \to p\pi^-\pi^-$ and $\overline{\Xi}^+ \to \overline{\Lambda}\pi^+ \to \overline{p}\pi^+\pi^+$ decays, as well as in $\Omega^- \to \Lambda K^- \to p\pi^- K^-$ and $\overline{\Omega}^+ \to \overline{\Lambda}K^+ \to \overline{p}\pi^+ K^+$ decays. We report on the final result from the Ω search, and give a status report on the Ξ search using the full HyperCP dataset of about one billion events.

Searches for Standard Model and Charged and Neutral MSSM Higgs Production

Ben Kilminster

Ohio State University

on behalf of the CDF collaboration.

We present the results on the searches for the Standard Model and the MSSM Higgs boson production in proton-antiproton collisions as $\sqrt{s}$ = 1.96 GeV with the CDF detector. The Higgs bosons are searched for in various production and decay channels, with data samples corresponding to 400 pb^{-1}. Using these measurements, we set an upper limit on the production cross section times branching fraction for the Standard Modle Higgs as a function of the Higgs mass, and we obtain exclusion regions in the tanβ vs mass for both charged and neutral MSSH Higgs bosons.

DØ Search for the Standard Model Higgs Boson

Hyunwoo Kim
University of Texas, Arlington

on behalf of the DZero collaboration.

We present three searches for the standard model Higgs boson at $\sqrt{s} = 1.96$ TeV in $p\bar{p}$ collisions using data taken with the DØ detector during Run II of the Fermilab Tevatron collider. The first study is a search for the Higgs boson in $H \to WW^{(*)} \to \ell^+\nu\ell'^-\nu$ decays. The data correspond to an integrated luminosity of 325 pb^{-1} in the e^+e^-, 318 pb^{-1} in the $e^\pm\mu^\mp$ and 299 pb^{-1} in the $\mu^+\mu^-$ final state. The number of events observed is consistent with expectations from standard model backgrounds. Limits from the combination of all three channels on the production cross section times branching ratio $\sigma \times BR(H \to WW^{(*)})$ are presented.

The second study is a search for the associated Higgs boson production in the process $p\bar{p} \to WH \to WWW^{(*)} \to \ell^\pm\ell^\pm\nu\bar{\nu}q\bar{q}$ in the ee, $e\mu$, and $\mu\mu$ channels. We require two like sign isolated leptons (electrons or muons) with $p_T > 15$ GeV plus additional selection cuts. We observe one event in the ee channel, 3 events in the $e\mu$ channel, and 2 events in the $\mu\mu$ channel, in agreement with the predicted Standard Model background, and set 95% CL upper limits on $\sigma(WH) \times BR(H \to WW^{(*)})$ between 3.9 and 2.1 pb for Higgs masses from 115 to 175 GeV.

The third study is a search for WH production in the $Wb\bar{b}$ final state. The search is performed in events containing one electron, an imbalance in the transverse enegy(E_T) and two b-tagged jets. Since no excess of events is observed in the $b\bar{b}$ invariant maess, we set 95% C.L. upper limits on the WH production cross section between 6.9 pb and 8.6 pb for Higgs boson masses between 105 and 135 GeV.

D0 Search for the Higgs Boson in Multijet Events

Alexander Melnitchouk
University of Mississippi

on behalf of the DZero collaboration.

We present two searches for the Higgs boson in multijet events at $\sqrt{s} = 1.96$ TeV in $p\bar{p}$ collisions using data taken with the DØ detector during Run II of the Fermilab Tevatron collider. The first study is a search for neutral Higgs bosons produced in association with bottom quarks in $p\bar{p}$ collisions. The cross sections for these processes are enhanced in many extensions of the standard model (SM), such as in its minimal supersymmetric extension at large $\tan\beta$. The results of our analysis agree with expectations from the SM, and we use our measurements to set upper limits on the production of neutral Higgs bosons in the mass range of 90 to 150 GeV.

The second study is a search for the standard model Higgs boson produced in association with the Z boson at DØ . We study the $p\bar{p} \to ZH \to \nu\bar{\nu}b\bar{b}$ channel, which is one of the most sensitive ways to search for light Higgs bosons because of the large $Z \to \nu\bar{\nu}$ and $H \to b\bar{b}$ branching ratios. The analysis starts with a sample of multijet events with large imbalance in transverse momentum. We then select events with two b-tagged jets and search for a peak in their invariant mass distribution. After subtracting the backgrounds, we set the 95% C.L. upper limits on the $\sigma(p\bar{p} \to ZH) \times BR(H \to b\bar{b})$ for Higgs masses between 105 and 135 GeV.

On Heavy Quarkonia and new Higgs Physics Effect -Theory and Phenomenology

Gennady A. Kozlov

Joint Institute for Nuclear Research

We establish a new effect of Higgs-boson interplay with heavy quarks which induces a strong attractive force between the constituents $\bar{Q}Q$ of a heavy quarkonium. An important application is the decay of heavy quarkonium into a Higgs-boson associated with gauge bosons. The criterion for making the $\bar{Q}Q$ bound state is established. We also show that non-perturbative effects due to gluonic field fluctuations are rather small in such a heavy quark flavor sector. Possible enhancement for the production and decays of $\bar{Q}Q$ bound states originated from the extra fourth generation quarks is discussed. The probabilty of an extra gauge boson Z' decay into a Higgs-boson and a bound state composed of heavy quarks is predicted. In the framework of the extended SU(2) gauge model we investigated new decay modes of Z' bosons. The data analysis results of the Fermilab Tevatron allows one to establish not only the lower bound of the Z' decay probabilities, but also to estimate the mixing angle between the states Z' and Z. We found that an investigation of radiative decays of Z' bosons at the acting collider Tevatron or at forthcoming LHC, would allows one to clarify the question of the efficiency of the extended gauge group $SU(2)\star SU(2)$, and to give the estimation of the coupling constants of Z' boson interaction with fermions. We have got the Higgs-boson mass sum rules which allows one to estimate the upper limits of stop-quark masses as well as the lower bounds on the scalar Higgs-boson masses. The bounds on the scale of the quark-lepton compositeness derived from the Tevatron CDF and D0 data applying to new extra gauge boson search are taken into account.

G.A. Kozlov et al., J.Phys.G: Nucl.Part.Phys. 30 (2004) 1201;// G.A. Kozlov, hep-ph/050115 (2005);// G.A. Kozlov and T. Morii, Phys. Rev. D67 (2003) 055001;// G.A. Kozlov and T. Morii, Phys. Lett. B545 (2002)127;// G.A. Kozlov, Phys. Atom. Nucl. 63 (2000) 2293;// G.A. Kozlov, Nuovo Cim. A112 (1999) 1103.

VIII.2 Neutrino Physics: *Double Beta Decay and Underground Laboratories*

The Majorana Project: A Next-Generation Double-Beta Decay Experiment

Victor M. Gehman

Los Alamos National Laboratory/University of Washington

on behalf of the Majorana collaboration.

The Majorana Project will endeavor to provide direct limits on the effective Majorana mass of the electron neutrino through the measurement of neutrinoless double-beta decay in ^{76}Ge. Our goal is an experiment with a scalable sensitivity ranging from a few hundred meV to 50 meV (corresponding to the mass scale indicated by the atmospheric neutrino oscillation results). The experiment will consist of several modules, each a close-packed array of many germanium detectors, enriched to 86% in ^{76}Ge, in a single cryostat. The objective of the first experimental phase of the Majorana Collaboration is to build a 180 kg detector array consisting of three cryostats containing 57 detectors each. This array will need to reach a background level on the order of one count per ton of Ge per year in the four keV region of interest around the double-beta decay endpoint. This background will allow us to reach an ultimate effective Majorana-neutrino mass sensitivity of approximately 100 meV, which is about five times better than current results and covers the quasi-degenerate mass solution region. Here, we present an overview of the project with emphasis on science goals, current R&D efforts and reference plan for the project.

GERDA, the GERmanium Detector Array for the search of neutrinoless double beta decay in Ge-76

Luciano Pandola

Gran Sasso National Laboratory

on behalf of the GERDA collaboration.

The study of neutrinoless double β decay (DBD) is the most powerful approach to the fundamental question if the neutrino is a Majorana particle, i.e. its own anti-particle. The observation of neutrinoless DBD would not only establish the Majorana nature of the neutrino but also represent a measurement of its effective mass. So far, the most sensitive results have been obtained with ^{76}Ge, and a group has claimed for the first time positive indications for neutrinoless DBD in ^{76}Ge. The new GERDA experiment [1] will operate in the Gran Sasso underground laboratory an array of bare enriched ^{76}Ge diodes in a shield of extremely radiopure liquid nitrogen or argon. This shield together with an additional water layer will reduce the external backgrounds by more than two orders of magnitude as compared to previous DBD experiments. In this talk the physics reach as well as the status of GERDA will be discussed.

[1] http://www.mpi-hd.mpg.de/ge76/proposal.pdf

Prospects for CUORE and Latest Results from CUORICINO

Eric B. Norman

Lawrence Livermore National Laboratory

on behalf of the CUORE collaboration.

CUORE (Cryogenic Underground Observatory for Rare Events) is a proposed next generation experiment designed to search for the neutrinoless DBD of ^{130}Te using a bolometric technique. The source/detector will be composed of 988 5x5x5–cm single crystals of TeO_2 all housed in a common dilution refrigerator and operated at a temperature of 8–10 mK. The total mass of ^{130}Te contained in CUORE will be approximately 204 kg. Attached to each crystal will be one or more neutron–transmutation doped (NTD) germanium thermistors that will measure the small temperature rise produced in a crystal when radiation is absorbed. The estimated sensitivity of CUORE is sufficient to cover essentially the entire inverted mass hierarchy region deduced from neutrino oscillation experiments. There are several compelling reasons to study ^{130}Te DBD. Because of its large decay energy and large expected nuclear matrix element, the half–life of ^{130}Te is predicted to be shorter than that of a number of other candidate isotopes. Secondly, based on the sensitivity needed to reach the mass scales inferred from the oscillation experiments, the ^{130}Te experiment can be done utilizing the natural abundance of ^{130}Te (34%), without the time and expense of obtaining separated isotopes. Of all the proposed next generation DBD experiments, only CUORE can reach the needed sensitivity without isotopic enrichment. CUORE has been approved by the Scientific Committee of the Gran Sasso National Laboratory (LNGS) in Italy and has already been assigned space in this facility. Recently, the INFN approved CUORE and has already committed 1.2M Euro to fund the construction of the large new dilution refrigerator need for CUORE. A prototype experiment, CUORICINO, which consists of 62 TeO_2 crystals, is now running at the LNGS. CUORICINO is presently the largest operating double beta decay experiment in the world and has recently published its first physics result - a limit on neutrino mass only slightly less stringent than that obtained from previous ^{76}Ge experiments. In this talk, the present status of CUORE will be presented along with the latest results from CUORICINO.

The depth-sensitivity relation (DSR) for underground laboratories

Dongming Mei, Andrew Hime
Los Alamos National Laboratory

Muon-induced background can limit the sensitivity of next generation experiments searching for neutrinoless double beta decay and WIMP dark matter. We have established the DSR based upon the muon and muon-induced fast neutron fluxes and spectra for a number of underground laboratories. Our results indicate that the muon-induced neutron elastic and inelastic scattering processes create a significant background for germanium-based dark matter and double beta decay experiments, unless such experiments are staged deep underground. We use the measured neutron elastic and inelastic scattering processes with a segmented clover (germanium) detector on the surface to confirm our model predictions.

DEAP & CLEAN Detectors for Low Energy Particle Astrophysics

Andrew Hime[1], Daniel McKinsey[2], Mark Boulay[3]
[1]*Los Alamos National Laboratory*
[2]*Yale University*
[3]*Queen's University*

Liquid Neon (LNe) and liquid Argon (LAr) are promising targets for large-scale and conceptually simple detectors of low-energy solar neutrinos and cosmological dark matter. Using the unique properties of scintillation light in LNe, an ultra-pure and large fiducial volume can be realized and serve as a simultaneous detector of solar neutrinos and dark matter. Similar use of liquid scintillation light in LAr offers the possibility for a large volume detector of dark matter with unprecedented background rejection capability. The development program underway to realize such detectors, dubbed CLEAN and DEAP, will be presented.

XI.2 Nuclear and Particle Astrophysics and Cosmology:
Dark Matter and Cosmology

Phases of Dense Quark Matter and Compact Objects

Andrew W Steiner[1], Prashanth Jaikumar[2], Sanjay Reddy[3]

[1]*T-16, Los Alamos National Laboratory*
[2]*Argonne National Laboratory*
[3]*Los Alamos National Laboratory*

The presence of quark matter in neutron stars may affect several neutron star observables and the neutrino signal in core-collapse supernovae. These observables are sensitive to the phase of quark matter that is present in compact objects. We present the first calculation of the phase structure of dense quark matter which includes a six-fermion color-superconducting interaction and show that the effect of this term can destabilize the pairing interaction, favoring phases where fewer quarks are paired. In turn, this modification of the phase structure can modify the neutrino signal, the structure of the neutron star, and the long-term cooling. We also show that, contrary to the 20-year old paradigm of the surface structure of the “strange-quark stars”, the surface of these objects may consist of nuggets of strange quark matter screened by the electron gas.

Cryogenic Dark Matter Search Experiment: Latest Results and Status

Michael Dragowsky

Case Western Reserve University

on behalf of the Cryogenic Dark Matter Search collaboration.

Compelling evidence for non-luminous matter pervasively distributed at galactic and supergalactic length scales exists from astronomy, astrophysics and observational cosmology. Dark matter in the form of weakly interacting massive particles, or WIMPs, postulates particle properties that are consistent with predicted massive, stable particles from a variety of extensions to the standard model (e.g. Supersymmetry and Kaluza-Klein theories). Regardless of the specific theoretical framework, such neutral, massive particles would interact via elastic scattering from nuclei in particle detectors. Dark matter direct-detection would not only inform the general issue of cosmologic dark matter, but also provide particle mass and cross section measurements relevant for understanding physics beyond the standard model.

Dark matter detected in the laboratory would have elastic WIMP–nucleon scattering signatures associated with the galactic dark matter halo kinematics. The resulting nuclear recoil energies would be on the order of 10^0–10^2 keV, requiring detection techniques with good energy sensitivity in this range. The Cryogenic Dark Matter Search Collaboration has developed novel particle detectors incorporating athermal phonon as well as ionization sensors to discriminate between nuclear recoil interactions characteristic of WIMPs and electron recoils due to background interactions. These devices will be introduced and results from nearly one year of operations in the Soudan Underground Laboratory will be presented that exclude new regions of parameter space for both spin-dependent and spin-independent WIMP–nucleon interactions. Prospects for additional dark matter sensitivity from continued CDMS operations at Soudan will be presented, as well as plans to conduct a series of higher mass experiments (SuperCDMS) in the coming years that will greatly compliment LHC findings related to dark matter and elementary particle interactions.

The Dark Energy Survey

Huan Lin
Fermi National Accelerator Laboratory

on behalf of the Dark Energy Survey collaboration.

The Dark Energy Survey (DES) is a proposed 5-year, 5000 deg^2 optical imaging survey, to 24th magnitude in the SDSS griz bands, that will use a new wide-field 3 deg^2 mosaic CCD camera on the Blanco 4m telescope at the Cerro Tololo Inter-American Observatory (CTIO). The primary scientific goal of the DES is to probe the nature of dark energy using four complementary methods: galaxy clusters, weak gravitational lensing, galaxy angular correlations, and Type Ia supernovae. For each of these methods, the DES should determine the dark energy equation of state parameter w with a statistical precision of about 5-15%, assuming constant w but without strong priors on other cosmological parameters. By deriving dark energy constraints using four complementary sets of measurements made from the same data set and within a common analysis framework, we will obtain important cross checks of our systematic errors and thereby make a substantial and robust advance in the precision of dark energy measurements.

Status of the XENON Direct Dark Matter Detection Experiment

Richard D Hasty
Yale University

on behalf of the XENON collaboration.

The XENON collaboration is developing a dark matter detector using liquid xenon (LXe) as the target medium for detecting weakly interacting massive particles (WIMPs). The final experiment is projected to have a fiducial mass of 1000 kg and a detection threshold of 16 keV. The experiment will consist of ten independent dual phase time projection chambers (TPC), as depicted in Fig. 1. The scintillation and ionization from each event in the TPCs will be measured, allowing background events to be eliminated. Nuclear recoil events, the expected WIMP signal, have a scintillation to ionization ratio that is distinct from the dominant background. Active shielding and 3D position resolution will further suppress background events. I will present recent results from the research and development program and discuss the current status of the project.

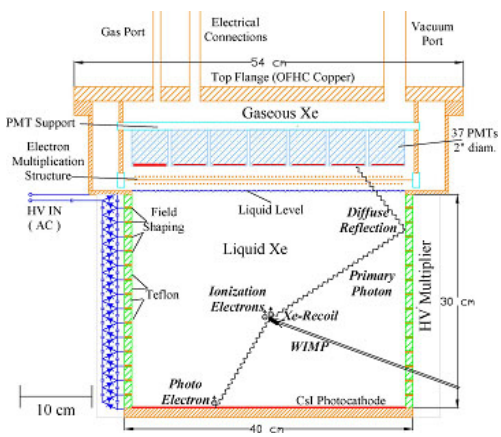

Fig. 1. A proposed XENON 100 kg module TPC. The scintillation light from an event would be detected by an array of photomultiplier tubes (PMTs) at the top and by a CsI photocathode. The ionized electrons will be detected via the proportional scintillation light emitted in the gas phase of the detector.

The XENON collaboration has made recent measurements that demonstrate the feasibility of using a dual phase Xe TPC to achieve improved sensitivity to dark matter. Two of the key measurements are the scintillation and ionization yield of LXe for low energy nuclear recoils. The scintillation efficiency for 10 keV nuclear recoils was measured to be greater than 10 percent of the efficiency for electron like recoils. The ratio of ionization to scintillation has also been measured for nuclear recoils, and the results indicate that nuclear recoils can be discriminated from gamma ray backgrounds.

The XENON collaboration is currently developing a prototype 10 kg fiducial volume detector (XENON10) with both good light collection and position resolution. The XENON10 prototype will be similar to the proposed 100 kg module in Fig. 1. This prototype will be installed and operated at Gran Sasso National Laboratory in Italy.

Search for Dark Matter Annihilations in Draco

Maxwell Chertok, et al.
University of California, Davis

on behalf of the CACTUS team.

CACTUS is a ground–based Air Cherenkov Telescope at the Solar 2 facility located near Barstow, California and operated by UC Davis. It uses an array of 160 large solar tracking mirrors (heliostats) and a camera with 80 photomultiplier tubes, in a multiplexed fashion, providing an effective camera with about 300 channels. CACTUS has also incorporated novel techniques of time projection imaging and triggering to improve upon the first generation sampling arrays of its kind.

We have recently completed observations of Draco, a dwarf spheroidal galaxy within the Milky Way local group that is known to be rich in dark matter content. Supersymmetry–inspired models for dark matter predict observable annihilation rates producing gamma rays. We will present the first results from our Draco campaign.

In earlier measurements of the gamma–ray emissions from the Crab nebula, we have established that CACTUS is sensitive in the 50–500 GeV energy range. We will describe our calibrations and present a preliminary energy spectrum for gamma–rays from the Crab and for background cosmic–rays.

The Atacama Cosmology Telescope Project

Arthur B Kosowsky
University of Pittsburgh

on behalf of the Atacama Cosmology Telescope collaboration.

The Atacama Cosmology Telescope (ACT) is a collaboration to produce maps of the cosmic microwave background radiation at an unprecedented combination of sensitivity, angular resolution, and sky coverage in three frequency bands. A complementary optical survey of the same sky region, primarily using the new Southern African Large Telescope (SALT), will also be performed. I will give an overview of the scientific motivations for this survey, including measurements of the primary microwave anisotropies reflecting the universe at a redshift of $z = 1100$ and secondary anisotropies from cosmic structures arising at much lower redshifts. I will also review the remarkable technology which enables such measurements and give a progress report on construction of the microwave telescope and its detectors. Potential constraints relevant to particle physics, such as the dark energy equation of state and neutrino masses, will be emphasized.

Dark Energy and Condensate Stars

Emil Mottola[1], Pawel O. Mazur[2]

[1]*Los Alamos National Laboratory*
[2]*Univ. of South Carolina*

A new final state of gravitational collapse is proposed. The dark energy equation of state, p $= -\rho$ acts as a kind of repulsive condensate core for the interior of a compact object with an exterior Schwarzschild geometry of arbitrary total mass M. The two regions are separated by a thin phase boundary layer wherein the vacuum energy and equation of state changes rapidly. The new solution is cold and dark, but has no singularities, no event horizons, and a global time. Its entropy is maximized under small fluctuations and is some 20 orders of magnitude less than the Bekenstein-Hawking formula for a 10 solar mass black hole. Hence unlike a black hole, the new solution is thermodynamically stable and there is no information paradox.

XII.2 Facilities and Instrumentation: *New Accelerator Facilities II*

Design of the AGS Upgrade for a Broad Band Neutrino Superbeam

Deepak Raparia, T. Roser, A. Ruggiero, W. R. Weng

BNL

BNL plans to create a very long base line super neutrino beam facility by upgrading the AGS from the current 0.14 MW to 1.0 MW and beyond. The proposed facility consists of two major components. First is a 1.5 GeV superconducting linac to replace the booster as injector for the AGS, second is the performance upgrade of the AGS itself for higher intensity and repetition rate. The major contribution for the higher power is from the increase of the repetition rate of the AGS from 0.3 Hz to 2.5 Hz, with moderate increase from the intensity. The accelerator design considerations to achieve high intensity and low losses for the new linac and the AGS will be presented. The design aspect for high power operation and easy maintenance will also be covered.

U.S. Participation in the LHC – Commissioning and Upgrades

Michael J Syphers

Fermilab

The U.S. LHC Accelerator Research Program was established to enable U.S. accelerator specialists to take on active and important roles in the LHC accelerator project during its commissioning and early operations, and to be a major collaborator in future LHC performance upgrades. In particular, LARP will support U.S. institutions in LHC commissioning activities and accelerator science, accelerator instrumentation and diagnostics, and superconducting magnet R&D to help bring the LHC on and up to luminosity quickly, to help establish robust operation, and to improve and upgrade LHC performance. Furthermore, this effort will improve the capabilities of the U.S. accelerator community in accelerator science and technology to more effectively use, develop, and preserve unique U.S. resources and capabilities. In this talk the present status of LARP efforts, near-term commissioning plans, and longer-term upgrade studies will be presented.

The SuperKEKB Project

Tatsuya Kageyama
KEK

on behalf of the KEKB team.

SuperKEKB is a challenging project to explore new luminosity frontiers beyond 10^35 cm^-2 s^-1 by upgrading the KEKB collider, the asymmetric electron-positron collider currently providing the highest luminosity (1.58 x 10^34 cm^-2 s^-1) on the planet. The design luminosity of SuperKEKB is 4 x 10^35 cm^-2 s^-1, where the beam currents need to be increased up to 4.1 A and 9.4 A for the high energy ring (8 GeV) and the low energy ring (3.5 GeV), respectively. In this talk, the overall design of SuperKEKB is introduced and followed by RF and vacuum technological issues related to the high current beam.

The ultracold neutron facility at PSI, a status report

Manfred Daum
Paul Scherrer Institut

on behalf of the PSI-UCN collaboration.

A new type of ultracold neutron (UCN) source based on the spallation process is under construction at PSI. The essential elements of this source are a pulsed proton beam with highest intensity ($I_p \geq 2\,mA$) and a low duty cycle ($\sim 1\,\%$), a heavy-element spallation target, a large moderator and converter system consisting of about $4\,m^3$ of heavy water at room temperature and $30\,dm^3$ of solid Deuterium (sD_2) at a low temperature ($\sim 6\,K$) for the production of ultracold neutrons. Operating the UCN source in a pulsed mode makes it possible to hold the sD_2 at low temperatures despite the large power deposition during the beam pulse of a few seconds. Spallation neutrons are thermalized in the D_2O, further cooled in the sD_2 and finally, some of them are down-scattered into the ultra-cold neutron range ($T_{kin} \leq 250\,neV$).

For the proton beam to the new UCN source, all beam line elements are installed and operational. New boxes, with center-of-intensity and intensity distribution (beam profile) monitors, which are able to handle the full intensity of the proton beam, have been built. The read out electronics of these monitor systems was refurbished to today's standards. Furthermore, two harp monitors for measuring the beam size and intensity distribution in front of the spallation target have been built.

After the general design of the spallation target, several tests have been performed for quality control of the fabrication process. The collimator for trimming off the beam tails in front of the target is designed and in the manufacturing process; the corresponding collimator exchange mechanism for handling this element is close to completion. Finally, calculations have been performed for the use of Lead filled Zircaloy cylinders as target material. This new target layout results in an increase of neutron production of a factor of about two compared to a target made of Zircaloy.

In summary, many activities in design and construction of the UCN source components have been started. First UCN are expected at the end of 2007. The status of the source will be presented at the conference.

Deuterium for Ultra-cold Neutron Sources

Peter Fierlinger[1], F. Atchison[1], B. Blau[1], K. Bodek[2], et al.
[1]*Paul Scherrer Institut*
[2]*Jagiellonian University*

A high intensity source of ultra-cold neutrons (UCN) using a solid Deuterium (sD_2) converter is being constructed at the Paul Scherrer Institut (PSI). The performance of the source depends on the initial production rate of UCN and the efficiency of the extraction from the sD_2. The extraction depends on the lifetime of UCN in the converter and the mean free path, which results from the scattering cross section. Therefore, investigations of the interaction of slow neutrons with D_2 were performed: (i) the UCN production cross section of cold neutrons in a sD_2 converter and (ii) scattering cross sections, covering the range from cold to ultra-cold neutrons. The basic neutron-D_2 interactions were studied in gaseous, liquid and solid ortho-D_2. The UCN production mechanism could be clarified using incident polarized cold neutrons and analyzing the UCN polarization.

Diamond-like Carbon for Ultra-cold Neutrons

Peter Fierlinger, F. Atchison, T. Brys, M. Daum, et al.
Paul Scherrer Institut

As a part of the ultra-cold neutron (UCN) source project at the Paul Scherrer Institut (PSI), the performance of diamond-like Carbon (DLC) as a novel material for the storage of UCN was investigated and promising results were obtained. Neutrons with kinetic energies $<$ 300 neV are usually referred to as ultra-cold, which is in the same energy range as the Fermi pseudo potential of Beryllium, Nickel or Diamond. For UCN storage, mainly two parameters are of major concern: (i) the Fermi potential V_F, which is proportional to the bound coherent scattering length and the density of the material, (ii) the loss coefficient per wall collision η, which is related to the nuclear absorption cross section and the temperature of the material and (iii) the spin flip probability per wall collision β. The theoretical estimation for η is in the order of 1-2$\cdot 10^{-7}$ for Beryllium or Diamond at low temperatures. At room temperature the losses are dominated by inelastic energy gain during collisions at the walls. Contrary to the commonly used material Beryllium, DLC is not toxic and widely used in industry. It combines a low nuclear absorption cross section and a high density, which causes a low loss coefficient, low inelastic scattering and a large Fermi potential. We performed systematic investigations of different DLC coatings by various surface analysis methods, as well as studies using UCN. The measured values of DLC with a loss coefficient $\eta = (7 \pm 0.9) \cdot 10^{-5}$ at 70 K and a depolarization probability $\beta = (7.5 \pm 2) \cdot 10^{-7}$ are competitive to Beryllium. Using this experience, a new facility to produce high density DLC coatings is currently being built at PSI.

Tuesday, October 25th

9:00 AM–12:30 PM, Plenary Session #2

Lattice Flavourdynamics

Christopher T Sachrajda
University of Southampton

I will review recent results in flavourdynamics obtained using lattice simulations. The talk will include a survey of the current status of the computations of quark-masses and of the weak matrix elements relevant for the determination of CKM-Matrix elements. Prospects for improvements in the precision of lattice calculations and in the range of physical quantities which can be studied will be discussed.

Phases of QCD

Krishna Rajagopal
Massachusetts Institute of Technology

Search for the Quark Gluon Plasma: Status

James L Nagle
University of Colorado

We present the current status of the experimental investigation into nuclear matter at the highest possible temperatures from the Relativistic Heavy Ion Collider at Brookhaven National Laboratory. Since its commissioning in 2000, experiments BRAHMS, PHENIX, PHOBOS and STAR have published a substantial data set categorizing the nature of the matter created. There have been many surprises and a new coherent picture of hot nuclear matter is coming into focus. We will present an overview of results and how this new picture meshes with our understanding of the Quark Gluon Plasma.

Probing the Fundamental Symmetries of the Early Universe

Michael Ramsey-Musolf
Caltech

Precision tests of the symmetries of the Standard Model provide a powerful tool for probing what lies beyond it. In this talk, I review present and future symmetry tests being carried out at low energies that may provide new clues about the particle physics of the early universe. I emphasize the implications of these tests for issues left unsolved by the Standard Model, such as the nature of unification, the origin of the matter antimatter asymmetry, and the properties of the neutrino.

Search for the Electric Dipole Moment of the Electron

David DeMille
Yale University

Tests of Fundamental Symmetries with Neutrons

Bradley Filippone
California Institute of Technology

2:30–4:00 PM, Parallel Session #3

I.5 Quarks and Gluons in Hot/Cold and Dense Matter:
QGP Thermodynamics and Dense Quark Matter

Baryon-strangeness correlations as a diagnostic tool

Jorgen Randrup, Volker Koch, Abhijit Majumder
LBNL

The correlation between baryon number and strangeness, $C_{BS} = -3\sigma_{BS}/\sigma_S^2$, elucidates the nature of strongly interacting matter, such as that formed transiently in high-energy nuclear collisions. This diagnostic can be extracted from lattice QCD calculations by means of its expression in terms of flavor susceptibilities, $C_{BS} = 1 + (\chi_{us} + \chi_{ds})/\chi_{ss}$. The smallness of the mixed-flavor susceptibitities severely limits the presence of $q\bar{q}$ bound states above the critical temperature, thus supporting a mean-field picture of independent (quasi)quarks.

Susceptibilities in sQGP

Ismail Zahed
SUNY Stony Brook

I will discuss recent issues in relation to the sQGP and their relevance to the bulk susceptibilities.

QCD Thermodynamics with an almost realistic quark mass spectrum

Christian Schmidt, et al.
Brookhaven National Laboratory

on behalf of the RBC-Bielefeld collaboration.

Since finite lattice cut-off effects are particularly large at finite temperature, it is mandatory to use an improved lattice action for thermodynamic calculations. Our results are obtain with a new highly improved staggered fermion action. The dispersion relation of the action is rotational invariant up to the fourth order in the momentum ($O(p^4)$) and in addition the flavor symmetry is improved by a gauge field smearing procedure which involves three, five and seven link terms that are designed to improve flavor symmetry.

Phases of QCD: lattice thermodynamics and a field theoretical model

Claudia Ratti, Michael A. Thaler, Wolfram Weise
Physik-Department T39, Technical University Munich

We investigate three-colour QCD thermodynamics at zero and finite quark chemical potential. Our investigation is based on a synthesis of a Nambu Jona-Lasinio (NJL) model and the non-linear dynamics involving the Polyakov loop [1]. In this Polyakov-loop-extended (PNJL) model, quarks develop quasiparticle masses by propagating in the chiral condensate, while they couple at the same time to a homogeneous background (temporal) gauge field representing Polyakov loop dynamics. This so-called PNJL model thus includes features of both deconfinement and chiral symmetry restoration. The parameters of the Polyakov loop effective potential are fixed in the pure gauge sector. The chiral condensate and the Polyakov loop expectation values as functions of temperature and quark chemical potential are calculated by minimizing the thermodynamic potential of the system. The resulting equation of state, (scaled) pressure difference and quark number density at finite quark chemical potential are then confronted with corresponding Lattice QCD data [2,3]. Some of our results are shown in Fig. 1.

Bibliography

[1] C. Ratti, M. A. Thaler, W. Weise, hep-ph/0506234, Submitted to Phys. Rev. D.
[2] A. Ali Khan *et al.*, Phys. Rev. D **64**, 074510 (2001).
[3] C. R. Allton *et al.*, Phys. Rev. D **68**, 014507 (2003).

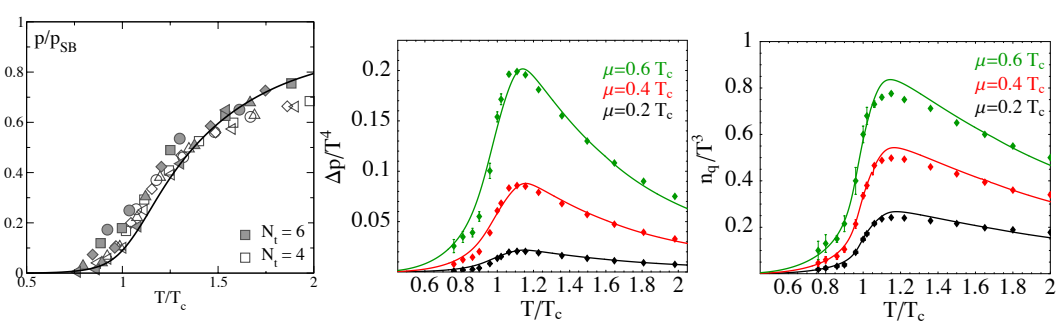

Fig. 1. Left panel: comparison between our results for the scaled pressure as a function of T/T_c at zero chemical potential, and the corresponding lattice data taken from Ref. [2]. Central panel: comparison between our results for the scaled pressure difference as a function of T/T_c at finite μ and the lattice data taken from Ref. [3]. Right panel: comparison between our results for the scaled quark number density as a function of T/T_c at finite μ, and the corresponding lattice data taken from Ref. [3].

Phase Diagram and Instability of Dense Neutral Three-Flavor Quark Matter

Kenji Fukushima
RIKEN BNL Research Center

We explore the phase diagram of dense three-flavor quark matter under color and electric neutrality conditions. On the phase diagram we identify the instability regions for each gluon in connection with the gapless color-flavor locked (gCFL) state, namely, chromomagnetic instability, that has been well investigated in the two-flavor case but is first clarified in our work for the gCFL phase. Our findings are summarized in Figs. **??**, **??**, and **??**.

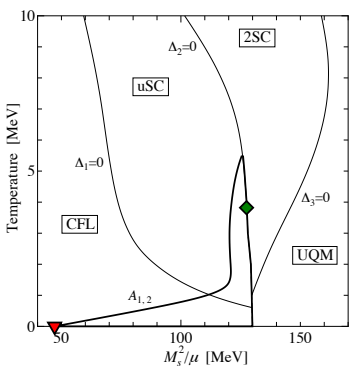

Fig. 1. Enclosed with solid thick lines is the unstable region for A_1 and A_2 on the phase diagram.

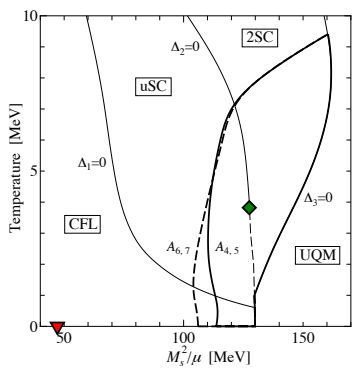

Fig. 2. Enclosed with solid and dashed thick lines are the unstable regions for A_4, A_5, and A_6, A_7 respectively.

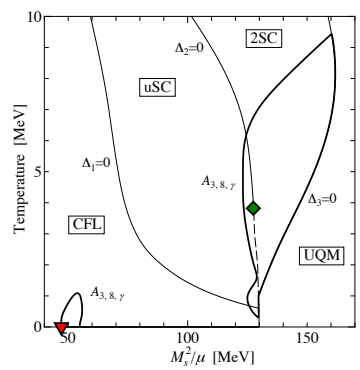

Fig. 3. Enclosed with solid thick lines is the unstable region for A_3, A_8, and A_γ.

In the region enclosed with thick lines in Fig. **??** A_1 and A_2 have imaginary Meissner masses. The instability starts at the gCFL onset and never penetrates into the 2SC phase nor unpaired quark matter (UQM). In the 2SC phase A_4, A_5, A_6, A_7 become rather unstable and this instability penetrates into the uSC and CFL sides.

The results for A_3, A_8, and A_γ (electromagnetic field) are somewhat tricky. This is because the phase diagram involves the first-order phase boundary which is model-dependent, and the gCFL always has almost quadratic dispersion relations for quark excitations. We disclose the physical origin and the mutual relationship of respective instability regions.

We also stress that these instability boundaries have definite physical meaning and can be regarded as the phase boundaries into crystalline-type color superconductivity.

Thermal unpairing transitions affected by neutrality constraints and chiral dynamics

Hiroaki Abuki, Teiji Kunihiro

Yukawa Institute for Theoretical Physics

Surprisingly rich phase structure which quark matter exhibits under high pressure are being revealed by extensive efforts. Two key ingredients whic play a crucial role for phases realized in QCD and those nature are (i) the strange quark mass, and (ii) the charge neutrality constraints in addition to the β-equilibrium condition. Some theoretical studies suggest that the effect of (ii) in the CFL phase completely cancels that of (i) down to some critical density below which a window for a novel gapless CFL (gCFL) phase opens. The neutrality constraints are also known to bring about an interesting phase even at finite temperature $(T \neq 0)$. It is shown in the Ginzburg-Landau analysis, that the d quark pairing (dSC) phase only with u-d and d-s pairings accompanied, shows up as the secondary hottest (coldest) pairing phase next to the 2SC (CFL) phase. The existence of such kind of an intermediate pairing phase has also been confirmed in the NJL model analysis.

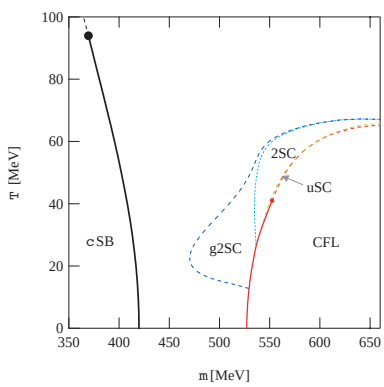

Fig. 1. Phase diagram calculated with a weak attraction in the scaler diquark (qq) channel.

In this talk, we will report our recent work [2] which is aimed at presenting a systematic and unified picture for the thermal unpairing transitions under the charge neutrality constraints. By extending the earlier work with the higher order effects of the strange quark mass on the pairing taken into account, we shall show how the window for the dSC-realizaion in the high density regime tends to close towards lower densities. In particular, it should be stressed that an analytic expression for the doubly critical point where the dSC would be energetically taken over by the u quark pairing (uSC) phase can be derived in our framework. We shall also present, how the phase structure of quark matter in (μ, T)-plane varies with changing level of coupling strength in (qq) channel (FIG. 1 is an example for a weak coupling); based on these, we shall discuss some of interesting features regarding thermal phase transitions with a special attention paid to the competition between the chiral and diquark dynamics. The talk will be based in part on [2].

1] H. Abuki and T. Kunihiro, in preparation.

2] H. Abuki, M. Kitazawa and T. Kunihiro, Phys. Lett. B **615**, 102 (2005) [arXiv:hep-ph/0412382].

I.6 Quarks and Gluons in Hot/Cold and Dense Matter:
High-pt and High-pt Correlations II

PHENIX Measurement of Particle Yields at High pT with Respect to Reaction Plane in Au+Au collisions at sqrt(s) = 200 GeV

David L Winter

Columbia University / Nevis Labs

on behalf of the PHENIX collaboration.

One of the most intriguing puzzles in RHIC physics is the origin of the azimuthal anisotropy of particle yields at high pT (> 5 GeV/c). Traditional flow and parton energy loss pictures have failed to describe the magnitude of this anisotropy. Measurement of the azimuthal asymmetry v2 at high pT will shed light on the contributions from flow, recombination, and energy loss, as well as the transition from soft to hard production mechanis ms.

The PHENIX Run4 dataset provides a powerful opportunity for exploring the angular anisotr of identified particle yields at high pT. Complementing traditional v2 measurements, we present pi0 yields as a function of angle with reaction plane, up to pT of at least 10 GeV/c. The centrality dependence of the angular anisotropy allows us to probe the density and path-length dependence of the energy loss of hard-scattered partons. We will discuss various mechanisms for particle production in this high pT region.

Systematic study of the medium modification of the away side jet in AuAu/CuCu collsions in PHENIX

Jiangyong Jia

Columbia University

on behalf of the PHENIX collaboration.

Two particle correlations in relative azimuth and pseudorapidity are an excellent probe of the dense medium created in heavy-ion collisions. Modifications of away side jet shape and strength, relative to p+p collisions, can give insight on the opacity of the medium and how the lost energy of the jet is redistributed into the medium. Detailed jet tomography study via Hadron-hadron and photon-hadron is make possible with the large AuAu dataset(> 1 billion minium bias events) and CuCu dataset (8 billion sampled minimum bias events) collected by PHENIX in 2004 and 2005.

We present the results of the di-hadron correlation in $\Delta\phi$ for both AuAu and CuCu collisions. The away side jet shape and yield from hadron-hadron and photon-hadron correlation are presented as function of centrality, trigger pT and associated hadron pT. The away side hadron - hadron correlation revealled a mach cone structure at low pT (< 4 GeV/c), as one moves to higher pT, the cone strucure is gradually filled up and a nice clean peak structure emerges for high trigger and associated hadron pT (> 5 GeV/c). We checked the robustness of this observation by studing the away side jet shape as function of the relative angle between the trigger hadron and the reaction plane. In addition to the jet shape, we also quantify the away side jet yield (I_{AA}) as function of centrality and compared between AuAu and CuCu. Although the away side jet structures are clearly visible, their magnitudes are found to be strongly suppressed in the most central AuAu and CuCu collisions. This study provide tight constraint on the opacity of the medium.

Near-side Delta eta correlations of high-pt hadrons from STAR

Joern Putschke

Lawrence Berkeley National Lab

on behalf of the STAR collaboration.

Systematic measurements of pseudorapidity (Delta eta) and azimuthal (Delta phi) correlations between high-pt charged hadrons and associated particles from the high statistics 200 GeV Au+Au and Cu+Cu datasets will be presented. In previous measurements differences in the near-side Delta Eta correlation between central Au+Au and the lighter systems d+Au and p+p were observed, including an additional long-range near-side correlation in Au+Au collisions. The near-side Delta eta correlation structure is most likely due to jet interactions with the longitudinally expanding medium. With the increased kinematic reach and statistical precision in Au+Au and Cu+Cu systematic studies of the Delta eta widths and correlated yield dependence on centrality, pt of the trigger and associated particles will be shown. In addition measurements to characterize the properties of the additional long-range correlation in Au+Au will be presented and discussed within different possible physics scenarios.

Probes of jet topology using two and three particle azimuthal correlations

Nuggehalli Ajitanand

SUNY Stony Brook

on behalf of the PHENIX collaboration.

Recent theoretical studies coupled with experimental observations have made away side jet modification a major issue in the study of medium induced effects at RHIC. In this work we present new results from the analysis of two and three particle azimuthal correlations. In particular the use of different coordinate representations (e.g. leading particle reference) tests the presence of ”Mach cone” like emissions of the away side jet fragments. The study is done as a function of event centrality for specific pt and flavor of the associated particles for both Au+Au and Cu+Cu collisons at RHIC.

Systematic Study of Azimuthal Charged Di-Hadron Correlations in Au+Au Collisions at $\sqrt{s_{NN}}$=200GeV from the STAR Experiment

Mark J Horner

Lawrence Berkeley National Laboratory

on behalf of the STAR collaboration.

Di-hadron correlations have proved to be a valuable technique to study the hot and dense medium created in AuAu collisions at RHIC through the interaction of jet fragments with the medium. Recent results show novel behaviour in azimuthally differential $< p_T >$ with respect to a high p_T trigger particle. We present here the results of a systematic study of $h^{\pm}$ azimuthal di-hadron correlations in different ranges of associated p_T correlated with a high p_T trigger particle. The data presented are from the high statistics year-4 $\sqrt{s_{NN}}$=200GeV Au+Au dataset. The results will be discussed in the context of different theoretical interpretations.

Partonic transverse momentum k_T and the fragmentation

Jan Rak

UNM

on behalf of the PHENIX collaboration.

Measurements of modifications to jet properties can give detailed information on the interactions of the outgoing parton with the dense nuclear medium and thereby on the nature of the QCD matter produced in heavy-ion collision. The method of leading high-p_T particle azimuthal correlations is used for an analysis of the π^0 fragmentation function and the partonic intrinsic momentum k_T. The potential of this method for for determination of the gluon/quark jet ratio as a function of the trigger jet momentum is discussed.

II.3 Quantum Chromodynamics: *Lattice Calculations*

Partially Quenched Chiral Perturbation Theory to NNLO

Timo Lähde

Lund University, Department of Theoretical Physics

At present, the most promising way to obtain information on low-energy hadronic observables from first principles is by means of numerical Lattice QCD simulations. However, for technical and computational reasons, simulations with dynamical sea quark masses of a few MeV cannot be performed at the present time. Rather, the physical values of the light sea quark masses have to be reached by means of a chiral extrapolation from simulations of Partially Quenched QCD (PQQCD) with sea quark masses of a few tens of MeV.

The generalization of Chiral Perturbation Theory (χPT) to the case where the sea quark masses are different from those of the valence quarks (PQχPT) provides a practical method for the extrapolation to physical quark masses from Lattice simulations of PQQCD. The low-energy constants (LEC:s) in PQχPT have a simple relation to the physically interesting LEC:s of (unquenched) χPT. Thus, once the LEC:s of PQχPT have been obtained from fits to Lattice QCD data, estimates of the physical LEC:s are also available.

The present work gives an overview of the NNLO, or two-loop calculations in PQχPT, which have been performed at Lund University during the last year. Complete results in PQχPT for the pseudoscalar meson masses and decay constants at NNLO have been obtained for 2 and 3 flavors of sea quarks. These results extend the earlier NLO work of Sharpe and Shoresh.

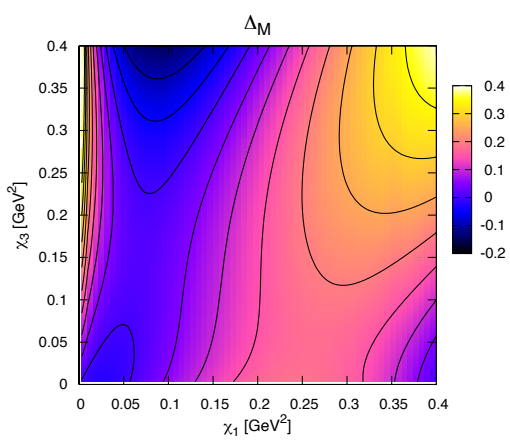

Fig. 1. The relative change in the squared pseudoscalar meson mass, with a trial set of LEC:s, to NNLO in two-flavor PQχPT, for a degenerate sea quark mass m_3 and a degenerate valence quark mass m_1. The sea and valence inputs are defined as $\chi_i = 2B_0\, m_i$.

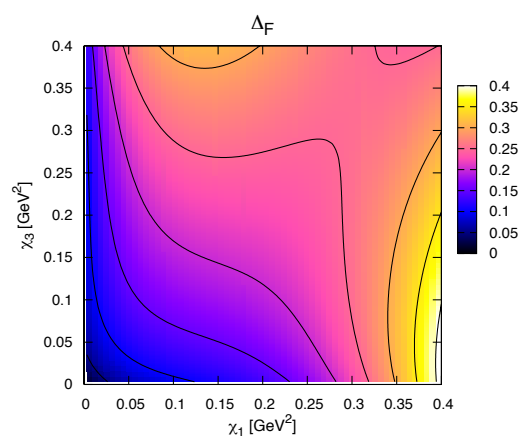

Fig. 2. The relative change in the pseudoscalar meson decay constant to NNLO in two-flavor PQχPT. Notation, definitions and LEC:s are similar to the results for the pseudoscalar meson mass.

Scaling behavior of quark propagator in full QCD

Maria B Parappilly
University Of Adelaide

on behalf of the CSSM team.

We study the scaling behavior of the quark propagator on two lattices with similar physical volume in Landau gauge with 2+1 flavors of dynamical quarks.

We use configurations generated with an improved staggered ("Asqtad") action by the MILC collaboration. The calculations are performed on a $28^3 \times 96$ lattice with a lattice spacing of $a = 0.09$ fm and on a $20^3 \times 64$ lattice with a lattice spacing of $a = 0.125$ fm. We calculate the quark mass function and wave-function renormalization function for a variety of bare quark masses. We compare the behavior of $Z(q^2)$ and $M(q^2)$ on two lattices with different lattice spacing and similar physical volume. We found that $Z(q^2)$ and $M(q^2)$ on both lattices shows good scaling behaviors.

Quark mass dependence of nucleon observables and lattice QCD

Massimiliano Procura, B. U. Musch, T. R. Hemmert, W. Weise
Physics Department, TU Munich

Lattice QCD on one side and chiral effective field theory on the other are progressively developing as important tools to deal with the nonperturbative nature of low-energy QCD and the structure of hadrons. At present, however, there is a gap between the relatively large quark masses accessible in fully dynamical lattice simulations of nucleon properties and the small quark masses relevant for comparison with physical observables. In our work we study a way to merge Chiral Perturbation Theory (χPT) which predicts the quark mass dependence of a nucleon observable and lattice simulations where the quark mass is a tunable parameter. We explore the feasibility of a systematic approach based on chiral effective Lagrangian for the extrapolation of nucleon properties from lattice QCD.
In Ref.[1] we have analyzed the quark mass, *i.e.* the pion mass expansion of the axial-vector coupling constant g_A of the nucleon. We compare two versions of nonrelativistic chiral effective field theory: one scheme restricted to pion and nucleon degrees of freedom only, and an alternative approach which incorporates explicit $\Delta(1232)$ degrees of freedom. It turns out that, in order to approach the physical value of g_A in a leading-one-loop calculation, the inclusion of the explicit $\Delta(1232)$ degrees of freedom is crucial. With information on couplings constrained from analyses of the $\pi N \to \pi\pi N$ reaction, a chiral extrapolation function $g_A(m_\pi)$ is obtained, which works well from the chiral limit across the physical point into the region of present lattice data. The outcome of Ref.[1] has been confirmed by the most recent data available.
The quark mass dependence of the nucleon mass M_N is the subject of Refs.[2,3]. An interpolation of this observable, between a selected set of fully dynamical two-flavor lattice QCD data and its physical value, is studied using manifestly covariant baryon χPT up to order p^4 in the framework of the so-called infrared regularization [4]. In order to minimize uncertainties due to lattice discretization and finite volume effects, our numerical analysis takes into account only simulations performed with lattice spacing $a < 0.15\,\mathrm{fm}$ and lattice spatial size L such that $m_\pi L > 5$. We have also restricted ourselves to data with $m_\pi < 600\,\mathrm{MeV}$ and $m_{sea} = m_{val}$. A good interpolation function is found already at one-loop level and chiral order p^3. We show that the next-to-leading one-loop corrections are small, for the whole range of quark masses that we analyze. From the p^4 numerical analysis we deduce the nucleon mass in the chiral limit, $M_0 \approx 0.88\,\mathrm{GeV}$, and the pion-nucleon sigma term $\sigma_N = (49 \pm 3)\,\mathrm{MeV}$ at the physical value of the pion mass. The inclusion of explicit $\Delta(1232)$ degrees of freedom is not essential to obtain a satisfactory description of the quark mass dependence M_N [3]. We have also performed a careful statistical analysis which confirms and sharpens our previous results and we have included finite volume effects in the expressions used in the fitting procedure [3].

[1] T. R. Hemmert, M. Procura and W. Weise, Phys. Rev. **D68**, 075009 (2003).

[2] M. Procura, T. R. Hemmert and W. Weise, Phys. Rev. **D69**, 034505 (2004).

[3] M. Procura, B. U. Musch, T. Wollenweber, T. R. Hemmert and W. Weise, *forthcoming*.

[4] T. Becher and H. Leutwyler, Eur. Phys. J. **C9**, 643 (1999).

f_D and f_{D_s} in lattice QCD with exact chiral symmetry

Ting-Wai Chiu, et al.
Physics Department, National Taiwan University

We determine the masses and decay constants of pseudoscalar mesons D, D_s, and K in quenched lattice QCD with exact chiral symmetry. For 100 gauge configurations generated with single-plaquette action at $\beta = 6.1$ on the $20^3 \times 40$ lattice, we compute point-to-point quark propagators for 30 quark masses in the range $0.03 \leq m_q a \leq 0.80$, and measure the time-correlation functions of pseudoscalar and vector mesons. The inverse lattice spacing a^{-1} is determined with the experimental input of f_π, while the strange quark bare mass $m_s a = 0.08$, and the charm quark bare mass $m_c a = 0.80$ are fixed such that the masses of the corresponding vector mesons are in good agreement with $\phi(1020)$ and $J/\psi(3097)$ respectively. Our results of pseudoscalar-meson decay constants are $f_K = 152(6)(10)$ MeV, $f_D = 235(8)(14)$ MeV, and $f_{D_s} = 266(10)(18)$ MeV.

Multi-Quarks and Two-Baryon Interaction in Lattice QCD

Hideo Suganuma[1], Takumi Doi[2], Fumiko Okiharu[3], Toru T. Takahashi[4]

[1]*Department of Physics, Kyoto University*
[2]*RIKEN-BNL Research Center, BNL*
[3]*Department of Physics, Nihon University*
[4]*Yukawa Institute for Theoretical Physics, Kyoto University*

We perform the detailed studies of the three-quark (3Q) potential [1,2], the tetra-quark (4Q) potential [3] and the penta-quark (5Q) potential [4] in SU(3) lattice QCD. The 3Q potential is found to be well described by the Y Ansatz [1,2]: the sum of the Coulomb term and the Y-type linear term based on the flux-tube picture. Actually, the 3Q potential subtracted by the Coulomb part is proportional to Y-shaped flux-tube length L_{min} as shown in Fig.1 [3].

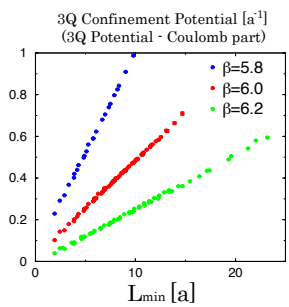

Fig. 1. 3Q confinement potential V_{3Q}^{conf}, i.e., 3Q potential subtracted by the Coulomb part, plotted against Y-shaped flux-tube length L_{min} in lattice unit.

We perform the first study of the multi-quark potential in lattice QCD [3,4] to clarify the inter-quark interaction in multi-quark systems. The 5Q potential V_{5Q} for the QQ-$\bar{Q}$-QQ system is found to be well described by the "OGE Coulomb plus multi-Y Ansatz" [4]: the sum of the one-gluon-exchange (OGE) Coulomb term and the multi-Y-type linear term based on the flux-tube picture. The 4Q potential V_{4Q} for the QQ-$\bar{Q}\bar{Q}$ system is also described by the OGE Coulomb plus multi-Y Ansatz [3], when QQ and $\bar{Q}\bar{Q}$ are well separated. We observe a lattice-QCD evidence for the "flip-flop", i.e., the flux-tube recombination between the connected 4Q state and the "two-meson" state [3].

We study also the nuclear force, i.e., the interaction between two nucleons, in SU(3) lattice QCD at the quenched level. These lattice-QCD studies give an important bridge between elementary particle physics and nuclear physics.

1. T.T. Takahashi, H. Matsufuru, Y. Nemoto and H. Suganuma, *Phys. Rev. Lett.* **86** (2001) 18; *Phys. Rev.* **D65** (2002) 114509.
2. T.T. Takahashi and H. Suganuma, *Phys. Rev. Lett.* **90** (2003) 182001; *Phys. Rev.* **D70** (2004) 074506.
3. F. Okiharu, H. Suganuma, T.T. Takahashi, *Phys. Rev.* **D72** (2005) 014505.
4. F.Okiharu, H.Suganuma, T.T.Takahashi, *Phys. Rev. Lett.* **94** (2005) 192001.

Nuclear Force in Lattice QCD

Toru T. Takahashi[1], Takumi Doi[2], Hideo Suganuma[3]

[1] *Yukawa Inst. for Theor. Phys., Kyoto Univ.*
[2] *RIKEN-BNL Research Center, BNL, Upton, New York 11973, USA*
[3] *Department of Physics, Kyoto University, Kyoto 606-8502, Japan*

The nuclear force, i.e., the interaction between two nucleons, is one of the most fundamental quantities in nuclear physics. While its long-distance part is understood by the light meson-exchange process proposed by Yukawa about 70 years ago, its short-distance part has been treated phenomenologically from the experimental data and is still mysterious at the level of quarks and gluons, more fundamental degrees of freedom in the strong interaction.

In the spirit of the elementary particle physics, it is desired to comprehend nuclear physics in terms of QCD, the underlying theory of the strong interaction. Among theoretical approaches, the lattice QCD calculation is considered as the most reliable nonperturbative method, which is called a ”numerical experiment”. In contrast to many studies on the hadron spectroscopy, there have been however a few lattice QCD studies on hadronic interactions.

In this paper, we aim to understand the nuclear force (inter-baryon force) directly based on QCD. We investigate the nuclear force, especially its repulsive core, using quenched lattice QCD as a successive work of the detailed lattice-QCD studies of the three-quark potential [1,2], the tetra-quark potential [3] and the penta-quark potential [4]. We also evaluate the contribution to the nuclear force from each Feynman diagram such as the quark-exchange diagram individually, which enables us to single out the effects of Pauli principle or quark exchanges and to extract the essence of the nuclear force. This lattice-QCD work is expected to give an important bridge between elementary particle physics and nuclear physics.

References

1. T.T. Takahashi, H. Matsufuru, Y. Nemoto and H. Suganuma,
Phys. Rev. Lett. **86** (2001) 18; *Phys. Rev.* **D65** (2002) 114509.
2. T.T. Takahashi and H. Suganuma, *Phys. Rev. Lett.* **90** (2003) 182001;
Phys. Rev. **D70** (2004) 074506.
3. F. Okiharu, H. Suganuma, T.T. Takahashi, *Phys. Rev.* **D72** (2005) 014505. 4. F.Okiharu, H.Suganuma, T.T.Takahashi, *Phys. Rev. Lett.* **94** (2005) 192001.

III.5 Nucleon Structure: *Flavor Decomposition and GPDs*

Measurement of ΔS in the nucleon at HERMES from semi-inclusive DIS

Harold E Jackson, Jr

Argonne National Laboratory

on behalf of the HERMES collaboration.

The polarization of the strange quarks in the proton is of particular interest, because an explanation of the small net contribution to the nucleon spin from the quark spins under the assumption of SU(3) symmetry implies a significant negative value for this quantity. Such a value would explain the violation of the Ellis-Jaffe sum rule in inclusive DIS. However, recent results from HERMES for a flavor decomposition of quark helicity distributions based on semi-inclusive DIS(see Fig.1) suggest that the strange sea polarization is zero.

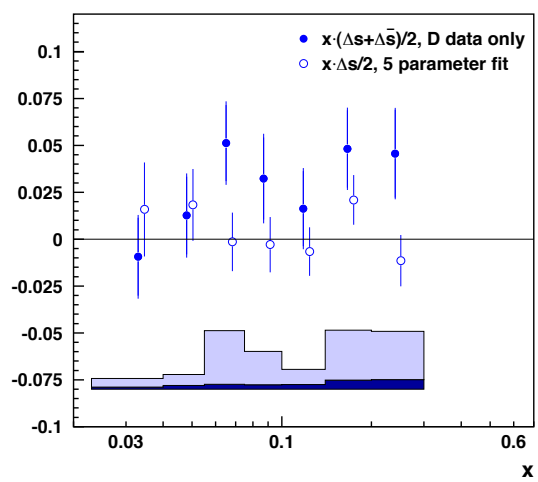

Fig. 1. The measured strange quark helicity density $x \cdot [\Delta s(x) + \Delta \bar{s}(x)]/2$.For comparison the open symbols denote the results from a five parameter fit to proton and deuteron data. The band in the bottom part gives the total systematic uncertainty on the results from the isoscalar extraction including(light shaded area) the uncertainty in fragmentation functions extrapolated from higher energies.

The total strange quark helicity density $\Delta S(x) \equiv \Delta s(x) + \Delta \bar{s}(x)$ carries no isospin. It can be extracted from measurements of scattering off of deuterium alone which is isoscalar. Effectively, measurements of the inclusive spin asymmetries provide an estimate of the helicity density of the non-strange sea. Using the spin asymmetries measured for charged kaons as the second experimental data set it is possible to extract directly $\Delta S(x)$. Furthermore, by measuring the charged kaon multiplicities at HERMES kinematics, the fragmentation functions relevent to the extraction procedure can be obtained without resort to other experiments. Because only the more recently acquired deuterium data base is used, the analysis can be carried out with higher statistics than that used in the analysis of Fig.1. Aside from that of isospin symmetry between the proton and the neutron, the only assumption made in this analysis is charge-conjugation invariance, No Monte-Carlo simulations of the fragmentation process are required. The results of a direct leading-order extraction of $\Delta S(x)$ using this approach will be presented.

Global analysis for determining polarized parton distribution functions in the nucleon

S. Kumano[1], M. Hirai[1], N. Saito[2]

[1]*IPNS, KEK, 1-1, Ooho, Tsukuba, Ibaraki, 305-0801, Japan*
[2]*Department of Physics, Kyoto University, Kyoto, 606-8502, Japan*

on behalf of the Asymmetry analysis collaboration.

Polarized parton distribution functions (PDFs) in the nucleon are determined by a global χ^2 analysis of polarized electron and muon scattering data. Here, we report the studies of the Asymmetry Analysis Collaboration (AAC) [1,2]. The first AAC parametrization was proposed in Ref. [1]. In the second version [2], additional data are included in the analysis data set, uncertainties of the polarized PDFs are estimated, and error-correlation effects are investigated between polarized antiquark and gluon distributions. The polarized PDFs are determined by analyzing the data on the spin asymmetry A_1. Then, their uncertainties are estimated by the Hessian method. The asymmetry A_1 is expressed in terms of the polarized structure function g_1, the unpolarized structure function F_2, and the longitudinal-transverse structure function ratio R: $A_1(x, Q^2) = g_1(x, Q^2) 2x[1 + R(x, Q^2)]/F_2(x, Q^2)$. The SLAC analysis results are used for the function $R(x, Q^2)$. The function $F_2(x, Q^2)$ is calculated by the GRV98 parametrization for the unpolarized PDFs. The function g_1 is calculated by the polarized PDFs with a number of parameters, which are determined by the χ^2 analysis.

Analysis results are shown in Fig. 1 for the polarized PDFs at Q^2=1 GeV^2. The dotted curves indicate uncertainties for the AAC00 parametrization [1], and the shaded areas are for the recent one [2]. One of the major differences between the two data sets is the addition of the SLAC-E155 proton data in Ref. [2]. The figure illustrates how the accurate E155 data improve the determination of each PDF. It is interesting to note that the gluon uncertainties are also reduced, and it should come from an error correlation between antiquark and gluon distributions. In order to discuss such a correlation, we also show global analysis results with the condition $\Delta g(x) = 0$ at the initial scale, $Q^2 = 1$ GeV^2. Recently, our analysis is in progress with an updated data set by adding new data from JLab, COMPASS, and HERMES.

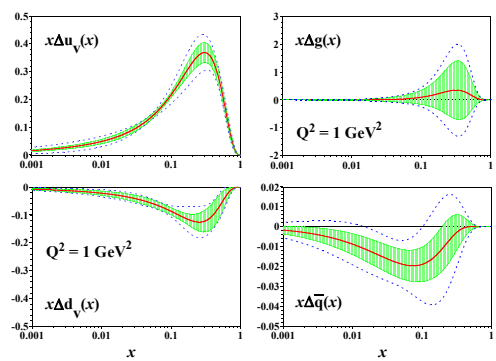

Figure 1. Polarized PDFs Δu_v, Δd_v, $\Delta\bar{q}$, and Δg and their uncertainties are are shown at Q^2=1 GeV^2 [2].

References

[1] Y. Goto *et al.* (AAC), Phys. Rev. D62 (2000) 034017.

[2] M. Hirai, S. Kumano, and N. Saito (AAC), Phys. Rev. D69 (2004) 054021.

Opportunities with Drell-Yan scattering: Probing the sea quark distributions of the proton

Paul E. Reimer

Argonne National Laboratory

on behalf of the Fermilab E866/E906 collaboration.

The Drell-Yan mechanism offers a unique, selective probe of antiquarks in the nucleon. This probe was successfully exploited by Fermilab E866 to explore the origins of the nucleon sea by measuring the ratio of $\bar{d}(x)/\bar{u}(x)$ in the proton and by Fermilab E772 to look for the effects of nuclear pions. Both experiments yielded very surprising results. Fermilab has approved a new Drell-Yan experiment, E906, that will investigate both of these results with significantly better resolution and kinematic reach.

With only $1/3$ of the proton's momentum carried by its valence quarks and the remainder carried by the sea quarks and gluons, the origin of the sea is remarkable in how poorly it is understood. The large $\bar{d}(x)/\bar{u}(x)$ ratio observed by E866 convincingly demonstrated that the sea is not simply a result of pQCD, but neither could meson cloud models fully explain the observed kinematic dependence. The data from E906 will probe this distribution more completely, especially into the large-x region which was inaccessible to earlier experiments.

When the proton is contained in a nucleus, the proton's parton distributions, as measured by DIS experiments, appear to be modified. Drell-Yan, with the ability to selectively view the antiquark distributions, is an ideal tool to study this effect. Because pions in meson exchange models of nuclear binding lead to an enhancement of the antiquark distributions, similar effects were expected in Drell-Yan. Fermilab E772, however, did not see this effect. Since E772, the expectations from theory have been revised to be within the uncertainty of the E772 data. The upcoming Drell-Yan experiment will be able to provide much more precise measurement over a wider kinematic range to guide and challenge the theoretical expectations.

In addition to probing the properties of the target nucleon, Drell-Yan can be used to study properties of the partons in the incoming beam. These properties include the energy loss of partons in cold nuclear matter and the high-x parton distribution in the beam proton.

This talk will discuss the results of the previous Drell-Yan experiments, and then compare these results with what we will learn from Fermilab E906.

Spin Physics with W's at RHIC

Ernst P Sichtermann

Lawrence Berkeley National Laboratory

on behalf of the STAR and Phenix collaborations collaboration.

The spin physics program at the Relativistic Heavy Ion Collider (RHIC) at Brookhaven National Laboratory presents a unique opportunity to measure, at hard scales and with high accuracy, the contributions from the light quark and anti-quark spins to the proton spin. These future measurements will be made at a center of mass energy of 500 GeV and make use of helicity properties in weak boson production. The (anti-)quark contributions can be flavor separated by determining the charge and momentum of the leptons from W boson decays in the central and forward rapidity regions.

The capabilities at RHIC with the current detector configuration and future upgrades will be discussed.

New results on Deeply Virtual Compton Scattering at HERMES

Elke C. Aschenauer
DESY

on behalf of the HERMES collaboration.

Recent theoretical progress in studying the internal structure of the nucleon is mostly related to exclusive reactions and their description in terms of generalized parton distributions (GPDs). This theoretical framework takes into account the dynamical correlations between partons of different momenta in the nucleon. The well-known parton distribution functions and form factors turn out to be the limiting cases and moments of GPDs. Of particular interest is the second moment of two unpolarized quark GPDs, which for the first time offers a possibility to determine the total angular momentum carried by the quarks in the nucleon.

We report our latest observations of azimuthal asymmetries in the hard electroproduction of real photons, the so-called deeply virtual Compton scattering (DVCS) process, with respect to the spin and the charge of the incoming lepton beam or with respect to the spin of the target. In particular the observation of a target spin asymmetry for a transversely polarized hydrogen target is reported for the first time. The asymmetries are attributed to the interference between the Bethe-Heitler process and the DVCS process, which gives access to the latter at the amplitude level. The DVCS process appears to be the theoretically cleanest way to access GPDs. All the data have been accumulated by the HERMES experiment at DESY, scattering the HERA 27.6 GeV electron/positron beam off proton, deuterium, neon, krypton and Xenon gas targets.

Exclusive Meson Production at Hermes

Jeroen Dreschler
NIKHEF

on behalf of the HERMES collaboration.

Exclusive electroproduction of pions and vector mesons has been measured on internal hydrogen and deuterium gas targets at HERMES using the 27.6 GeV positron beam of HERA. From these processes, more information can be obtained about generalized parton distributions (GPDs), which provide a unified description of the structure of hadrons. Preliminary results for the total π^+ production cross section and earlier measurements of the cross sections for exclusive vector meson production are shown and compared with GPD based calculations. The transverse target spin asymmetry A_{UT} in exclusive ρ^0 production has been measured. This is an observable sensitive to the GPD E^q and hence, in conjunction with the GPD H^q, to the total quark angular momentum. Preliminary results for A_{UT} are shown.

IV.5 Hadrons, Nuclei, Hypernuclei - Light Quarks: *Strange Quarks*

Study of pentaquark and $\Lambda(1405)$

Hidekatsu Nemura[1], Choki Nakamoto[2]

[1]*Advanced Meson Science Laboratory, DRI, RIKEN*
[2]*Suzuka National College of Technology*

Recent experimental report[1] on a new observation of strange tribaryon $S^0(3115)$ has had a significant impact on nuclear physics. The existence of deeply bound $\bar{K}$-nuclear systems has been predicted by Akaishi and Yamazaki[2], based on an assumption of $\Lambda(1405)$ being a bound state of $\bar{K}+N$. However, the $S^0(3115)$ is different from that was originally predicted since the isospin ($I=1$) of $S^0(3115)$ determined by the isospin conservation does not match the isospin ($I=0$) predicted by the theory. Moreover, the mass of $S^0(3115)$ is about 100 MeV lighter than the value by the theoretical prediction.

The $\Lambda(1405)$, $J^\pi = \frac{1}{2}^-$, has the smallest mass in the negative parity states of the baryon spectrum. Several constituent quark-model studies have been mentioning that the contribution of $(q^4\bar{q})$ configurations could be large in the $\Lambda(1405)$[3,4]. Here all of the five quarks may occupy their lowest $(0s)^5$ orbits, since an antiquark has the intrinsic negative parity. If we assume that the flavor $SU(3)$ is an exact symmetry, we found that two kinds of the $(q^4\bar{q})$ states for $\Lambda(1405)$,

$$\Psi(\Lambda(1405)) = [5]_R[222]_C[222]_F[32]_S, \tag{1}$$

(Subscripts (RCF and S) stand for the position coordinates, color, flavor and spin space, respectively.) give strongly attractive color-magnetic interactions:

$$\left\langle \sum_{i<j} (\boldsymbol{\lambda}_i^c \cdot \boldsymbol{\lambda}_j^c)(\boldsymbol{\sigma}_i \cdot \boldsymbol{\sigma}_j) \right\rangle = \begin{cases} 16 & (\text{ for } [22]_S \text{ for } (q^4)), \\ 80/3 & (\text{ for } [31]_S \text{ for } (q^4)), \end{cases} \tag{2}$$

which make lower the mass calculated for the $(q^4\bar{q})$ state than that given for the (q^3).

Towards a description of the strange tribaryon, as a first step, the purpose of this study is to describe a five-body calculation of pentaquark for $\Lambda(1405)$ by using the stochastic variational method[5,6].

References

1. T. Suzuki *et al.*, Phys. Lett. **B 597**, 263 (2004).
2. Y. Akaishi and T. Yamazaki, Phys. Rev. C **65**, 044005 (2002).
3. F. Brau, C. Semay and B. Silvestre-Brac, Phys. Rev. C **66**, 055202 (2002).
4. C. Helminen and D. O. Riska, Nucl. Phys. A **699**, 624 (2002).
5. H. Nemura, Y. Akaishi and Y. Suzuki, Phys. Rev. Lett. **89**, 142504 (2002).
6. H. Nemura *et al.*, Phys. Rev. Lett. **94**, 202502 (2005).

Experimental study of strange tribaryons in the ^{4}He(K^-_{stop}, p) reaction

Masaharu Sato
Tokyo Institute of Technology

on behalf of the KEK PS-E549 collaboration.

Our recent experiment performed at KEK (KEK-PS E471) has observed a distinct peak structure in the ^{4}He(K^-_{stop}, p) spectrum. This state is unexpected, which we denoted as strange tribaryon $S^0(3115)$ with the charge 0 and the total isospin 1 [1].

For the confirmation and further study of this state, recently we have carried out a new experiment at KEK (KEK PS E549 experiment). The goals of the E549 experiment are;

1. inclusive spectroscopy of the ^{4}He(K^-_{stop}, p) at high statistics,
2. determination of the width and the formation ratio of S^0 state, and
3. search for excited states of S^0.

In the e549 experiment, we installed new tracking devices and TOF start and stop counters for the proton measurement which enables us to measure the proton with high resolution under the inclusive condition. As the result of this improvement, we have achieved 2$\sim$3 times better resolution and about 10 times higher statistics. We also enlarged the momentum acceptance of the proton by minimizing the material between TOF counters, so that we can search for excited state of the S^0.

Data was taken for about one month from the end of this May and data analysis is in progress. At this conference, preliminary results from the ^{4}He(K^-_{stop}, p) reaction will be presented.

[1]. T.Suzuki et al., Phys. Lett. B 597(2004)263

[2]. M.Iwasaki et al., Nucl. Instr. Meth. A473, (2001)286

Lambda(1520) and Sigma(1385) in the nuclear medium

Murat M. Kaskulov, E. Oset
Universidad de Valencia − CSIC and IFIC

Recent studies of the Lambda(1520) resonance within chiral unitary theory with coupled channels find the resonance as a dynamically generated state from the interaction of the decuplet of baryons and the octet of mesons, essentially a quasibound state of the pion and Sigma(1385) in this case. This decay channel of the Lambda(1520) is forbidden in free space for the nominal mass of the Sigma(1385), but the coupling of the pion to p–h components in the nuclear medium opens new decay channels of the Lambda(1520) in the nucleus and produces a width more than five times bigger than the free one. We perform the calculations by dressing simultaneously the Lambda(1520) and the Sigma(1385) resonances, finding moderate changes in the mass but substantial ones in the width of both resonances.

Chiral dynamics of the $\Lambda(1520)$ in coupled channels tested in the $K^-p \to \pi\pi\Lambda$ reaction

Sourav Sarkar
IFIC, University of Valencia, Spain

The $\Lambda(1520)$ resonance is studied in a chiral coupled channel approach. This resonance appears as dynamically generated from the interaction of the decuplet of baryons and the octet of mesons in s-wave. Its treatment is improved greatly with the phenomenological inclusion of the $\bar{K}N$ and $\pi\Sigma$ channels in d-wave and the experimental mass and decay width of the $\Lambda(1520)$ are obtained accurately. Since the most important building block in the $\Lambda(1520)$ appears to be the $\pi\Sigma^*$ channel, we study the $K^-p \to \pi\Sigma^*(\pi\Lambda)$ reaction in the region of the $\Lambda(1520)$ and above, and compare the results with recent experimental data. With the coupling of the $\Lambda(1520)$ to the $\pi\Sigma^*$ channel predicted by the theory we find a cross section in good agreement with the data and there is as well agreement for the invariant mass distributions which show a neat peak for the Σ^* in the $(\pi\Lambda)$ spectrum. We also show the consistency of the results with the partial wave amplitudes of the $\bar{K}N \to \bar{K}N$ and $\bar{K}N \to \pi\Sigma$ in $I = 2$.

Θ^+ and $\Lambda(1520)$ production in pp reactions at high energies

Ilya Narodetskiy
ITEP

We estimate the production cross sections of various hyperons at high energies. Using the K exchange model we perform a comparative study of the Θ^+ and $\Lambda(1520)$ production in inclusive proton-proton reactions pp $\to$ Θ^+X and pp $\to$ $\Lambda(1520)X$ at high energies. Assuming that $J^P(\Theta^+) = \frac{1}{2}^+$ we obtain

$$\frac{d\sigma}{dxdk_\perp^2}(pp \to \Theta^+X) = \frac{1}{4\pi}\frac{G^2_{\Theta KN}}{4\pi}\sqrt{\frac{\lambda(s_1, q^2, m_p^2)}{\lambda(s, m_p^2, m_p^2)}} \cdot \frac{p}{E_\theta} \cdot \varphi(q^2)F^4(q^2) \cdot \sigma^{tot}_{K^0p}(s_1, q^2), \quad (1)$$

where $x = p_{\Theta\|}/p$ ($p(\sqrt{s})$ is the initial proton momentum in the center-of-mass frame), $k_\perp^2$ is the transverse Θ^+ momentum squared, $G^2_{\Theta KN}/4\pi = 0.16 \cdot \Gamma_{\Theta\ KN}/1$ MeV, $\sqrt{\frac{\lambda(s_1,q^2,m_p^2)}{\lambda(s,m_p^2,m_p^2)}}$ is the ratio of flux factors in the pp and K_0p reactions,

$$\varphi(q^2) = \frac{(m_p - m_\theta)^2 - q^2}{(q^2 - m_K^2)^2}, \quad (2)$$

and $F(q^2)$ is the form factor taken from the study of exclusive reactions. For the pp $\to$ $\Lambda(1520)X$ reaction we obtain

$$\frac{d\sigma}{dxdk_\perp^2} = \frac{1}{4\pi} \cdot \frac{G^2_{\Lambda NK}}{4\pi}\sqrt{\frac{\lambda(s_1, q^2, m_p^2)}{\lambda(s, m_p^2, m_p^2)}} \cdot \frac{p}{E_\Lambda} \cdot \varphi(q^2) \cdot F^4(q^2) \cdot \frac{\lambda(m_\Lambda^2, m_p^2, q^2)}{6m_\Lambda^2 m_K^2} \cdot \sigma^{tot}_{K^0p}(s_1, q^2), (3$$

where

$$\Gamma_{\Lambda(1520)} = \frac{G^2_{\Lambda NK}}{4\pi} \cdot \frac{\lambda(m_\Lambda^2, m_p^2, m_K^2)^{3/2}}{48 m_K^2 m_\Lambda^5}[(m_\Lambda - m_p)^2 - m_K^2] \quad (4)$$

Using the fact that $\sigma_{tot}(K^0p)$ is approximately constant ($\sim$ 20 mbarn) up to logarithms at $\sqrt{s} \gtrsim$ 10 GeV we obtain $\sigma(pp \to \Theta^+X) \sim 0.8$ μbarn. For the pp $\to$ $\Lambda(1520)X$ reaction we use the Rarita-Schwinger vector-spinor formalism to treat the spin 3/2 $\Lambda(1520)$ relativistically. IN this way we obtain sigma($pp \to \Lambda(1520)^+X$) $\sim$ 25 μbarn

We also extend our calculations to include K^* exchange. The contribution due to the K^* exchange is estimated as

$$\sigma(pp \to \Theta^+X) \sim 50 \text{ nbarn}, \quad \sigma(pp \to \Lambda(1520)^+X) \sim 90 \text{ nbarn} \quad (5)$$

A rough estimate of possible interference effects between the diagrams with K and K^* exchanges yields our final estimate

$$\sigma(pp \to \Theta^+X) \sim 0.8 \pm 0.2\ \mu\text{barn}, \quad \sigma(pp \to \Lambda(1520)^+X) \sim 25 \pm 2\ \mu\text{barn} \quad (6)$$

Anisotropic lattice QCD studies of penta-quarks and tetra-quarks

Noriyoshi Ishii[1], Takumi Doi[2], Hideaki Iida[3], Yukio Nemoto[4]

[1]*Department of Physics H-27, Tokyo Institute of Technology*
[2]*RBRC, Brookhaven National Laboratory, USA*
[3]*Department of Physics H-27, Tokyo Institute of Technology, Japan*
[4]*Department of Physics, Nagoya University, Japan*

Anisotropic lattice QCD studies of the penta-quark(5Q) with the quantum numbers, $J^P = 1/2^\pm$ and $3/2^\pm$ together with tetra-quarks(4Q) are presented at the quenched level. We use the standard gauge action at $\beta = 5.75$ on the anisotropic lattice with the renormalized anisotropy $a_s/a_t = 4$ and the $O(a)$ improved quark (Clover) action with $\kappa = 0.1410(0.010)0.1440$. To distinguish a compact 5Q resonance from an NK scattering state, we propose a new method of "*hybrid boundary condition (HBC)*", which is a flavor dependent spatial BC to raise the NK and NK* thresholds by $200 - 300$ MeV in the spatial lattice of the size $L \sim 2$ fm.

We first consider the $J^P = 1/2^\pm$ penta-quarks employing the diquark-type interpolating field using 504 gauge configurations [1]. For $J^P = 1/2^-$, we obtain $m_{5Q} \simeq 2.25$ GeV, which is too heavy to be identified as $\Theta^+(1540)$. For $J^P = 1/2^+$, we obtain $m_{5Q} \simeq 1.75$ GeV. Although it is close to the empirical value, the analysis with HBC shows that it is an NK scattering state, which cannot be identified as $\Theta^+(1540)$.

We next consider the $J^P = 3/2^\pm$ penta-quarks using a large number of gauge configurations as $N_{conf} = 1000$ employing three Rarita-Schwinger interpolating fields, (a) the NK*-type, (b) the color-twisted NK*-type and (c) a diquark-type [2]. Note that the spin of Θ^+ has not yet determined experimentally, and that the $J^P = 3/2^-$ assignment provides a possible solution to the puzzle of the narrow decay width of Θ^+. Thus it is one of the important candidates of the quantum number of $\Theta^+(1540)$. After chiral extrapolations, we obtain only massive states, i.e., $m_{5Q} \simeq 2.4 - 2.6$ GeV for $J^P = 3/2^+$, and $m_{5Q} \simeq 2.1 - 2.2$ GeV for $J^P = 3/2^-$. In addition, the HBC analysis shows that these 5Q states are not compact 5Q resonances.

Tetra-quarks(4Q) are another interesting exotic hadrons other than the penta-quarks. There are a series of scalar mesons known as the scalar nonet, i.e., $f_0(600)$, $\kappa(800)$, $f_0(980)$ and $a_0(980)$, whose structures and mass spectrum are naturally understood as bound states of a diquark and an anti-diquark rather than conventional $q\bar{q}$'s. In addition, a recently discovered charmed meson $D_s(2317)$ is considered to be another candidate of a tetra-quark. We consider these exotic tetra-quark states presenting our preliminary anisotropic lattice QCD results using the HBC method [3].

ferences

[1] N. Ishii, T. Doi, H. Iida, M. Oka, F. Okiharu, H. Suganuma, Phys. Rev. **D71**, 034001 (2005).
[2] N. Ishii, T. Doi, Y. Nemoto, M. Oka, H. Suganuma, hep-lat/0506022.
[3] H.Suganuma, N.Ishii, F.Okiharu, K.Tsumura, A talk given at Lattice 2005, Jul. 2005, Dublin, Ireland.

V.3 Heavy Flavor Physics - Search for New Particles: *Quarkonium Physics*

Recent developments in the modeling of heavy quarkonia

Stanley F Radford[1], Wayne W. Repko[2]

[1]*Department of Physics , Marietta College*
[2]*Department of Physics and Astronomy, Michigan State University*

We examine the spectra and radiative decays of the charmonium and bottomium systems using a model which incorporates the complete one–loop spin–dependent perturbative QCD short distance potential plus a linear confining term including (spin–dependent) relativistic corrections to $O(v^2/c^2)$, and a fully relativistic treatment of the kinetic energy. We compare the predictions of this model to experiments, including states and decays recently measured at Belle, BaBar, CLEO and CDF. The results of these comparisons allow a discussion of the spin–dependence of the long–range potential. We also discuss the behavior of the wave functions and decay widths in response to perturbative and non–perturbative treatments of the spin–dependent terms.

Fragmentation, NRQCD and Factorization in Heavy Quarkonium Production

Gouranga C. Nayak[1], Jian-Wei Qiu[2], George Sterman[1]

[1]*C.N. Yang Institute for Theoretical Physics, Stony Brook University, SUNY, Stony Brook, NY 11794, USA*
[2]*Department of Physics and Astronomy, Iowa State University, Ames, IA 50011, USA*

We study factorization in heavy-quarkonium production in high energy collisions using NRQCD. We find uncancelled infrared divergences at NNLO which are not matched by conventional NRQCD matrix elements. However, we show that gauge invariance and factorization require that conventional NRQCD production matrix elements be modified to include Wilson lines or non-abelian gauge links. With this modification NRQCD factorization for heavy quarkonium production is restored at NNLO.

Bottomonium Spectrum and Decays

David Besson
University of Kansas

on behalf of the CLEO collaboration.

$\psi(3770)$ non-$\bar{D}D$ Decays

Hajime Muramatsu
Cornell

on behalf of the CLEO collaboration.

ψ(2S) and J/ψ results from CLEO

Guangshun Huang
Purdue University

on behalf of the CLEO collaboration.

---

h_c discovery and $\Gamma(\gamma\gamma)$ χ_{c2} from CLEO

Kam Seth
Northwestern University

on behalf of the CLEO collaboration.

VI.3 Fundamental Symmetries: *Charm Mixing, Bs Mixing, and Lepton Flavor Violation*

Constraints on Charm Mixing and Doubly-Cabibbo Suppressed Decays

Werner Sun
Cornell

on behalf of the CLEO collaboration.

Due to the quantum correlation between D^0 and $\bar{D}^0$ from the $\psi(3770)$, the time-integrated single and double tag decay rates depend on charm mixing amplitude, doubly Cabibbo suppressed amplitudes and the relative strong phase δ between D^0 and $\bar{D}^0$. Using the $\sim 300\text{pb}^{-1}$ collected with the CLEO-c detector at $\psi(3770)$ energy, we measure the absolute branching fraction of D^0 decays to hadronic flavor states, CP eigenstates and semileptonic final states to determine the relative strong phase $\cos\delta$ and limit the mixing amplitude y.

Charm Mixing at Babar

Ray F Cowan
MIT

on behalf of the BABAR collaboration.

The Babar experiment at the PEP-II asymmetric storage ring offers excellent opportunities in charm physics. We present an investigation of $D\bar{D}$ oscillations using hadronic and semileptonic D decays.

CLEO results on $\tau^+\tau^-$ and LFV decays of $\Upsilon(1,2,3S)$

Istvan Danko
RPI

on behalf of the CLEO collaboration.

CLEO is putting its large $\Upsilon(1,2,3S)$ data samples to use to set limits on Beyond The Standard Model effects in Υ decay. Two examples will be discussed: 1. We report on measurements of $B(\Upsilon(1,2,3S) \to \tau^+\tau^-$, with the first observation in the case of $\Upsilon(3S)$ and the first precision measurement in the case of $\Upsilon(2S)$, where the yields of these decays relative to those for $\Upsilon(1,2,3S) \to \mu^+\mu^-$ imply important lepton universality limits in the Υ sector. 2. We present the first search for Lepton Flavor Violation (LFV) in the decays of $\Upsilon(1,2,3S)$ resonances. We discuss the analysis technique, Monte Carlo simulation studies, the background calibration method based on data, and preliminary results of our analysis.

Search for B_s^0 Oscillations

Stephanie Menzemer
MIT

on behalf of the CDF collaboration.

We report on a search for B_s^0 oscillations using data from $p\bar{p}$ collisions at $\sqrt{s} = 1.96$ TeV recorded by the CDF detector operating at the Fermilab Tevatron. The search is performed separately in semileptonic decays, $B_s^0 \to D_s l X$, and fully reconstructed decays of the B_s^0 meson. Limits are set separately in each channels and combined for the final result.

Search for B_s^0 Oscillations and Measurement of the Lifetime Difference in the B_s^0 System

Tulika Bose

Columbia University

on behalf of the DZero collaboration.

Constraints on the mass difference, Δm_s, between mass eigenstates of the B_s^0 system provide important input to the standard CKM triangle. Measurements of the width difference between the same two eigenstates, $\Delta\Gamma_s$, also probe for CP violation as well as new physics beyond the Standard Model.

Recent results on searching for B_s^0 oscillations in the DØ detector are presented. A large semileptonic data sample collected at the Tevatron Collider in the period 2002–2005 was used in the analysis. The decays $B_s^0 \to D_s^- \mu^+ \nu$, $D_s^- \to \phi\pi^-, K^*(892)K^-$ have been reconstructed and the initial state flavour of the B_s^0 meson has been determined using the opposite-side tagging technique. Limits on Δm_s are presented.

We also present a study of the untagged decay $B_s^0 \to J/\psi\phi$. We obtain the CP-odd fraction in the final state at time zero, $R_\perp$, the average lifetime of the $(B_s^0, \bar{B}_s^0)$ system, and the relative width difference, $\Delta\Gamma/\bar{\Gamma} \equiv (\Gamma_L - \Gamma_H)/\bar{\Gamma}$.

Minimal Flavor Violation in the Lepton Sector

Vincenzo Cirigliano[1], Benjamin Grinstein[2], Gino Isidori[3], Mark B Wise[4]

[1]*California Institute of Technology*
[2]*University of California at San Diego*
[3] *INFN, Laboratori Nazionali di Frascati (ITALY)*
[4]*California Institute of Technology*

We extend the notion of Minimal Flavor Violation to the lepton sector. We introduce a symmetry principle which allows us to express lepton flavor violation in the charged lepton sector in terms of neutrino masses and mixing angles. We explore the dependence of the rates for flavor changing radiative charged lepton decays ($\ell_i \to \ell_j\gamma$) and μ-to-e conversion in nuclei on the scales for total lepton number violation, lepton flavor violation and the neutrino masses and mixing angles. Measurable rates are obtained when the scale for total lepton number violation is much larger than the scale for lepton flavor violation.

VII.1 Fundamental Interactions in Atomic and Neutron Physics: *EDM of Electrons, Muons, Neutrons, Atoms*

P- and T-invariance violating nuclear Schiff moment, new upper limit for the proton electric dipole moment

Vladimir Dmitriev

Budker Institite of Nuclear Physics

The best upper limit on electric dipole moment (EDM) of anything has been obtained from the measurement of the atomic EDM of ^{199}Hg [1].

$$|d(^{199}\mathrm{Hg})| < 2.1 \times 10^{-28}\ \mathrm{e\ cm}.$$

The nuclear part of the atomic dipole moment associated with the EDM of the ^{199}Hg nucleus manifests itself through the Schiff moment which is the first nonzero term in the expansion of the nuclear electromagnetic potential after accounting the screening by the atomic electrons. There are two kinds of contributions to the Schiff moment. The first one is nonzero only in the presence of parity- and time-invariance violating nucleon-nucleon interaction

$$\mathbf{S_1} = \frac{1}{10}\sum_N^A e_N \left(r_N^2 \mathbf{r}_N - \frac{5}{3}\langle r^2\rangle_{ch} \mathbf{r}_N \right),$$

where e_N equal $|e|$ for a proton and zero for a neutron. The second part of the Schiff moment operator connected with the internal EDM of the nucleons

$$S_2^i = \frac{1}{6}\sum_N^A d_N^i \left(r_N^2 - \langle r^2\rangle_{ch} \right) + \frac{1}{5}\sum_N^A \left(r_N^i (\mathbf{r}_N \cdot \mathbf{d}_N) - d_N^i r_N^2/3 - d_N^k \langle Q_{ik}\rangle/3 \right),$$

where Q_{ik} is the nuclear quadrpole moment.

For ^{199}Hg the last unpaired nucleon is a neutron. Nevertheless, due to core polarization, via proton - neutron interaction the proton dipole moment contributes to the Schiff moment as well. We found that for ^{199}Hg the Schiff moment is

$$S(^{199}\mathrm{Hg}) = (0.2 d_p + 1.9 d_n)\ \mathrm{e} \cdot \mathrm{fm}^3.$$

Combining it with the result of experiment we obtained a new constraint for the proton EDM [2]

$$d_p < 0.54\, 10^{-23} \mathrm{e} \cdot \mathrm{cm},$$

which is almost one order of magnitude better than the previous upper limit.

References

[1] M.V. Romalis, W.C. Griffith, J.P. Jacobs, and E.N. Fortson, Phys. Rev. Lett. **86**, 2505 (2001).

[2] V.F. Dmitriev and R.A. Sen'kov, Phys.Rev.Lett. **91**, 212303, (2003).

Prospective candidates for the EDM experiments of new type: calculations of enhancement of P,T-odd effects in HI^+ and liquid Xe.

Timur A. Isaev, Aleksander N. Petrov, Nikolay S. Mosyagin, Anatoly V. Titov
Petersburg Nuclear Physics Institute

The search for the P,T-parity non-conservation (PNC) effects is of fundamental importance in physics and such experiments are performed on TlF and YbF, and are prepared on PbO and HgH. Recently some new approaches were suggested, such as the search for P,T-odd effects in liquid xenon [1] and on HI^+ molecular ion [2]. For preparation and interpretation of these experiments high-precision calculations of the electronic densities on the heavy nuclei are required and other molecular properties which cannot be measured are usually need to be computed. Recently developed theoretical methods [3] allow one to analyze the atomic-molecular systems from the point of enhancement of P,T-odd effects and recommend such or another system as a prospective candidate. We calculated enhancement factor for electron EDM in the ground state of HI^+ molecular ion, this factor is required for experiment of new type on electron EDM search suggested in [2]. The results of calculations of P,T-odd effects in liquid xenon will be also discussed.
This work is supported by the RFBR grant 03–03–32335.
REFERENCES:

(1) Romalis M.V. and Ledbetter M.P., Phys.Rev.Lett, 87, 067601 (2001).
(2) Stutz R. and Cornell E., Bull.Am.Phys.Soc., 49, 76 (2004).
(3) Titov A.V., Mosyagin N.S., Petrov A.N. and Isaev T.A., Int.J.Quantum Chem., 104, 223 (2005), [arXiv: physics/0506038]; Petrov A.N. et al., Phys.Rev.A, in press.

Lorentz Violating Supersymmetric Quantum Electrodynamics

Pavel A Bolokhov[1], Stefan G. Nibbelink[2], Maxim Pospelov[1]
[1]*University of Victoria*
[2]*Shanghai*

We extend the Supersymmetric QED by the interactions with external tensor backgrounds which are assumed to be generated by some Lorentz-noninvariant dynamics at an ultraviolet scale M. Exact supersymmetry is compatible with operators of dimension five and higher, solving the naturalness problem in the Lorentz-violating sector. The Lorentz-noninvariant extension at dimension five level is studied in detail, including the renormalization group properties of these operators and their phenomenological consequences. The low-energy precision measurements set typical constraints on the size of the dimension five operators at 10^{-10} level from the inverse Planck mass.

Light Ion EDM Searches using a Magnetic Storage Ring

Cornelis J.G. Onderwater, et al.
KVI/Rijksuniversiteit Groningen

on behalf of the Storage Ring EDM collaboration.

The existence or absence of large permanent electric dipole moments (EDMs) of subatomic particles is one of the most pressing questions in physics today. An EDM violates both parity (P) and time-reversal (T) symmetries. Assuming the combined CPT symmetry is conserved, EDMs also violate CP. It could therefore help explain the matter antimatter asymmetry in the universe. Within the current Standard Model, EDMs are immeasurably small because they can only be induced by known CP-violation mechanisms in higher order radiative corrections. An EDM of sizable strength would therefore indicate a new source of CP-violation. Many Standard Model extensions predict EDMs that may be in reach of experiment. Therefore, many efforts are underway world wide to design new experiments to reveal these possibly large EDMs.

The most stringent EDM limits are those for the electron, neutron and the mercury atom. There are two reasons why the potentially very interesting light nuclei have not been explored so far. The experimental signature of an EDM is the dependence of the spin precession frequency on the strength of an electric field. Due to the rearrangement of the atomic electrons, the nucleus is shielded from an external electric field, severely reducing the experimental sensitivity for nuclear EDMs using typical atomic physics methods. Only large and heavy nuclei, such as mercury, have a sufficiently large so-called Schiff moment to allow experimental access. In addition to this fundamental problem, the need to use strong electric fields has prevented precise direct measurements on charged particles. All precise measurements to date are made using electrically neutral systems (neutrons or atoms), from which the more fundamental EDMs of their constituents must be inferred using theoretical models.

We will describe a new, highly-sensitive method of probing for EDMs on charged particles, such as muons and deuterons, using magnetic storage rings. These techniques utilize the strong electric fields present in the particle's rest frame due to relativistic effects. We will discuss the physics reach for a range of sensitivities: 10^{-27} to 10^{-29} e·cm for the deuteron and $< 10^{-24}$ e·cm for the muon. We will compare ring designs that (a) cancel the precession of the anomalous magnetic moment using electric fields and (b) accumulate an EDM precession using a resonance between the anomalous precession and synchrotron oscillations. The mere existence of an EDM for a fundamental particle at these levels would imply a new source of CP-violation that is several orders of magnitude above Standard Model predictions but within the range of speculative models containing new physics.

Electric dipole moment of Radium–225

Nicholas D. Scielzo, et al.

Argonne National Laboratory

The discovery of a permanent electric dipole moment (EDM) larger than the undetectably small value predicted by the Standard Model would signify a new source of time–reversal violation and CP violation. Many extensions to the Standard Model, such as supersymmetry, predict atomic EDMs just below current experimental sensitivity. A new source of CP violation could also explain the matter–antimatter asymmetry seen in the universe.

The radium atom is an excellent system for future EDM measurements. In isotopes such as ^{225}Ra ($t_{1/2}$=14.9 days) that have an octupole–deformed nucleus, the signature of an EDM is expected to be amplified by over two orders of magnitude relative to previously studied systems such as ^{199}Hg. In addition, ^{225}Ra has a nuclear spin of ½ which eliminates systematic effects due to electric quadrupole moments and relatively large quantities of this rare isotope can be obtained from the decay of ^{229}Th.

The overall plan is to collect ^{225}Ra atoms in a magneto–optical trap and transfer the sample to an optical dipole trap where the EDM measurement can be performed. However, several of the atomic properties needed to cool and trap ^{225}Ra atoms had either never been measured or had not been measured with sufficient precision. We have measured the frequency of the $^1S_0$–$^3P_1$ transition and the lifetime of the $^3P_1$ state by detecting fluorescence from a thermal atomic beam. Development of a magneto–optical trap based on this transition is currently underway.

This work was supported by the U.S. Department of Energy, Office of Nuclear Physics, under Contract No. W–31–109–ENG–38.

An electron EDM search using trapped molecular ions

Russell Stutz[1], Aaron Leanhardt[2], Laura Sinclair[3], Eric Cornell[2], et al.

[1]*JILA/University of Colorado*
[2]*JILA/NIST*
[3]*JILA/Univerisity of Colorado*

We report on an experiment to search for the electron electric dipole moment using trapped molecular ions. Currently, we are considering HfH+ and PtH+ as promising candidates for our experiment. The triplet Delta ground states of these molecules should provide large effective electric fields to enhance the EDM signal, and also provide highly polarized samples of ions in relatively weak (10's to 100's of V/cm) rotating electric fields due to a small Omega–doublet splitting. This talk will discuss our current experimental plans to create and trap HfH+ and PtH+, cool the molecules to their rovibrational ground state, and perform electron spin resonance spectroscopy in parallel electric and magnetic fields.

VIII.3 Neutrino Physics: *Accelerator and High Energy Neutrinos*

Recent Charm Production and Neutrino Oscillation Results from the CHORUS Experiment

Aysel Kayis Topaksu
University of Cukurova

From 1994 to 1997, the emulsion target of the CHORUS detector, which combines nuclear emulsion and electronic detector techniques, was exposed to the neutrino beam of the CERN SPS. In total about 100.000 CC neutrino interactions were located in the nuclear emulsion target and fully reconstructed.

The emulsion scanning is performed by fully automatic microscopes. With the present performance of emulsion scanning systems, it has become possible to perform large area volume scanning. All tracks belonging to an interaction vertex can be recognised and measured precisely. This technique has been used for the recognition of events where charmed particles are produced. More than 2000 events with a recognised charm decay have been collected and fully measured.

A comprehensive study of charm production by neutrinos is being made. The measurement of charm production by anti-neutrinos will be presented. Using a high statistics D^0 sample, a study of fragmentation parameters was performed. The results of this study will be shown and a comparison will be made with other experiments. Also measurements of the inclusive topological decay rate, including the decay rate into muons, and total D^0 production rate based on the final statistics will be given. In addition the result on the cross section measurement of D^{*+} production in neutrino-nucleon charged current interactions will be shown.

A systematic search for hyperfragments (strange nuclei) and superfragments (charmed nuclei) has been performed in neutrino-emulsion interactions. For the first time, a production rate of hyperfragments in neutrino–emulsion interactions was obtained. The absence of superfragment candidates provides an upper limit for the superfragment production rate.

Final results on the search for the tau-lepton decays and the analysis of ν_{mu} - ν_{tau} oscillation will be presented.

Status of the MINOS Experiment

George S Tzanakos

University of Athens

on behalf of the MINOS collaboration.

The MINOS Experiment consists of two detectors in the Fermilab NuMI beam: 980 ton one at 1 Km and 5.4 Kton one at 735 Km from the target. The far detector construction and commissioning was concluded in August 2003, and cosmic ray and atmospheric neutrino data have been collected routinely since that time. The far MINOS detector is the only large underground neutrino detector which employs a magnetic field, allowing identification of muon neutrinos and antineutrinos. The construction and commissioning of the near detector was finished at the end of 2004. The NuMI beam line, which uses 120 GeV protons from Fermilab's Main Injector to produce an intense neutrino beam in the few GeV range, was completed and commissioned in early 2005. The current MI proton intensity on NuMI target is about 2.0E+13 per pulse (2 – 3.6s cycle time). As of this date 4.7E+19 protons on target have been delivered resulting in a large number of recorded neutrino interactions in the near detector, and also some in the far detector.

In this talk the physics goals of the MINOS experiment will be presented along with a description of the NuMI beam and MINOS detectors. We shall present preliminary results from measurements of up-going muons and fully contained atmospheric muon neutrino and antineutrino interactions in the far detector, corresponding to an exposure of about 400 days. In addition, preliminary analysis of neutrino beam data from the near and far detectors shall be shown.

E907: Hadron Production Measurements for Neutrino Flux Calculations

Jonathan M Paley
Indiana University

on behalf of the MIPP collaboration.

Neutrino cross-section measurements as well as precision measurements of neutrino mixing angles and mass differences depend heavily on neutrino flux calculations. Such calculations rely on hadron-nucleus interaction cross-section data, and yet the data are scarce. The Main Injector Particle Production (MIPP) experiment at Fermilab, currently in-progress and collecting data, is a full acceptance spectrometer with excellent particle identification abilities. MIPP aims to provide a comprehensive hadron production data set for p's, π's and K's at various momenta (from 5 to 120 GeV) on several targets including beryllium and carbon. In particular, MIPP has collected hadron production data on the actual MINOS target using 120 GeV/c protons from the Main Injector. I will review the physics goals, detectors and status of the experiment.

MINERνA: A High Statistics, Neutrino-Nucleus Scattering Experiment in the NuMI Beam at Fermilab

Jorge G. Morfin

Fermilab

on behalf of the MINERvA collaboration.

The extremely intense NuMI neutrino beam at Fermilab, constructed for the MINOS Neutrino Oscillation Experiment, is an ideal beam for a high-statistics, low-energy neutrino scattering experiment. The MINERvA Collaboration has received Stage I approval to put a fine-grained scintillator detector directly upstream of the MINOS near detector to study topics of interest to both particle and nuclear physicists.

With final states as varied as high-multiplicity deep-inelastic reactions, coherent single-p^0 production and quasi-elastic neutrino scattering, the MINERvA detector is a hybrid of a fully active, fine-grained detector and a traditional calorimeter. The fiducial volume for most analyses is in the inner Active Target, shown in the figure on the left below, where the only material is triangularly-shaped, plastic scintillator strips. Since the scintillator detector does not fully contain events due to its low density and low Z, the MINERvA design surrounds it with sampling detectors with different absorbers acting as electromagnetic calorimeters (ECALs) and hadronic calorimeters (HCALs). The upstream ECAL and HCAL act as Pb and Fe nuclear targets respectively. The outer detector (OD) acts a muon identifier as well as an HCAL for sideward going muons and hadrons. The entire detector is placed just upstream of the MINOS near detector that acts as a forward-going muon identifier/spectrometer.

In a 4-year run MINERvA expects to accumulate at least 8.5 million events in the fiducial volume of the active detector and around 2.5 million events in the nuclear targets

Quasi-elastic	0.8 M events
Resonance (1 – p)	1.6 M events
Transition: Resonance to DIS	2.0 M events
DIS	4.1 M events
Coherent Pion Production	85 K CC / 42 K NC events
Strange particle Production	> 230 K Fully reconstructed events
Generalized Parton Distributions	O 10 K events
Nuclear Effects	C: 1 M events, Fe and Pb: 2.5 M events each

As an example of the physics potential of MINERvA, the right hand figure below shows the expected measurement of coherent p^+ productions (in red) compared to existing measuremets. The expected results for other important channels will be shown.

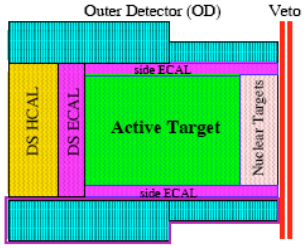

Figure 44: A side view schematic of the MINERvA detector

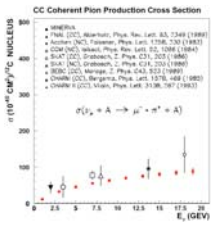

The ANTARES Neutrino Telescope

Teresa Montaruli
University of Wisconsin

on behalf of the ANTARES collaboration.

ANTARES is a project for the construction of a high energy neutrino telescope in the Mediterranean sea at a depth of 2.5 km, 40 km offshore La Seyne sur Mer (Toulon, France). ANTARES main scientific aims are the detection of neutrinos produced by cosmic accelerators, such as gamma-ray bursters, active galactic nuclei and pulsars embedded in supernova remnants, and the detection of dark matter particles. Twelve lines anchored at sea bed, spaced by about 70 m, will hold 75 optical modules each, which will contain photomultipliers for Cherenkov light detection. The results of two test lines, that have been recently deployed, will be presented. The first of the final detector lines will be deployed and connected to the electro-optical cable to shore by the end of 2005. The status of the project and the expected performance are going to be described.

The Production of Λ and Σ^0 Hyperons in Antineutrino-Proton Collisions

Stephan L Mintz, Lingling Wen
Physics Department, Florida International University

We obtain total and differential cross sections for strangeness changing charged current reactions $\overline{\nu}_L + p \longrightarrow \Lambda + L^+$ and $\overline{\nu}_L + p \longrightarrow \Sigma^0 + L^+$ where L stands for an electron, muon, or tau lepton. We calculate these cross sections from near threshold to several GeV. We also obtain the contributions of the various form factors to the total and differential cross sections. We do this in support of possible experiments which have been proposed by the MINERνA Collaboration. The calculation is phenomenologically based and makes use of SU(3) relations to obtain the standard vector current form factors. The axial current form factor for the Λ reaction is obtained from Λ beta decay data but for the Σ^0 process is obtained via SU(2) relations from Σ^- beta decay data since Σ^0 does not undergo beta decay. We also make theoretical estimates for the contributions of the pseudoscalar form factor and for the F_E and F_S form factors to the total and differential cross sections. We note that the latter two form factors are second class form factors and are forbidden by G-parity for the $p \leftrightarrow n$ transition but are not forbidden here. We discuss our results and show that for the Λ case that most of the contributions come from the vector and axial vector form factors and that for the Σ^0 case only the vector current form factor makes a substantial contribution. Thus this later reaction would be a particularly suitable test for the SU(3) obtained form factors. This has now become an interesting question. Data from Ξ^0 beta decay indicates that the SU(3) form factors hold over the range of q^2 available for this decay and Cabibbo has speculated that they may hold for higher q^2 values. We also indicate what might be learned if data for the inverse process, $e^- + p \longrightarrow \Lambda + \nu_e$ might become available from experiments at TJNAF.

IX.1 Muon Physics: *Overview and Muon Decay Parameters*

Recent Results and Future Prospects in Muon Physics

David W Hertzog
University of Illinois at Urbana-Champaign

The muon is a unique particle: It is used to penetrate hadronic matter in deep-inelastic scattering; to characterize the parameters of the weak interaction through its decay properties; to improve our understanding of QCD at low energies from capture rates; and, to test sensitively the standard model. And, this list does not even include μSR, which serves a different community. I will attempt to meld many of these disparate topics into a brief overview of the "field" of muon physics. The combination of new results with the promise from ongoing and planned experiments, demonstrates that the muon continues to play a key role in both particle and nuclear physics disciplines.

Muon decay: Measurement of the transverse e^+ polarization and its implications on G_F (Fermi coupling constant) and TRI (time reversal invariance).

Wulf Fetscher, et al.
ETH Zurich

on behalf of the ETH-Cracow-PSI-Katowice collaboration.

The two transverse polarization components P_{T_1} and P_{T_2} of the e^+ from the decay of polarized μ^+ have been measured as a function of the e^+ energy. Their energy averaged values are $\langle P_{T_1} \rangle = (6.3 \pm 7.7 \pm 3.4) \times 10^{-3}$ and $\langle P_{T_2} \rangle = (-3.7 \pm 7.7 \pm 3.4) \times 10^{-3}$. From the energy dependence of P_{T_1} and P_{T_2} the decay parameters η, η'' and α'/A, β'/A are derived, respectively.

Assuming only one additional coupling besides the dominant $V - A$ interaction improved limits on η, β'/A, and the scalar coupling constant g^S_{RR} are derived: $\eta = (-2.1 \pm 7.0 \pm 1.0) \times 10^{-3}$, $\beta'/A = (-1.3 \pm 3.5 \pm 0.6) \times 10^{-3}$, $\mathrm{Re}\{g^S_{RR}\} = (-4.2 \pm 14.0 \pm 2.0) \times 10^{-3}$ and $\mathrm{Im}\{g^S_{RR}\} = (5.2 \pm 14.0 \pm 2.4) \times 10^{-3}$.

High Precision Measurements of Muon Decay at TWIST

Jingliang Hu
TRIUMF

on behalf of the TWIST collaboration.

As a test of the Standard Model in the purely leptonic decay interaction, the TWIST experiment is designed to precisely measure Michel parameters describing the energy and angle dependence of positrons emitted from the decay of polarized positive muons. TWIST has just published its first measurements of Michel parameters ρ and δ from the 2002 data, with a precision 2 to 3 times better than the previous results. The physics analyses of the 2004 data, which were taken under better conditions, are in progress. Some improvements in reducing the systematic uncertainties have been achieved. This talk will describe the operation of the experiment and the techniques which are used to extract the decay parameters. Recent progress and results will be presented.

Constraints on Muon Decay Parameters from Neutrino Mass

Rebecca J. Erwin, Jennifer E. Kile, Michael J. Ramsey–Musolf, Peng Wang
California Institute of Technology

The TWIST experiment at TRIUMF will probe the Michel parameters, which parameterize contributions to muon decay from beyond the Standard Model, to unprecedented precision. Because some of these parameters are sensitive to chirality–violating four–fermion operators that also contribute to neutrino mass, limits on the mass can be used to put constraints on these operator coefficients. In my talk, I will discuss our analysis of these constraints and their subsequent implications for the Michel parameters.

XI.3 Nuclear and Particle Astrophysics and Cosmology: *Gamma Rays I*

Exploring the Physics of Active Galactic Nuclei in the Era of Neutrino and Gamma-Ray Astronomy

Paolo S. Coppi
Yale University

I review the outstanding issues in our understanding of Active Galactic Nucleus (AGN) phenomenon, focusing in particular on the subclass of AGN objects known as blazars. These objects have powerful relativistic outflows originating near their central black holes that produce intense and highly variable gamma-ray emission. They have also been proposed as strong sources of high-energy neutrinos. I will comment on how the next generation of gamma-ray and neutrino observatories will address some of the current puzzles we face.

H.E.S.S. Performance and Results

Wystan Benbow
Max Planck Institut fuer Kernphysik

on behalf of the H.E.S.S. Collaboration collaboration.

The High Energy Stereoscopic System (H.E.S.S) is an array of four imaging atmospheric-Cherenkov telescopes located in the Khomas Highlands of Namibia. The low energy threshold ($\sim$100 GeV), excellent background rejection ($>$99%), and good angular resolution ($<$0.1 deg) of H.E.S.S. allow the detection of a 1% Crab flux source in $\sim$25 hours of observation. This enables H.E.S.S. to perform searches for VHE gamma-ray emission from astrophysical objects with unprecedented sensitivity. H.E.S.S. has already detected more than 30 sources of VHE gamma rays, from a number of source classes. The performance of H.E.S.S. and the results of recent observations will be reported here.

VERITAS: the next generation very high energy gamma-ray telescope.

Trevor C Weekes
Harvard-Smithsonian Center for Astrophysics

on behalf of the VERITAS Collaboration team.

VERITAS (the Very Energetic Radiation Imaging Telescope Array System) is the next generation ground-based gamma-ray observatory that is being built in southern Arizona by a collaboration of ten institutions in Canada, Ireland, the U.K. and the U.S.A. It uses the atmospheric Cherenkov imaging technique that was developed by the collaboration at the Whipple Observatory and which has been used to detect both galactic and extragalactic sources of TeV gamma rays. VERITAS is designed to operate in the range from 50 GeV to 50 TeV with optimal sensitivity near 200 GeV; it will overlap with the next generation of space-based gamma-ray telescopes.

The design of VERITAS will be described, its scientific objectives outlined, and the present status of construction detailed. In addition to lowering the energy threshold of the technique by a factor of 4, the flux sensitivity will be improved by a factor of 10-20. The first two telescopes have been built and their properties will be described. The first phase of VERITAS, consisting of four telescopes, of 12 m aperture, will be operational by the time of the GLAST launch in 2007. Eventually it is hoped to expand the array to include seven telescopes on a filled hexagonal grid of side 80 m.

Flux of light antimatter nuclei near Earth, induced by cosmic rays in the Galaxy and in the atmosphere

Konstantin V. Protasov

Laboratoire de Physique Subatomique et de Cosmologie

Antiprotons in cosmic rays have been extensively studied both experimentally and theoretically over the last few decades, with the general purpose of measuring their flux and understanding their origin. Recently some new prospects have been outlined, strengthening the motivations for the study of the $\bar{p}$ flux, and extending the interest for cosmic rays antimatter to other light antinuclei, antideuterons $\bar{d}$ in particular. The $\bar{p}$ and $\bar{d}$ production in neutralino annihilation has been considered as a possible signature for the dark matter constituents in the Universe. $\bar{p}$ and $\bar{d}$ have also been considered as evaporation products of primordial black holes. This requires the secondary galactic contribution to be accurately known for a significant search of the former to be considered.

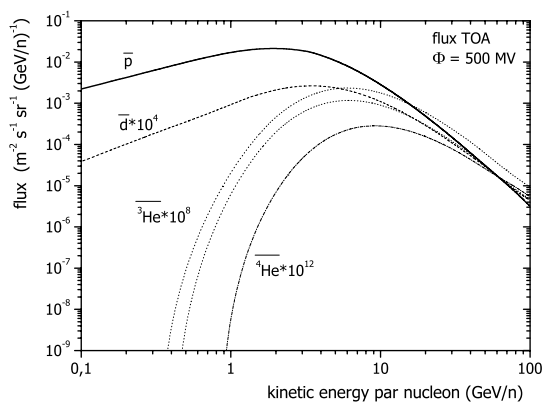

Fig. 1. The Galactic flux for $\bar{p}$, $\bar{d}$, $^3\bar{H}e$, and $^4\bar{H}e$ antimatter particles.

This contribution presents new calculations [1] of the light antinuclei $\bar{p}$, $\bar{d}$, $^3\bar{H}e$, $^4\bar{H}e$ fluxes produced by cosmic rays collisions on the interstellar matter in the Galaxy, and the first calculations of the fluxes produced by cosmic rays in the atmosphere for the same particles. For the flux, a new production channel $\bar{p}p \rightarrow \bar{d}X$ has been included in the calculations and was shown to contribute significantly to the total flux. The cross sections involved in the calculations were based on existing accelerator data analyzed recently in [2-4]. The results are found significantly different from previous calculations.

[1] R. Duperray et al., Phys. Rev. **D71**, 083013 (2005)

[2] R. Duperray, K. Protasov, and A.Yu. Voronin, Eur. Phys. J. **A16**, 27 (2003)

[3] R. Duperray, K. Protasov, L. Derome, and M. Buénerd, Eur. Phys. J. **A18**, 597 (2003)

[4] R. P. Duperray et al., Phys. Rev. **D68**, 094017 (2003)

XII.3 Facilities and Instrumentation: *New Detector Systems - Silicon Detectors*

The CMS Silicon Tracker - Status and Challenges

Gabriella Pasztor
University of California, Riverside

The CERN LHC is scheduled to start colliding proton beams at a centre-of-mass energy of 14 TeV in 2007. For the detection and study of diverse signatures for new physics at the LHC, robust charged particle tracking and vertex reconstruction within a strong magnetic field are essential. The CMS collaboration is constructing the largest Silicon Tracker ever built, consisting of 16000 silicon strip modules with an active silicon area of 200 m^2 and almost 10 million readout channels. While module mass production started in 2004 and is expected to finish in early 2006, the integration of modules into larger substructures of the barrel and endcap subdetectors just began in earnest. In this presentation, after the introduction of the detector design, the experiences and challenges of silicon module mass production will be discussed with particular attention to the key components, the silicon sensors and the front-end hybrids. The progress and plans of the integration of modules into the substructures and the construction of the large inner- and outer barrel and endcap detectors will then be presented. To conclude, the performance of the substructures will be reviewed as measured in test beam experiments and system tests.

Status of the construction of the ALICE Silicon Pixel Detector

Vito Lenti

INFN BARI (Italy)

on behalf of the SPD Project in the ALICE Collaboration collaboration.

The Silicon Pixel Detector (SPD) constitutes the two innermost layers of the ALICE Inner Tracking System (ITS). The two layers in barrel configuration are located at average radii of 3.9 and 7.6 cm, with a corresponding pseudorapidity coverage of $|\eta| < 1.98$ and $|\eta| < 0.9$, respectively. The main goal of the SPD is to give precise measurements of the impact parameters of secondary tracks from weak decays of particles with open heavy-flavour. High granularity and spatial precision are required to obtain accurate tracking information in a region where track density, in the most central heavy-ion collisions, could reach 80 tracks/cm^2. The expected total ionizing dose and fluence, integrated over 10 years, are 2.5 kGy and 3×10^{12} n/cm^2 (1 MeV neutron equivalent) respectively. The material budget is required to be less than 1% X_0 in each layer.

The SPD is based on hybrid silicon pixels; the sensors are 2-D arrays of reverse-biased silicon diodes, bump bonded to readout chips. The pixel cell dimensions are 50μm (rϕ) and 425μm (z). The pixel ASIC, in 0.25 μm CMOS with radiation tolerant design, is a mixed-signal chip with 8192 pixel cells arranged in 32 columns and 256 rows. Each cell contains a preamplifier-shaper with leakage current compensation, followed by a discriminator. Five readout chips are flip-chip bonded, using Pb-Sn solder bumps, to a single silicon sensor matrix of 256x160 cells, 200 μm thick; this assembly constitutes a “ladder”. The basic detector module is the half-stave, where 2 ladders are glued to an aluminium-polyimide multi-layer flex bus which carries signal and power lines. Each half stave is controlled and read out via a multi-chip module (MCM) with several ASICs, also in 0.25 μm CMOS with radiation tolerant design. The MCM includes a custom design optical transceiver for data communication with the back-end electronics via optical fibres. The two SPD layers contain 120 half-staves mounted on 10 low-mass carbon fibre support sectors in which very thin tubes are embedded for the cooling with C4F10 in an evaporative system.

The assembly of the half staves and the mounting on the carbon fiber sectors are carried out on precision coordinate measuring machines. The tools and procedures developed for the assembly are described. The status of construction is overviewed.

A high–performance silicon tracker for the CBM experiment at FAIR

Johann M. Heuser, et al.

GSI

on behalf of the CBM collaboration.

The Compressed Baryonic Matter (CBM) experiment planned at the Facility for Antiproton and Ion Research (FAIR) is designed to study strongly interacting matter at high baryon densities where the QCD phase diagram is poorly known.
The experiment is based on a novel concept for charged–particle tracking and heavy–flavor decay vertex measurement in fixed–target heavy–ion collisions as it was recently applied for the first time in NA60 at CERN. The core of CBM is a silicon vertex tracker of unprecedented performance. Tracking is exclusively performed with most advanced pixel and microstrip detectors, arranged in a magnetic dipole field between the target and detector systems for particle ID and calorimetry. The technological challenges include ultra low–mass silicon sensors and support, extreme radiation hardness, and fast self–triggered readout.
The paper outlines the physics and detector concept of CBM and focuses on the performance required from the silicon tracker.

The Status of the CMS Forward Pixel Detector

Ping Tan
Fermilab

on behalf of the CMS Forward Pixel collaboration.

The silicon pixel detector is the inner–most component of the CMS tracking system. It consists of three barrel layers and two end disks on each side. The pixel detector provides precise measurements of space points to allow effective pattern recognition in the multiple track environments near the LHC interaction point. The end disks, known as the Forward Pixel detector, will be located at a mean distance of 34.5 cm and 46.5 cm from the interaction point. One of the main challenges in the design of the pixel detector is the expected high level radiation in LHC environment. The pixel detector is required to remain operational with a fluence up to 6×10^{14} n_{eq}/cm^2.

The Forward Pixel detector is based on hybrid silicon pixels: the 2–D arrays of silicon sensors are bump–bonded to readout chips. The p–stop technique is used in fabrication of the n^+ on n sensors. The dimensions of the pixel cell are 100 μm × 150 μm. The pixel readout chip, fabricated in 0.25 μm CMOS with radiation–tolerant design, is organized in 26 double columns with 80 rows on each column. It consists of a total of 4096 readout channels. Each channel contains a preamplifier–shaper, followed by a discriminator. Analog information of the pulse height is read out to improve the position resolution. The basic detector unit is called plaquette where a number of readout chips (from 2 to 10) are connected by bump–bond to the silicon sensors. Several plaquettes are used to form turbine blade shaped panels. The panels are mounted to V–shape Aluminum channels, one on each side, to form a blade. These V–shape cooling channels also provide positioning. There are 24 blades on each disk. The Forward Pixel contains a total of 96 blades. The control and readout of each panel is realized in the front–end electronics through a token bit manager.

The Forward Pixel will be assembled and tested with full DAQ system at Fermilab. Currently the Forward Pixel detector is in the preproduction phase. The activities on the production preparation and system tests will be described.

Heavy quark detection with a forward silicon micro-vertex detector in the PHENIX Experiment

Patrick L McGaughey

Los Alamos National Laboratory

on behalf of the PHENIX collaboration.

Intriguing evidence that a new state of matter, the quark-gluon plasma, is formed in collisions of ultra-relativistic heavy ions has emerged during the past year from experiments done at the Relativistic Heavy Ion Collider (RHIC) at Brookhaven National Laboratory. We are developing a unique experimental capability at RHIC for the direct identification of heavy quarks, which will be used to help accurately determine the properties of this new state of matter. We will construct a silicon micro-vertex detector (SVD) covering the forward rapidity region, which will provide an excellent measurement of charm quark decays in the high multiplicity environment of nuclear collisions. Based upon electronics developed for the BTeV experiment, the SVD will cover one quarter of the acceptance of a PHENIX muon arm and will serve as a first step towards a full vertex detector covering both muon arms. LANL internal funds will support the construction costs.

The HERMES Recoil Detector

Ralf Kaiser
University of Glasgow, Dept. of Physics and Astronomy

on behalf of the HERMES collaboration.

Generalised parton distributions (GPDs) offer a way to unify the previously disjunct pictures of the nucleon given by parton distribution functions on the one hand and form factors on the other. For the first time GPDs may provide detailed information on the localisation of partons inside hadrons and access to their orbital angular momentum. GPDs can be accessed experimentally through the measurement of hard exclusive reactions, the cleanest of which is deeply virtual Compton scattering (DVCS). At the beam energy of HERMES (27.5 GeV) the reaction ep $\rightarrow$ e$'\gamma$p is dominated by bremsstrahlung (Bethe-Heitler). However, measurable asymmetries in beam spin and beam charge arise from the interference of both processes. The beam spin asymmetry is proportional to the imaginary part of the DVCS amplitude, while the beam charge asymmetry is proportional to the real part of the DVCS amplitude. Both can in turn be expressed in terms of GPDs. The HERMES Recoil

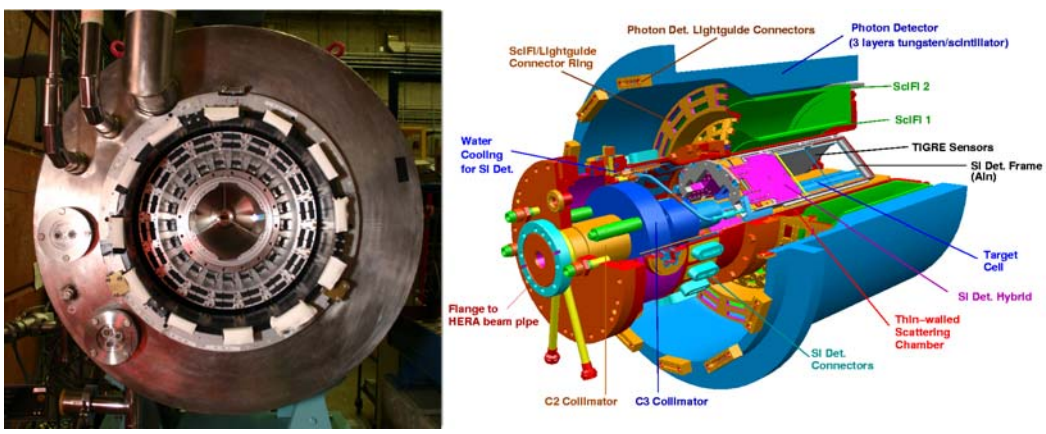

Fig. 1. Photo and schematic view of the HERMES Recoil Detector.

Detector consists of three active components: a silicon detector surrounding the target cell inside the beam vacuum, a scintillating fibre tracker and a photon detector consisting of three layers of tungsten/scintillator. All three detectors are are located inside a solenoidal magnetic field of 1 Tesla. The Recoil Detector will identify the recoiling proton from a hard exclusive reaction and measure it's momentum. In this way it will ensure the exclusivity of the given event. The components of the HERMES Recoil Detector have been tested extensively in test beams. Currently the entire detector is being tested with cosmic rays. It will be installed in the HERMES experiment at the end of 2005 for data taking until summer 2007. This talk will present the detector itself, results from test beam measurements and physics projections for the upcoming HERMES data taking with the Recoil Detector.

4:00–6:30 PM, Poster Session

Quarks and Gluons in Hot/Cold and Dense Matter

Can we distinguish energy loss from hadron absorption?

Alberto Accardi
Iowa State U.

Knowing wether a hadron is formed inside or outside the nuclear medium is very important for correctly interpreting jet-quenching data. The cleanest experimental environment to study the space-time evolution of hadronization is semi-inclusive DIS on nuclear targets.

Two frameworks are presently competing to explain the observed attenuation of hadron production: [1] quark energy loss (with hadron formation outside the nucleus) and [2] nuclear absorption (with hadrons formed inside the nucleus), see Fig. 1. In this presentation I explore the possibility to distinguish them using the A-dependence of the hadron attenuation ratio in nuclear DIS, and propose an observable which will help comparing theory models and and experimental data.

Contrary to common expectations, I find that the A-dependence of hadron attenuation cannot distinguish energy loss from hadron absorption. To accomplish this goal we need more exclusive observables.

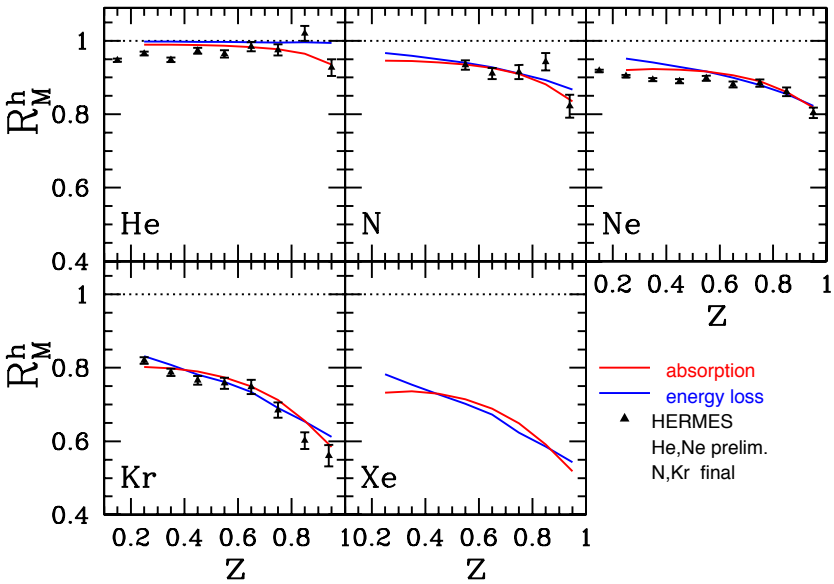

Fig. 1. Energy loss (red) and absorption model (blue) computations of the hadron attenuation ratio $R_M^h(z) = \left(\frac{1}{N_A^{DIS}}\frac{dN_A^h(z)}{dz}\right) \Big/ \left(\frac{1}{N_D^{DIS}}\frac{dN_D^h(z)}{dz}\right)$, compared to final HERMES data for N and Kr, and to preliminary data for He and Ne. Predictions for Xe are presented.

References

[1] E. Wang and X. N. Wang, Phys. Rev. Lett. **89** (2002) 162301. F. Arleo, JHEP **0211** (2002) 044 and reference therein.

[2] A. Accardi, D. Grunewald, V. Muccifora and H. J. Pirner, Nucl.Phys.A in press [arXiv:hep-ph/0502072] and references therein.

Conical Flow Induced by Quenched QCD Jets

Jorge Casalderrey Solana, Edward V. Shuryak, Derek Teaney
SUNY Stony Brook

Quenching is a recently discovered phenomenon in which QCD jets created in heavy ion collisions deposit a large fraction or even all their energy and momentum into the produced matter . At RHIC and higher energies, where that matter is a strongly coupled Quark-Gluon Plasma (sQGP) with very small viscosity, we suggest that this energy/momentum propagate as a collective excitation or "conical flow". Similar hydrodynamical phenomena are well known, e.g. the so called sonic booms from supersonic planes. We solve the linearized relativistic hydrodynamic equations to detail the flow picture. We argue that for RHIC collisions the direction of this flow should make a cone at a specific large angle with the jet, of about 70°, and thus lead to peaks in particle correlations at the angle $\Delta\phi = \pi \pm 1.2$ rad relative to the large-p_t trigger. This angle happens to match perfectly the position of the maximum in the angular distribution of secondaries associated with the trigger recently seen by the STAR and PHENIX collaborations. The interaction of hard processes (jets) with the medium form at RHIC may allow to measure some of the properties of the sQGP, in particular, the speed of sound.

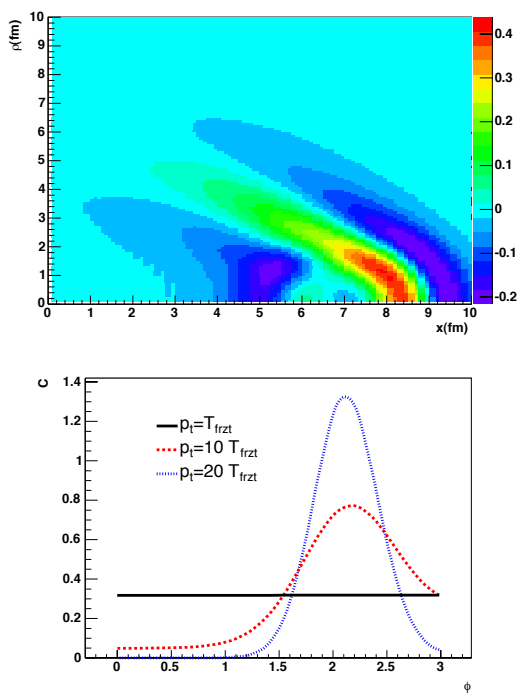

Fig. 1. (a)Velocity field v_x created by a jet moving along the $\hat{x}$ direction ($c_s^2 = 1/3$, $\Gamma_s = 1/(4\pi T)$, $\sigma = \Gamma_s$). The jet is assumed to disappear at $t = 7$ fm. Note that matter moves preferentially in he Mach direction (b) The normalized spectrum of associated secondaries versus the azimuthal angle ϕ. Three curves are for different p_t at $y = 0$ for $c_s^2 = 1/3$, $\Gamma_s = 1/(4\pi T)$, $\sigma = \Gamma_s$. The jet disappears completely at $t = 7$ fm while the spectrum is calculated at $t = 10$ fm.

Azimuthal anisotropy of charged hadrons at RHIC

Michael S Issah
SUNY Stony Brook

on behalf of the PHENIX collaboration.

The high energy density matter created at RHIC during energetic Au+Au collisions has been shown to behave hydrodynamically with very low viscosity. Hydrodynamics provides a link between the equation of state and the flow patterns revealed in measured hadron spectra and azimuthal anisotropy. The fine structure of azimuthal anisotropy, that is its detailed dependence on transverse momentum (p_T), centrality and particle type can provide valuable constraints on the range of validity of hydrodynamics and the onset of competing mechanisms. We report on the azimuthal anisotropy of charged and identified hadrons from the high statistics Au+Au and Cu+Cu data recorded by the PHENIX Collaboration. The p_T, centrality, beam energy and system size dependence of the azimuthal anisotropy of hadrons, together with an investigation of its scaling properties, will be presented and discussed.

Analysis of nuclear parton distribution functions

S. Kumano, M. Hirai, T.-H. Nagai

IPNS, KEK, 1-1, Ooho, Tsukuba, Ibaraki, 305-0801, Japan

Nuclear modifications of parton distribution functions have been investigated particularly since the EMC finding. Although available data are limited in comparison with the nucleonic case, we should be able to extract information on their nuclear modifications from the experimental measurements of deep-inelastic-scattering (DIS) and Drell-Yan processes. We have been investigating optimum nuclear parton distributions (NPDFs) for explaining available DIS and Drell-Yan data. We report our recent studies on the NPDFs and their uncertainties [1,2]. The NPDFs are expressed by the corresponding nucleonic ones multiplied by weight functions w_i:

$$f_i^A(x, Q_0^2) = w_i(x, A) f_i(x, Q_0^2), \quad w_i(x, A) = 1 + \left(1 - \frac{1}{A^\alpha}\right) \frac{a_i + b_i x + c_i x^2 + d_i x^3}{(1-x)^{\beta_i}}. \quad (1)$$

The initial scale Q_0^2 is taken as Q_0^2=1 GeV^2. We consider modifications for valence-quark, antiquark, and gluon distributions: w_{u_v}, w_{d_v}, $w_{\bar{q}}$, and w_g, which are expressed by the parameters in Eq. (1). The parametrized distributions are evolved to each experimental Q^2 point by the DGLAP evolution equations. Then, the parameters are determined by a χ^2 fit to the experimental data on F_2 structure-function and Drell-Yan cross-section ratios. Uncertainties of the obtained NPDFs are estimated by the Hessian method. Typical results are shown for the calcium nucleus in Fig. 1, where the weight functions w_{u_v} (=w_{d_v}), $w_{\bar{q}}$, and w_g are shown at Q^2=1 GeV^2 with their uncertainties. The solid curves are the optimum functions and shaded areas indicate their uncertainties.

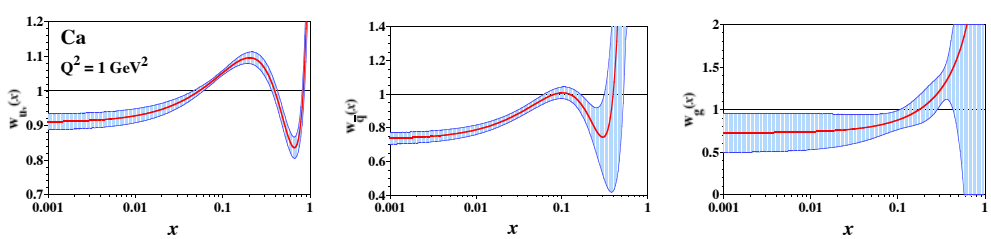

Fig. 1. Modifications of valence, antiquark, and gluon distributions are shown at Q^2=1 GeV^2 for the calcium nucleus [2].

The uncertainties of the NPDFs indicate that the valence-quark distributions are well determined. The antiquark distributions at small x are also determined well, but they cannot be fixed at large x. The uncertainties of the nuclear gluon distributions are very large at this stage in the whole-x range. From the analysis results, we proposed NPDFs from the deuteron to a heavy nucleus. A code is available on our web site [2] for calculating the NPDFs at given x and Q^2.

References

[1] M. Hirai, S. Kumano, and M. Miyama, Phys. Rev. D64 (2001) 034003.

[2] M. Hirai, S. Kumano, and T.-H. Nagai, Phys. Rev. C70 (2004) 044905. The NPDF code could be obtained from http://research.kek.jp/people/kumanos/nuclp.html.

Evidence for a long–range pion emission source in Au+Au Collisions at $\sqrt{s_{NN}} = 200$ GeV

Roy A. Lacey

SUNY Stony Brook

on behalf of the PHENIX collaboration.

A deconfined phase of nuclear matter is expected to be formed at the high energy densities created in Au+Au collisions at RHIC. It is widely believed that an important signature for the formation of such a phase is a particle emission source of large space–time extent.

The PHENIX experiment at RHIC, has recently acquired ~ 1.5 billion Au+Au events at sqrt(s)=200GeV during the year–2004. This high statistics data set allows for the extraction of detailed information about the emission sources for various particle types. The source images in turn provide a window in the dynamics of the high energy density nuclear matter created. Results from a recent analysis of the data using state of the art 1D and 3D Source Imaging indicate a previously undetected long–range structure in the two–pion source image. The presentation will focus on this new finding and provide detailed information about the 3–Dimensional structure of pion and proton emission sources.

Properties of the baryonic chemical potential and specific heat of hadronic matter from RHIC/CERN experiments

Aram Z Mekjian

Rutgers University

Properties of the baryonic chemical potential and associated specific heat of hadronic matter are investigated. The specific heat, mean hadronic mass excited and its fluctuation are connected to production yields and properties of the baryonic and electric chemical potentials. Expressions are developed which directly connect the specific heat to the behaviors of these chemical potentials through their value, slope and curvature. Various situations are studied such as particle yields with and without anti–baryons. This enables a determination of the importance of each element. A possible divergence of the specific heat is connected to the vanishing of the chemical potential with increasing excitation energy. A Hagedorn mass spectrum in the hadronic phase which varies as $\rho(m) \sim m^{-\tau} \exp(\beta_h m)$ is used to study this possible divergence in the hadronic phase below the Hagedorn critical temperature $T_h = 1/\beta_h$. The importance of the prefactor exponent τ is discussed. The prefactor exponent determines the behavior of the chemical potential with energy. The chemical potential will go to zero as $T \to T_h$ as ($T - T_h)^{5/2-\tau}$ if$\tau \le 5/2$. For $\tau > 5/2$, the chemical potential will go to a constant. Moreover, if $5/2 < \tau \le 7/2$ the constant is approached with infinite slope, while for $\tau > 7/2$ this slope is also finite. The specific heat per particle will diverge for $\tau \le 7/2$. Limitations of the Hagedorn model are show to be related to the formation of a quark–gluon plasma. These limitation arise because of the infinite density of particles and anti–particles as $T \to T_h$. Thus a transition is reached at a lower temperature than T_h.

Production of Λ and $\bar{\Lambda}$ in Au + Au collisions at $\sqrt{s_{NN}}$ = 200 GeV

Debsankar Mukhopadhyay
Vanderbilt University

on behalf of the PHENIX collaboration.

The measurement of Λ and $\bar{\Lambda}$ in relativistic heavy ion collisions is important to study the net baryon density, strangness production and nuclear modification factors in the particle production. Intermediate and high p_T (anti) lambda yields and the $\bar{\Lambda}$ to Λ ratio can provide information about the hadronization mechanism in the hot and dense medium and parton energy loss.

The PHENIX experiment at RHIC has recorded 1.5×10^9 Au+Au collisions during 2003-2004 run. This large data sample coupled with high resolution particle identification capabilities allows for a detailed study of the Λ and $\bar{\Lambda}$ production over a large number of centrality classes and in a broad p_T range. The latest results on the spectra, yields, ratios and nuclear modification factors for (anti) lambdas will be presented.

BCS-BEC crossover in relativistic superfluid and its possible realization in QCD

Yusuke Nishida[1], Hiroaki Abuki[2]

[1]*Department of Physics, University of Tokyo*
[2]*Yukawa Institute for Theoretical Physics, Kyoto University*

To reveal the nature of strongly interacting matter under extreme conditions is one of the most challenging problems in hadron physics. An interesting possibility suggested in the color superconducting phase in the dense quark matter and the pion superfluid phase at finite isospin density is the crossover from Bardeen-Cooper-Schrieffer pairing to Bose-Einstein condensation (BCS-BEC crossover).

In this presentation, we will report our recent work [arXiv:hep-ph/0504083] which aims to explore the BCS-BEC crossover in a relativistic system. Using the four-Fermi interaction model and employing the Gaussian approximation in the partition function, we calculate the critical temperature T_c and the chemical potential μ as a function of the coupling G with the total number density fixed. The numerical result of T_c is shown in Fig. 1, from which we find two crossovers where the behavior of T_c changes. One is the ordinary BCS-BEC crossover, but with some unconventional non-plateau behavior of the critical temperature because of the relativistic effect. The other is from the BEC state to the novel state, *the relativistic BEC (RBEC)*, where the critical temperature increases to the order of the Fermi energy. The physical characteristics of the BCS, BEC and RBEC phases will be discussed in detail in our presentation.

The dashed line shown in Fig. 1 is the dissociation temperature T_{diss} where the bound boson decouples from the spectrum. T_{diss} line separates the normal phase into two regions; a normal phase without stable bosons for $T > T_{diss}$, and a *preformed boson phase* with stable bosons for $T_c < T < T_{diss}$.

Also, we will make some speculative remarks on the relevance of the two crossovers to QCD; there may be a band of superfluid phases (BCS-BEC-RBEC) between the hadronic phase and the quark-gluon plasma phase in the QCD phase diagram. The preformed boson phase above T_c will also have close relevance to the qq bound states discussed by Shuryak and Zahed.

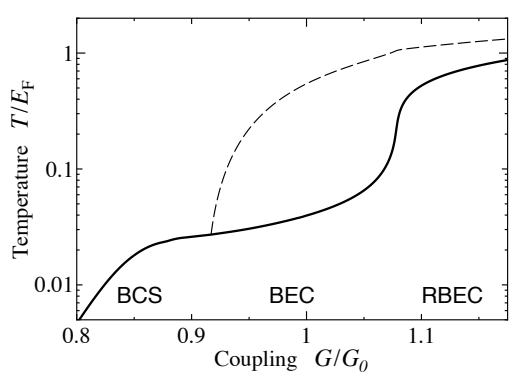

Fig. 1. Critical temperature T_c normalized by the Fermi energy (thick solid line) as a function of the coupling G/G_0. G_0 is defined by $G_0 = \pi^2/\Lambda^2$.

The Parton Momentum Distribution and the Equation of State in Nuclear Matter.

Jacek Rozynek

Institute For Nuclear Studies , Warsaw, Poland.

In the frame of properly formulated covariant parton model (1), we calculated the nuclear modifications of the transverse momentum distribution in the nucleon inside nucleus. The modifications concern the nucleon rest energy which changes the Bjorken x in the nuclear medium giving the good agreement (2) with the experimental data (the EMC effect for $x > 0.15$ and the nuclear lepton-pair production). In the model we discuss a connection between the average value of the parton transverse distribution square and the Bjorken variable x for bound nucleons which interact inside nuclear medium. In this way we introduce a final state interaction between the scattered nucleon and the rest of the nucleus. For large x, in the Bjorken limit (large Q^2 momentum transfer), the final state nucleon-nucleon interaction is negligible and the average transverse parton momentum in the bound nucleon is smaller then in the free one. Contrary, for $x < 0.3$ the influence of the nuclear medium on the transverse momentum parton distribution is strongly reduced due to the presence of nuclear interaction. The possible experimental evidence is discussed.

The quark anti-quark content of bound nucleon simulated by pion structure function is changed as a function of nuclear matter density. Finally we derive the equation of state for dense nuclear matter which is softer then EOS in the standard vector - scalar (Walecka) relativistic mean field approach with eventual transition to quark phase.

(1) R.G.Roberts, ”The Structure of the Proton - Deep Inelastic Scattering” Cambridge University Press (1990).

(2) ”The Single Particle Sum Rules in the EMC effect”, J.Rozynek G. Wilk, Phys. Rev. C 71, 068202 (2005).

Measurement of non-photonic electrons in $\sqrt{s}$=200 GeV p+p, d+Au, and Au+Au collisions in STAR

Thomas S Ullrich

BNL

on behalf of the STAR collaboration.

The measurement of heavy flavor production in relativistic heavy ion collisions is both an extreme experimental challenge and rich with physics information. Final state effects, such as heavy quark energy loss in the medium, and nuclear initial state effects can be studied by comparison of their yields and spectra in p+p, p+A and A+A collisions. The measurement of their azimuthal anisotropy (v_2) can potentially help to further our understanding of the mechanisms that lead to early equilibration in the hot and dense matter.

As direct D meson measurements are limited in statistics and thus in p_T reach, non-photonic single electron measurements from semi-leptonic decays of D and B mesons can serve as a substitute. They are thought to constitute the leading source of non-photonic electrons.

In this talk we will present spectra of non-photonic electrons in Au+Au collisions for transverse momenta from 1.5 GeV/c up to 10 GeV/c for different centralities. They are compared to those from p+p and d+Au collisions in order to infer information about in-medium modifications of heavy quarks. We also will discuss recent single electron v_2 measurements from minimum bias Au+Au collisions in the p_T region of 2-5 GeV/c.

Proposal for a High Energy Nuclear Database

Ramona Vogt[1], David Brown[2]

[1]*Lawrence Berkeley National Lab and University of California, Davis*
[2]*Lawrence Livermore National Lab*

We propose to develop a high-energy heavy-ion experimental database and make it accessible to the scientific community through an on-line interface. The database will be searchable and cross-indexed with relevant publications, including published detector descriptions. It should eventually contain all published data from the Bevalac, AGS, SPS and FNAL fixed-target programs to the RHIC and LHC colliders; proton-proton, proton-nucleus to nucleus-nucleus collisions as well as other relevant systems; and all measured observables. Such a database would have tremendous scientific payoff as it makes systematic studies easier and allows simpler benchmarking of theoretical models to a broad range of experiments. To enhance the utility of the database, we propose periodic data evaluations and topical reviews.

Secondary pairing in gapless color-superconducting quark matter

Qing-hai Wang
University of Connecticut

We calculate secondary pairing in a model of a color superconductor with a quadratic gapless dispersion relation for the quasiquarks of the primary pairing. Our model mimics the physics of the sector of blue up and red strange quarks in gapless color-flavor-locked quark matter. The secondary pairing opens up a gap Δ_s in the quark spectrum, and we confirm Hong's prediction that in typical secondary channels $\Delta_s \propto G_s^2$ for coupling strength G_s. This shows that the large density of states of the quadratically gapless mode greatly enhances the secondary pairing over the standard BCS result $\Delta \propto \exp(-\mathrm{const}/G)$. In all of the secondary channels that we analyzed we find that the secondary gap, even with this enhancement, is from ten to hundreds of times smaller than the primary gap at reasonable values of the secondary coupling, indicating that secondary pairing does not generically resolve the magnetic instability of the gapless phase.

Jets and α_s measurements in ep collisions

Yuji Yamazaki
DESY

on behalf of the H1 and ZEUS collaboration.

Through a deep understanding of detectors and the underlying physics, measurements of jet cross sections at HERA are the most precise in the world. This allows a detailed study of parton evolution schemes, the dynamics of QCD and precise extractions of the strong coupling constant, α_s. Recent measurements have produced values of α_s which are competitive in precision with that of the world average and shown tantalising hints of BFKL dynamics.

Quantum Chromodynamics

Gauge Invariance of the Vacuum Condensate of Dimension Two in Yang–Mills Theory

Angelo Raffaele Fazio

Universidad Nacional de Colombia, sede de Bogota

We discuss the gauge parameter independence of the condensate of dimension mass squared constructed in Yang–Mills theories. We prove that the above mentioned gauge independence considering Yang–Mills theories as a limiting case of non–commutative gauge field theories where the commutative parameter tends to zero. We assume that these theories admit a gauge invariant regularization and that in the regularized theory the commutative limit is not singular. Outlook and perspectives related to these hypotheses are finally discussed.

From Dense Dilute Duality to Selfduality of High Energy QCD

Michael Lublinsky

University of Connecticut

I will report on a recent theoretical progress in understanding QCD evolution at high energies. A question of BFKL Pomeron loop resummation will be addressed within a functional operator approach. A new duality transformation relating dilute and dense regime will be introduced. A complete evolution kernel for high energy QCD must be selfdual under this dense-dilute duality transformation.

Measurement of the Charged D Meson Pseudoscalar Decay Constant

Hanna Mahlke

Cornell

on behalf of the CLEO collaboration.

Using 300 1/pb of data obtained with the CLEO-c detector at CESR on the $\psi(3770)$ resonance, the branching ratio for the purely leptonic decay of the charged D meson into a charged muon and neutrino has been measured. At this energy changed D mesons are produced as D^+D^- pairs. We use a "double-tag" technique where one D is fully reconstructed and only the muon from the other D is detected. The presence of the neutrino, and only the neutrino, is then inferred from energy and momentum conservation. Measurement of this fully leptonic branching ratios provides a determination of the pseudoscalar decay constant of charged D mesons.

Nucleon Structure

Relativity and Wavemechanism

Kapil Prasad Chandra

Guru Ghasidas University,Bilaspur

A relation for the wave and particle properties is derived, when a body is moving with high velocity than the total energy or Relativistic energy is the sum of two energy. Rest mass energy and energy due to moving of body to accordingly Dual nature this energy is wave properties energy, this leads us to a equation for wave and particle properties of matter, which gives successful theoretical base for Bohr's complementary principle and solve many drawbacks of De Broglies dual nature equation of matter.

Polarization Observables in Deuteron Electro-Disintegration

Renee Fatemi

Massachusetts Institute of Technology

on behalf of the BLAST collaboration.

Electron scattering from polarized deuterium provides insight into the nucleon form factors as well as the structure of the internucleon potential. The comparison of the measured single spin tensor asymmetry (A_d^T) to theory tests our knowledge of the D-state contribution to the deuteron wavefunction. While double spin beam-vector symmetries (A_{ed}^V) probe the accuracy of the form factors used to describe the charge and magnetic distributions of the individual nucleons. Measurements of these asymmetries have been made by the BLAST Collaboration, utilizing the 850 MeV polarized electron beam provided by the MIT-Bates Accelerator. Electrons were scattered from a vector and tensor polarized deuterium gas target, located on the Bates South Hall Electron Storage Ring. The Bates Large Acceptance Spectrometer Toroid detector (BLAST) allowed simultaneous determination of both asymmetries over a Q^2 range of 0.1-0.5 $(GeV/c)^2$. Asymmetry results and comparisons with theory will be presented along with target polarization measurements.

Λ^0 Polarization in $pp \to p\Lambda^0 K^+(\pi^+\pi^-)^N$, $N = 1, 2, 3, 4, 5$, at 27.5 GeV

Julian Felix

Instituto de Fisica, Universidad de Guanajuato

on behalf of the BNL e766 collaboration.

The polarization of Λ^0's from the specific reactions $pp \to p\Lambda^0 K^+(\pi^+\pi^-)^N$, $N = 1, 2, 3, 4, 5$, created from 27.5 GeV incident protons on a liquid Hydrogen target, as function of x_F, P_T, and $M_{\Lambda^0 K^+}$, is reported. The data is from the BNL e766 experiment[1] which collected 300×10^6 events; from those events, 1% resulted as exclusive events, from where the present analyzed data come. The Λ^0 polarization is a function of x_F, P_T, and $M_{\Lambda^0 K^+}$ [2]. The Λ^0 polarization as function of x_F and P_T is a very well known result -they agree with published inclusive results-[3]; the Λ^0 polarization as function of $M_{\Lambda^0 K^+}$, a new one -which do not agree with previous published results [4]. Here are reported the whole results, which show that Λ^0 polarization depends on the Λ^0 production mechanism.

References

[1] J. Uribe *et al*, Phys. Rev. D49, 4373(1994). E. P. Hartouni *et al*, Nucl. Inst. Meth. A317, 161(1992). E. P. Hartouni *et al*, Phys. Rev. Lett. 72, 1322(1994). E. E. Gottschalk *et al*, Phys. Rev. D53, 4756(1996). D. C. Christian *et al*, Nucl. Instr. and Meth. A345, 62(1994). B. C. Knapp and W. Sippach, IEEE Trans. on Nucl. Sci. NS 27, 578(1980). E. P. Hartouni *et al*, IEEE Trans. on Nucl. Sci. NS 36, 1480(1989). B. C. Knapp, Nucl. Instrum. Methods **A289**, 561(1980).

[2] J. Félix *et al*, Phys. Rev. Lett. 76, 22(1996). J. Félix, Ph.D. thesis, Universidad de Guanajuato, México, 1(1994). J. Félix *et al*, Phys. Rev. Lett. 82, 5213(1999).

[3] K. Heller *et al*, Phys. Lett. **B68**, 480(1977). G. Bunce *et al*, Phys. Lett. **B86**, 386(1979).

[4] T. Henkes *et al*, Phys. Lett. B283, 155(1992). J. Félix *et al*, Phys. Rev. Lett. 88, 061801-4(2002).

Acknowledgements

We acknowledge the assistance of the technical staff at the AGS at Brookhaven National Laboratories and the superb efforts by the staffs at the University of Massachusetts, Columbia University, and Fermilab. This work was supported in part by National Science Foundation Grants No. PHY90-14879 and No. PHY89-21320, by the Department of Energy Contracts No. DE-AC02-76CHO3000, No. DE-AS05-87ER40356 and No. W-7405-ENG-48, and by CoNaCyT of México under Grants 458100-5-4009PE and 2002-CO1-39941.

Pion-Field Theoretical Description of the Δ^{++}(1236)-Resonance without QCD

Helmut Jahn

Faculty of Physics and Research Center Karlsruhe

Excited states of the nucleon were predicted by Wentzel already in 1940. Wentzel showed that such kind of states can be derived from models of meson field theory if they are treated above a certain coupling strength. In particular for a pseudo-scalar meson field theory such kind of states were derived by Pauli and Dancoff in 1942 with equal amount of spin and isospin. They can be understood as arising from excitation of the pionic cloud of the nucleon by which the main part of nuclear forces also is coming out. The excitation of these states also is the mechanism by which the pion-nucleon resonance scattering is originated which firstly was experimentally discovered by Fermi in 1955. This connection was confirmed by Wentzel in 1975 on occasion of his decoration with the Max-Planck-Medal of the German Physical Society.

On the other hand there has been the development of the particle physics leading to the concept of the quark model by Gell-Mann and Zweig. Attempts to incorporate the excited nucleon states of Wentzel, Pauli & Dancoff and Fermi into the quark model show that this would require to introduce a new degree of freedom to which the name "'colour"' has been given and which is not needed in the case of the excited nucleon states of Wentzel and Pauli & Dancoff. Moreover it has been stated by Thomas Walcher that simple observables of the hadrons as mass, spin and magnetic moment cannot be derived from the quantum colour dynamics (QCD) and the same is true for the nuclear forces. Thus genuine field theoretical methods of strong coupling had to be developed in order to be able to derive the pion-nucleon resonance scattering from a model of pion field.

In the following contribution a completion of the method of Wentzel and Pauli & Dancoff is sketched following a work of the author and treating the pion-nucleon resonance scattering. By means of a canonical and nonlinear transformation of variables the original meson field is split into a free meson part and a self field part of the nucleon. The transformation is defined such that the interaction between the compound nucleon system thus arising and the free mesons vanish in the case of infinitely strong coupling. The solution of this field splitting problem is presented and the problem of calculating the pion-nucleon resonance scattering from this strong-coupling theory is treated on this basis. Numerical results obtained from such a calculation are discussed. For the sake of simplicity the symmetric pseudoscalar fixed-and-extended-source meson field theory is used and found that the lowest pion-nucleon resonance scattering is quite well reproduced with essentially the same parameters necessary to reproduce the nucleon-nucleon-potential. The present investigation will serve to guide more extended considerations in this direction.

The sum rule which relates the spin dependent structure function g_1 to the cross section of the photopruduction

Susumu Koretune

Shimane University

It has been known that some sum rules derived from the canonical quantization on the null-plane get the contribution from the nonlocal quantity corresponding to the matrix element of the bilocal currents which is absent in the equal-time formalism. The sum rule for the spin dependent function g_1^{ab} corresponding to the moment at $n = 0$ is one example. Here, a, b denotes the flavor dependence of the currents. Now,the Nachtmann moment of the structure function $g_1 + g_2$ at $n = 0$ takes the form $\int_0^1 dx(g_1 + g_2)/x$ and exactly agrees with the form of the current algebra sum rule, and can be smoothly continued to the $Q^2 = 0$ limit. The situation is completely different from the moment at $n = 1$. Since the integral of the matrix element of the bilocal current is Q^2 independent, we can consider that the current algebra sum rule holds even at $Q^2 = 0$. Here we consider this possibility, and show that the sum rule which relates the spin dependent function g_1^{ab} to the cross section of the photoproduction exists. In case of the current commutation relation, it is for the anti-symmetric combination with respect to a, b. Thus it is for the cross sections of the isovector photon. Then we find that the phtoproduction part is zero if a similar sum rule as the Cabibbo-Radicati sum rule known in the equal time formalism holds. In this case we get that the Q^2 dependent part is also zero. These are exactly the two sum rules obtained by the equal-time formalism. In our case, these two sum rules are related and it has a chance to be valid even when the each sum rule is violated due to the high energy behavior. In case of the current anticommutator, it is for the symmetric combination with respect to a, b. Thus we obtain the sum rule which relates the cross section of the phtoproduction and g_1^p. Since the sum rule in case of the moment at $n = 1$ is known as Ellis Jaffe sum rule in the deep inelastic reaction and Drell Hern Gerasimov sum rule in the photoproduction, and since the sign change in the course to reach the limit $Q^2 = 0$ is not well understood, we investigate the issue in our approach. Then we show that there is a deep connection between the elastic and the resonance contributions, and argue that it is this relation and the rapid change of the elastic contribution in the low Q^2 region which explains why the sign change discussed by the Drell Hern Gerasimov sum rule and Ellis Jaffe sum rule occurs in the very small Q^2 region.

Predicting Minimum Bias and Underlying Event at LHC

The ATLAS Collaboration[1]

[1]*CERN*

A knowledge of minimum bias events and the underlying event at the LHC is required in order to develop robust analysis strategies, reconstruction algorithms. Minimum bias data from the SppS and the Tevatron, and underlying event data from the Tevatron have been used to tune current physics models (PYTHIA and HERWIG) in order to predict particle multiplicities and pt distributions in minimum bias and underlying events at LHC energies. First studies on how ATLAS can measure these distributions will also be presented.

Baryon charge transfer and production asymmetry of $\Lambda_c/\bar{\Lambda}_c$ in hadron interactions.

Olga Piskunova

Lebedev Physics Institute of Russian Academy of Sciences

The predictions were done for asymmetry between production spectra of Λ^0 and $\bar{\Lambda}^0$ at the energy of LHC experiments. The value of A(s) should be situated in the corridor between two curves that are calculated in Quark-Gluon String Model with two possible intercepts of $\alpha_{SJ}(0)$=0,5 and 0,9. Both curves describe the asymmetries measured at lower energies up to RHIC experiments. The data of H1 experiment can be fitted only with $\alpha_{SJ}(0)$=0,9.

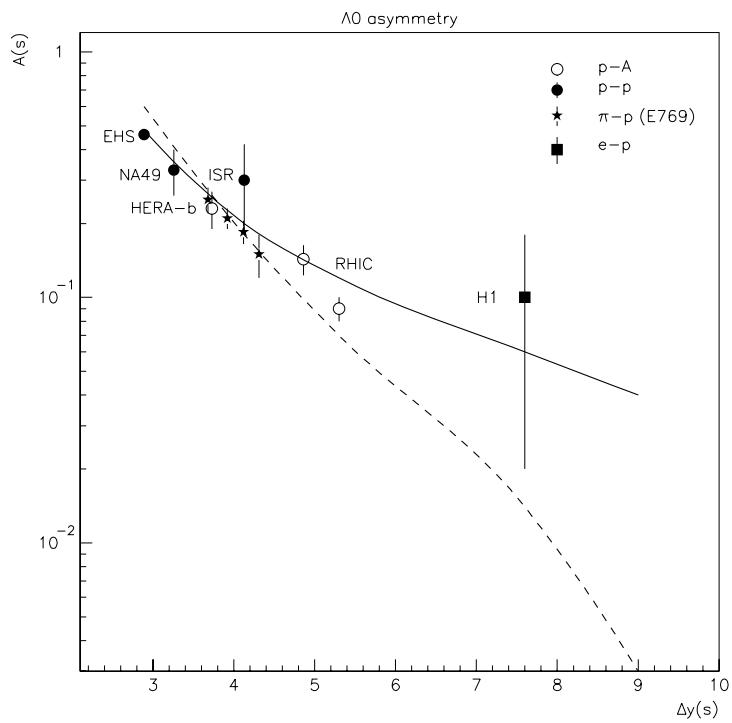

Fig. 1. Asymmetry in Λ^0 and $\bar{\Lambda}^0$ production and QGSM curves: $\alpha_{SJ}(0)$=0,5(dashed line) and $\alpha_{SJ}(0)$=0,9 (solid line).

Transverse single spin asymmetries from muons at forward rapidity in polarized p+p collisions at $\sqrt{s_{NN}} = 200$ GeV

Anuj K Purwar

Los Alamos National Lab

on behalf of the PHENIX collaboration.

The spin structure of the proton has revealed itself to be extremely complex and is an area of ongoing research. In particular its transverse spin structure remains poorly understood. Large transverse single-spin asymmetries were observed in forward pion production by the E704 collaboration at Fermilab ($\sqrt{s} = 19.4$ GeV) and have been found by the STAR and BRAHMS experiments to persist at RHIC energies. In addition, single-spin azimuthal asymmetries were observed recently in semi-inclusive deep-inelastic scattering experiments. Such large asymmetries were initially surprising because at leading order, perturbative quantum chromodynamics predicted only small effects. Thus, transverse single spin asymmetries (A_N) have the potential to be an important tool in understanding the quark spin distributions in a polarized proton. We measure the production of single muons using the PHENIX muon arms (pseudorapidity range: $1.2 < |\eta| < 2.4$). By using the PHENIX muon arms we can make this measurement at non zero values of X_F, complementing earlier mid-rapidity results for neutral pions and charged hadrons, thus allowing us to study A_N in different kinematical regimes. We present the latest results of A_N for single muons from collisions of polarized p+p collisions at $\sqrt{s_{NN}} = 200$ GeV at RHIC.

Diffractive vector meson production at COMPASS and plans for GPD's measurements

Andrzej M. Sandacz

Soltan Institute for Nuclear Studies, Warsaw

Exclusive vector meson production is a part of the COMPASS on-going physics program. The data for ρ^0, ϕ and J/ψ production cover typically a Q^2 range $10^{-3} < Q^2 < 25$ GeV^2 at an average W equal to about 10 GeV. Here we present two preliminary results on spin dependence of diffractive production of ρ^0 meson from COMPASS polarised target.
First, the Q^2 dependence of several spin density matrix elements and of R = σ_L/σ_T is presented. The data are consistent with a substantial increase of R with Q^2 and a weak violation of SCHC. Second, the longitudinal double-spin asymmetry A_1^ρ for incoherent ρ^0 production on polarised deuterons is shown as a function of Q^2 and x_{Bj}. The asymmetry is in general compatible with zero in the whole kinematic range.
Finally we discuss prospects for measuring DVCS and exclusive meson production at COMPASS in order to investigate GPD's. This will require modifications of the COMPASS present setup by replacement of the target by a liquid hydrogen target and adding a recoil detector. Estimates of expected accuracy for the future studies of DVCS and other exclusive reactions will be given.

Longitudinal Double Spin Asymmetry for η production at mid-rapidity in polarized p+p collisions at $\sqrt{s_{NN}} = 200$ GeV

Joseph P Seele

University of Colorado at Boulder

on behalf of the PHENIX collaboration.

The gluon helicity distribution of the nucleon remains poorly constrained by existing data from polarized deep inelastic scattering. Longitudinal double spin asymmetries, A_{LL}, measured for inclusive hadron production in polarized proton-proton collisions at high energies have been shown to be sensitive to the gluon helicity distribution, Δg.

Polarized proton-proton collisions at RHIC will provide measurements of A_{LL} with unprecedented accuracy. Precision measurements of the longitudinal spin asymmetries in inclusive hadron production are a cornerstone of the RHIC-spin program. The extraction of Δg from these data depends on the experimental knowledge of the relevant fragmentation functions. However, the measurement of A_{LL} for different hadrons with independent experimental uncertainties and different fragmentation functions will lead to robust estimates of experimental and theoretical uncertainties in the extraction of Δg.

We have used the central rapidity detectors of the PHENIX spectrometer to measure the production of η particles at mid-rapidity ($|\eta| < 0.35$). We present results for A_{LL} for η production in polarized p+p collision at $\sqrt{s_{NN}} = 200$ GeV at RHIC.

Spin Duality on the Neutron (^{3}He)

Patricia H Solvignon[1], Nilanga Liyanage[2], Jian-Ping Chen[3], Seonho Choi[4]

[1]*Temple University*
[2]*University of Virginia*
[3]*Jefferson Lab*
[4]*University of Seoul*

on behalf of the Jefferson Lab Hall A collaboration.

Jefferson Lab experiment E01-012 used the polarized ^{3}He target in Hall A for a measurement of the virtual photon asymmetry $A_1^{^3He}$ and the spin structure function $g_1^{^3He}$ in the resonance region over a Q^2 range from 1.0 to 4.0 $(GeV/c)^2$. The same quantities are extracted for the neutron. Data from E01-012 combined with deep inelastic scattering data will provide a test of quark-hadron duality predictions. This will be one of the first test of the spin and flavor dependence of quark-hadron duality. The demonstration of duality for spin structure functions will enable us to use the resonance data to study the nucleon spin structure in the large x_{bj} region. Some details of the experiment and preliminary results will be presented.

Investigation of Nonlinear Effects in Inelastic Rosenbluth Separations

Vladas Tvaskis, et al.

Hampton University / Jefferson Lab

Jefferson Lab Hall C Experiment E94–110 measured precision inclusive electron–proton cross sections in the nucleon resonance region ($1 < W^2 < 4$ GeV^2), spanning the four–momentum transfer range $0.2 < Q^2 < 4.5$ GeV^2. To obtain new measurements of the separated longitudinal and transverse proton structure functions in this regime, 195 Rosenbluth–type separations were performed, typically with over 5 points for each fixed (W^2, Q^2), and covering a broad range in epsilon. SLAC Experiment E140 previously obtained a now well–known precision data set for Rosenbluth–type separations in the deep inelastic regime, with 88 separations covering the ranges $2.5 < W^2 < 29.7$ GeV^2 and $0.6 < Q^2 < 20.0$ GeV^2.

These two data sets, by far the largest available for Rosenbluth separation studies, have recently been evaluated for potential nonlinearities caused by two photon exchange effects. Such effects have been posited as the explanation for the substantial discrepancy in elastic data between form factor results obtained from Rosenbluth separation and polarization transfer methods. Results of this analysis will be presented, including both the measured constraints on the size of such nonlinearities and the epsilon dependence thereof. A detailed study of the delta resonance in particular will also be presented.

Inclusive π^0 Production in Polarized pp Collisions Using the STAR Endcap and Barrel Electromagnetic Calorimeters

Jason C Webb

Indiana University

on behalf of the STAR collaboration.

The two-spin helicity asymmetry A_{LL} for inclusive π^0 production in pp collisions has sensitivity to the gluon's contribution to the proton spin comparable to that attainable by full jet reconstruction [1]. The STAR collaboration has recently added large-acceptance electromagnetic calorimeters with Shower-Maximum detectors which provide discrimination between high-energy π^0's and single photons [2]. Data with longitudinally polarized proton beams have been accumulated with a partial installation of these subsystems in 2004 (sampled luminosity $\approx 0.3\text{pb}^{-1}$ with beam polarizations $\approx 40\%$) and a more complete installation in 2005 ($\approx 3\text{pb}^{-1}$, $\bar{P} \approx 45 - 50\%$). As configured in 2005, the Endcap and Barrel Electromagnetic Calorimeters provide the capability to reconstruct high-p_T π^0's over the pseudorapidity range $0 \leq \eta \leq 2$ with full azimuthal coverage. We present the current status of analyses of these data, with emphasis on π^0 reconstruction algorithms and backgrounds.

[1] B. Jager, M. Stratmann and W. Vogelsang, Phys. Rev. D **70**, 034010 (2004) [arXiv:hep-ph/0404057].

[2] K. H. Ackermann *et al.* [STAR Collaboration], Nucl. Instrum. Meth. A **499**, 624 (2003).

Hadrons, Nuclei, Hypernuclei - Light Quarks

Low Energy Pions in Nuclear Matter and Double-pion Photoproduction in Nuclei

Luis Alvarez Ruso, O. Buss, P. Muehlich, U. Mosel

Institut fur Theoretische Physik, Universitat Giessen

The main interest in reactions where pion pairs are produced close to threshold in the nuclear medium follows from the conjecture that partial restoration of chiral symmetry makes the σ meson lighter and narrower. This would manifest itself in the form of an enhancement of the cross section near the 2π threshold. Photons are the ideal probe for this kind of studies; they penetrate deeper and can test high densities. A recent experiment with photons of energies between 400 and 460 MeV by the TAPS collaboration shows a shift to low $\pi\pi$ invariant masses with increasing target mass (C, Ca, Pb). The effect seems to be present in the $\pi^0\pi^0$ but not in the $\pi^\pm\pi^0$ final state. This has been interpreted as an indication that the $\pi\pi$ interaction in the σ channel is modified.

Our goal has been to study the effects of pion final state interactions (FSI) in this reaction using a coupled-channel transport model based on the semi-classical BUU equation. Produced pions can scatter elastically with the surrounding nucleons, change their charge or be absorbed on their way out of the nucleus.

As a first step we have investigated low energy scattering of pions with nuclei. Implementing different scenarios of in-medium modifications, the pion mean free path in nuclear matter has been obtained and pion absorption simulations have been compared to data for pion kinetic energies between 10 and 130 MeV and different targets (C, Al, Au). The nice agreement with data gives us confidence in applying this semiclassical method at energies as low as 20 MeV.

We have then considered $\pi^0\pi^0$ and $\pi^\pm\pi^0$ photoproduction on nuclei. For the pion-pair production on the nucleons we have used a theoretical model developed in Valencia, which describes well not only the total cross sections but also the differential distributions. We observe that elastic and charge-exchange scattering of the final state pions with the nucleons in the surrounding nuclear medium yields a downward shift of the $\pi\pi$ invariant mass distribution. We show that the target mass dependence of the measured $\pi^0\pi^0$ invariant mass spectrum can be explained without introducing medium effects beyond absorption and quasi-elastic scattering of the final state particles. On the other hand, we find considerable discrepancies with the data in the $\pi^\pm\pi^0$ channel, in part due to the fact that we obtain a large contribution from side feeding from $\pi^+\pi^-$ photoproduction followed by charge exchange. This discrepancy with the data is a standing problem because the apparently stronger pion absorption in the $\pi^\pm\pi^0$ channel than in the $\pi^0\pi^0$ channel, as indicated by the measurements, is not understood.

We conclude that conventional FSI effects play a relevant role in low-energy two-pion photoproduction in nuclei and should be taken to account. Given our present understanding, the observed target mass dependence of the $\pi^0\pi^0$ invariant mass spectrum does not provide an unmistakable evidence of the modification of the $\pi\pi$ interaction at finite nuclear densities.

Application of the mathematical theory of partitions on the description of nuclear and solid state problems

Alfonso M. Anzaldo-Meneses

Universitat Autonoma Metropolitana Mexico D.F.

Important success in solving nuclear and solid state problems has been demonstrated by Alfonso Anzaldo-Meneses, who as the first physicist has applied the mathematical theory of partitions on the description of the nuclear and solid state problems. This mathematical theory of partitions has been originated by Hardy and Ramanujan and established in a book by Andrews. Anzaldo has carried through the application of this theory to the description of the following problems:

.) The description of the pricompound model of nuclear reactions up to 14 MeV neutron energy by taking into account the so-called excitons which firstly have been found by Torlife Ericson using the quantum mechanical perturbation but improve confirmed by Anzaldo using the theory of partitions.

.) Moreover Anzaldo has demonstrated how the nuclear shell structure can be incorporated into the nuclear level density description using the theory of partitions and

.) last but not least it is shown by Anzaldo how the influence of small (nano) metal particles on specific heat and magnetic susceptibility can be calculated by using the theory of partitions. Topic session directed towards nuclei and theory.

Exotic narrow resonance searches in the system ΛK^0_s in p+propane collisions at 10 GeV/c

Petros Zhora Aslanyan

Joint Institute For Nuclear Research, VBLHE

Experimental data from the 2m propane bubble chamber have been analyzed to search for an exotic baryon states, in the ΛK^0_s decay mode for the reaction p+C_3H_8 at 10 GeV/c. The invariant mass spectrum ΛK^0_s observe a narrow peaks at 1750$\pm$18, 1795$\pm$18,1850$\pm$19 MeV/c^2 and full widths of $\Gamma_{exp.}$= 32$\pm$6, 44$\pm$15, 29.0$\pm$8 MeV/c^2. The statistical significance of these peaks has been estimated as 5.6, 3.3 and 3.0 S.D., respectively. There are the small enhancements in mass regions of (1650-1675) and (1925-1950) MeV/c^2. These would be candidates for the N^0 pentaquark or the Ξ^0 states.

Analysis of $U_A(1)$ symmetry breaking and restoration effects on the pseudoscalar meson observables

Pedro Costa[1], M. C. Ruivo[1], C. A. de Sousa[1], Yu. L. Kalinovsky[2]

[1]*Departamento de Física da Universidade de Coimbra, Coimbra, Portugal*
[2]*Laboratory of Information Technologies, Joint Institute for Nuclear Research, Dubna, Russia*

We explore the effects of breaking and restoration of chiral and axial symmetries using an extended three-flavor Nambu-Jona-Lasinio model that incorporates explicitly the axial anomaly through the 't Hooft interaction. We implement a temperature (density) dependence of the anomaly coefficient motivated by lattice results for the topological susceptibility. The spectrum of scalar and pseudoscalar mesons is analyzed bearing in mind the identification of chiral partners and the study of its convergence (see Fig. 1). We also concentrate on the behavior of the mixing angles that give us relevant information on the issue under discussion. The results suggest that the axial part of the symmetry is restored before the possible restoration of the full U(3)⊗U(3) chiral symmetry might occur. We also study the influence of these symmetries on the anomalous decays $\pi^0, \eta \to \gamma\gamma$ at finite temperature or density.

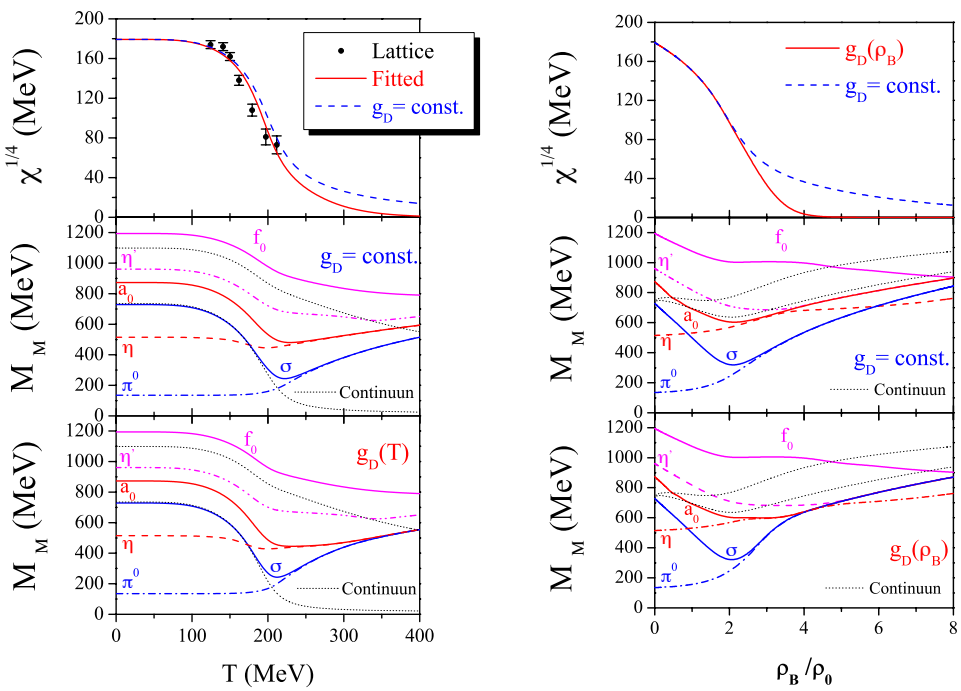

Fig. 1. Topological susceptibility and meson masses as functions of temperature (left panel) and density (right panel), with g_D = cte. and $g_D(T(\rho_B))$.

Energy Dependence on ρ^0 Mass Distribution

Swapan Das
Nuclear Physics Division, B.A.R.C

The rho meson production in the (p, p') reaction on a nucleus can be thought as a potential tool to investigate its in-medium properties. According to the model presented here, the virtual ρ^0 meson, emitted at the $\rho pp'$ vertex, interacts with the nucleus. This interaction places this virtual particle to its mass-shell. The excess momentum of the virtual rho meson is adjusted by the recoiling nucleus. Naturally, the on-shell rho meson in the final state would carry the information about the nuclear medium effect on it.

The T-matrix T_{ch}, describing the mechanism for the present reaction, is given by

$$T_{ch} = \int\int d\mathbf{r}d\mathbf{r}' \; \chi^{(-)*}(\mathbf{k}_\rho, \mathbf{r}')\Pi_\rho(\mathbf{r}')G_\rho(\mathbf{r}' - \mathbf{r})\chi^{(-)*}(\mathbf{k}_{p'}, \mathbf{r})(\bar{N}|\hat{\Gamma}_{\rho NN}|N)\chi^{(+)}(\mathbf{k}_p, \mathbf{r}). \quad (1)$$

Where $(\bar{N}|\hat{\Gamma}_{\rho NN}|N)$ denotes the vertex function for the virtual ρ^0 emission at the $\rho pp'$ vertex. $G_\rho(\mathbf{r}' - \mathbf{r})$ describes the propagation of this virtual rho meson from the production point $\mathbf{r}$ to another point $\mathbf{r}'$, where it gets scattered by the optical potential $V_{O\rho}(\mathbf{r}')$. This potential is appeared in the above equation through the ρ self-energy $\Pi_\rho(\mathbf{r}')[= 2q_0 V_{O\rho}(\mathbf{r}')]$. Here, q_0 denotes the energy of the virtual ρ^0 emitted at the $\rho pp'$ vertex. χs appearing in this equation denote the distorted wave functions for the in-continuum particles, i.e., p, p' and ρ^0.

The calculated double differential cross sections, $\frac{d^2\sigma}{dm d\Omega_{p'}}$, for the ρ^0 mass distribution are presented in the Fig.1.

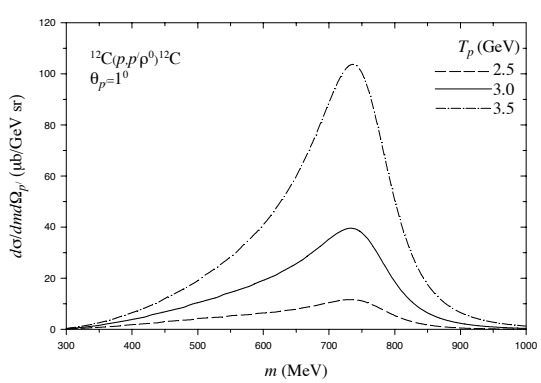

Fig. 1. Beam energy dependence on the cross section

The above figure shows that the calculated cross section increases with the increase in beam energy.

S–wave pion nucleon scattering lengths from πN, pionic hydrogen and deuteron data

M. Doering, E. Oset, M.J. Vicente Vacas
IFIC, University of Valencia

The precise values of the isoscalar and isovector πN scattering lengths are one of the important issues in hadronic physics. Together with low energy πN scattering data they determine parameters of the chiral Lagrangian which allows to make predictions even below πN threshold using chiral perturbation theory.

The scattering lengths (b_0, b_1) are determined [1] using a unitarized coupled channel approach based on chiral Lagrangians. Using experimental values of pionic hydrogen and deuterium as well as low energy πN scattering data, the free parameters of the model are calculated. Isospin violation is incorporated to a certain extent by working with physical particle masses. For the deuterium scattering length $a_{\pi^- d}$ new significant corrections concerning real and imaginary parts are evaluated, putting new constraints from π^-d scattering on the values of (b_0, b_1). In particular, the dispersion correction, the influence of the $\Delta(1232)$ resonance, and crossed terms are considered. Also, the Fermi motion is taken into account. The sum of these effects, together with values from the literature [2], shifts the pion deuteron scattering length $a_{\pi^- d}$ by a value of

$$\Delta a_{\pi^- d} = (104 \pm 24) \cdot 10^{-4} m_\pi^{-1}.$$

In a multiple scattering series, $a_{\pi^- d}$ is then parametrized in terms of the particle channels, and together with the experimental $a_{\pi^- p}$, $a_{\pi^- p \to \pi^0 n}$, and low energy πN scattering data, the parameters of the chiral model are determined, which are the subtraction constants for the meson–baryon loops, an isoscalar piece, and the real part of the loop that is generated by the $\pi N \to \pi\pi N$ reaction.

The findings for (b_0, b_1) are in quantitative agreement with other studies [3,4], although the theoretical error is found to be significantly larger. The isospin breaking from different physical masses is small.

Altogether, a parametrization of the πN potential from zero energy to around 200 MeV above threshold is obtained, that can be used in further studies as the one of pionic atoms.

[1] M. Doring, E. Oset and M. J. Vicente Vacas, Phys. Rev. C **70**, 045203 (2004)

[2] T.E.O. Ericson, B. Loiseau and A.W. Thomas, Phys. Rev. C **66**, 014005 (2002)

[3] S. R. Beane, V. Bernard, E. Epelbaum, U. G. Meissner, and D. R. Phillips, Nucl. Phys. A **720**, 399 (2003)

[4] J. Gasser, M. A. Ivanov, E. Lipartia, M. Mojzis and A. Rusetsky, Eur. Phys. J. C **26**, 13 (2002)

NNbar bound states in a constituent quark model

David R Entem, F. Fernndez
Universidad de Salamanca

The recent observation of a near threshold narrow enhancement in the $p\bar{p}$ invariant mass spectrum from the radiative $J/\psi \to \gamma p\bar{p}$ decay by the BES collaboration [1] has renewed the interest for the $p\bar{p}$ interaction and the possible baryonium states. If the near threshold enhancement is fitted with an S-wave Breit-Wigner resonance function the resulting peak mass is $M = 1859 \pm 6$MeV below $2m_p$. If a P-wave fit is performed the peak mass is very close to the threshold, $M = 1876 \pm 0.9$MeV, with a very narrow width $\Gamma = 4.6 \pm 1.8$MeV. The photon polar angle distribution is consistent with $1 + \cos^2\vartheta$ which suggest that the angular momentum is very likely to be J=0. So this structure may have quantum numbers $J^{pc} = 0^{-+}$ or $J^{pc} = 0^{++}$ which do not correspond to any known meson resonance. The purpose of this contribution is to look for bound states or near threshold resonances in the $p\bar{p}$ scattering. To do that we use a t-channel $N\bar{N}$ potential derived by G-parity transformation of a quark model NN potential which has been shown very successful to describe the NN phase shifts and the hadron phenomenology[2]. The use of this potential avoid the strong attraction generated by the G-parity transform of the ω exchange appearing in the conventional meson exchange models. Annihilation is taken into account by a complex interaction being the real part generated by a s-channel one-pion and one-gluon exchange and taken the imaginary part as an energy independent potential of gaussian form $iW_i e^{-\frac{q^2 b'^2}{3}}$. The two parameters of this potential are fixed to reproduce the $p\bar{p}$ annihilation cross section. This parametrization allows us to reproduce the $p\bar{p}$ total cross section and the total and annihilation $p\bar{n}$ cross sections, showing that our potential has the right real part and isospin dependence. Solving the Schrödinger equation we do not find any bound state in S or P waves. Above threshold only one resonance on the $^3P_0$ partial wave with isospin 0 appears, having a mass of $M = 1895.0$ MeV and a width of $\Gamma = 16.8$ MeV, and being OPE the most important contribution in this partial wave. Without the optical potential the resonance appears like a bound state 1.3 MeV below the $p\bar{p}$ threshold. We discuss the relationship between this resonance and the large shift observed for the $^3P_0$ state in protonium.

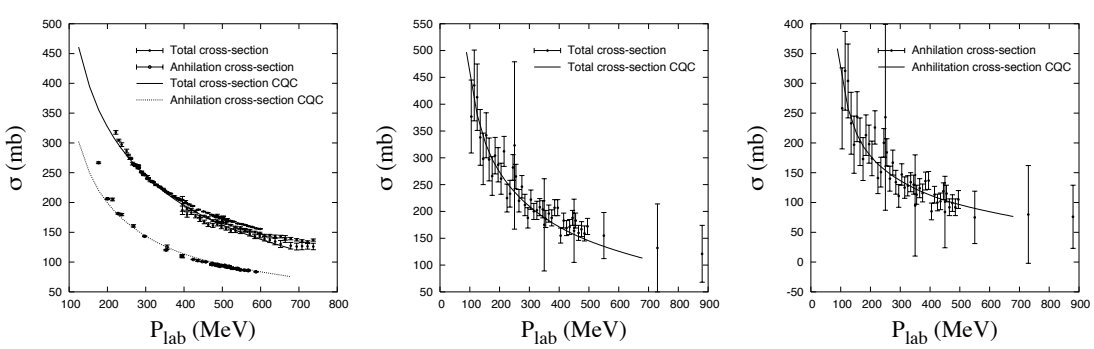

[1] BES Collaboration, Phys. Rev Lett. **91**, 22001 (2003).

[2] D.R. Entem, F. Fernández and A. Valcarce, Phys. Rev. C **62**, 034002 (2000); A. Valcarce, H. Garcilazo, F. Fernández and P. González, Rep. Prog. Phys. **68**, 965 (2005); J. Vijande, F. Fernández and A. Valcarce, J. Phys. G **19**, 2013 (2005).

Hadronic Range Effects in πN Scattering at Threshold

Torleif E. O. Ericson[1], B. Loiseau[2], S. Wycech[3]

[1]*Theory Division, CERN, CH-1211 Geneva 23, Switzerland*
[2]*LPTE, F-75252 Paris, France*
[3]*Soltan Institute for Nuclear Studies, PL-00681 Warsaw. Poland*

We have previously demonstrated that the iteration of the Coulomb interaction in the scattering of a charged pion on a nucleon near threshold generates model independent contributions to the threshold πN amplitude as a consequence of gauge invariance [1]. This assumes a short range interaction whatever its origin as compared to the combined (π^-p) charge distribution. In terms of the Coulomb and hadronic scattering lengths a_C and a^h and of the hadronic range parameter b^h one has:

$$a_C = a^h(1-2\mu\alpha a^h\langle r\rangle_{em}) + 2\mu\alpha\langle 1/r\rangle_{em} b^h - 2\mu\alpha(a^h)^2\left[\log(\alpha) + 2\gamma - 1 + \langle\log(2\mu r)\rangle_{em}\right] . \quad (1)$$

Here, the low energy expansion of the hadronic amplitude is $\tan\delta^h_{l=0}/q = a^h + b^h q^2 + ..$. The physical modifications in Eq. (1) correspond to the correct wave function for an extended charge at the origin, to the shift in energy due to the Coulomb potential of the extended charge at the origin and to the cusp-like renormalization of the wave function due to final state interaction in the Coulomb field, respectively. We made plausible that the approximation was a good one, but we could not provide an expansion in terns of a small parameter. Here we show that the crucial finite range parameter is $\frac{1}{2}\langle r^2_{str}\rangle/(\langle r^2_\pi\rangle + \langle r^2_p\rangle) \simeq 1/6$. This small parameter means that the Coulomb contributions of Eq. (1) can be removed from the (complex) Coulomb scattering length derived from the π^-p atom without loss of information at the present level of precision.

The contributions discussed above do not assume any particular theory apart from the range condition. It can be applied formally to any consistent theory under the same conditions and in particular to Chiral EFT. It corresponds in this case to the full non-perturbative amplitude. However, since the contribution from form factors depend on the full momentum shape, this should be correctly represented. They generate mostly explicit values for chiral constants in an expansion under the same conditions. We compare to the results of Ref. [2] in the heavy baryon limit. Counting EFT powers in the usual way, the extended wave function correction $-\alpha\mu a^h\langle r\rangle$ is a term of 3rd order, while the Coulomb energy one $\mu\alpha a^h\langle(1/r)\rangle$ is of 2nd order. The charge distribution dependence of the double scattering term $-\alpha\mu(a^h)^2\langle\ln\mu r\rangle$ is of 4th order. The Coulomb term can be linked to the chiral constant f_2 related to the np e. m. mass difference in the heavy baryon limit [3]. Although beyond experimental accuracy, perfect consistency requires the following relation between the strong isovector form factor and e. m. ones: $F^-_{str}(q^2)F_\pi(q^2) = F_{1;p}(q^2)$. With the empirical values for the pion and proton form factors, this suggests that the isovector strong form factor is implicitly governed by the ρ-meson mass by this chiral relation.

References

[1] T. E. O. Ericson, B. Loiseau and S. Wycech, Phys. Lett. **B 594**, 76 (2004).

[2] J. Gasser, *et al.*, Eur. Phys. J. C **26** (2002) 13.

[3] V. E. Lyubovitskij and A. Rusetsky, Phys. Lett. B **494**, 9 (2000).

Isospin Breaking in πN Scattering at Threshold

Torleif E. O. Ericson[1], A. Ivanov[2], B. Loiseau[3], S. Wycech[4]

[1]*Theory Division, CERN, Geneva*
[2]*Atomic Institute and SMI of Austrian Academy of Sciences, A-1040 Wien, Austria*
[3]*LPNHE, F-75252, Paris, France*
[4]*Soltan Institute for Nuclear Studies, PL-00681 Warsaw, Poland*

The present high precision in the measurements of the strong interaction shift and width in pionic hydrogen and deuterium opens the possibility to realistically test isospin symmetry relations for the threshold elastic πN amplitudes.

Recent advances in the theoretical understanding of the symmetry breaking [1,2] suggest a classification of the mechanisms as follows:

Class I : Kinematic mass effects and external e. m breaking.

Class I.a. Kinematic effects due to physical mass differences [3].

Class I.b. Effects induced by the symmetry breaking by the iterated Coulomb field [1].

Class II. Symmetry breaking from internal structure.

Class II.a. Strong e. m breaking, such as that due to quark mass differences [3].

Class II.b. Internal e. m. breaking, such as that due to an internal photon [2].

A meaningful test of Class II violating terms requires that the contributions from Class I terms are well understood and under control. We examine the violating terms both from the view point of Chiral Perturbation Theory (ChPt) as well as from that of gauge invariance applied to the hadronic amplitude. In the analysis, we follow the philosophy of Fettes et al. [3] for the relevant ratios of amplitudes. As pointed out in Ref. [3], kinematic identity in the amplitudes is crucial to a meaningful test. We work as in Ref. [3] in the heavy baryon limit using amplitudes with the pion energies $\omega_{i,f}$ averaged over their initial and final state values. We discuss this situation for different scenarios involving first the expected violation based purely on effects from Class I. We use the πN low energy expansion together with gauge invariance in different approximations corresponding to different orders in the chiral EFT expansion. We then compare these results to the predictions of Class II terms. We identify and discuss the critical points for a realistic test of isospin symmetry at threshold. The physical mechanisms of the breaking effects are emphasized.

References

[1] T. E. O. Ericson, B. Loiseau and S. Wycech, Phys. Lett. **B 594**, 76 (2004).

[2] T. E. O. Ericson and A. N. Ivanov, hep-ph/0503277.

[3] N. Fettes, Ulf–G. Meißner, and S. Steininger, Phys. Lett. B **451**, 233 (1999); N. Fettes and U.–G. Meißner, Phys. Rev. **C 63** 045201 (2001); (hep-ph/0008181).

Strange Tribaryons

T. Fernandez Carames[1], A. Valcarce[2], H. Garcilazo[3], P. Gonzalez[1]

[1]*Universidad de Valencia*
[2]*Universidad de Salamanca*
[3]*IPN, Mejico*

Recently an exotic tribaryon resonance $S^0(3115)$ has been discovered using the stopped K^- absorption experiment, $^4He(K^-_{stopped}, p)$, at KEK-PS [1]. The proton energy distribution shows a monoenergetic peak, with a significance of 13σ, interpreted as the formation of a new kind of neutral tribaryon with isospin $I = 1$ and strangeness $S = -1$. The extracted mass and width of the state are $3117.0^{+1.5}_{-4.4}$ MeV and $<$ 21 MeV, respectively, and its main decay mode is found to be ΣNN. The recent detailed analysis of the neutron spectrum in $^4He(K^-_{stopped}, n)$ [2] has made manifest a second monoenergetic peak assigned to the formation of another strange tribaryon $S^+(3140)$ with a significance of 3.7σ. The mass and width of this state are deduced to be $3140.5^{+3.0}_{-0.8}$(syst) $\pm$ 2.3(stat) MeV and $<$ 21.6 MeV, respectively, its main decay mode being $\Sigma^{\pm}NN$. The isospin of the state is assigned to be zero. The experimental determination of spin-parity of these strange tribaryons is awaited.

In this work we study the possible existence of tribaryon resonances in the ΣNN system. For this purpose we follow the same procedure that we used in the past to study three-body systems made of N's and Δ's. The three-body calculations are performed using a truncated T-matrix approximation where the inputs of the three-body equations are the two-body T-matrices truncated such that the orbital angular momentum in the initial and final states is equal to zero. These two-body T-matrices, however, have been constructed taking into account the coupling to the $\ell = 2$ states due to the tensor force. This approximation in the case of the three-nucleon system, with the NN interaction taken as the Reid soft-core potential, leads to a triton binding energy which differs less than 1 MeV from the exact value. Like in our previous studies of the bound-state problem of the $NN\Delta$, $N\Delta\Delta$, and $\Delta\Delta\Delta$ systems we deal with real integral equations since we do not consider the imaginary terms arising from the coupling of the baryon-baryon subsystems to lower mass channels. Thus, in this work we neglect the imaginary terms arising from the coupling of the ΣN subsystem to the ΛN channel. The real terms arising from the $\Sigma N \to \Lambda N$ transition are taken into account in an effective way since our potentials are fitted to the $\Sigma N \to \Sigma N$ cross section.

The two-body interactions correctly reproduce the low-energy observables of the NN and ΣN systems. We have not found any ΣNN bound state. However, our results show that there are only two attractive $S-$ wave channels, they are the $(I, J) = (1, 1/2)$ and $(0, 1/2)$, with a resonance close above the three-body threshold. The channel with $I = 1$ is always more attractive than that with $I = 0$. The isospin quantum numbers and the energy ordering correspond exactly to the recently measured strange tribaryons from the $^4He(K^-_{stopped}, N)$ reactions in the KEK PS E471 experiment. We predict quantum numbers $J^{\pi} = 1/2^+$ for the two reported strange tribaryon resonances. The awaited experimental determination of J^{π} can serve as a stringent test of our model dynamics against others.

[1] T. Suzuki *et al.*, Phys. Lett. B **597**, 263 (2004).

[2] T. Suzuki *et al.*, nucl-ex/0501013. M. Iwasaki *et al.*, nucl-ex/0310018.

Observation of a K^-pp bound state and future prospects at the FINUDA

Hiroyuki Fujioka

Department of Physics, University of Tokyo

on behalf of the FINUDA collaboration.

The FINUDA experiment mainly aims to study the Λ-hypernuclear spectroscopy and its decay processes with the (K^-_{stop}, π^-) reaction [1], where the negative kaon is abundantly provided by the e^+e^- collider DAΦNE as a decay particle of a $\phi(1020)$ meson. The kaon has the momentum as slow as $\sim 127\,\mathrm{MeV/c}$ and can be stopped in a very thin nuclear target ($\sim 0.2\,\mathrm{mg/cm^2}$), which enables us to have a good momentum resolution for emitted particles from the reaction vertex. The FINUDA spectrometer covers a solid angle larger than 2π sr, which allows us to detect multi-particles. These features also have advantages to look for a deeply-bound kaonic state formed in the stopped K^- reactions; the most important is to detect a Λ hyperon through the $\Lambda \to p + \pi^-$ decay. We chose 5 kinds of targets (^{6}Li, ^{7}Li, ^{12}C, ^{27}Al and ^{51}V) in the first run (2003–2004). We have succeeded to observe a deeply-bound K^-pp state through the decay into $\Lambda + p$ [2]. The Λ and proton clearly showed back-to-back angular correlations for various targets, which suggests the K^-pp system is produced as a fragment in the stopped K^- reaction. The binding energy and the width were obtained from the invariant mass of the $\Lambda + p$ system (Fig. 1). In this talk, I will discuss the detail of this decay mode and the prospects in the coming run in 2006.

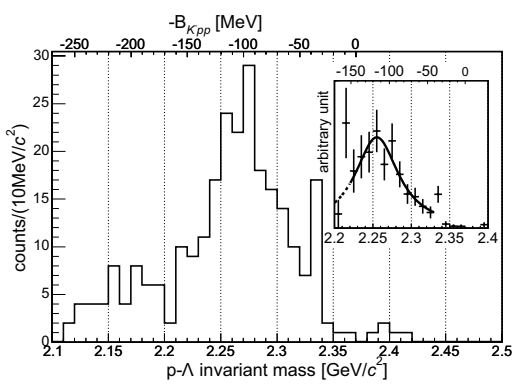

Fig. 1. Invariant mass of a Λ and a proton in back-to-back correlation from lithium and carbon targets before the acceptance correction. The inset shows the result after the acceptance correction.

References

[1] M. Agnello *et al.*, Phys. Lett. B **622**, 35 (2005).

[2] M. Agnello *et al.*, Phys. Rev. Lett. **94**, 212303 (2005).

Pentaquark traces in kaon-nuclear phenomenology

Avraham Gal[1], Eli Friedman[2]

[1]*Racah Institute of Physics, Hebrew University, Jerusalem*
[2]*Racah Institute of Physics, Hebrew University, Jerusalem*

Substantially improved fits to K^+ - nucleus integral cross-section data were obtained, as shown in Fig.1, by incorporating also *true* K^+ absorption into the K^+ - nucleus optical potential [1]. The derived upper bound on the absorption cross section per nucleon, $\sigma_{abs}^{(K^+)}/A \sim 3.5$ mb, may be relegated to the underlying microscopic absorption reaction $K^+nN \to \Theta^+(1540)N$. It was estimated that $\sigma(K^+d \to \Theta^+p)$ is a fraction of millibarn.

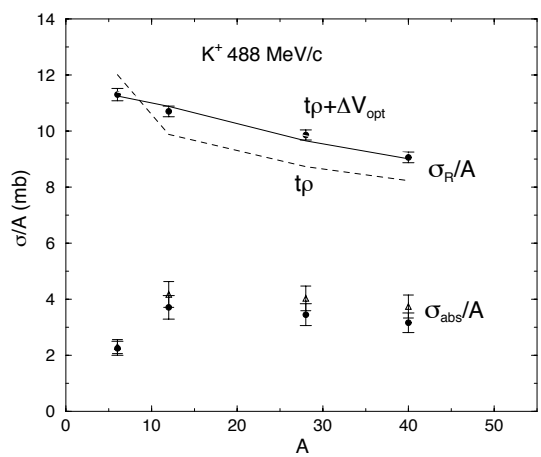

Fig. 1. Fits to K^+ reaction cross sections and derived K^+ absorption cross sections

In this presentation we demonstrate that our conclusions remain in effect also when differential cross sections are included in the fit (potential 3 in Fig.2), and offer a comprehensive discussion of suggested relevant experiments with K^+ beams.

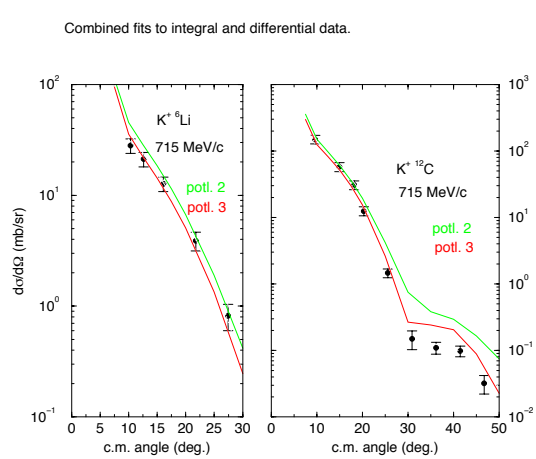

Fig. 2. Combined fits to integral and differential cross sections at 715 MeV/c

Spectroscopy of the superheavy hydrogen isotopes $^{4-7}$H

Yuri Gurov *et al.*

Moscow Engineering Physics Institute (State University)

The formation of superheavy hydrogen isotopes was studied in the reactions induced by stopped π^--mesons absorbed by the ^{9}Be and ^{11}B nuclei. The experiment was carried out at the LEP channel of the LAMPF with a multilayer semiconductor spectrometer [1]. Structures, associated with resonance states in $^{4-7}$H have been observed in the missing mass spectra obtained in correlation measurements of the particles pairs (p, d, t, ^{3,4}He).

Three resonance states of the ^{4}H were observed in the reaction channel ^{9}Be(π^-,dt)X. The missing mass spectrum is consistent with the ^{4}H ground state at E_r =1.6±0.1 MeV, and of reduced width ^{2} = 0.4±0.1 MeV. When these results are compared with the data obtained in other experiments, it is apparent that the ^{4}H is more bound and narrow.

Peaks in missing mass spectra for the ^{9}Be(π^-,pt)X and ^{9}Be(π^-,dd)X reactions were attributed to the ^{5}H resonance states. The lowest state was observed at E_r = 5.5±0.2 MeV (Γ = 5.4±0.5 MeV). All three excited states are above the threshold of the ^{5}H decay into five nucleons.

Four states of ^{6}H were proposed in the reaction channels ^{9}Be(π^-,pd)X and ^{11}B(π^-,p^{4}He)X. The lowest state was observed at E_r = 6.6±0.7 MeV (Γ = 5.5±2.0 MeV). Excited states of ^{6}H are observed for the first time. As for ^{5}H these states are above the threshold of the decay into nucleons.

Bound states of ^{7}H were not observed in the ^{9}Be(π^-,pp)X reaction. Some evidences were obtained for high-excited states at E_r = 16±1 MeV ($\Gamma \cong$ 2 MeV) and E_r = 21±1 MeV ($\Gamma \cong$ 5 MeV).

The work was supported by the CRDF grant NMO-011-0 and the “Russian Universities” grant RU.02.01.147.

References

1. M.G.Gornov et al., NIM, A466, 461 (2000).

Structure and Formation of Mesic Atoms and Mesic Nuclei

Satoru Hirenzaki

Dept. of Physics, Nara Women's University

The light pseudoscalar mesons are interpreted as the Nambu-Goldstone bosons and their properties, especially meson mass spectra, are explained as the consequences of the symmetry breaking pattern of QCD in vacuum. Thus, it seems very interesting to study the meson properties in nucleus to obtain new information on chiral dynamics at finite density, especially the partial restoration of chiral symmetry around normal nuclear density. In this context, meson-nucleus bound systems (mesic atoms and mesic nuclei) are one of the most interesting systems. We study the structure and formation of these systems and discuss the experimental feasibilities.

References

(1) H. Nagahiro, D. Jido, S. Hirenzaki; 'Formation of mesic nuclei by (gamma, p) reactions'; Nuclear Physica A, accepted; nucl-th/0504081.

(2) H. Nagahiro and S. Hirenzaki; 'Formation of Eta'(958)-mesic nuclei and axial U(1) anomaly at finite density '; Phys. Rev. Lett. 94 (2005) 232503 1-4.

(3) J. Yamagata, H. Nagahiro, Y. Okumura, S. Hirenzaki; 'Formation of kaonic atoms and kaonic nuclei by In-flight (K,p) reactions'; Progress of Theoretical Physics, accepted; nucl-th/0503039.

(4) K.Suzuki, M.Fujita, H.Geissel, H.Gilg, A.Gillitzer, R.S.Hayano, S.Hirenzaki, K.Itahashi, M.Iwasaki, P.Kienle, M.Matos, G.M"unzenberg, T.Ohtsubo, M.Sato, M.Shindo, T.Suzuki, H.Weick, M.Winkler, T.Yamazaki,T.Yoneyama; 'Precision spectroscopy of pionic 1s states of Sn nuclei and evidence for partial restoration of chiral symmetry in the nuclear medium'; Phys. Rev. Lett. 92 (2004) 072302 1-4.

(5)H. Nagahiro, D. Jido, S. Hirenzaki; 'Eta-Nucleus interactions and in-medium properties of N*(1535) in chiral models'; Phys. Rev. C68 (2003) 035205 1-9.

(6) D. Jido, H. Nagahiro, S. Hirenzaki; 'Medium effects to N(1535) resonance and eta mesic nuclei'; Phys. Rev. C66, 045202 (2002).

(7) H. Geissel, H. Gilg, A. Gillitzer, R. S. Hayano, S. Hirenzaki, K. Itahashi, M. Iwasaki, P. Kienle, M. Mu"nch, G. Mu"zenberg, W, Schott, K. Suzuki, D. Tomono, H. Weich, T. Yamazaki, T. Yoneyama; 'Experimental indication of a reduced chiral order parameter from the 1s pi- state in 205Pb'; Phys. Lett. B549, 64-71 (2002).

Nucleon electromagnetic form factors in nuclear matter.

Tai Horikawa, W.Bentz
Tokai University

We use the quark-diquark picture to construct the nucleon, and calculate its electromagnetic form factors. Furthermore, we estimate the medium effects for electromagnetic form factors by using the equation of state of nuclear matter in the mean field approximation. In this contribution, I explain the effect of the diquark intrinsic form factor, and the renormalization from the vector meson and pion cloud around the constituent quarks.

Phenomenology of spin 3/2 baryons with pentaquarks

Tetsuo Hyodo, Atsushi Hosaka
RCNP (Research Center for Nuclear Physics)

We examine several assignments of spin and parity for the pentaquark Θ^+ state ($J^P = 1/2^\pm, 3/2^\pm$) in connection with known baryon resonances. Assuming that the Θ^+ belongs to an antidecuplet representation which mixes with an octet, we calculate the mass spectra of the flavor partners of the Θ^+ based on the SU(3) symmetry. The decay widths of the Θ^+ and nucleon partners are analyzed for the consistency check of the mixing angle obtained from the masses. It is found that a suitable choice of the mixing angle successfully reproduces the observed masses of $\Theta(1540)$ and $\Xi_{3/2}(1860)$, when their spin and parity are assigned to be $J^P = 3/2^-$, together with other $J^P = 3/2^-$ resonances. The decay widths of $\Theta \to KN$, $N(1520) \to \pi N$, and $N(1700) \to \pi N$ are also reproduced simultaneously[1].

References

[1] T. Hyodo and A. Hosaka, Phys. Rev. **D71**, 054017 (2005), hep-ph/0502093.

Multibarion excitation - evidence for the QCD degree of freedom in nuclear reactions ?

Vladimir I. Komarov
DLNP, JINR Dubna

There exists a wide range of data on proton-nucleus collisions at high energy-momentum transfers to few-nucleon groups (the lightest nuclei or clusters inside nuclei) where specific features are observed, that are not yet reproduced within any comprehensive meson-nucleon approach. We have analyzed two types of such data - on subthreshold particle production and on the emission of protons with momenta far beyond the kinematical boundary for the free NN-collision. A phenomenological model [ROC-model, H. Mueller, Z.Phys. **A353**(1995)103; Eur. Phys. J. **C18**(2001)563] was used. The main idea of the model consists in considering both nucleons and few-nucleon groups equally as hadrons which may be excited by a projectile hadron. Subsequent decay of the excited states proceeds in accordance with quark statistics. Momentum- energy conservation is satisfied at all stages of the process and any poorly known factors, such as high-momentum components of the nuclei, medium modification of the particle properties, etc, are eliminated from consideration. A small set of free parameters is fixed, mainly by fitting them to the pp-data and scaling to the few-nucleon groups. Then, a wide range of experimental data [Y. Sugaya et al., Nucl. Phys. **A634**(1998)115] on subthreshold antiproton production may be reproduced along with pion and kaon production for various initial energies, momentum spectra, projectile types ($p, d, {}^4He$), target mass- numbers [V. Komarov et al., J.Phys. **G30**(2004)921; H. Mueller and V.Komarov, J.Phys. **G30**(2004)1379; J.Phys. **G31**(2005)285]. With the same parameters of the multibaryon excitations, the model describes data on backward production of fast protons at 1 GeV. The possibility of reproducing similar data at 400 GeV is considered, too. Characteristic properties of multibaryon excitations revealed in such reproduction of experimental data may be treated as a strong hint for it being desirable to consider them within the npQCD approach. It is quite reasonable since the typical excitation energies are sufficient for rearrangement of the quark structure of nucleons, and the high density required for fusion of the quark-gluon content of several nucleons may be found in the ground state of nuclei, due to density fluctuation of nuclear matter or produced by its scraping by a fast projectile. It means that the events of interest may be generated already at intermediate energies and be selected by criteria of energy transfers to few-nucleon groups higher than ~ 0.3 GeV and momentum transfers $>\sim 2\ \mathrm{fm}^{-1}$. The relatively low multiplicity of secondaries in such conditions allows a complete kinematical reconstruction of events and therefore, the direct measurement of the continues excitation spectrum of the multibaryon system, momentum transfer to it, decay channels, spectra of the decay products. It may be stressed that the information is not obscured by the complicated scenario of the process, as it reveals in the production and decay of quark-gluon plasma at heavy-nuclei collisions. An appropriate systematic study, experimental and theoretical, of the phenomena of transition from nucleon-meson systems to multibaryons with a common quark-gluon content would contribute a new field for applying efforts in resolving the problem of the QCD structure of vacuum and hadrons.

Pentaquarks as Chiral Solitons and as Multiquark States

Vladimir Benedikt Kopeliovich,
Institute for Nuclear research of Russian Academy of Sciences

The spectra of pentaquarks are discussed within chiral (topological) soliton model and compared with simplified quark picture. Similarity of spectra of baryon resonances obtained within quark model and chiral soliton model takes place, especially for higher multiplets. Certain differences take place as well, which require careful interpretation. In particular, considerable variation of strange antiquark mass in different SU(3) multiplets of pentaquarks is required to fit their spectra obtained from chiral solitons, as well as difference of energies of ”good” and ”bad” diquarks. The partners of lowest exotic states with different values of spin, which belong to higher SU(3) multiplets, have the energy considerably higher than that of lowest states, and this could be a point where the difference from simple quark models is striking. Some deficiences in the argumentation against validity of the chiral soliton approach, existing in the literature, are pointed out. Different quantization schemes of chiral solitons lead to considerable spread in position of exotic baryon states, which could make easier comparison with existing and future data.

Flavored Multibaryons and Hypernuclei in Topological Soliton Model

Vladimir Benedikt Kopeliovich,
Institute for Nuclear research of Russian Academy of Sciences

The binding energies of the ground states of strange (S=-1) hypernuclei are calculated in the ”rigid oscillator” version of the bound state soliton model, proposed by Klebanov and Westerberg [1]. Good qualitative and even quantitative agreement has been reached for light hypernuclei, with atomic numbers up to 12 [2]. The binding energies of charmed and beautiful hypernuclei are found to be greater than that of strange hypernuclei [2].

The energies of baryon states with positive strangeness, or anti-charm (-beauty) are estimated within same approach [3]. Positive strangeness states can appear as relatively narrow nuclear levels (Theta-hypernuclei), the states with heavy anti-flavors can be bound with respect to strong interactions in the original Skyrme variant of the model (SK4 variant). The binding energies of anti-flavored states are estimated also in the variant of the model with 6-th order term in chiral derivatives in the lagrangian as solitons stabilizer (SK6 variant). The latter variant is less attractive, and nuclear states with anti-charm or anti-beauty can be unstable relative to strong interactions. The chances to get bound hypernuclei with heavy antiflavors are greater within ”nuclear variant” of the model with rescaled model parameter (Skyrme constant e or e’ decreased by 30expected to be valid for baryon numbers greater than B 10. The rational map approximation is used to describe multiskyrmions with baryon number up to 30 and to calculate the quantities necessary for their quantization (moments of inertia, sigma-term, etc.).

1. K.M.Westerberg and I.R.Klebanov, Phys. Rev. D50, 5834 (1994)
2. V.B.Kopeliovich, JETP 96, 782 (2003); nucl-th/0209040
3. V.B.Kopeliovich and A.M.Shunderuk, JETP 100, 929 (2005); nucl-th/0409010

Quasielastic Knock out of Light Nuclear Fragments from C-12 and O-16 by Intermediate Energy Pions

Vyacheslav Kulikov, et al.

Institute of Theoretical and Experimental Physics

on behalf of the MTS collaboration.

The quasielastic deuteron and triton knock out from ^{12}C and ^{16}O has been studied at pion beam of 0.72 GeV/c in full kinematics. Momentum distributions of the intranuclear motion of quasideuterons, excitation energy spectra of the rest nuclei and values of quasideuteron effective numbers were obtained. Parameters of quasideuteron intranuclear motion are in a reasonable agreement with the measurements made at other beams. Quasideuteron effective numbers in nuclei from ^{6}Li to ^{16}O, measured in full kinematics, are practically independent from atomic number that is different from inclusive deuteron knock out by protons. Triton knock out from these nuclei has been seen. It made possible to estimate the backward pion triton elastic scattering not measured yet at so high energy and momentum transfer.

Strange Dibaryons and Tribaryons as Hexa- and Nona-Quark States

Yuu Maezawa, Tetsuo Hatsuda, Shoichi Sasaki
Department of Physics, The University of Tokyo

Recently, an exotic tribaryon state $S^0(3115)$ was reported with $13\,\sigma$ significance level in a stopped K^- absorption, $K^- + {}^4He \to S^0 + p$, at KEK-PS [PLB **597** 263]. S^0 has the baryon number $B = 3$ and the strangeness $S = -1$. The mass is approximately 3115 MeV (111 MeV below the K^-pnn threshold) with the decay width less than 21 MeV. Moreover, an exotic dibaryon state with $B = 2$ and $S = -1$ (the same quantum numbers with K^-pp system), was announced by FINUDA Collaboration [PRL **94** 212303] in K^- absorption reaction on nuclear targets. We call it tentatively as F^+. Its mass is about 2258.5 MeV (115 MeV below the K^-pp threshold) with a width about 67 MeV.

Because of the small widths and large binding energies from the KNN and KNNN thresholds, these states are the strong candidates of deeply bound kaonic nuclei predicted by Akaishi and Yamazaki [PRC **65** 044005], or even the compact multi-quark states [Maezawa, Hatsuda and Sasaki, hep-ph/0412025]. We explore the latter possibility further by identifying $F^+(2260)$ as hexa-quark (six-quark) state with the $(3u)(2d)(1s)$-structure and $S^0(3115)$ as a nona-quark (nine-quark) state with the $(3u)(5d)(1s)$-structure.

For the multi-quark spectra, the color-magnetic interaction, the strange-quark mass, and the flavor-dependent interaction due to pion cloud play crucial roles. By the group theoretical consideration, we find that flavor-multiplets with small dimensions have relatively small masses. Therefore, we identify F^+ and S^0 as a member of the lowest flavor multiplet, (flavor, isospin, spin)=$(8, \frac{1}{2}, 1)$ and $(27, 1, \frac{1}{2})$, respectively. Also we have carried out quantitative investigation on the based of the chiral bag model. Spectral structure for multi-quark dibaryons and tribaryons with the inputs $F^+(2260)$ and $S^0(3115)$ are shown in Fig. 1. From the figure, we conclude that, for the hexa-quark system (a), all states including H dibaryon are *above the hadronic thresholds*, whereas, for the nona-quark system (b), the states in $(8, \frac{1}{2}, \frac{1}{2})$ with $S = -2$ and $(1, 0, \frac{3}{2})$ with $S = -3$ can be *true bound states* below the hadronic thresholds. The latter is due to the strong color-magnetic effect compensating for the $SU_F(3)$ breaking effect.

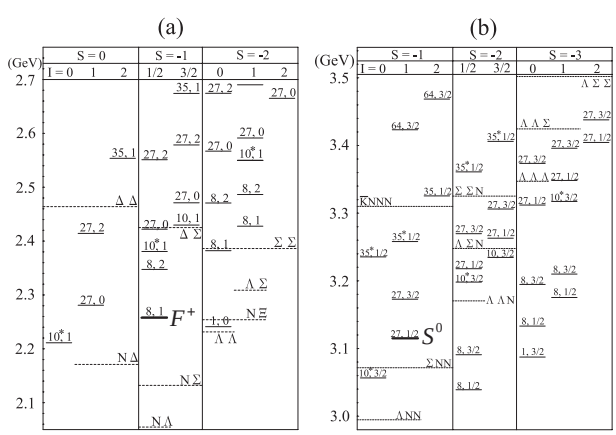

Fig. 1. The mass spectra for (a) the hexa-quark system and (b) the nona-quark system. Flavor multiplet and spin are described on each state.

Radiative Decays of the Υ(1S) to a Photon and Two Charged Tracks

The CLEO Collaboration

Using the CLEO III detector, we report on a new study of exclusive radiative $\Upsilon(1S)$ decays into the final states $\gamma\pi^+\pi^-$, γK^+K^- and $\gamma p\bar{p}$. We present branching ratio and helicity amplitude measurements for the decay modes $\Upsilon(1S) \to \gamma f_2(1270)$ and $\Upsilon(1S) \to \gamma f_2'(1525)$, and upper limits for the decay $\Upsilon(1S) \to \gamma f_J(2200)$ with $f_J(2220) \to \pi^+\pi^-$, K^+K^- and $p\bar{p}$.

Study of Two-Body Radiative $\Upsilon(1S)$ Decays

The CLEO Collaboration

We report on a new study of exclusive radiative decays of the $\Upsilon(1S)$ resonance into the final states $\gamma\pi^0\pi^0$, $\gamma\pi^0\eta$ an $\gamma\eta\eta$ with $\eta \to \gamma\gamma$ which were collected with the CLEO III detector operating at the Cornell Electron Storage Ring. In the channel $\gamma\pi^0\pi^0$ we present branching ratio and helicity amplitude measurements for the decay mode $\Upsilon(1S) \to \gamma f_2(1270)$. In addition, we place upper limits on branching ratios for the isoscalar resonances $f_0(1500)$ and $f_0(1710)$ in the $\pi^0\pi^0$, $\pi^0\eta$ and $\eta\eta$ decay channels.

$\bar{K}$-nuclear deeply bound states in a dynamical model

J. Mares[1], E. Friedman[2], A. Gal[2]

[1]*Nuclear Physics Institute, 250 68 Rez, Czech Republic*
[2]*Racah Institute of Physics, The Hebrew University, Jerusalem 91904, Israel*

New results from DAΦNE suggest deep binding for $\bar{K}$ mesons in light nuclei such as Li and C [1]. Here we explore limits on the possible existence of narrow $\bar{K}$-nuclear states and on their width, in ^{12}C and in other light nuclei, using the RMF model for a system of nucleons and one $\bar{K}$ meson which interact via scalar and vector boson fields [2]. Deeply bound $\bar{K}$-nuclear states are generated dynamically. Substantial polarization of the core nucleus is found in light nuclei. Absorption modes are also included dynamically, considering explicitly both the resulting compressed nuclear density and the reduced phase space for $\bar{K}$ absorption from deeply bound states (top of Fig.1). Varying the strength of $\bar{K}$-nuclear couplings, the behavior of the calculated width as function of the $\bar{K}$ binding energy is studied, as demonstrated in the bottom part of Fig.1 for several RMF versions in ^{12}C and in ^{16}O. The implications for interpreting the FINUDA Collaboration results [1] will be discussed.

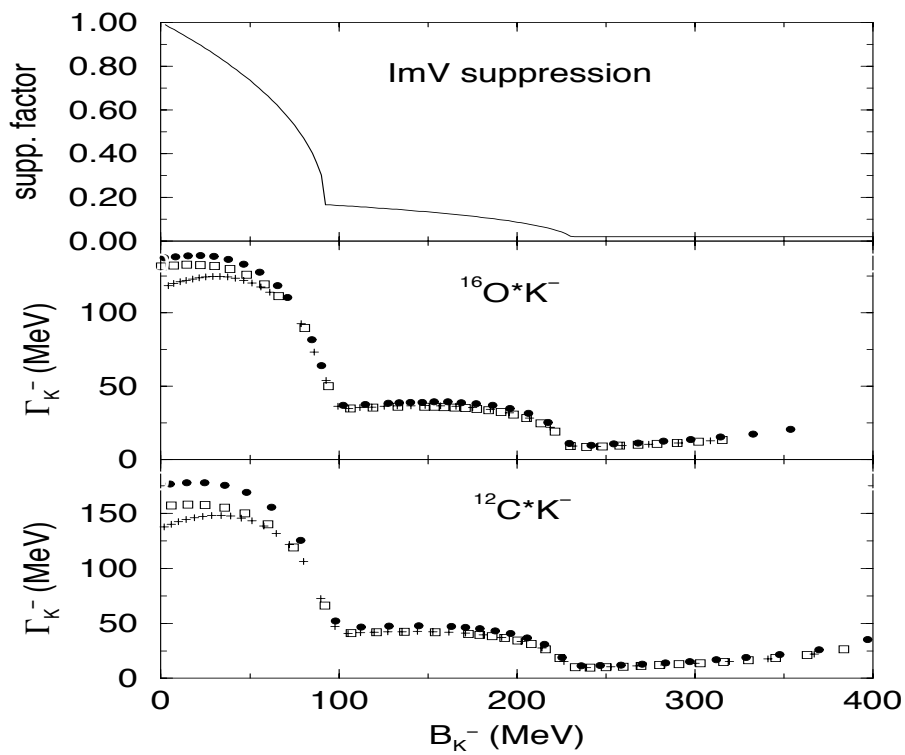

Fig. 1. Phase-space suppression factor for Im V_{opt} (top) and the width of the 1s K^--nuclear state in ^{12}C and in ^{16}O as function of the K^- binding energy [2].

[1] M. Agnello *et al.*, Phys. Rev. Lett. **94** (2005) 212303.
[2] J. Mareš, E. Friedman, A. Gal, Phys. Lett. B **606** (2005) 295.

Neutron-deuteron scattering at 95 MeV - a signature of three-nucleon forces

Philippe Mermod,
Department of Neutron Research, Uppsala University, Sweden

We have measured the full angular distribution of neutron-deuteron elastic scattering at 95 MeV with two independent experimental setups. The results are in very good agreement with predictions based on three-nucleon forces, and incompatible with predictions based on two-nucleon forces only. As by-products of the neutron-deuteron experiments, we obtained also new neutron-proton scattering data.

Radii of Hadrons/Lighter Nuclei and the Geometrical Picture

Mohammad Alam Saeed, Fazal-e-Aleem, Atif Alvi
Centre for High Energy Physics, University of the Punjab

A study of hadronic form factors of proton, deuteron and alpha in the light of geometrical picture is undertaken to account for the internal structure of hadrons/lighter nuclei. These form factors throw light on the distribution of matter inside the hadron/nuclei (deuteron and alpha) reveal interesting information. It is found that radii of deuteron, alpha and proton increase with increase in energy implying that these particles become more opaque at higher energies.

Dynamically generated spin $\frac{3}{2}^-$ resonances from octet meson - decuplet baryon interactions

Sourav Sarkar

IFIC, University of Valencia

The s-wave interactions of the baryon decuplet with the octet of pseudoscalar mesons is studied using the lowest order chiral Lagrangian in a unitarized coupled channel approach. We have perfomed a systematic study of the $\frac{3}{2}^-$ resonances which are generated dynamically by this interaction by searching for poles of the transition matrix in the complex plane in different Riemann sheets. We find two bound states in the $SU(3)$ limit corresponding to the octet and decuplet representations. These are found to split into eight different trajectories in the complex plane when the $SU(3)$ symmetry is broken gradually. Using natural values for the subtraction constants in the meson-baryon loop function, which is the only free parameter in our approach, we are able to provide a reasonable description for a good number of 4-star $\frac{3}{2}^-$ resonances listed by the Particle Data Group. In particular, the $\Xi(1820)$, the $\Lambda(1520)$ and the $\Sigma(1670)$ states are well reproduced. We predict a few other resonances and also evaluate the couplings of the observed resonances to the various channels from the residues at the poles of the scattering matrix which allows us to make predictions for partial decay widths into a decuplet baryon and a meson.

Exclusive Measurements of pp $\rightarrow$ NN$\pi\pi$ from Threshold up to the $\Delta\Delta$ region - Dynamic σ and $\pi\pi$ Low-Mass Enhancement

Tatiana Skorodko, et al.

Physikalisches Institut - Univ. Tübingen

on behalf of the CELSIUS-WASA collaboration.

The $\pi\pi$ production in pp collisions has been measured at CELSIUS in the energy range $T_p = 775 - 1360$ MeV exclusively using the WASA 4π detector with hydrogen pellet target. The WASA detector containing magnetic field, tracking detectors and calorimeter, allows the detection of both charged and neutral particles. This way the measurements were carried out with 4 - 6 overconstraints for the pp$\pi^+\pi^-$ and pp$\pi^0\pi^0$ channels. At energies close to threshold the data can be well described by either the Roper resonance concept or a dynamic formation of the σ meson.

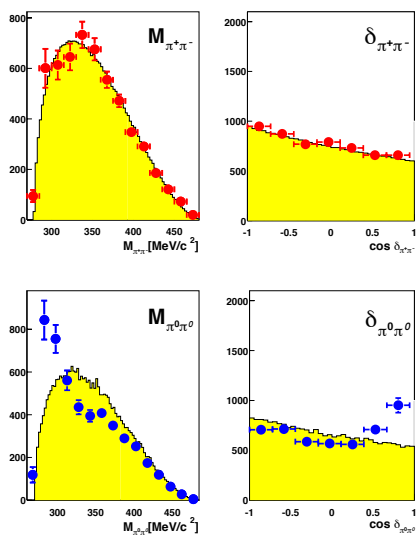

Fig. 1. $\pi\pi$ invariant-mass ($M_{\pi\pi}$) and opening angle ($\delta_{\pi\pi}$) distributions for the $\pi^0\pi^0$ (bottom) and $\pi^+\pi^-$ (top) channels at $T_p = 1100$ MeV. The shaded areas show the phase-space distributions.

At higher energies - above 1 GeV - the formation of the $\Delta\Delta$ system is expected to get dominant. However, the $M_{\pi\pi}$ spectrum does not exhibit the predicted double-hump structure. In the $\pi^+\pi^-$ channel it rather behaves like phase-space, whereas in the $\pi^0\pi^0$ channel it systematically exhibits a pronounced enhancement at small invariant masses accompanied with a corresponding one at small $\pi\pi$ opening angles. A scenario for this enhancement could be the presence of Bose-Einstein correlations (BEC) for identical bosons - as observed in heavy-ion and in elementary reactions.

However, a first analysis of our data on the very difficult to access nn$\pi^+\pi^+$ channel shows no low-mass enhancement there - excluding thus BEC and revealing the observed structure rather as a σ channel phenomenon - in resemblence of the so-called ABC effect, which so far was thought to be present only in bound nuclear systems.

Pentaquarks with spin 1/2 and 3/2 in QCD sum rules

Jun Sugiyama[1], Takumi Doi[2], Makoto Oka[1]

[1]*Tokyo Institute of Technology*
[2]*RIKEN BNL Research Center*

QCD sum rules are derived for pentaquark baryons, Θ^+ and Ξ^{--} with spin 1/2 and 3/2. We focus on its parity because it is closely related with the structure.

It is shown that the positive parity $J = 1/2^+$ state is not allowed in low energy region, while the negative parity $J = 1/2^-$ state of mass around $1.5\mathrm{GeV}$ is obtained. It is pointed out that the obtained state is not clearly separated from the meson-baryon scattering state because it is expected to be broad.

For $J = 3/2$ it is shown that both positive and negative-parity pentaquarks were exist for Θ^+ while neither is obtained for Ξ^{--}. It is found that the sum rules depend on the choice of the interpolating field operator and we discuss which one is suitable. The masses of the Θ^+ pentaquark states are predicted around 1.5 GeV, where the negative parity state is slightly lighter than the positive parity state.

An Experimental Search for Deeply Bound Kaonic Nuclear States

Takatoshi Suzuki

RIKEN

on behalf of the KEK E471 collaboration.

As the first experimental search for deeply bound kbar nuclear states, proton/neutron energy spectra from K^- absorption at rest on liquid helium4 target were measured by means of time-of-flight (KEK-PS E471 experiment).

On the proton side, a very significant peak structure was found in the $^4\mathrm{He}(K^-_{\mathrm{stopped}}, pX)$ spectrum, and it was assigned to the formation of a new kind of neutral strange tribaryon $S^0(3115)$ with total isospin 1. The width was extremely narrow, and the upper limit was estimated to be 21.6 MeV. Since tribaryonic kbar nuclear state with total isospin 1 with triton-like nuclear core $[NNN]_{T=1/2}$ was originally predicted to be shallow and broad, this discovery was quite unexpected. The mass value was deduced to be $3117.7^{+4.7}_{-2.9}$ MeV/c^2, and its main decay mode is ΣNN. If it is interpreted as the $K^-pnn^{T=1}$ state, the binding energy is 193.4 MeV with respect to $K^- + p + n + n$ rest mass. At present, there exist several possible interpretations of this state, and whether this state can be interpreted as one species of $\bar{K}NNN$ states is not definite. This talk is mainly devoted to the analysis and the result of this part, and the $^4\mathrm{He}(K^-_{\mathrm{stopped}}, nX)$ spectra are briefly discussed.

Λ(1405) as a $q^4\bar{q}$ state

Sachiko Takeuchi[1], Kiyotaka Shimizu[2]
[1]*Japan College of Social Work*
[2]*Department of Physics, Sophia University*

Recent experiments with the kaon beam show that there are a few kinds of $\bar{K}$-nuclei which are deeply bound. For example, the binding energy of S^0(3115) is 194 MeV if the state is considered as K^-pnn [1]. It is argued that such a deeply bound state can exist if there is strong attraction between the I=0 $N\bar{K}$ pair: the required attraction is so strong that the Λ(1405) becomes actually the K^-p bound state [2]. It is also reported that the state can also be understood as $N\bar{K}$ and $\Sigma\pi$ states by new data analysis [3].

From the quark model view points, Λ(1405) has been considered as the flavor-singlet q^3 state with the orbital excitation. The calculated mass, however, is usually much heavier than the observed one [4]. In this work, we examine the possibility that Λ(1405) has a $q^4\bar{q}$ component by using the method developed for the pentaquark systems [5].

It is known that the $N\bar{K}$ (IJ^P)=(0 1/2$^-$) state does not have a repulsion from the color-magnetic interaction, CMI. By introducing the mixing among the $q^4\bar{q}$ flavor multiplets, we have found that there are two states where CMI is strongly attractive. In Table 1, a simple estimate with the orbital $(0s)^5$ configuration is shown. $q^4\bar{q}$(A) consists of uds$(u\bar{u}+d\bar{d})$, whose main components are $\Sigma\pi$, $N\bar{K}$, and $\Lambda\eta$. $q^4\bar{q}$(B) is udss$\bar{s}$, which consists mainly of ΞK and $\Lambda\eta$. The pseudoscalar mesons, π and K, are treated as $q\bar{q}$ states in this simple estimate. It seems that the $q^4\bar{q}$(A) may become a bound state of $N\bar{K}$, which can contributes to the observed Λ(1405).

In the present talk, we will discuss the features of the $q^4\bar{q}$ systems with strangeness -1 and (IJ^P)=(0 1/2$^-$). We argue that these components can be important and should be mixed to the q^3 Λ(1405) state.

Table 1
Estimate with the orbital $(0s)^5$ configuration. (in MeV).

	K+N	π+Σ	$q^4\bar{q}$(A)	$q^4\bar{q}$(B)
Quark mass	1774	1774	1774	2191
Kinetic energy	680	664	894	738
CMI	-322	-400	-524	-419
Total-(K+N)	0	-94	13	445

[1] T. Suzuki *et.al*, Phys. Lett. **B597**(2004) 263.
[2] Y. Akaishi and T. Yamazaki, Phys. Rev. **C65**(2002) 044005.
[3] V.K.Magas, *et.al.* hep-ph/0503043.
[4] M. Furuichi, K. Shimizu, and S. Takeuchi, Phys. Rev. **C68**(2003)034001
[5] S. Takeuchi and K. Shimizu, Phys. Rev. **C71**(2005) 062202.

Hypernuclei and Recent Hyperon-Nucleon Potentials

Yiharn Tzeng[1], S.Y. Tsay Tzeng[2], T.T.S. Kuo[3]

[1]*Institute of Physics, Academia Sinica,*
[2]*Department of Photonics, National Taipei University of Technology, Taipei,Taiwan, ROC*
[3]*Department of Physics, State University of New York, Stony Brook,NY11794, USA*

The Nijmegen NSC89 and the recent NSC97 hyperon-nucleon potentials are adopted to study the structures of hypernuclei. Investigations are carried on by using our two-frequency shell model folded diagram approach. We first calculate the YN G matrix with the exact Pauli exclusion operator. The nucleon frequency for the harmonic oscillator basis wave function is chosen from the empirical formula $\hbar\omega_N = 45A^{-1/3} - 25A^{-2/3}$, while the hyperon one is obtained as the frequency when the lowest hyperon single particle energy in the hypernucleus reaches a saturation minimum. The magnitude of $\hbar\omega_N$ is 14 MeV , 11 MeV and that of $\hbar\omega_\Lambda$ is about 10 MeV and 8 MeV for ${}^{16}_{\Lambda}O$ and ${}^{40}_{\Lambda}Ca$ respectively. The energy-independent effective interaction V_{eff} is then obtained from the YN G matrix elements, using a $\hat{Q}$-box folded-diagram framework. The spin-dependence parameters derived from the Nijmegen NSC89 and NSC97f potentials are similar, but both are rather different from those obtained with the $J\ddot{u}lich - B$ potential. We will examine how our calculated spectra vary via these different versions of the realistic hyperon-nucleon potentials. Special attention is drawn on the contribution of the $\Lambda N - \Sigma N$ coupling diagram. Although this diagram contributes significantly to V_{eff} in most cases, it does not alter much to the final spectrum.

In-Flight (K^-, p) Reactions for theFormation of Kaonic Atoms and Kaonic Nuclei

Junko Yamagata[1], Hideko Nagahiro[2], Satoru Hirenzaki[1]

[1]*Department of Physics, Nara Women's University*
[2]*Research Center for Nuclear Physics, Osaka University*

We study the kaonic atom and kaonic nucleus formation by the in-flight (K^-, p) reactions for C, O, Si and Ca target cases theoretically. Deeply bound kaonic atoms were predicted to exist as quasi-stable states and were expected to be observed in some proper experimental methods. Kaonic nuclear states are also expected to exist with large decay widths. We evaluate the formation cross sections of the kaonic atoms and kaonic nuclei using the Green function method with the appropriate energy dependent optical potentials. We will discuss the possibilities to observe the kaonic states in the (K^-, p) reactions based on the realistic theoretical calculations.

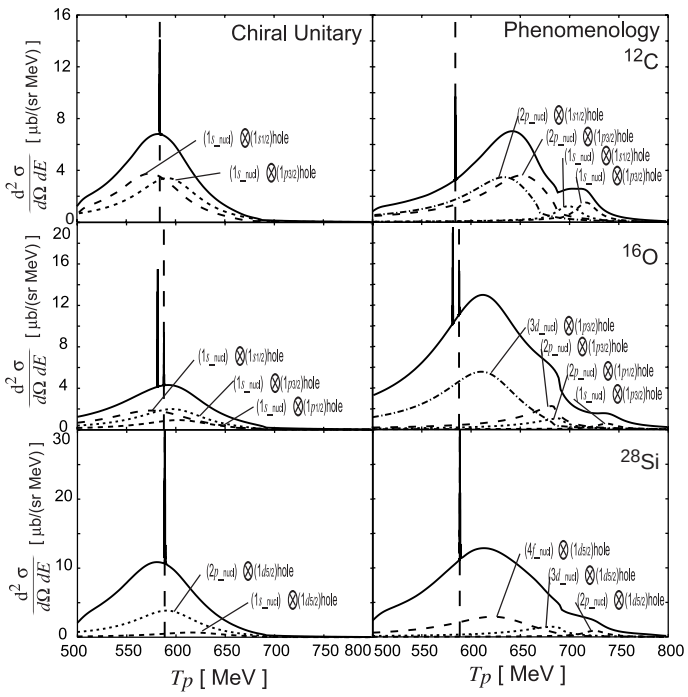

Fig. 1. Kaonic nucleus formation cross sections in ^{12}C, ^{16}O and ^{28}Si(K^-, p) reactions plotted as functions of the emitted proton energies at $\theta_p^{Lab} = 0$ [degrees] and $T_K = 600$ MeV for (left) the chiral unitary model and (right) the phenomenological K-nucleus optical potential. The vertical dashed lines indicate the threshold energies, and the sharp peaks around the threshold are due to the atomic state formations. The energy dependent decay widths for kaonic states are used.

Reference

J. Yamagata, H. Nagahiro, Y. Okumura, S. Hirenzaki, Prog. Theor. Phys. accepted, nucl-th/0503039

Heavy Flavor Physics - Search for New Particles

Leptonic and semileptonic bottom hadron decays

Conrado Albertus, et al.

Departamento de Fisica Moderna, Universidad de Granada

We present different calculations of bottom hadron decays evaluated within the common framework of a nonrelativistic quark model. The reactions include baryon $\Lambda_b \to \Lambda_c$ and $\Xi_b \to \Xi_c$ semileptonic decays [1], leptonic decay of B and B^* mesons [2], semileptonic $B \to D$ and $B \to D^*$ decays [2], and the semileptonic $B \to \pi$ decay [3].

For the $\Lambda_b \to \Lambda_c$ and $\Xi_b \to \Xi_c$ semileptonic decays we used coordinate space wave functions obtained from a variational approach [4] made posible by the simplifications introduced by heavy quark symmetry. We also developed a novel expansion of the electroweak current operator in coordinate space. The calculation of form factors was supplemented with heavy quark effective theory (HQET) constraints. These improvements allowed us to predict form factors and decay distributions for all q^2 values allowed in the physical decays. We could extract the Cabibbo-Kobayashi-Maskawa matrix element $|V_{cb}|$ for which we found a value $|V_{cb}| = 0.40 \pm 0.005(\mathrm{stat})^{+0.001}_{-0.002}(\mathrm{theory})$ in good agreement with a recent determination by the DELPHI Collaboration [5].

Calculations with mesons were done in momentun space. Our values for the vector decay constants $f_{B_s} = 239^{+9}_{-7}$ MeV and $f_{B_s^*} = 236^{+14}_{-11}$ MeV are in very good agreement with lattice QCD [6] and QCD sum rules results [7]. The agreement is not that good for f_B and f_{B^*} for which we obtained the values $f_B = 155^{+15}_{-12}$ MeV and $f_{B^*} = 151^{+15}_{-13}$ MeV while lattice data are in the range 200 ± 30 MeV[8].

In the evaluation of form factors for the $B \to D$ and $B \to D^*$ semileptonic decays we improved the nonrelativistic quark model prediction by imposing HQET constraints. The results are in good agreement with experiment and lattice data close to the zero recoil point. This allows, by comparison to experiment, another independent determination of $|V_{cb}|$. From the $B \to D$ decay we got $|V_{cb}| = 0.040 \pm 0.006$, in perfect agreement with the above determination based on the $\Lambda_b \to \Lambda_c$ semileptonic decay.

The semileptonic $B \to \pi$ decay was studied starting from a simple quark model that included the contribution of the B^* pole. This pole plays a role only near q^2_{max} being strongly suppresed by a soft hadronic vertex that we evaluate within the model. To extent the model to all q^2 values accessible in the physical decay we used a novel multiply-subtracted Omnès dispersion relation. The final results agree with lattice data from the UKQCD and APE Collaborations. The same scheme also leads to excellent results for the $D \to K$ and $D \to \pi$ semileptonic decays.

[1] C. Albertus, E. Hernández and J. Nieves, Phys. Rev. D 71 (2005) 014012.

[2] C. Albertus, E. Hernández, J. Nieves and J.M. Verde Velasco, Phys. Rev. D 71 (2005) 113006.

[3] C. Albertus, J.M. Flynn, E. Hernández, J. Nieves and J.M. Verde-Velasco, Phys. Rev. D in print.

[4] C. Albertus, J.E. Amaro, E. Hernández and J. Nieves, Nucl. Phys. A 740 (2004) 333.

[5] J. Abdallah *et al.* (DELPHI Collaboration), Eur. Phys. J. C 33 (2004) 213.

[6] S. Hashimoto, plenary talk at the 32nd International Conference on High-Energy Physics (ICHEP 2004), hep-ph/0411126.

[7] S. Narison, Phys. Lett. B 520 (2001) 115.

[8] C. Bernard, Nucl. Phys. B Proc. Suppl. 94 (2001) 159.

Recent results on hadronic B decays at BaBar

Babar Collaboration
SLAC

We present recent results on B mesons hadronic decays using 230 million $B\bar{B}$ pairs collected by the BABAR detector at the SLAC PEP-II storage ring. The results include new measurements of rare decays and studies of the decay modes that might be useful for the measurement of CKM parameters.

Origin of the Light Neutral Boson Observed in Heavy Ion Collisions

Mohamed El-Sayed El-Nagdy

on behalf of the EMUO3 collaboration.

We report the results of (e+ e- pairs) produced during the interactions of 200A GeV 32S with emulsion nuclei. The results for the electron pairs suggest that they originate from light neutral bosons emitted during the collision. The origin of such neutral bosons due to de-excitation of the produced fragment 4He, 8Be and 12C resulting in 32S fragmentation. The masses of the neutral bosons were estimated from electron kinematics and found to be equal 1.500.29 and 9.821.52 MeV/c2 and life time of orders 10-15 - 10-16s. The data and results obtained could explain and put conclusion to the puzzles which were going on during the last 50 years around the anomalous mean free path of a-particles produced during high energy particle collisions. The depression of average shower particles muliplicities produced in the collisions of secondary helium fragments as compared to those of primary helium at similar energy put forward as a possible signature of formation of a neutral boson.

Dedicated to the souls of Professors M. El-Nadi and O. E. Badawy of Cairo University, Egypt.

Measurement of B^0 Oscillations

The CDF Collaboration

We report on a measurement of B^0 oscillations using data from $p\bar{p}$ collisions at $\sqrt{s} = 1.96$ TeV recorded by the CDF detector operating at the Fermilab Tevatron. B^0 are measured separately in semileptonic decays, $B0 \rightarrow DlX$, and fully reconstructed decays of the B^0 meson. This sample is also used to calibrate the performance of the flavor taggers for the B_s^0 Oscillation search.

B Hadron Lifetime Measurements

The CDF Collaboration

We present lifetime measurements performed using data from $p\bar{p}$ collisions at $\sqrt{s} = 1.96$ TeV recorded by the CDF detector operating at the Fermilab Tevatron. These measurements include new high precession measurements of the B_s^0 meson the production and study of which is currently unique to the Tevatron Experiments.

Selected Topics in B and Charm Physics at CDF

The CDF Collaboration

Selected new topics of interest from the Beauty and Charm physics program at CDF are reviewed. Latest results from CDF on CP violation, Mixing and spectroscopy will be shown.

Wavelet analysis of data in physics of resonances: application to the R measurement

Victor Henner, Tatyana Belozerova

Perm State University

The advantages that the wavelet analysis (WA) provides for resolving the structures in experimental data are demonstrated. Due to good scaling properties of the wavelets one can consider the data with various resolution which allows to separate the resonances from background and from each other. The WA is much less sensitive to the noise than any other analysis and allows substantially reduce the role of statistical fluctuations in data. In this work we apply the WA to reanalyze the data on the total cross section for hadron production in e^+e^- annihilation. The smearing the *R* data with WA gives a way to find the value of α_s constant more precisely. Above open flavor thresholds, the WA analysis of *R* allows us to determine parameters of vector resonances more reliably.

Charmed Molecules

Evgeni Kolomeitsev[1], M.F.M. Lutz[2], J. Hofmann[2]

[1]*University of Minnesota*
[2]*GSI and TU, Darmstadt, Germany*

We discuss the formation of charmed meson and baryon resonances as predicted by the chiral SU(3) symmetry of QCD. Based on the leading order term of the chiral Lagrangian a rich spectrum of molecules is generated, owing to final-state interactions. Charmed scalar and axial-vector meson resonances and s- and d-wave baryon states will be discussed. The obtained mesonic and baryonic spectra are remarkably consistent with the empirical pattern.

Chiral SU(3) predicts new multiplet structures. Chiral excitations of charmed pseudo-scalar and vector mesons form an anti-triplet and a sextet representation of the SU(3) group. So far unobserved narrow isospin-singlet mesons with negative strangeness are anticipated. For charmed baryons we suggest the existence of resonance states that form an anti-quindecimplet, two sextet and two anti-triplet representations of the SU(3) group. In particular, narrow states with anomalous isospin (I) and strangeness (S) quantum numbers $(I, S) = (1/2, +1)$ can be formed.

Measurement of the Cross Section for $e^+e^- \to$ hadrons at $E_{cm} = 3773$ MeV

CLEO Collaboration

Using 281pb^{-1} of CLEO-c data taken at $E_{cm} = 3773$MeV as well as 21pb^{-1} taken at $E_{cm} = 3671$MeV, we measure the hadronic cross section of the $\psi(3770)$ and compare it with the reported cross section for $D\bar{D}$ production.

Dalitz-plot Analyses from CLEO

The CLEO Collaboration

Model uncertainty in the Dalitz plot analysis of $D^0 \to K_s\pi^+\pi^-$ may become the limiting systematic uncertainty in the determination of CKM angle γ/ϕ_3 from the decay $B^+ \to D_{cp}K^+$, $D_{cp} \to K_s\pi^+\pi^-$. We exploit the quantum correlation of D's produced from $\psi(3770)$ to simultaneously measure D^0, $\bar{D}^0$, D_{CP+}, D_{CP-} decay to $K_s\pi^+\pi^-$ and thereby reduce the model dependence on γ/ϕ_3. Other decay modes useful for probing γ/ϕ_3 are also under study including $D^0 \to \pi^+\pi^-\pi^0$, $K^+K^-\pi^0$ and $K_SK\pi$. We compare various methods of analysis including K-matrix and Breit-Wigner Models.

Spectator effects and lifetimes of heavy hadrons

Alexey A Petrov
Wayne State University

We present a calculation of subleading $1/m_b$ corrections to spectator effects in the ratios of beauty hadron lifetimes in heavy-quark expansion. We find that these effects are sizable and should be taken into account in systematic analyses of heavy hadron lifetimes. In particular, the inclusion of $1/m_b$ corrections brings into agreement the theoretical predictions and experimental observations of the ratio of lifetimes of Λ_b-baryon and B_d meson. We obtain $\tau(B_u)/\tau(B_d) = 1.06 \pm 0.02$, $\tau(B_s)/\tau(B_d) = 1.00 \pm 0.01$, $\tau(\Lambda_b)/\tau(B_d) = 0.86 \pm 0.05$.

SUSY searches and SUSY phases

Yudi Santoso
University of Victoria

The search for supersymmetry is currently dominated by two venues: through direct susy particle search at colliders and through susy dark matter search. However, there is another aspect that is also worth to look at. Supersymmetry provides many complex phases in addition to the Standard Model phase. Although phenomenology strongly constrains the values of these phases, there is no compelling theoretical argument for having zero susy phases at this moment. Electric dipole moment (EDM) for elementary particle, which is forbidden in the Standard Model, could arise in supersymmetric models with phases. Therefore it is natural to look at EDM to study susy phases. I would like to discuss current results, and to what extent EDM can compete with or complement colliders in the near future.

X(3872): a $q\bar{q}$-$c\bar{c}$ molecule with attractive diquarks

Sachiko Takeuchi[1], V. E. Lyubovitskij[2], Th. Gutsche[2], Amand Faessler[2]
[1]*Japan College of Social Work*
[2]*Institute for Theoretical Physics, University Tuebingen*

The $q\bar{q}c\bar{c}$ systems are investigated by a quark model with diquark correlation, which enables us to describe a meson molecular system which has quark dynamics in the short range region. The model includes the instanton-induced interaction (INS) and the color-magnetic interaction (CMI) as the hyperfine interaction for quarks. It is found that $J/\psi\rho(1^{++})$ state can actually be a molecule whose color-octet component gains attraction from both of these interactions. We argue that the peak X(3872) can be this state. The possibility to find the states $J/\psi\omega$ with $J^{PC} = 1^{++}$ or 2^{++} and $J/\psi\rho$ with 2^{++} will also be discussed [1].

The model hamiltonian, H, consists of the nonrelativistic kinetic term, K, the linear confinement potential, V_{Conf}, the one-gluon exchange interaction, V_{OGE}, the instanton-induced interaction, V_{INS}, the zero-point energy, $V_{const.}$, to fit the average meson mass, and the σ-meson exchange, V_σ, for the overall attraction:

$$H = K + V_{Conf} + V_{OGE} + V_{INS} + V_{const.} + V_\sigma \ . \tag{1}$$

The strength of V_{OGE} and V_{INS} is determined empirically. A bound state(s), if any, can be obtained by the stochastic variational approach. This model can describe properties of the baryons and mesons successfully [2,3].

INS has originally been introduced to solve the $U_A(1)$ problem. It generates the η-η' mass difference, and also gives extra attraction to the color-octet flavor-octet spin-1 $q\bar{q}$ pair, which is found in the $J/\psi\rho(1^{++})$ state.

In the table below, we show the binding energy, E_B, size of the component, N, rms, and relative distances between quarks, ($r_{q\bar{q}}$, r_{qc}, $r_{c\bar{c}}$), and sizes of CMI and INS of the $J/\psi\rho(1^{++})$ state. The system has two components: the one where both of $u\bar{d}$ and $c\bar{c}$ are color-singlet, $(J/\psi\rho)_{11}$, and the other is color-octet: $(J/\psi\rho)_{88}$. Since E_B is small, the former component is dominant. Note, distance between the light quarks and between $c\bar{c}$ is close (ρ and J/ψ), while these two clusters are kept apart from each other. The probability of the color-octet component is large considering that the binding energy is small. Its spacial size is small, reflecting the fact that it is affected by the attraction both from CMI and from INS. Unlike to the color-singlet component, there is not much deformation. Thus, this bound state can be considered as a J/ψ-ρ molecule with the deeply bound DD^* component in the short range.

Content	J^{PC}	E_B [MeV]		N	rms	$r_{q\bar{q}}$	r_{qc}	$r_{c\bar{c}}$	$\langle V_{CMI}\rangle$	$\langle V_{INS}\rangle$
$J/\psi\rho$	1^{++}	2.0	total	1	1.99	0.91	1.63	0.49	61.3	-1.3
			$(J/\psi\rho)_{11}$	0.92	2.05	0.89	1.68	0.45	74.5	0
			$(J/\psi\rho)_{88}$	0.08	1.11	1.08	0.81	0.81	-74.6	-16.3

[1] S. Takeuchi, V. E. Lyubovitskij, Th. Gutsche, and Amand Faessler, in preparation
[2] M. Furuichi, K. Shimizu, and S. Takeuchi, Phys. Rev. **C68**(2003)034001
[3] T. Shinozaki, M. Oka, S. Takeuchi, and K. Shimizu, in preparation

Heavy flavour production in ep collisions

Yuji Yamazaki
DESY

on behalf of the H1 and ZEUS collaboration.

The study of heavy quark production is a rich area for understanding QCD and is under extensive examination by the H1 and ZEUS experiments at HERA. The production of heavy quarks is sensitive to the structures of the incoming proton and photon complimenting the inclusive measurments in ep and eγ deep inelastic scattering. Results from HERA have contributed significantly to what previously appeared to be a serious problem in QCD with the inadequate description of Tevatron data for beauty production. Measurements at HERA of fragmentation parameters also test the concept of the universality of fragmentation.

Fundamental Symmetries

Liquafaction

Carl A. Brannen

.

Some quantum gravitation theorists find Euclidean Quantum Gravity the “only sane” methoc [hep-th/0507171] for quantum gravitation. This suggests that Euclidean coordinates should be explored for use in particle theory, especially with the Geometric Algebra methods of obtaining gravitation on a Euclidean coordinate system by several authors [gr-qc/9910039, physics/0410035].

Euclidean relativity poses both a challenge and an opportunity for particle theorists. Traditional particle theory has been restricted by perfect Lorentz symmetry, but it has also been very successful. The strongest restriction is the Coleman-Mandula theorems, which prevent the internal particle symmetries from being written in terms of external geometry. How can we loosen this restriction on the internal symmetries of particles, without losing perfect Lorentz symmetry for their kinematics?

In Hestenes’ Geometric Algebra (GA), the tangent vectors of a space-time manifold are associated with the basis vectors of a Clifford Algebra (CA). This provides an algebra that automatically obeys Lorentz symmetry. We will loosen the association by allowing the tangent vectors of the manifold to be associated with arbitrary elements of the CA, provided that the elements we choose satisfy the same commutation relations that the basis vectors satisfy. The resulting algebra is called the “Particle Internal Symmetry Algebra” or PISA.

For any spinor, the PISA and the GA will be indistinguishable as they are subalgebras of the same CA. Where there are differences is in how distinct subalgebras, which we can associate with different particles, are related to each other. The natural relations are exponential in form and will produce the sort of symmetry breaking needed to distinguish between different fermions.

For several choices of the space-time manifold, including several varieties of Euclidean relativity, we will obtain parameterizations for converting back and forth between GA and PISA calculations.

Restoration of Supersymmetry against arbitrary small quantum corrections using feedforward neural network

Ashish Chaturvedi
ICIS, Dr. B. R. Ambedkar University, Agra, India

In this paper, the study of restoration of Supersymmetry, broken at tree level, has been undertaken. In the present model we have lucratively applied the method of back propagation based on gradient descent along the error surface to restore the supersymmetry against arbitrary tiny quantum corrections in the form of small thermal agitations. Back propagation method brings the potential stability against supersymmetry breaking due to small thermal agitations by updating the connection strengths in different layers of feedforward neural network. Keywords: Artificial Neural Network, Back propagation, Supersymmetry.

Measurements of $\sin(2\beta+\gamma)$ at Babar

Babar Collaboration
SLAC

We present a measurement of the time-dependent CP-violating asymmetries in decays of neutral B mesons to the final states $D^*\pi$, $D\pi$ and $D\rho$ using approximately 232 million $B\bar{B}$ events recorded by the BaBar experiment at the PEP-II e^+e^- storage ring. The other B meson in these events is determined to be a B^0 or a $\bar{B}^0$ from its decay products. With some theoretical assumptions, we interpret our results in terms of limits on $\sin(2\beta+\gamma)$.

Measurements of direct CP violation at Babar

Babar Collaboration
SLAC

We present searches for and measurements of direct CP violation in B decays, by using data collected by the Babar detector at the PEP-II e^+e^- asymmetric storage ring.

The QWeak Experiment

Michael T Gericke
TRIUMF / University of Manitoba

on behalf of the QWeak collaboration.

The Qweak experiment at Jefferson Lab aims to make a 4% measurement of the parity-violating asymmetry in elastic scattering at very low Q^2 of a longitudinally polarized electron beam on a proton target. The experiment will measure the weak charge of the proton, and thus the weak mixing angle at low energy scale, providing a precision test of the Standard Model. Since the value of the weak mixing angle is approximately 1/4, the weak charge of the proton $Q_w^p = 1 - 4\sin^2\theta_w$ is suppressed in the Standard Model, making it especially sensitive to the value of the mixing angle and also to possible new physics. The experiment is approved to run at JLab, and the construction plan calls for the hardware to be ready to install in Hall C in 2007. The experiment will be a 2200 hour measurement, employing: an 80% polarized, 180 μ A, 1.2 GeV electron beam; a 35 cm liquid hydrogen target; and a toroidal magnet to focus electrons scattered at 9deg, a small forward angle corresponding to $Q^2 = 0.03\ (\mathrm{GeV/c})^2$. With these kinematics the systematic uncertainties from hadronic processes are strongly suppressed. To obtain the necessary statistics the experiment must run at an event rate of over 6 GHz. This requires current mode detection of the scattered electrons, which will be achieved with synthetic quartz Čerenkov detectors. A tracking system will be used in a low-rate counting mode to determine average Q^2 and the dilution factor of background events. The theoretical context of the experiment and the status of its design are discussed.

Atomic Trapping of Radioactive Isotopes to Study Time Reversal Violation

K. Jungmann, C.J.G. Onderwater, L. Willmann, H.W. Wilschut
Kernfysisch Versneller Instituut

At KVI a program of multidisciplinary research has been started with the main focus on studying fundamental interactions and symmetries. The basic principle is to use radioactive nuclei as a testing ground for time reversal invariance. Although the Standard Model does not forbid time reversal violation (TRV), the effect is vanishingly small in nuclei and atoms compared to the experimental accuracy reachable at present and the foreseeable future.

We are setting up a facility at KVI in which radiactive isotopes can be produced with various production mechanisms including fusion-evaporation, fragmentation and direct reactions. We separate the desired isotope in a magnetic double separator from the incoming beam and unwanted other isotopes. After slowing down, the ions are cooled and bunched in an RFQ device. The actual experiments on TRV will take place in optical neutral atom traps.

The TRIμP (Trapped Radioactive Isotopes: μicrolaboratories for fundamental Physics) facility [1,2] is an open users facility providing beam according to the advice of a Program Advisory Committee. First experiments using energetic beams after the separator have already been conducted. The further build-up of the facility is progressing.

The local research group concentrates on studies of β-ν correlations and the search for permanent EDMs[3], for which radioactive Ra isotopes are good candidates. β-decay of light isotopes provides an alternative route. Both methods depend on atomic trapping techniques to reach the required accuracy. The first steps in studying the β-decays of $^{2}1$Na have been taken. By first attempting to trap Ba the trapping of Ra is pursued.

Current progress and the complementarity of the approach with other activities in both low and high energy experiments will be described.

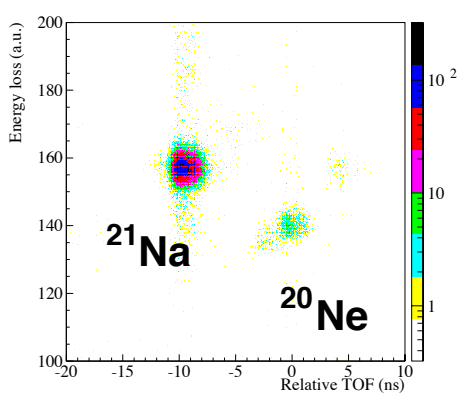

Fig. 1. Example for the TRIμP separator performance: ^{21}Na has been produced with better than 99.5% purity with the only visible contamination of (stable) ^{20}Ne. For the first experiment caried out – a measurement of the ^{21}Na branching ratio – this was of no conern.

This report is on behalf of the TRIμP group at KVI [1,2]. This work is supported by the Dutch organization FOM and the EU in the framework of the NIPNET and ION-CATCHER RTD networks.

[1] G.P. Berg et al., NIM B **204**, 532 (2003) and Nucl.Phys. **A721**, 1107c (2003)
[2] J.W. Turkstra et al., Hyperf. Interact. **127**, 533 (2000)
[3] K. Jungmann, Nucl. Phys. **A751**, 87c (2005) and physics/0501154

Limits on Weak Annihilation in Inclusive Charmless Semileptonic B Decays

The CLEO Collaboration

Theoretical predictions for the weak decay $b \to u l \nu$ are subject to the contributions of higher-order terms that must be neglected in making practical phenomenological calculations. One such term that arises at order $(\Lambda/M_B)^3$ in the non-perturbative expansion describes "weak annihilation" (WA). While the contribution of this term to the total rate is expected to be small, it is predicted to have a non-trivial distribution across phase space, concentrated near the maximal value of q^2. The significance of WA relative to the leading-order rate in this restricted region is thus greatly enhanced, and values for the CKM element $|V_{ub}|$ extracted from inclusive measurements of $b \to u l \nu$ made in the high q^2 regime are subject to a corresponding but unknown correction from WA. We constrain the magnitude of WA relative to the total inclusive $b \to u l \nu$ rate and, consequently, the associated uncertainty on extracted values of $|V_{ub}|$. We find the magnitude of weak annihilation effects are not statistically significant and present limits for a series of different models of weak annihilation kinematics.

Exclusive semileptonic decays of D mesons produced in the reaction $\psi(3770) \to D\bar{D}$

The CLEO Collaboration

Initial running of the CLEO-c detector in the fall of 2003 and the winter of 2004 has provided the world's largest sample of $\psi(3770)$ decays. Using this data sample, we have reconstructed D mesons decaying to hadronic final states and have used them to tag events with a charm-anti-charm meson pair. Measurements of absolute branching ratios for a variety of semileptonic decay modes of D^0 and D^+ mesons will be presented.

Inclusive Semileptonic Branching Fractions and Electron Momentum Spectra

The CLEO Collaboration

We present a precise measurements of the inclusive charm branching fractions and electron momentum spectra for the decays: $D^+ \to Xe\nu$ and $D^0 \to Xe\nu$ using CLEO-c detector at the CESR e^+e^- collider. Tagged D samples collected at $\psi(3770)$ center-of-mass energy are used in these measurement.

Search for Rare and Forbidden Decays $D^+ \to h^\pm e^\mp e^+$

The CLEO Collaboration

Using 0.8 million D^+D^- pairs collected with the CLEO-c detector at the $\psi(3770)$ resonance, we have searched for flavor-changing neutral (FCNC) and lepton-number-violating (LNV) decays of D^+ mesons to final states with dielectrons. We find no indication fo either, obtaining 90% confidence level upper limits of $B(D^+ \to \pi^+e^+e^-) < 7.4 \times 10^{-6}$, $B(D^+ \to \pi^+e^+e^+) < 3.6 \times 10^{-6}$, $B(D^+ \to K^+e^+e^-) < 6.2 \times 10^{-6}$, and $B(D^+ \to K^+e^+e^+) < 4.5 \times 10^{-6}$.

Leptons and Quarks in discrete subgroups of the Standard Model gauge group

Franklin Potter

Sciencegems. com / Formerly at U C Irvine

The continuous gauge group of the Standard Model could be acting like a “cover group” for underlying discrete symmetries of specific finite binary rotational subgroups, one of its subgroups for each lepton and quark family. The mathematical properties of these finite subgroups will dictate the same physical properties of the leptons and quarks as achieved by the SM. In addition, this finite rotational subgroup approach determines their mass ratios correctly from the j-invariant related to their elliptic modular functions, explains the family relationships through subgroup mathematical relationships, and achieves electroweak symmetry breaking without requiring a Higgs. Predictions for the detection at the LHC of the effects of these subgroups will be discussed.

On the Unified System of the Nucleons in Nuclei

Rasulkhozha Sultonkhozhaevich Sharafiddinov,

Institute of Nuclear Physics of Uzbekistan Academy of Sciences

Measurement of the ratio R_K between the Branching Ratio of K––> e nu and K––>*μ* nu decays

Mayda M. Velasco

Northwestern University

on behalf of the NA48 collaboration.

The measurement of the ratio R_K between the Branching Ratio of K+ to e+ nu and K+ to mu+nu decays is a sensible test of lepton universality and of V–A structure of the weak interactions. This measurement is predicted with good theoretical precision, but its actual accuracy is affected by the lack of a statistically proportionate sample of K+– to e+– nu. The NA48/2 experiment, at the CERN SPS accelerator, has collected already more than 4 times the world total K+– to e+– nu statistics, during 2003 data taking. Such data set, obtained in an experimental condition that keeps an adequate control of the possible systematic effects, allows a significative test of theory prediction and, for the first time ever, a comparison of R_K between positive and negative Kaon decays. After the description of the most relevant features of the collected data, it will be presented the preliminary result based on 2003 data set.

Precise measurement of form factors for KL––> pi e nu and KL–––>pi *μ* nu decays

Mayda M. Velasco

Northwestern University

on behalf of the NA48 collaboration.

A sample of 5.6 million reconstructed Ke3 events recorded by the NA48 experiment was used to measure the Dalitz plot density their decay. Admitting all possible Lorentz–covariant couplings, the form factors f+(q2), fS, and fT for vector, scalar, and tensor interactions were measured. Assuming only V–A couplings, λ+ = 0.0288 +/– 0.0012 was obtained. Alternatively, a quadratic fit was performed but contrary to recent claims, we do not pbserved a significant non–linear contribution. In addition, over 2.5 million Kμ3 decays from the same minimum bias run period were analysed, resulting in a preliminary measurement of the form factors of λ+ = 0.0260 +/– 0.0007 +/– 0.0010 and λ0 = 0.0120 +/– 0.0008 +/– 0.0015. In both cases, pole form factors have been performed and will be discussed.

First observation for Ks–->pi0ee and Ks–->pi0mumu

Mayda M. Velasco
Northwestern University

on behalf of the NA48 collaboration.

To further study Direct CP Violation in the rare decay KL to π0e+e− and π0μ+μ−, the π0*l* +*l* − component due to KS−KL mixing has to be bound. A high sensitivity search for KS to π0 e+ e− and π0 μ+μ− has been conducted by the NA48 experiment using data collected in 2002 from an intense short kaon neutral beam. The sensitivity over the previous results is extended by about two orders of magnitude and clear signals for barching fractions of the order of 10−9 are observed and measured. The final results of these searches will be presented along with their impact on future searches.

Direct CP Asymmetry in Charmless Hadronic Two-body B Decays

Chung-Hsiang Wang
National United U., Taiwan

on behalf of the Belle collaboration.

We report improved measurements of the partial-rate CP asymmetry in two-body cha rmless *B* decays with a large data sample collected by the Belle detector a t KEKB e^+e^- collider. The modes we report include $K^+\pi^0$, $\pi^+\pi^0$, $K^+\pi^-$, ηK^+, $\eta\pi^+$, ωK^+ and $\omega\pi^+$.

Simplified Extension of Electroweak Mixing and the Generation of Massive Gauge Bosons

Thomas E. Ward

Techsource Inc.

Details of a simplified extension of electroweak mixing using off–diagonal mixing of scalar (Higgs sector), vector (electroweak) and tensor (spin–2) gauge fields with the massive vector boson field that removes the degeneracy of the multiple gauge boson states will be presented. Mixing in this manner allows for unique solutions of the multiplets and masses of the massive neutral gauge boson states. The series of two state off–diagonal matrices are solved using the best–fit value of the EW mixing angle $\sin^2\theta_W = 0.2313$, the experimental masses of the W and Z bosons, and the mass less photon and graviton. The analysis predicts the following massive neutral gauge boson values: Higgs scalar singlet (112.65 GeV), Higgs psuedoscalar doublet (charged 169.58 GeV and neutral 218.94 GeV), and the neutral tensor gauge boson (8.087 GeV). The top quark mass extracted from the Higgs mass sector is 169.54 GeV. The extracted off–diagonal EW mixing matrix elements for the scalar (89.80 GeV), vector (21.93 GeV) and tensor (3.413 GeV) interactions agree to better than 1% with the mixing matrix elements found within the well known dynamical Lagrangian that describes the interaction of the massive vector boson field (A_μ) with the massive scalar field (η) following spontaneous symmetry breaking.

Deep inelastic cross sections at HERA with polarized lepton beam

Yuji Yamazaki

DESY

on behalf of the H1 and ZEUS collaboration.

Total and differential cross sections for charged and neutral current deep inelastic scattering in e^+p and e^-p collisions with longitudinally polarised electron beams have been measured with the H1 and ZEUS detectors at HERA. The cross sections measured at positive and negative longitudinal-polarisation values of the electron beam are compared with the predictions of the Standard Model. These measurements provide a classic test of the helicity structure of electroweak interactions.

Fundamental Interactions in Atomic and Neutron Physics

Parity and time reversal violation in atoms and test of the Standard Model

Victor Flambaum
University of New South Wales

In this talk I want to present two different topics:

1. Recent measurements of Cs weak charge by Boulder group led by Nobel Laureate Carl Wieman indicated possible deviation from the Standard Model predictions. We performed new calculations of parity violation in Cs including all-orders summation of dominating diagrams in many-body theory and strong Coulomb field radiative corrections. The theoretical error was reduced two times. Conclusions for the Standard Model and possible ”new physics” will be discussed.
Atomic and molecular experiments can also be used to detect nuclear anapole moment - magnetic multipole which violates parity.

2. Parity and time invariance violating nuclear forces produce P,T-odd nuclear moments. In turn, these moments can induce electric dipole moments (EDM) in atoms. EDM of diamagnetic atoms is induced by nuclear Schiff moment. We explain the origin of Schiff moment and mechanism of collective enhancement (up to 1000 times) in deformed nuclei, describe electric field produced by the Schiff moment, perform atomic calculations of EDM in atoms of experimental interest and present tests of CP violation models. Suggestion of new experiments: EDM of certain odd isotopes of Ra and Rn may exceed EDM of lighter atoms by 3 orders of magnitude!

Ultracold Neutron Storage in a Magnetic Trap made of Permanent Magnets

Peter W Geltenbort[1], Victor F Ezhov[2], Joachim J Hartmann[3], N A Kovrizhnykh[4]
[1]*Institut Laue−Langevin*
[2]*Petersburg Nuclear Physics Institute, Gatchina, Russia*
[3]*Technical University Munich, Germany*
[4]*Research Institute of Electrophysical Apparatus, St. Petersburg, Russia*

The measurement of the neutron lifetime τ_n is one of the important experiments of fundamental physics. Together with the determination of one of the correlation parameters characterizing neutron decay it allows to fix the element V_{ud} of the Cabibbo−Kobayashi−Maskawa (CKM) matrix. With the 2004 world average for τ_n from the Particle Data Group (τ_n = 885.7 ± 0.8 s) and the latest value for the neutron â−decay asymmetry (A = −0.1189 ± 0.0007) the unitarity of this matrix, an important test of the Standard Model of electro−weak interaction, is violated at the 3ó level. A very recent experimental result,τ_n = 878.5 ± 0.8 s, differs by six standard deviations from the 2004 world average. Therefore, a new experiment with a different approach is necessary.
In the experiment presented here ultra−cold neutrons (UCN) are stored in a permanent−magnet trap and the number of surviving neutrons is determined as a function of time. This allows to measure the neutron lifetime with a method complementary to that usually used, UCN storage in material bottles, with an error comparable to the world average of today.
The new experimental set−up is described in detail and first preliminary results are given.

The CryoEDM Experiment

Philip G Harris, et al.
University of Sussex

on behalf of the CryoEDM collaboration.

A series of measurements of the neutron electric–dipole moment (nEDM) have, over the course of more than half a century, played an important role in shaping and constraining numerous models of CP violation. The latest of these is now entering the final stages of its development at the ILL, Grenoble. It will use a so–called superthermal source, in which ultracold neutrons are produced by the down–scattering of polarised 8.9 Å neutrons in superfluid helium. Its sensitivity is expected to exceed that of the previous generation by two orders of magnitude. This talk will outline the techniques involved, the progress to date, and the anticipated schedule of measurements.

Schiff Theorem and the Electric Dipole Moments of Hydrogen-Like Atoms

Cheng-Pang Liu, et al.
Kernfysisch Versneller Instituut

The permanent electric dipole moment (EDM) of a physical system is an indication of time-reversal (T) violation, and can be related to CP violation if CPT symmetry is exact. Although a neutral atomic system is ideal for such a precision test, much of its EDM evades the detection because the re-arrangement of its constituents to screen the applied electric field: the so-called Schiff theorem.

Despite this difficulty, a lot of progresses have been made and they provide stringent constraints for quantities like the electron EDM, the nucleon EDM, the P- and T- odd electron-nucleon, and nucleon-nucleon forces. In this work, we revisit the Schiff theorem and consider its application to the hydrogen-like atoms (atom with only one electron). The special attention is a qualitative understanding about how different mechanisms compete to give the resulting atomic EDM.

Nuclear Spin–Dependent Parity Nonconservation in Molecules

Dennis Murphree, Sidney Cahn, David Rahmlow, David DeMille
Yale University, Department of Physics, New Haven, CT 06520

The effects of nuclear spin–dependent parity nonconservation (NSD–PNC), which are of relevance in and particle physics, can be dramatically enhanced in diatomic molecules. These observable effects from two underlying physical causes: *fundamental couplings of the* Z^0 *boson* (parameterized by the cons nd *nuclear anapole moments* . A nuclear anapole moment is a P–odd electromagnetic moment that appears interactions between nucleons. Besides being of intrinsic interest, anapole moments can provide a new me imentally investigating purely hadronic weak interactions.[1,2] Only a single measurement of a nuclear ana that of ^{133}Cs by Wieman *et al* .,[3] has been made to date. The $C_{-2P,N}$ constants, which describe the –vector electronic coupling of the Z^0 to protons and neutrons, are two of the most poorly character rs of the Standard Model. Neither has been measured directly, and uncertainties on the measurements of li tions of the closely related electron–quark couplings $C_{-2u,d}$ are at the level of 300% and 70% respectivel on, it has been predicted that certain 4–fermion contact interactions at an energy scale of 12 TeV could lead iation in these constants from their expected values.[6] Thus precise measurement of the $C_{-2P,N}$ param o provide evidence for new physics at high energy scales.

Here we outline an experimental program that will allow dramatic improvement on previous effor both nuclear anapole moments and the C_2 constants. By exploiting the properties of diatomic molecules to measure the anapole moments of at least nine different nuclei. This will effectively double the numb a points for interpreting hadronic weak interactions[1]. Furthermore, our ultimate precision in measuring the oupling constant C_{2N} should reach an unprecedented uncertainty of ~20%, as well as yielding a compet nent of C_{2P} .

The basic idea of our technique is to study NSD–PNC in molecular transitions using laser uency spectroscopy. In particular, we will measure the NSD–PNC mixing between hyperfine/rotational le ound electronic state of molecules with a single valence electron in a $^2\Sigma$ state. A rotationally cold bea free radical species will be created via laser ablation[7] and passed through a superconducting solenoidal mag netic field will be tuned to bring two states of opposite parity to near degeneracy, hence maximizing luced mixing between the levels. An oscillating electric field will drive Stark transitions between these y measuring interference between the naturally occurring PNC mixing and the Stark–induced mixing, we ize the strength of the weak interaction. Because the anapole and tree–level Z^0 exchange contributions to ect scale differently with atomic number, by performing the experiment in a series of different molecules we the anapole moment contribution from the $C_{2P,N-}$ contribution. We expect to have excellent control ics because the weak–Stark interference changes sign with several experimentally controllable parameters. generation of our experiment, we will study the ^{137}BaF molecule, which should be primarily sensitive to moment of ^{137}Ba. In this molecule, we expect an asymmetry of around 8%, which should allow a measure SD–PNC effect to the target 10% uncertainty within a few minutes of integration.

We report on the current status of our efforts to construct the apparatus for this experiment, focu opment of the free radical beam and a system to actively shim and stabilize the magnetic field at the des -0.1 ppm.

kton and C. Wieman, ˆAtomic parity nonconservation and nuclear anapole moments˜, Ann. Rev. Nucl. Part. Sci. **51**, 261 (2001).
kton, C.–P. Liu, and M.J. Ramsey–Musolf, ˆNuclear anapole moments˜, Phys.Rev. **C 65** (2002) 045502.
ilbert, M.C. –Noecker, R.N. –Watts, and C.E. –Wieman, –*Phys. Rev. Lett.* **55**, 2680 (1985); Gilbert and –Wieman, *Phys. Rev. A* **34**, 7
rescott *et al.* , ˆFurther measurements of parity non–conservation in inelastic electron scattering˜, Phys. Lett. B **84**, 524 (1979).
ty *et al.* , ˆStrange magnetism and the anapole structure of the proton˜, Science **290**, 2117 (2000).
), ˆThe Future˜, pp. 977–1005 in ˆPrecision Tests of the Standard Electroweak Model˜, ed. P. Langacker (Singapore, World Scientific,
butt *et al.* , ˆA jet beam source of cold YbF radicals˜, J. Phys. B: At. Mol. Opt. Phys. **35**, 5013 (2002).
guyen, D. Budker, D. DeMille, and M. Zolotorev, Phys. Rev. A **56**, 3453 (1997).

Toward a New Measurement of the Neutron Electric Dipole Moment

Oscar Naviliat-Cuncic, et al.
Universite de Caen Basse-Normandie and LPC-Caen

on behalf of the nEDM collaboration.

Precision measurements of particle electric dipole moments (EDMs) provide extremely sensitive means to search for non-standard mechanisms of T (or CP) violation. For the neutron EDM, the upper limit has been reduced by eight orders of magnitude in 50 years thereby excluding several CP violation scenarios. The current limit on the neutron EDM, which is dominated by statistics, was obtained in measurements using ultra-cold neutrons (UCNs) produced in a reactor and stored in a vacuum chamber. We report here on a new effort aiming at improving the neutron EDM limit by more than an order of magnitude, down to a level of 10^{-27} e·cm. The two central elements of the approach are: *i)* the use of the higher UCN densities which will be available at the new dedicated spallation UCN source at the Paul Scherrer Institute; and *ii)* the optimization of the in-vacuum Ramsey resonance technique, with storage chambers at room temperature, to reach new limits of sensitivity. The control of systematic effects required by the new sensitivity level calls for new magnetometry schemes. An array of laser optically pumped Cs magnetometers will actively stabilize the frequency and phase coherence of the Ramsey pulses. The optimization of the in-vacuum technique includes active control of the static magnetic field, the use of a multi-chamber setup, improvements in the coatings of large area cells and guides and the use of fast UCN detectors. The paper will present the status of the project and the ongoing R&D activities.

A Superconducting Magnetic UCN trap for Precise neutron Lifetime Measurements

Ruediger Picker

Constraints on non-Newtonian gravity and on axion from the experiment on neutron quantum states in the Earth's gravitational field

Konstantin V. Protasov

Laboratoire de Physique Subatomique et de Cosmologie

According to the predictions of unified gauge theories, supersymmetry, supergravity, and string theory, there would exist a number of light and massless particles. An exchange of such particles between two bodies gives rise to an additional force. Additional fundamental forces at short distances were intensively studied following the hypothesis about supplementary spatial dimensions. In this contribution, we estimate an upper limit on an additional attractive short-range force, which could be established from the experiment on neutron quantum states in the Earth's gravitational field [1] in a model-independent way [2].

The simplest upper limit on the strength of an additional interaction follows from the condition that this additional interaction does not itself create any bound state. This limit is presented in Figure (the solid line) in comparison with the limits from the Casimir-like and van der Waals force measurement experiments (the short dashed lines), as well as from experiments on protonium atoms (solid horizontal line). The long dashed line shows a limit which can be easily obtained by an improvement of this experiment. α_G and λ are strength and characteristic range of this interaction.

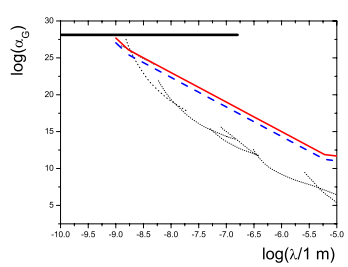

Axions are well-known as a possible solution to the strong CP problem as well as an interesting darkmatter candidate. One of the most remarkable predictions associated with the axion is that it yields a parity and time-reversal violating, giving monopole-dipole coupling between spin and matter. Experimental and astrophysical observations imply that the mass of the axion must lie between 1 μeV and 1 meV, corresponding to a range between 20 cm and 0.2 mm.

The limit on the axion coupling constant can be also established from the experiment on neutron quantum states in the Earth's gravitational field. For instance for the characteristic axion Compton wave length $\lambda = 1$mm, we obtain the limit for the coupling $g_p g_s/4\hbar c = 2 \cdot 10^{-17}$ which is at least a few orders of magnitude better than existing limits.

[1] V.V. Nesvizhevsky et al., Phys. Rev. **D67**, 102002 (2003).

[2] V.V. Nesvizhevsky, K.V. Protasov, Quant. Class. Grav. **21**, 4557 (2004).

Search for tensor couplings in the weak interaction using $^6He^+$ ions and a novel transparent Paul trap

Daniel Rodríguez

LPC-Caen

on behalf of the LPCTrap collaboration.

Nuclear β decay is a sensitive tool to investigate weak processes. According to the Standard Model (SM), nuclear β decay is mediated by the exchange of $W^{\pm}$ bosons which result in vector (V) and axial-vector (A) couplings. Other couplings such as scalar (S), pseudoscalar (P) or tensor (T), are permitted by Lorentz invariance but forbidden within the SM. The search for the presence of such interactions requires high-precision experiments. In this contribution, we report on an experiment aimed at determining the β-ν angular correlation coefficent a in the decay of ^{6}He. This is a pure Gamow-Teller decay and according to the SM, a $= -1/3$. So far, the most precise measurement of the β-ν angular correlation coefficient in the decay of ^{6}He has led to a $= -0.3308 \pm 0.0030$ [1,2]. A more precise value of a, by a factor of two improved accuracy (δa $= 0.0015$), could be achieved using novel techniques.

A new correlation experiment is under commissioning at GANIL after coupling the LPCTrap to the low energy beam line of the SPIRAL source. The LPCTrap is a novel transparent Paul trap made out of two sets of concentric rings centered on the beam axis. This configuration permits injection and extraction of the decaying ions, and detection of the decay products. The device enables to confine the ions almost at rest, in a small volume without interaction with matter. The radioactive $^6He^+$ ion beam with an energy of 10-34 keV is decelerated and cooled down to energies of the order of eV. The ions are then captured in the trap. Deceleration and cooling are accomplished by means of a Radio Frequency Quadrupole (RFQ)-cooler and buncher [3]. The parameter a is determined by measuring the time of flight of the recoil ions ($^6Li^{++}$) in coincidence with the β particles. The detection system consists of a set of Micro Channel Plates (MCP's) detectors and a β-telescope placed in a back-to-back geometry around the trap volume. In this contribution, a detailed description of the system will be given, the results from the first experiment with $^6He^+$ ions will be presented, and the different sources of uncertainty in the determination of a will be discussed.

[1] C.H. Johnson *et al.*, Phys. Rev. **132**, 1149 (1963).

[2] F. Gluck *et al.*, Nucl. Phys. A **628**, 493 (1998).

[3] G. Ban *et al.*, Nucl. Instrum. Methods Phys. Res. A **518**, 712 (2004).

This work has been supported by the European Commission within the RTD project EXOTRAPS under contract number HPRI-CT-1998-00018, and is supported within the NIPNET network under contract number HPRI-CT-2001-50034. D.R. acknowledges support from the EU under a Marie Curie Intra-European Fellowship under contract number MEIF-CT-2005-011269.

Nuclear and Particle Astrophysics and Cosmology

Nuclear Mass Systematics with Neural Nets and Astrophysical Nucleosynthesis

Sotiris T. Athanassopoulos[1], E. Mavrommatis[1], K. A. Gernoth[2]

[1]*Physics Department, Division of Nuclear & Particle Physics, University of Athens, Greece*
[2]*Department of Physics, UMIST, Manchester, United Kingdom*

One of the main subjects of Nuclear Astrophysics is the study of the various nucleosynthesis processes and the justification of the present abundances [1]. The input for such studies from Nuclear Physics involves among others masses, separation energies and Q-values for nuclei far from stability line. The experimental activity with the existing and under construction radioactive ion-beam and heavy-ion facilities will provide partially this input. Reliable models of these quantities will supplement the rest.

In this work [2] we present new global statistical models of the atomic mass-excess and related quantities (separation energies, Q-values) using neural networks that model the differences between the experimental mass-excess values ΔM^{exp} [3] and the theoretical values ΔM^{th} given by the finite range droplet model (FRDM) of Möller et al [4]. The model of the differences seems to catch subtle regularities of nuclear structure not yet embodied in the best microscopic/phenomenological models of atomic-mass systematics. It is for this reason that the predictive performance of the above constructed models outperforms in the majority of the case those of FRDM and of models developed by training neural networks solely on the masses [5]. We will present mainly results of the mass excess, one and two neutron and proton separation energies and Q-values for -decay that are used as input for the astrophysical nucleosynthesis processes r and rp.

[1] "Opportunities in Nuclear Science: A Long Range Plan in the Next Decade" DOE/NSF, 2002); "NUPECC Long Range Plan 2004: Perspectives for Nuclear Physics Research in Europe in the Coming Decade and Beyond" (NUPECC, April 2004)
[2] S. Athanassopoulos, E. Mavrommatis, K.A. Gernoth, and J.W. Clark in preparation.
[3] A.H. Wapstra, G. Audi, and C. Thibault, Nucl. Phys, A729, 337 (2003).
[4] P. Möller, J.R. Nix, W.D. Myers, and W.J. Swiatecki, At. Data Nucl. Data Tables 59, 185 (1995).
[5] S. Athanassopoulos, E. Mavrommatis, K.A. Gernoth, and J.W. Clark, Nucl. Phys. A743 (2004) 222 and references therein.

QCD as an interface between particle-physics and astrophysics

Manjari Bagchi
Presidency College, Kolkata, India.

After extensive theoretical works on free quark phase, when we search for it in laboratories, disappointing results come out. Four experimental groups reporting on relativistic heavy ion collisions (RHIC) show that quark gluon plasma (QGP) with asymptotic freedom (AF) and chiral symmetry restoration (CSR) may never be realised in RHIC although a non-hadronic phase is reached. This phase is strongly interacting and is not fully understood theoretically but it is certainly not QGP with AF and CSR. Therefore we should turn into astrophysics and the possibility of strange star (SS) deserve renewed attention. Strange stars are very compact astrophysial objects made off free u, d, s quarks. Yet the existence of strange quark matter (SQM) was proposed by Witten more than two decades ago, even today it is still difficult to prove or disprove the existence of a state of strange quark matter in its purest form. Extensive research by different groups are going on and besides the equation of states (EOS) and mass radius relations, efforts are being made to find observational signatures for the existence of quark stars.

In our model, strange star properties has been calculated using large N_c approximation with built-in CSM. A relativistic HF calculation has been performed using Richardson potential as an interquark interaction. This potential has the asymptotic freedom (AF) and a confinement-deconfinement mechanism built into it. Richardson potential which is well tested in hadronic property calculations has only one scale parameter with value nearly equal to 400 MeV. But our present calculation has employed a modified version of the potential with two scale parameters;- one to take care of confinement, having a value of 350 MeV and the other to take care of asymptotic freedom having a value of 100 MeV. This form of the potential is also tested in baryonic property calculations. We have obtained a set of EOS's for β equilibrated charege neutral SQM and solving TOV equations, we have also get the mass radius relations for the strange stars. To calculate the properties of strange stars at high temperatures, we have taken the effect of temperature (T) on gluon mass in a simple way, following Alexanian and Nair in addition to the usual density dependence and find that the transition temperature from hadronic matter to strange matter is 80 MeV, close to the 100 MeV estimated by Witten in 1984. Therefore formation of strange stars may be the only signal for formation of QGP with AF and CSM.

Open Heavy Flavor Production as a Probe of Nuclear Effects and High Density matter in pp, dAu and AA collisions at $\sqrt{s_{NN}}$ =200 GeV

Xiaorong Wang

New Mexico State University

on behalf of the PHENIX collaboration.

Heavy flavor production in hadron collisions is dominated by gluonic processes and is a sensitive probe of the gluon structure function in the nucleon and its modification in nuclei. A study of heavy flavor production in different collision systems in various kinematic regions presents an opportunity to probe cold nuclear medium and hot dense matter effects. In pp and dAu collisions, parton shadowing, color glass condensate, initial state energy loss, and coherent multiple scattering in final state interactions can be studied. Nuclear modification in hot dense matter can also be studied by looking at open charm flow and energy loss in nucleus-nucleus collisions.

The PHENIX detector can measure the semi-leptonic decays of open charm and open bottom through the single electron and single muon channels. Single electrons can be measured at mid-rapidity ($|y| < 0.35$) with the PHENIX central arms and single muons can be measured at forward and backward rapidity in the range $1.2 < |\eta| < 2.4$ with the muon spectrometers. We investigate nuclear medium effects on heavy flavor production via single muons and single electrons in pp dAu and AA collisions over wide kinematic ranges. Preliminary PHENIX results and the current status of these analyses will be presented.

Neutrino and Photon radiation from the surface of Quark Stars

Prashanth Jaikumar
Argonne National Laboratory

Thermal photon and neutrino rates are important determinants of neutron star cooling. They are also sensitive probes of the underlying dense phase of matter. We present results from a theoretical investigation of these rates in the context of strange quark stars. We focus on the importance of a proper treatment of the bremsstrahlung process for neutrino and photon emission. In-medium modifications are also analyzed and found to have competing influences on the bremsstrahlung rate. As an application of this study, two specific cases are examined: the long-term cooling of neutron stars with possibly color-superconducting quark matter in the interior; and the cooling of bare quark stars. Our results prove equally useful in quantifying observable signatures of quark matter in stars, and determining neutrino signals from other astrophysical objects such as Gamma-ray bursters (GRBs) and black-hole accretion torii. Finally, an alternative to a bare quark star, i.e., one with a thick crust is proposed, and its observational consequences are discussed in detail.

Characterization of the Neutron Response To A Liquid Xenon Based Detector For Dark Matter Studies

Sharmila Kamat

Columbia University

on behalf of the XENON collaboration.

Liquid Xenon as a radiation detection medium finds application in fields such as dark matter studies, neutrinoless double beta decay and gamma ray astrophysics. The use of Liquid Xenon in the direct detection of dark matter particles called WIMPs has received renewed attention due to its easy scalability to large masses and its potential to improve the limits to WIMP detection to 1 event/100kg/year. The XENON experiment uses a dual phase liquid Xenon time projection chamber to search for WIMPs through the simultaneous measurement of ionization and scintillation signals from particle interactions with Xenon atoms. The ratio of primary to secondary scintillation from ionization for nuclear recoils from WIMPs or neutrons, and for electron recoils from background, allows for the event-by-event discrimination by the detector. As neutrons constitute the limiting background for a dark matter search, it is essential to fully characterize the response of liquid Xenon to a neutron background. This poster discusses the measurements and results obtained by irradiating a liquid Xenon liquid/gas phase detector with neutrons. The detector output was simulated using Monte Carlo techniques and the observed and expected recoil energy spectrum compared. The various neutron interactions in Xenon and the material surrounding the detector were examined. Understanding the neutron response to Xenon is critical in estimating contribution of backgrounds for dark matter searches.

Lattice QCD Constraints on Hybrid and Quark Stars

Evgeni Kolomeitsev[1], Yu.B. Ivanov[2], A.S. Khvorostukhin[3], V.V. Skokov[4], et al.
[1]*University of Minnesota*
[2] *GSI, Darmstad, Germany and Kurchatov Institute, Moscow, Russia*
[3]*JINR, Dubna, Russia*
[4]*GSI, Darmstad, Germany and JINR, Dubna, Russia*

A QCD-motivated dynamical-quasiparticle model with parameters adjusted to reproduce the lattice-QCD equation of state is extrapolated from region of high temperatures and moderate baryonic densities to the domain of high baryonic densities and zero temperature. The resulting equation of state matched with realistic hadronic equations of state predicts a phase transition into the quark phase at higher densities than those reachable in neutron star interiors. This excludes the possibility of the existence of hybrid (hadron-quark) stars. Pure quark stars are possible and have low masses, small radii and very high central densities. Similar results are obtained for a simple bag model with massive quarks, fitted to reproduce the same lattice results. Self-bound quark matter is also excluded within these models. Comparison with standard bag models is made.

Cosmic Rays, Superbubbles and Interstellar Mixing

Richard E. Lingenfelter[1], James C. Higdon[2]
[1]*University of California, San Diego*
[2]*Claremont Colleges*

The question of how freshly synthesized metals from supernovae are mixed into the interstellar medium is a long standing problem. We show that recent studies of cosmic ray nuclear interactions and abundances provide three independent measures of the first phase of the mixing process in the evolution of the metallicity in the supernova active cores of superbubbles, which form around OB star associations in giant molecular clouds. We discuss these measurements of cosmic-ray produced Li, Be and B in the early Galaxy, and the anomalous abundances of ^{22}Ne and the actinides in the cosmic rays which define the metallicity in these cores, which are the primary sites of cosmic ray acceleration. We also explore the implications of these measurements on the nature and time scales of the mixing process.

Quantum Celestial Mechanics

Franklin Potter[1], Howard G. Preston[2]

[1]*Sciencegems. com Formerly at U C Irvine*
[2]*Preston Research Formerly at U C Irvine*

A Schrödinger-like wave equation for a dust-filled universe has an effective repulsive negative gravitational potential that explains the cosmological redshifts of distant supernovae and galaxies as gravitational redshifts instead of inflationary redshifts. Supernovae light curve durations are determined by different clock rates at the source and observer. A matter density of about 5% of the critical matter/energy density is sufficient to agree with the energy density of the universe. The CMB microwave blackbody spectrum would need to originate from equilibrium with galaxy luminosities, and for a photon mean free path length of the Hubble radius, the CMB would be at about 3 K, the actual value depending upon the average light flux per galaxy. Previous applications in the Solar System and in galaxies with the Schwarzschild metric confirm the universality of this approach. A torsion bar near a rotating mass may be the critical laboratory test. This large-scale gravitational quantization is not quantum gravity and does not require 'dark matter' nor 'dark energy'. More details are found at gr-qc/0303112.

Magnetic phase diagram of QCD and compact stars

Toshitaka Tatsumi[1], K. Nawa[1], E. Nakano[2], T. Maruyama[3]

[1]*Department of Physics, Kyoto University*
[2]*Yukawa Institute for Theoretical Physics, Kyoto University*
[3]*College of Boiresource Sciences, Nihon University*

Nowadays, many efforts have been devoted to understand QCD at finite density (ρ) and/or temperature (T). We are here concentrated on the magnetic phase diagram in $\rho - \mathrm{T}$ plane. Our studies have been stimulated by discovery of *magnetars* with huge magnetic field of 10^{15}G $\gg$ 10^{12}G for standard radio pulsars. The origin of the magnetic field observed in compact stars is a long standing problem since the first discovery of a pulsar. Since there is widely developed hadronic matter inside compact stars, it should be reasonable to consider the microscopic origin of magnetic field. We have considered the possibility of ferromagnetism in quark matter, in analogy with electron gas [1,2]. By a perturbative calculation with OGE interaction, we have suggested that ferromagnetism may appear at low densities, where the Fock exchange interaction favors spin alignment (Bloch mechanism). Subsequently we have done a self-consistent mean-field calculation [3], where we have also taken into account the possibility of color superconductivity. Axial-vector mean-field is then responsible to ferromagnetism, and thereby the single-particle energy breaks rotation symmetry. Accordingly two Fermi surfaces for two spin degrees of freedom are deformed in the "prolate" and "oblate" shapes. Quark pairing is possible by taking quark pairs with opposite momentum to each other on each Fermi surface, so that the gap function becomes anisotropic. Consequently we have found that ferromagnetism and color superconductivity can coexist with little interference.

In the intermediate densities we may expect another magnetic phase by taking into account the chiral restoration [4]. With the pseudo-scalar density as well as the scalar density, we can consider other chiral-restoration paths than the usual one only with the scalar density as quark density increases. Assuming the plane-wave configuration for both densities, which we call *dual chiral density wave (DCDW)*, we have demonstrated that quark matter becomes unstable against formation of DCDW at a certain density around the restoration density in the usual treatment. Thus the restoration density is shifted to be higher due to DCDW. DCDW phase also exhibits an interesting magnetic aspect, *spin density wave*.

These magnetic phases should have some implications on relativistic heavy-ion collisions (RHIC) or compact stars; e.g. possibility of magnetized strangelets produced in RHIC or hadron-quark phase transition in early universe. Assuming the magnetars as quark stars we can estimate the magnetic field to be 10^{15-17}G, enough for magnetars.

[1] For a review, T. Tatsumi, E. Nakano and K. Nawa, hep-ph/0502201; hep-ph/0506002.
[2]T. Tatsumi, Phys. Lett. B489(2000)280.
[3]E. Nakano, T. Maruyama and T. Tatsumi, Phys. Rev. D68(2003)105001.
T. Tatsumi, T. Maruyama and E. Nakano, Prog. Theor. Phys. Suppl. 153(2004)190;hep-ph/0312351.
[4] T. Tatsumi and E. Nakano, hep-ph/0408294; Phys. Rev. D71(2005)114006.

Facilities and Instrumentation

Development and Testing of Novel Strip–Pixel Detectors for the Silicon Vertex Tracker at PHENIX.

Christina Haegeman

University of New Mexico

on behalf of the PHENIX collaboration.

A new Silicon Vertex Tracker (VTX) is being constructed for the PHENIX experiment at RHIC. Our prime motivation is to provide precision measurements of heavy–quark production (charm and beauty) in A+A, p(d)+A, and polarized p+p collisions. The VTX comprises of two inner layers of pixel detectors followed by two layers of novel strip–pixel detectors which provide 2D information with single–sided readout. We present the design of the strip–pixel detectors and the QA procedures being developed for the sensors.

A novel idea for nondestructive measurement of single charged particle

Kensuke Homma
Hiroshima University

Novel methods of nondestructive measurement for charged particles lead us to challenge new type of experiments in both accelerator related and non-related applications. As an accelerator related application, there is a successful example as the nondestructive measurement[**?**], which was aming at measuring a short bunch length containing 10^9 electrons. More challenging subject is whether we can achieve the nondestructive measurements for single charged particle or not, since there is no precedent to succeed to measure single charged particle and if one succeeds, it would maximize the extent of the application to all of particle physics. The principle of the nondestructive measurement is to measure an instantaneous change of a local refractive index due to electric fields of charged particles passing by a sensor surface. The change of the refractive index is detectable through the phase retardation i.e. the change of polarization states of scanning laser lights in a crystal. In [**?**] the actually used crystal was $LiNbO_3$ which has the electro-optical property (Pockels effect) originated from the uniaxial structure of ferroelectics. However, in order to achieve the nondestructive measurement for single charged particle, much more elaborated ideas are necessary. I willl propose to use $\bar{4}2$m type crystal such as KH_2PO_4(KDP) and KD_2PO_4(DKDP) operated at the structual phase transition temperatures to maximize the sensitivity to external electric fields or minimize the energy loss per detector element. In this presentation, I will provide an idea to drastically improve the signal to noise ratio based on the local diffraction pattern of scanning laser lights compared to the nondestructive measurement performed by [**?**] toward the single charged particle measurement with above mentioned crystals. In addtion, I also provide a conceptual design for a nondestructive ToF measurement as a concrete application to end-point energy measurement of tritium beta decays, by which an incommensurable energy resolution to anti-electron neturino mass is expected for the future experiments.

References

[1] Semertzidis, Y. K. et al., Electro-optical detection of charged particles, *Nucl. Instrum. Meth.*, **A452**, 396-400 (2000).

A Study on the Afterpulse of Photomultiplier Tubes

Heejong Kim, Nural Akchurin
Texas Tech University

The afterpulse phenomenon has been known to occur in the photomultiplier tube (PMT) several hundred nanoseconds later than the main pulse. We report on Hamamatsu PMT R7525, which was chosen for CMS forward calorimeter. Normally, the effects of afterpulse can easily be avoided easily by gating the main pulse. In the absence of such gating, the afterpulse can fake physics events. Various tests were conducted to investigate the behavior of the afterpulse using R7525 photomultiplier tube. Dependence on main pulse height and high voltage of the afterpulse was measured. The photomultiplier tubes were operated under helium abundant condition to see the effect of helium on afterpulse. We present our results on different types of afterpulses and give details especially on He generated afterpulse. As an example, timing distribution of afterpulse for a PMT, which was operated at –1300V HV, is shown in Fig. 1. ADC gate timing to measure the charge of 3 different afterpulses is indicated by arrows in Fig. 1.

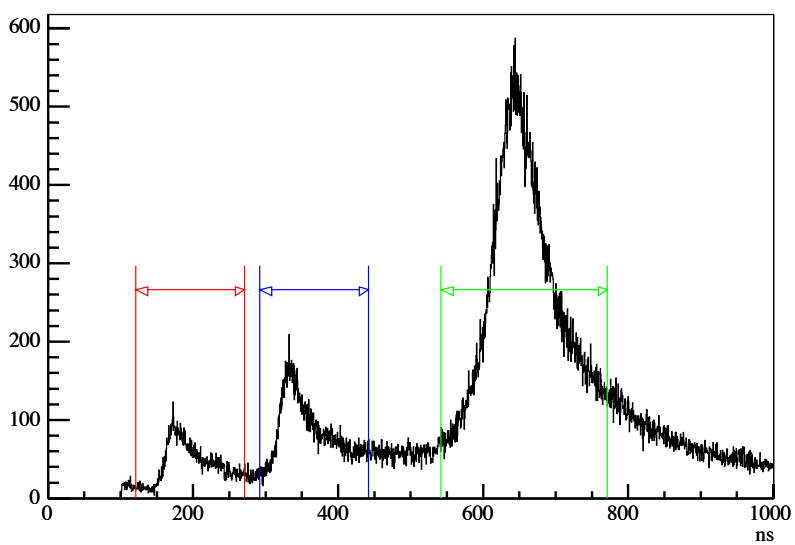

Fig. 1. Timing distribution of afterpulses from a PMT at –1300V HV. The leading edge of the main pulse was the reference for timing. The gate timing of 3 afterpulses is indicated by the colored arrows.

Separation of Scintillation and Cerenkov Light in an Optical Calorimeter

Heejong Kim
Texas Tech University

on behalf of the DREAM collaboration.

From a previous experiment, the Dual-Readout Module(DREAM) calorimeter showed that the energy resolution of hadronic shower can be improved by measuring the scintillation and the Čerenkov light simultaneously to eliminate the effect of fluctuation of electromagnetic shower fraction (f_{em}). The idea of the DREAM calorimeter can be applied to the optical calorimeter, even homogeneous calorimeter, if it is possible to separate the light into its scintillation and Čerenkov components. The scintillation lights are isotropically generated as a molecular de-excitation process while Čerenkov lights have spontaneous process, which have preferred angle with respect to the particle direction. Based on these different characteristics of the lights, 1) the time structure and 2) the angular distribution of light, two techniques to separate the lights into two components were tested with the DREAM calorimeter in H4 beam line of Super Proton Synchrotron at CERN from May to July 2004. We present our results of 2004 beam test. As an example, Fig. 1 shows the fraction of the signals recorded in ADC with Δt delayed gate to the original signals from 80 GeV electron beam data. It shows that Čerenkov light is faster than the scintillation light.

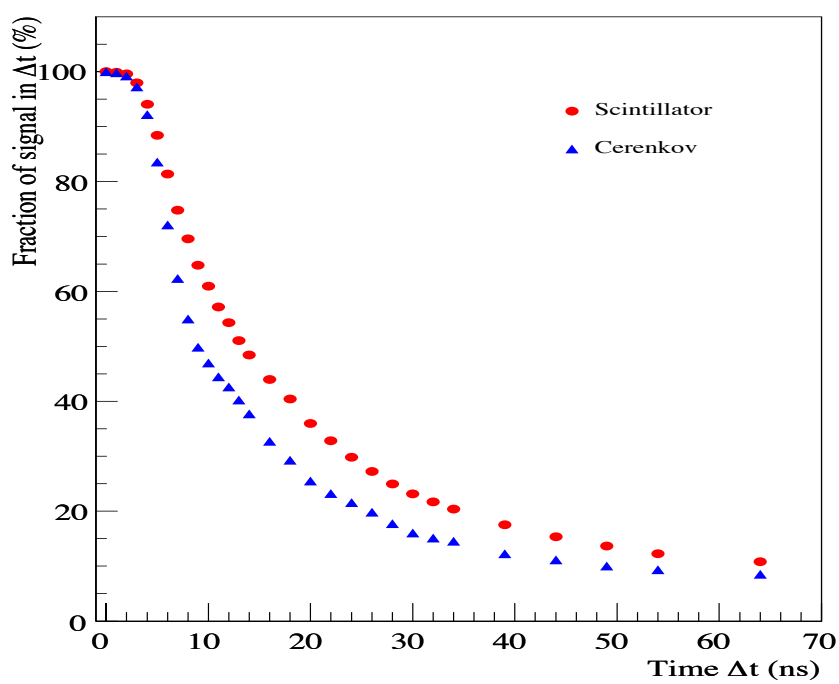

Fig. 1. The fraction of the signals measured in ADC with Δt delayed gate as a function of Δt.

Analysis of the Front End Electronics of the Low Voltage Distribution System

Oluwasoji Omotunde Omiwade
Abilene Christian University

on behalf of the PHENIX collaboration.

Miscellaneous

The Perception of Radioactive Waste among the People of Africa

Babagana Aubakar

BABAGANA RESEARCH

West Africa is one of the Africa's most populated regions, with a total population of approximately 200 million people. The West African sub–region comprises of sixteen different countries, which are as follows: Nigeria, Benin, Togo, Ghana, Cote Ivoire, Guinea, Guinea Bissau, Liberia, Sierra– Leone, Gambia, Senegal, Mauritania, Western Sahara, Mali, Burkina Faso and Niger Republique.

Apart from Nigeria, Senegal and Ghana all the other remaining countries are extremely poor and unviable. As a result of this the sub–region has been experiencing a lot of civil unrest, countries like Liberia, Sierra Leon and Code Ivore have been experiencing civil wars since the early 1990s. In addition to the already existing problems of trafficking in drugs, arms, humans and weaponry trade within the sub–region.

Today the sub–region is experiencing the coming of a new evil deal called "Trade in radio active waste"; which involves the transporting of radioactive wastes from the developed countries to it's waste bin in West Africa, where it is unsafely buried after collecting millions of dollars from It's original owners. Recent statistics have revealed that most of the people involved in the evil businesses of trafficking in drugs, human, arms and trading in weaponry, are diverting in to the so called evil business of "Trade in Radioactive waste" because this new illegal trade financially exceeds the rest of the above listed evil businesses.

Introduction of Appropriate Momentum Operator and the Role of Impulse–Momentum Theorem in Quantum Mechanics

Bunaro Eyasu Betalo

Physics

An appropriate momentum operator representation is introduced here. The earlier representation that follows from de Broglie postulate is in contradiction with the Compton Effect. Application of the new representation with Impulse–momentum theorem not only removes probability from heart of quantum mechanics but also forms straightforward approach for atomic/nuclear energy exploration.

SUSY Search at ATLAS

Gianluca Comune

Michigan State University

on behalf of the ATLAS SUSY GROUP collaboration.

We discuss the recent studies of Super Gravity models done with the ATLAS detector simulation. Detailed studies are performed with the realistic GEANT 4 simulation. The following two new results are focused in this talk. (1) Study of the background and the limitations to the sensitivity arising from different sources of systematic uncertainties: (2) The reconstruction of the characteristic signatures of SUSY models in the stau co-annihilation and Focus Point regions of parameter space, in which the predicted relic density of the Lightest Neutralino is consistent with cosmological constraints.

Coherent vector meson electroproduction off deuteron

Atilla Gonenc

Florida International University

on behalf of the CLAS collaboration.

QCD predicts Color Transparency (CT), which refers to nuclear medium becoming transparent to a small color neutral object produced in high momentum transfer reactions, due to reduced strong interaction. Despite several studies at BNL, SLAC, FNAL, DESY and JLAB, a definitive signal for CT still remains elusive. In this paper, we present the preliminary results of a new study at JLAB motivated by theoretical calculations that suggest fully exclusive measurement of coherent vector meson electroproduction off the deuteron as a favorable channel for studying CT.

Vector meson production has a large cross section at high energies, and the deuteron is the best understood and simplest nuclear system. Exclusivity allows the production and propagation to be controlled separately by controlling Q^2 , l_f (formation length), l_c (coherence length) and t. This control is important as the rapid expansion of small objects increases their interaction probability and masks CT.

The CT signal appears in a ratio of cross sections at high $-t$, where rescattering is significant, to low $-t$, where single nucleon reactions dominate.

Measurements of vector meson production were carried out using the CLAS detector in Hall B at Jefferson Lab and its large acceptance allowed measurements to span the range where vector meson dominance describes the process to the regime where pQCD becomes important.

Combined with photoproduction and proton target data, this study will allow systematic and complete study of the production and propagation of the qq in the nuclear medium which is important for understanding QCD in the transition region.

The Flow of Physics Knowledge from Laboratory to Members of the Public

Olumuyiwa Oladunni Oke
Ladoke Akintola University of Technology

The transfer of knowledge between groups of individuals of different levels of knowledge (physics researchers; members of the public) and orientation is discussed with reference to the manner in which physics knowledge is disseminated. A prototype system that allows easy access to knowledge at these different levels was designed in order to overcome the limits and obstacles associated with the more traditional linear model of knowledge transfer. The controversial relationship between physics researchers in the laboratory and members of the public is the basis of arguments in this paper.

Keywords: Knowledge Transfer, Knowledge Diffusion, Knowledge management, Knowledge Networks, Information Technology, Terminology Management and Physics

Student Posters

Magnetic Storms Formation in the Earth's Atmosphere.

Oladele I. Akintola[1], Adekunle A. Adegoke[2]

[1]*Physics Students Association of Nigeria (PSAN).*
[2]*Physics Students Association of Nigeria.(PSAN).*

The phenomenon of magnetic storms is one of the transient changes of the earth's magnetic field. It can last for hours and almost few days as compared with the regular periodic scalar variations of the earth magnetic field. The study of magnetic storms have significant in radio communications, the generation of power by the electric power authority. And the geophysical (Magnetic) survey in the solid mineral industry. This paper focused in tracing the origin of earth's magnetic storm down to the earth surface. More so Interplanetary magnetic field (IMF) intensity equations was derived by employing the magneto–hydro–dynamic theory (MHDT). It was observed that the field varies as r2 near the sun and r1 far away from the sun.

About Limit Masses of Elementary Particles in Quantum Field Theory with Fundamental Mass

Farruh Akramov

Samarkand State University

on behalf of the Umida Khodjaeva collaboration.

The construction of a sequential Quantum Field Theory (QFT) with a new, universal scale in the superhigh energy region - Fundamental Mass M emanates to V.G.Kadyshevskiy's work [1]. This Fundamental Mass and corresponding to it fundamental length, probably, are called to play the same key role in physical theory, as Planck's constant, the speed of light or Newtonian gravitational constant do, and sequentially in quantum field theory appear as a characteristic scale in the superhigh energy region.

In this work the simple examples of spontaneous breaking of various symmetries for the scalar theory with fundamental mass have been considered [1]. Higgs' generalizations on fundamental mass have been found.

In this work with the application of the concept of Markov's "Maximon" [2] shown, that the account of the spontaneous breaking of symmetry results in the appearance of goldstone scalar non-mass particle and material scalar particle, having defined mass, and this particle can be identified with Markov's "Maximon".

As we know, the local fields are referred to the lowest representations of appropriate compact groups of symmetry. As to particles' mass, this magnitude is Kazimir's operator of Poincare's noncompact group, and in those representations of the given group, which are being used in QFT, can take any values. In 1965 M.A. Markov put forward the hypothesis [2], according to that the spectrum of masses of elementary particles must break on "Planck's mass" $m_{Plank} = \sqrt{\frac{\hbar c}{G}}$ (G - gravitational constant) $M \leq m_{Plank}$. Particles with the limit mass $m = m_{Plank}$ M.A. Markov has defined as " maximons ". " Maximon's " concept has been put in the basis of Markov's script of the early Universe. In this work has been proved, that because of the spontaneous break of the symmetry both goldstone scalar non-mass particle and material scalar particle appear, that, if we accept it for maximon, then maximon will has the mass: $m_{Maximon} = \frac{2M}{(\sqrt{2}+1.25)^{1/2}}$.

Reference

[1] Kadyshevsky V.G., FERMILAB-Pub 78/70 THY, September, 1978. Ibadov R.M., Kadyshevsky V.G. Proc.5th Int. Symp. Selected Topics In Statistical Mechanics, Dubna-1989, world Scienfic p.131-156 (1989).

[2] Markov M.A. JETF 1966, v.51, page 878; Markov M.A. Preprint INR, P-0207,1981, P-0286, 1983; Kadyshevsky V.G. The quantum theory Fields and Markov's "maximon". Preprint JINR P2-84-753, JINR, Dubna, 1984, 11.

Transverse single spin asymmetries from muons in polarized p+p collisions at $\sqrt{s_{NN}} = 200$ GeV

Hisham Al Bataineh

New Mexico State University

on behalf of the PHENIX collaboration.

Measurement by E704 of non-zero single spin asymmetries(SSA) in inclusive particle production at fixed target energies have generated much interest since leading twist collinear factorized pQCD predicts that these asymmetries should be small. This interest has recently grown with the discovery by the STAR and BRAHMS collaborations that these asymmetries persist even to RHIC energies. Precision measurements of SSAs in different regions of x_F and p_T and their QCD analysis may serve to quantify contribution from the different mechanisms.

The PHENIX muon arms cover forward rapidity range of $1.2 < |\eta| < 2.4$, which corresponding to non-zero value of x_F. We study single spin asymmetries with single inclusive muons at different x_F and p_T ranges from collisions of polarized p+p collisions at $\sqrt{s_{NN}} = 200$ GeV. The current status of this analysis will be presented.

Detection of Cherenkov Light with Wavelength Shifting Acrylic Plastic

Brian Beckford, Naipy Perez, Joerg Reinhold

Florida International University

The collection efficiency for Cherenkov light from a fused silica radiator incident on a wavelength shifting acrylic plate (WLS) has been determined during a beam test at the proton synchrotron at the KEK facility. The yield of the photoelectrons produced through internally generated Cherenkov light as well as light incident from the radiator was measured as a function of the momentum of the incident beam. The yield is directly proportional to $\sin^2_\Theta$ where Θ is the angle of the Cherenkov light created. This allows the extraction of the photon collection efficiency of the WLS which is roughly 51% for photons created in the fused silica radiator. This is comparable to more traditional means of detecting photons in RICH detectors, like CsI photocathodes or large PMT arrays. Currently, small prototype tests and Monte Carlo simulations are being conducted to investigate the feasibility of using arrays of WLS bars as a means of constructing cost efficient one-dimensional RICH detectors.

Target Density Fluctuation Monitoring in the Happex Helium Parity Violation Experiment at Jefferson Lab

Lindsay Glesener

San Francisco State University

Background: The Happex-He experiment is a parity violation experiment using Jefferson Lab's continuous electron beam and a cryogenic helium gas target[1]. The summer 2004 run of Happex was limited to an electron beam current of 35 microamps[2] because of density fluctuations in the helium target. These fluctuations, which increased dramatically at high current, increased the statistical error of the experiment[3]. For the summer 2005 run of Happex, tests were conducted to determine the extent of the target density fluctuations and to find target and beam configurations that minimized these fluctuations.

Method: Eight quartz luminosity monitors, which were not sensitive to parity violating asymmetries, were used to measure the widths of asymmetry distributions due to target density fluctuations. The asymmetry widths were measured as the electron beam current, beam raster size, target fan speed, and target density were varied. These widths were then compared to widths for conditions which should not produce density fluctuations.

Results: With an electron beam current of 30 μA, target density fluctuations were found to contribute 480 ppm to the statistical error. This is an increase of 2% in the statistical error of the experiment. Low beam currents lessened fluctuations, as did a large beam raster, high target fan speed, and high target density.

Conclusion: In order to measure many electron-nucleus interactions while minimizing target density fluctuations, the Happex experiment should run at a moderate current of 30 to 40 microamps.

References: 1**.** D. Armstrong and R. Michaels, spokespersons, He4 Parity Experiment No. E00-114. 2**.** K.A. Aniol *et al*., Phys. Rev. C 69, 065501 (2004). **.** D. Armstrong, B. Moffit, R. Suleiman, "Target Density Fluctuations and Bulk Boiling in the Hall A Cryotarget," Tech Note JLAB-TN-03-017, 2003.

Vector Meson Mass Corrections at $O(a^2)$ in PQChPT with Wilson and Ginsparg-Wilson quarks

Hovhannes R Grigoryan[1], Anthony W. Thomas[2]

[1]*Thomas Jefferson National Laboratory / Louisiana State University*
[2]*Thomas Jefferson National Laboratory*

We derive the mixed as well as unmixed lattice heavy meson chiral Lagrangian up to order $O(a^2)$, with Wilson and Ginsparg-Wilson fermions. We consider two flavor partially quenched theory and calculate vector meson mass corrections up to order $O(a^2)$, including the corrections associated with the violation of O(4) rotational symmetry down to hypercubic group. The chiral extrapolation formula is then compared with that used in numerical simulations.

Spin Dressing Effects on Polarized Helium 3

David Howell, et al.

University of Illinois at Urbana-Champaign

The electric dipole moment (EDM) of the neutron provides a unique window into CP-violating processes in the light-quark baryons sector. A new experiment with ultracold neutrons aims to measure the neutron EDM with a sensitivity of 10^{-27} e-cm. The experiment will use a novel comagnetometry technique with polarized ^{3}He "dressed" by an RF magnetic field to match its effective magnetic moment to that of the neutron, allowing a sensitive measurement of the precession frequency of neutrons. We have studied the dressed ^{3}He spin system experimentally. Results on the spin dressing effects on the ^{3}He magnetic moment over a broad range of experimental conditions will be presented.

$B \to \rho(\omega)\gamma$, $B \to K^*\gamma$ and the Unitarity Triangle

Karsten Koeneke
Massachusetts Institute of Technology, Laboratory for Nuclear Science

on behalf of the Babar collaboration.

This poster discusses the most recent BaBar measurements of the branching fraction of the decays $B \to \rho(\omega)\gamma$ and $B \to K^*\gamma$ and its implications for the Unitarity Triangle.

The ratio of these branching fractions is proportional to the ratio of the Cabibbo-Kobayashi-Maskawa elements $|V_{td}/V_{ts}|$, and therefore measures the length of the far side of the Unitarity Triangle.

The results resented in this poster are based on the analysis of 211 million $\Upsilon(4S) \to B\bar{B}$ events collected by the BaBar detector between 1999 and 2004. These results have been recently published [Phys. Rev. Lett. 94, 011801, 2005].

Candidate Molecular Ions for an Electron EDM Experiment

Edmund R Meyer, et al.
JILA

An experiment has been proposed to trap heteronuclear diatomic molecular ions to search for the electron's electric dipole moment (eEDM) [1]. In order to pick a suitable molecule many parameters must be considered, including the polarizability, rotational constant and nuclear charge of the heavy atom, as well as the expected size of the science signal (the effective electric field experienced by the electron). We have developed an expedient method to estimate these properties using standard molecular structure software. This method enables us to investigate a large number of possible molecules, and points us toward the most promising candidates. We have used this technique to identify as promising candidates the hydrides HfH^+ and PtH^+.

[1] R. Stutz and E.A. Cornell, DAMOP 2004 Poster.

Exclusive η meson reconstruction in pp collisions with the HADES spectrometer

Anar Rustamov[1], Stefano Spataro[2]

[1]*GSI, Gesellschaft für Schwerionenforschung mbH, Germany*
[2]*INFN, Instituto Nazionale di Fisica Nucleare,Italy*

on behalf of the HADES collaboration.

HADES is a second generation experiment for high resolution spectroscopy of electron pairs produced in proton, pion and heavy ion induced reactions. The spectrometer is installed at the SIS at GSI Darmstadt and is operational since 2002. The main goal of this contribution is to present exclusive η meson reconstruction from both, hadronic and electromagnetic decay channels in proton-proton collisions at 2.2 GeV. The reconstruction procedure is based on selections made on missing mass distributions. In order to obtain better mass resolution and signal to background ratio, a kinematic fit algorithm has been developed, showing significant improvements for both decay channels. The ratio of reconstructed η mesons in the electromagnetic and hadronic decay channels will be shown both for data and simulation. The results will also be used to evaluate the HADES dielectron reconstruction efficiency. The performance of track reconstruction using pp elastic channel, a concept for particle identification without a start detector, based on reaction time reconstruction from known particle momentum and mass will also be shown.

Measurement of the Decay Rate and Form Factor Parameters of the Decay $K_L \to e^+e^-\gamma$

Michael J Wilking

University of Colorado - Boulder

on behalf of the KTeV collaboration.

We present a measurement of the branching ratio for the decay $K_L \to e^+e^-\gamma$ using data from the 1997 run of the KTeV (E799) experiment at Fermilab. We also report a measurement of the $K_L \to \gamma^*\gamma$ form factor using the parametrizations by Bergström Massó Singer (BMS) and by D'Ambrosio Isidori Portolés (DIP). Our result is a factor of 13 improvement in statistics over the previous most precise result.

Public Science Lecture

Frontiers of Cosmology: Recent Successes and Future Challenges

Wendy L. Freedman
Carnegie Institute of Washington

Wednesday, October 26th

9:00 AM–12:10 PM, Plenary Session #3

Heavy Ion Collisions at RHIC and at the LHC: Physics Challenges

Urs Achim Wiedemann
CERN Physics Department

The wider kinematical range accessible in nucleus-nucleus collisions at RHIC and LHC collider energies opens novel opportunities for studying the properties of dense QCD matter. In particular, a large class of abundantly produced high transverse momentum processes is highly sensitive to medium properties due to the phenomenon of jet quenching. This allows us to characterize with unprecedented detail partonic equilibration processes, and it has the potential to elucidate the microscopic dynamics underlying the most dominant bulk phenomena of heavy ion collisions, namely collective flow and approximate hadrochemical equilibrium. On the other hand, there is increasing evidence that understanding the origin and effectiveness of equilibration processes relies on a better characterization of the high initial parton densities, including the potentially large non-linear contributions to their evolution. The much wider longitudinal phase space at collider energies provides novel means to this end. Here, I present my view of what has been learnt already about dense QCD matter due to the wider kinematical reach of RHIC, and what are the most promising avenues for making further progress in the near future.

Nucleon Structure: Spin Content

Naohito Saito
University of Kyoto

Contribution of Strange Quarks to Proton Structure

Douglas H. Beck
Loomis Laboratory of Physics, University of Illinois at Urbana-Champaign

By measuring parity-violating elastic electron scattering from protons, the contributions of strange quarks to proton ground state properties can be determined. Several recent experiments have made such measurements, and a picture of this physics may be starting to emerge. In particular, the combined results of five measurements at Q^2 = 0.1 GeV^2 suggest the size of the strange quark contribution to the magnetic moment of the proton is at the 5-10% level. A summary of these recent measurements and the physics implications will be presented.

Status and New Opportunities in Neutrino Physics

Boris Kayser
Fermilab

New Results in Neutrino Measurements

William C. Louis III
Los Alamos National Laboratory

SM and Beyond: Clues from Recent Charm Measurements

Marina Artuso
University of Syracuse

Thursday, October 27th

9:00 AM–12:10 PM, Plenary Session #4

Connecting Dark Energy and Fundamental Physics

Mark Trodden
University of Syracuse

Dark Matter: Search for WIMPS

Daniel S. Akerib
Case Western Reserve University

New Prospects for Detection of the Highest Energy Cosmogenic Neutrinos

Peter Gorham
University of Hawaii

Rare B and K Decay

Jeff Richman
University of California, Santa Barbara

CP Violation in B Decays: Status of the Unitarity Triangle

Masanori Yamauchi
KEK

CP Violation in B Decays: Search for Physics Beyond the SM

Hassan Jawahery
University of Maryland

2:30–4:00 PM, Parallel Session #4

I.7 Quarks and Gluons in Hot/Cold and Dense Matter:
Collision Dynamics, Correlations and Fluctuations

Perfect fluidity of the sQGP core and dissipative hadronic corona

Tetsufumi Hirano, Miklos Gyulassy
Department of Physics, Columbia University

The agreement of hydrodynamic predictions of differential elliptic flow and radial flow patterns with Au+Au data at $\sqrt{s_{NN}} = 200$ GeV is one of the main lines of evidence suggesting the nearly perfect fluid properties of the strongly coupled Quark Gluon Plasma, sQGP, produced at RHIC. We study the sensitivity of this conclusion to different hydrodynamic assumptions on hadro-chemical and thermal freezeout after the sQGP hadronizes. In order that all the data on (1) hadronic ratios, (2) radial flow, as well as (3) differential elliptic flow be reproduced, the sQGP core must expand with a minimal viscosity that is even greater than the viscosity of its hadronic corona. However, because of the large entropy density difference of the two phases of QCD matter, the larger viscosity in the sQGP phase leads to nearly perfect fluid flow, while the smaller entropy density of the hadronic corona strongly hinders the applicability of Euler hydrodynamics. The “perfect fluid” property of the sQGP is thus not due to a sudden reduction of the viscosity at the critical temperature, but to a sudden increase of the entropy density of QCD matter and is therefore an important signature of deconfinement.

System Size and Energy Dependence of Elliptic Flow

Alice C. Mignerey
University of Maryland

on behalf of the PHOBOS collaboration.

Azimuthal correlations are proving to be an extraordinarily powerful tool in elucidating the initial conditions and dynamical evolution of matter created in relativistic heavy ion collisions. As our theoretical vision of heavy ion collisions evolves, differential flow measurements are providing both guidance and strong constraints. This work examines the elliptic flow as a function of pseudorapidity, centrality, transverse momentum, energy and species. The data presented were taken with the PHOBOS experiment at RHIC during Au–Au and Cu–Cu collisions ranging over an order of magnitude in energy. The broad and continuous pseudorapidity coverage of PHOBOS makes these results particularly useful in constraining the three–dimensional structure of the collisions. The implications of these data on the source initial conditions and dynamics will be discussed.

Rapidity Dependence of Elliptic Flow at RHIC

Erik Johnson[1], Hiro Ito[2]
[1]*University of Kansas*
[2]*Brookhaven National Laboratory*

The measured elliptic flow (v_2) of identified particles as a function of p_t and centrality at RHIC suggests the created medium in Au+Au collisions achieves early local thermal equilibrium that is followed by hydrodynamic expansion. These measurements of identified particle v_2 have been limited, however, to a narrow region about mid-rapidity. Charged-hadron v_2 measurements show a significant reduction at foward pseudorapidities. It is not known if this η dependence is a general feature of elliptic flow or reflects other changes in the particle spectra in going to the foward region. The BRAHMS experiment provides unique capabilities to measure v_2 at foward rapidities. Using the BRAHMS multiplicity array to determine the v_2 event plane, identified particle elliptic flow can be measured using the BRAHMS spectrometers. This talk will discuss the identified particle elliptic flow at η = 0, 1, 2.7 and 3.4 from Run 4 Au+Au collision at $\sqrt{s_{NN}}$ = 200GeV. In addition, the p_t-integrated flow for charged hadrons obtained using just the multiplicity array will be presented.

Evolution of event-by-event transverse energy (E_T) fluctuations over collision centrality in RHIC interactions

Raul L Armendariz

New Mexico State University

on behalf of the PHENIX collaboration.

A quark-gluon plasma (QGP) state of matter affecting E_T production in relativistic heavy ion interactions, and produced more frequently in central than in peripheral events, may leave a phase transition signature in event-by-event E_T distributions. Comparing the relative widths of distributions across centrality is done in a search for a QGP. The standard deviation, σ, and mean, μ, are moments of distributions and their ratio quantifies the relative fluctuation; the fluctuation measurement is made for each centrality class and its evolution is studied by $\frac{\sigma^2}{\mu}$ versus collision participant nucleons. Purely random combinations as a function of centrality is characterized by $\frac{\sigma^2}{\mu}$ remaining constant, and deviations from this are evaluated. We report on the current status of E_T fluctuations analysis performed using $\sqrt{s_{NN}} = 200$ GeV Au+Au, $p + p$, d+Au, and 62.4 GeV Au+Au data recorded by the electromagnetic calorimeter of the PHENIX detector. The relationship between E_T and multiplicity fluctuations will be explored.

Probing Collision Dynamics with Fluctuation and Correlation Studies at RHIC

Claude A Pruneau

Wayne State University

on behalf of the STAR collaboration.

We present results of net charge, transverse momentum, and kaon vs pion multiplicity fluctuations analyses in Au + Au collisions at $s_{NN}^{1/2}$ =20, 62, 130, and 200 GeV. Results are discussed based on theoretical predictions, and compared to those of PHENIX, CERES and NA49. Net charge fluctuations are finite and in qualitative agreement with resonance gas, and quark coalescence models. They exhibit the minimal beam energy dependence expected for a finite system due to constraints of charge conservation. Normalized transverse momentum correlations $< \Delta p_t, \Delta p_t >^{1/2} / < p_t >$ exhibit no sizable dependence on beam energy. These analyses were conducted with various azimuthal ranges to investigate radial flow, and resonance productions dependences on collision centrality. The p_t analysis is also done relative to the collision reaction plane. We present the first kaon vs pion multiplicity fluctuations at RHIC, and compare with results from NA49 at lower energy.

Quark-antiquark production from classical fields and chemical equilibration

Tuomas Lappi[1], F. Gelis[2], K. Kajantie[1]

[1]*University of Helsinki*
[2]*SPhT, CEA/DSM/Saclay*

Much attention has recently been given to the thermalization properties of QCD matter formed in ultrarelativistic heavy ion collisions. Hydrodynamic analysis have assumed rapid initial thermalization and essentially entropy conserving expansion thereafter. Now RHIC experiments suggest that this is the correct picture. However, the chemical equilibration of the initially gluonic system remains a theoretical problem.

The classical field approach has been used successfully in both analytical and numerical calculations to understand the gluonic part of the small-x wavefunction of a nucleus and gluon production in relativistic heavy ion collisions.

We compute the number of quark-antiquark pairs produced in the classical color fields of colliding ultrarelativistic nuclei. The calculation is done by numerically solving the Dirac equation in the background given by these classical fields. The backreaction of the created pairs on the color fields is not taken into account. While the number of $q\bar{q}$ pairs is parametrically suppressed in the coupling constant, we find that for realistic couplings at RHIC energies it could, in this classical field model, even be compatible with the thermal ratio to the number of gluons. After isotropization one could thus have quark-gluon plasma in chemical equilibrium.

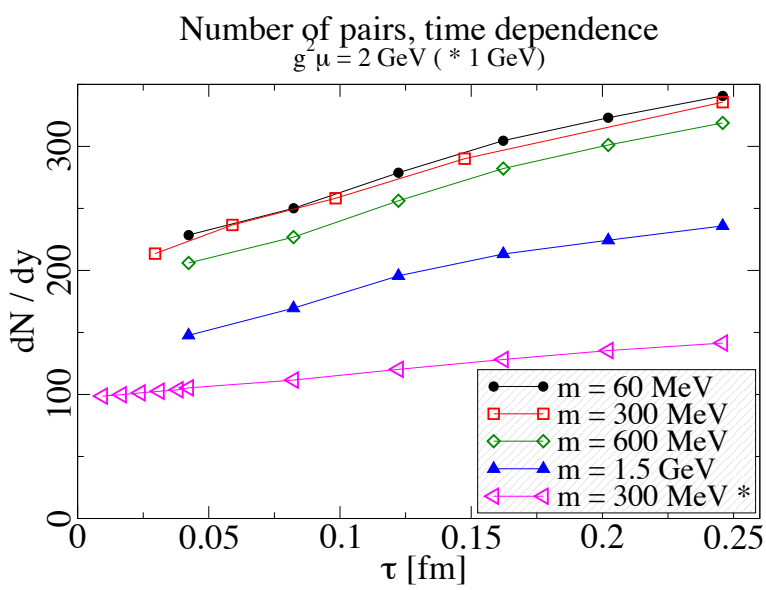

Fig. 1. Dependence on proper time τ of the number of pairs of one flavor per unit rapidity dN/dy. The value of the charge density of the classical color charges $g^2\mu$ is 2 GeV for the upper curves and 1 GeV for the lower curve. The values of quark masses used are marked on the figure.

I.8 Quarks and Gluons in Hot/Cold and Dense Matter:
Collision Dynamics, Particle Spectra and Strangeness

New Results from NA49

Zoltan Fodor
KFKI-Institute for Particle and Nuclear Physics

on behalf of the NA49 collaboration.

High p_T neasurements of pion, proton, K^0-s and Λ production at midrapidity in Pb+Pb collisions at 158GeV/nucleon beam energy are presented. The ratio of R_{CP} (as a function of p_T is extracted and compared to RHIC measurements. Particle yield ratios (proton/pion and Λ/K^0) are presented, showing a high p_T enhancement of the baryon/meson ratio for $p_T > 2\mathrm{GeV}/c$ in central collisions. Measured the flow of the Λ and compared to the flow of the pions and protons and the energy dependence of particle production on the range of SPS (20-158 Gev/nucleon).

Identified particle transverse momentum spectra in p+p and d+Au collisions at $\sqrt{s_{NN}}$ = 200 GeV

Pawan Kumar Netrakanti

Variable Energy Cyclotron Centre

on behalf of the STAR collaboration.

Identified transverse momentum spectra in p+p and d+Au collisions provides an important testing ground for perturbative quantum chromodynamics (pQCD) and to models based on multiple parton interactions in final state (EPOS). They also provide a reference spectra for quantifying the suppression of particle production at high transverse momentum in nucleus-nucleus collisions. Study of particle production in d+Au collisions in forward and backward rapidities will help in constraining the models based on initial multiple partonic scattering and those based on gluon saturation picture.

In this talk we present the transverse momentum spectra ($0 < p_T < 10$ GeV/c) for pions,protons and anti-protons at midrapidity ($|y| < 1.0$) in p+p and d+Au collisions at $\sqrt{s_{NN}}$ = 200 GeV measured in the STAR experiment at RHIC. We observe that the transverse momentum spectra of pions in p+p collisions are found to be consistent with both phenomenological model (EPOS) and with NLO pQCD calculations. We have found that both pion and proton spectra follows x_T scaling in p+p collisions. The Nuclear Modification Factor (R_{dAu}) for pions, protons and anti-protons in d+Au collisions at midrapidity are observed to be higher than unity at intermediate p_T ($2 < p_T < 6$ GeV/c). The value of proton R_{dAu} is higher than that of pions. This is consistent with the predictions based on a coalescence model calculations where the effect is treated as final state interaction. The p_T dependence of particle ratios for p+p and d+Au collisions will be presented. The eta-asymmetry ratio for identified pions in d+Au collisions will also be discussed.

Status of Strangeness Physics in Heavy-Ion Physics

Helen Caines

Yale University

A brief study of the yields and spectra of strange particles produced in heavy-ion and elementary collisions is presented using results from RHIC, SPS and the AGS.

The spectra of strange hadrons have been measured as a function of centrality for a variety of collision systems and energy. Thus, system size effects on strange particle production and their kinematics, such as flow and the nuclear modification factors can be studied. An excitation function of strange hadron production will be presented and the possible effects of entropy and the volume of the source on strangeness are discussed. Comparisons to theoretical models of strangeness production in heavy-ion collisions are also made

Thermodynamic properties of quark matter: droplets and strangelets formation

Celia A. de Sousa[1], P. Costa[1], M. C. Ruivo[1], Yu. L. Kalinovsky[2]

[1]*Physics Department*
[2]*Joint Institute for Nuclear Research, Dubna*

The study of finite lumps (droplets) of quark matter plays an important role for the search of quark gluon plasma (QGP) in recent relativistic heavy-ion collisions [1]. At low temperatures and densities the quarks are confined into hadrons. As the temperature or density increase there is the possibility from QCD that hadronic matter undergoes a phase transition. It is believed that the QGP lies in the chiral symmetric phase, where all symmetries of the QCD Lagrangian are restored. This motivates a growing activity devoted to the analysis of the thermodynamics of the quark matter, as well as to the study of the QCD phase diagram. Several QCD inspired models have been used to this purpose. The most interesting aspects of such investigations would be to observe signs of phase transitions. This is a challenging topic bearing in mind the results of present and future experiments to which the present lattice calculations are still away from giving definitive answers.

We perform our calculations in the framework of Nambu-Jona-Lasinio type models, by using a standard bosonization procedure [2,3]. At zero temperature the emphasis is put on investigating droplets formation, which can provide signs indicating a first order phase transition. In fact, the appearance of an absolute minimum of the energy per baryon signifies the possibility for finite droplets to be in mechanical equilibrium with the vacuum at zero pressure. Since for very low temperature the absolute minimum of the energy turns to be at zero density, the phase transition is still first order but the system is unstable against expansion. With increasing temperature we will have a crossover. We also consider the possibility of bound states in quark matter with the admixture of strange quark matter. We observe that the energy density is reduced by having three Fermi seas instead of just two in the absence of strangeness, and more significant bound states (strangelets) are obtained in this case.

Work supported by Caloust Gulbenkian Foundation (P. Costa), CFT and by FEDER/FCT under projects POCTI/FNU/50326/2003 and POCTI/FP/63412/2005.

[1] F. Karsch and E. Laremann, Phys. Rev. D 50, 6954 (1994); K. Kanaya, Prog. Theor. Phys. Suppl. 129, 197 (1997); C. Lourenço, Nucl. Phys. A 698, 54 (2002).
[2] P. Costa and M. C. Ruivo, Europhys. Lett. 60 (3), 356 (2002); P. Costa, M. C Ruivo, C. A de Sousa and Yu. L. Kalinovsky, Phys. Rev. C 70, 025204 (2004).
[3] P. Costa, M. C. Ruivo, C. A de Sousa and Yu. L. Kalinovsky, Phys. Rev. D 70, 116013 (2004); Phys. Rev. D 71, 116002 (2005).

Strangeness production in small and large collision systems at RHIC

Mark Heinz
Yale University

on behalf of the STAR collaboration.

We present measurements of strange and multi-strange hadrons in p+p and heavy ion collisions at sqrt(s) = 200 GeV. This data from different collision systems allows us to study the system size dependence of strangeness production. Firstly, we will compare strange particle production in p+p collisions to LO and NLO pQCD models and draw conclusions about their validity. Next, we will study the centrality dependence in heavy ion collisions of strange and multi-strange particle production. In particular we show that a non-linear dependency exists between (anti)-hyperon yields and the commonly used system size variable, N_{part}. This behavior disfavors widely used thermal equilibrium models. Other possible variables representing a better estimate of the correlation volume have been investigated and results will be shown.

Charge Transport in High-Energy Hadron Collisions

Paul Stankus
Oak Ridge National Laboratory

Precise measurement of net electrical charge density can reveal the transport of quarks in high-energy p + p or A+A collisions. Such measurements could shed interesting light on the “baryon anomaly” observed at RHIC, on the existence of baryon junctions, and on the general questions of initial stopping and transport in hadronic collisions. We will examine what constraints can be placed on charge transport from existing RHIC and ISR data, and discuss possible future high-precision measurements.

II.4 Quantum Chromodynamics: *Experimental Results I*

The structure of the proton measured at HERA

Yuji Yamazaki
DESY

on behalf of the H1 and ZEUS collaboration.

The structure of the proton is accurately constrained by measurements from the H1 and ZEUS experiments at HERA. Measurements in inclusive deep inelastic scattering over five orders of magnitude in the virtuality of the exchanged photon, Q^2, and Bjorken x are well described by next-to-leading order QCD. Recent jet and very high-x (up to 1) data have and will provide further constraints in this high Q^2 and x regime. The structure of the proton at low x and Q^2 is less well-understood and remains a challenge for phenomenology.

Rosenbluth Separation of electropion production cross-section from Hydrogen and Carbon

Xin Qian[1], Ben Clasie[2], Dipangkar Dutta[1], Haiyan Gao[1]
[1]*TUNL, Duke University, Durham, NC, USA*
[2]*Massachusetts Institute of Technology, Cambridge, MA, USA*

on behalf of the JLab E01107 collaboration.

Jefferson Lab (JLab) experiment E01-107 has collected data on pion electroproduction from hydrogen and several nuclear targets. The primary motivation of this experiment is to search for signatures of the phenomenon predicted by perturbative quantum chromodynamics (pQCD) known as Color Transparency (CT). CT refers to the suppression of final (and initial) state interactions of hadrons with the nuclear medium in exclusive processes at large momentum transfers. This involves using the ratio of semi-inclusive electroproduction of pions from nuclear targets to hydrogen target to extract the nuclear transparency of pions. This method relies on the assumption that the reaction mechanism of electropion production from hydrogen is similar to the quasi-free eletropion production from nuclear targets. In order to test this assumption, data were collected at forward and backward electron angles at two different values of momentum transfers squared (Q^2). By comparing the separated cross-section from hydrogen and heavier targets one can test this assumption.

We have extracted the longitudinal/transverse separated cross-sections at the lower of the two Q^2 settings from hydrogen and carbon targets and we have compared the separated cross-sections. These preliminary results will be presented. This work is supported by the U.S. Department of Energy under contract number DE-FG02-03ER41231.

Measurement of Light-Cone Wave Functions by Diffractive Dissociation

Daniel Ashery
Tel Aviv University

A powerful way to describe hadronic internal structure is through the Light-Cone Wave Functions (LCWF) which are solutions of the light-cone Hamiltonian. They encode the quarks and gluons momenta and helicities. These functions enter the calculation of a large variety of hadronic properties such as static and transition form factors, decay modes etc. Diffractive dissociation of particles have been demonstrated as a method to measure their valence light-cone wave functions. The valence LCWF of pions was measured by Fermilab E791 collaboration by diffractive dissociation to dijets . The effect of color transparency was demonstrated within the same experiment.

Measurements of the light-cone wave function of the photon yield information on both their electromagnetic and hadronic components. These were measured by the ZEUS collaboration in DESY. The electromagnetic component was studied by diffractive dissociation to $\mu^+\mu^-$ pairs. The hadronic $|q\bar{q}\rangle$ component of the photon was studied by diffractive dissociation to dijets and to $\pi^+\pi^-$ pairs.

The results of both experiments willbe presented and discussed.

Di-electron Widths of the Upsilon$(1, 2, 3S)$ Resonances

Jim Pivarski
Cornell

on behalf of the CLEO collaboration.

We have determined the di-electron widths (Γ_{ee}) of the $\Upsilon(1S)$, $\Upsilon(2S)$, and $\Upsilon(3S)$ to be 1.336 ± 0.009(stat) $\pm$ 0.019(syst)keV, 0.616 ± 0.010(stat) $\pm$ 0.009(syst)keV, and 0.425 ± 0.009(stat) $\pm$ 0.006(syst)keV, respectively. To measure these widths to their 2% precisions, the Cornell Electron Storage Ring scanned the production cross-section lineshapes of the three resonances in e^+e^- collisions, providing the CLEO detector with a total of 0.61fb^{-1} of lineshape data and 0.76fb^{-1} below resonance for background subtraction. These measurements are a precise check on lattice QCD calculations for an observable related to f_B.

Leptonic and Semileptonic Decays from CLEO

Sheldon Stone

Syracuse University

on behalf of the CLEO collaboration.

We report on a measurement of the decay width of the D+ meson into a muon and neutrino that lead to a value of the decay constant of (222.6 +- 16.7 {+2.8}{-3.4}) MeV. We also give values for the inclusive semileptonic decay rate of both D0 and D+ mesons. Finally, we show our measurements of exclusive semileptonic branching ratios in both Cabibbo favor and suppressed modes.

Observation of vector meson modification in 12-GeV p+A interaction

Satoshi Yokkaichi
RIKEN

on behalf of the KEK-PS E325 collaboration.

In QCD, spontaneous broken chiral symmetry is the origin of dynamical quark mass which constitute hadrons. In hot and/or dense matter, the broken chiral symmetry is thought to be restored toward to chiral critical temperature/density, and hadron mass could be modified in such matter. Even at the normal nuclear density, about 1/3 of restoration of chiral symmetry is expected, and mass/width modification of mesons are also predicted theoretically.

KEK-PS E325 experiment was performed to detect such modification on the invariant mass spectra in e^+e^- and K^+K^- from the low-mass vector meson (ρ, ω and ϕ) decays, which produced in 12GeV proton induced reactions and decaying in target nuclei. Data taking was completed in 2002. In e^+e^- invariant mass spectra, we observed clear peaks of ω and ϕ meson, with the mass resolution of 8.0 and 10.7 MeV/c^2 respectively. Such high resolution is the world best value of the e^+e^- invariant mass spectroscopy in hadronic reactions. We also observed the excesses which are not reproduced by known hadronic sources, at low-mass side of ω-meson peak (Fig.1) and also at low-mass side of ϕ-meson peak (Fig.2). Origin of the excesses can be thought as modified vector mesons decayed at the normal nuclear density of the target nuclei.

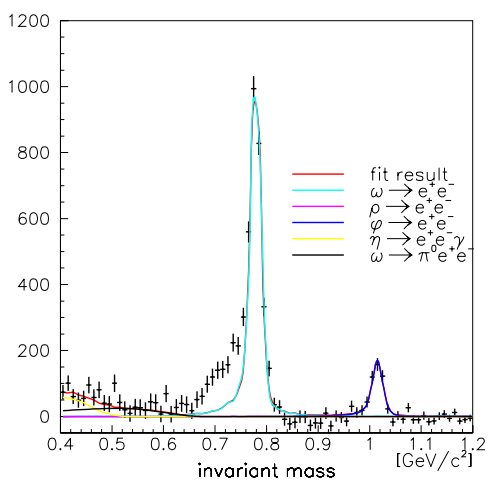

Fig. 1. .

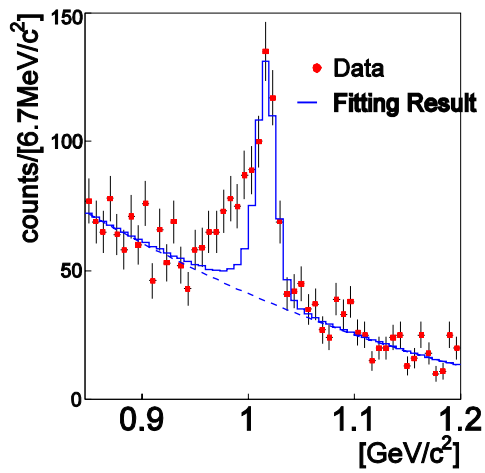

Fig. 2. .

We can reproduce the observed spectra in ω-meson region with our toy model calculation including an assumption that the mass decreasing is linearly depending on the density. In this case, we estimated that the mass of ρ and ω meson are decreased by 9% at the normal nuclear density. To explain the spectum of ϕ-meson region, we have to include another assumption of the width broadning in the nuclear matter. These results are consistent with some theoretical predictions about the meson modifications taking into account the chiral symmetry restoration.

III.6 Nucleon Structure: *Transverse Spin I*

Single Spin Asymmetry and Quark Orbital Motion in Nucleon

Feng Yuan
RBRC, Brookhaven National Lab

The Single Spin Asymmetries (SSA) in various high energy scattering processes are analyzed in the QCD factorization framework. From these studies we can obtain the information on the quark orbital angular momentum distribution in the nucleon. In particular, with the fit to the SSA in the semi-inclusive DIS, we make predictions for the relevant SSAs at hadron colliders such as RHIC. The connection between other measurements associated with the quark orbital angular momentum will also be discussed, including the high-x polarized structure functions and nucleon's form factors.

Transversity measurements at HERMES

Benedikt Zihlmann
University of Gent

on behalf of the HERMES collaboration.

Azimuthal single spin asymmetries (SSA) in semi inclusive deep inelastic lepton scattering (SIDIS) provide a tool to access transversity, the distribution of transversely polarized quarks in a transversely polarized nucleon. In addition the Sivers mechanism, the relation between the intrinsic transverse quark momentum and the transverse momentum of the final hadron, can give rise to a non zero SSA. For both the Collins and Sivers mechanism azimuthal moments are extracted from the HERMES data taken with a transversely polarized hydrogen target. Single and double hadron final states are investigated.

Tranversity signals in two hadron correlation at COMPASS

Rainer Joosten

Helmholtz Institut fr̈ Strahlen- und Kernphysik

on behalf of the COMPASS collaboration.

In lepton-nucleon scattering two hadron production the chiral odd interference fragmentation function $H_1^{\sphericalangle}(z, M^2)$ is considered a promising way to probe of the transverse spin distribution function $\Delta_T q(x)$. The measurement of $\Delta_T q(x)$ is one of the goals of the COMPASS experiment at CERN. In 2002, 2003, and 2004, COMPASS took data with a ^{6}LiD target polarised either longitudinally or transversally with respect to the 160 GeV/c μ^+ beam direction. About 20% of the beam-time was spent in the transverse configuration, allowing for the measurement of transversity effects. Results of the analysis of two hadron production will be reported.

Double Longitudinal Asymmetry in Jet k_t Measured in Di–hadron Correlations in Polarized p+p Collisions at sqrt–s = 200GeV in the PHENIX Experiment at RHIC

Robert Hobbs

University of New Mexico

on behalf of the PHENIX collaboration.

By measuring the azimuthal correlations between two high p_t hadrons, one can extract jet properties such as the fragmentation transverse momentum j_t and the "intrinsic" transverse momentum k_t. In longitudinally polarized p+p collisions, differences in the extracted average k_t for like and un–like helicity combinations (double asymmetry) may give information on the relationship between the polarization and the partonic transverse momentum, and thus the orbital angular momentum of the hard–scattered partons. This method is similar to a technique previously suggested by Meng Ta–chung et al. in the Drell–Yan channel. In this talk we present the physics technique, the anlysis method and the current status of the analysis for pi^0 – hadron azimuthal correlations in PHENIX with data from RHIC Run3 and Run5.

Spin Effects in Large Rapidity Neutral Pion Production at STAR

Steven F. Heppelmann
Penn State University

on behalf of the STAR collaboration.

First measurements of large Feynman x (x_F) neutral pion production in polarized proton collisions at $\sqrt{s}$=200 GeV were reported previously. Cross section measurements at η=3.3 and 3.8 and the analyzing power measurements at η=3.8 were completed for $0.3 < x_F < 0.6$.

The cross section was found to be consistent with next-to-leading order perturbative QCD calculations. In that framework, the dominant subprocess is partonic collisions of highly polarized valence quarks on low Bjorken x-gluons.

The analyzing power was found to be large and positive and increased with increasing x_F. The analyzing power was found consistent with phenomenological calculations based on the Collins effect, the Sivers effect and initial-state and final-state higher twist contributions.

Subsequent data has been acquired with both transverse and longitudinal polarized proton collisions at RHIC at $\sqrt{s}$=200 GeV and 410 GeV. The status of the analysis will be presented. Also future upgrade plans and status will be discussed.

Recent DIS Results from JLab: A_1^n at high-x, and, the Q^2-dependence of g_2^n

Todd Averett
College of William and Mary

on behalf of the Polarized 3He and Hall A Collaborations collaboration.

Recent experiments using $^3\vec{H}e(\vec{e}, e')$ in the deep-inelastic scattering region, have revealed interesting new information about the spin-structure of the neutron. Measurements of the asymmetry A_1^n at high-x have seen, for the first time, the expected cross-over of zero and positive slope as $x \to 1$. These data are in good agreement with constituent quarks model and have been further used to extract the ratios $\Delta d/d$ and $\Delta u/u$. A second experiment made precision measurements of the spin structure function, g_2^n as a function of Q^2, which has sensitivity to higher-twist contributions. These higher-twist contributions are directly related to the non-perturbative structure of the neutron and are sensitive to process such as gluon-exchange during the time of electron scattering. Recently published data will be shown, which indicate positive high-twist contributions at lower Q^2. These results were obtained using a polarized ^{3}He target in Hall A at Jefferson Lab.

IV.6 Hadrons, Nuclei, Hypernuclei - Light Quarks: *Miscellaneous Talks I*

The Radiative Pion Decay Anomaly Revisited

Willi Bertl

Paul Scherrer Institute

on behalf of the PIBETA collaboration.

The decay $\pi^+ \to e^+\nu\gamma$ is a commonly used tool to determine weak decay form factors of the pion. The most recent published value of the axial form factor [1] was obtained as a byproduct of the newest measurement of the pion beta-decay branching ratio, an experiment performed in the period 1999–2001 by the PIBETA collaboration at the Paul Scherrer Institute [2]. The measurement achieved a fourfold improvement in precision on the axial form factor, compared with earlier experiments. However, a deviation from Standard Model predictions was been observed in a specific region of phase space (high E_γ/low E_{e^+}), similar to the one found in 1990 by the ISTRA collaboration [3]. In both cases the deviation could not be explained by instrumental or analysis deficiencies. Theoretical attemps have been made over the years to attribute this anomaly to a small tensor component in the interaction, a possibility not ruled out by limits derived from other experiments [4]. In 2004, the updated PIBETA collaboration revisited this decay in a dedicated, lower rate experiment. The original PIBETA spectrometer with slight modifications served again as the detection device in a four month long run. Clean samples of about 20.000 radiative pion decays and, for cross checking, of approximately 100.000 radiative muon decays have been collected simultaneously. These data are presently being analyzed by 3 independent groups within the collaboration. Simultaneous and accurate description of all accessible pion and muon decay processes is the mandatory objective for all analysis work. Understanding the spectrometer's performance has been continuously improved over the years and has made possible simulations of unprecedented accuracy. First results on radiative pion as well as muon decay will be presented at the conference.

[1] "Precise Measurement of the Pion Axial Form Factor in the $\pi^+ \to e^+\nu\gamma$ Decay"
E. Frlež et al., Phys. Rev. Lett. **93** 181804(2004).

[2] "Precise Measurement of the $\pi^+ \to \pi^0 e^+\nu$ Branching Ratio" D. Počanić et al., Phys. Rev. 181803(2004).

[3] V.N. Bolotov et al., Phys. Lett. B **243**, 308, (1990).

[4] P. Herczeg, Phys. Rev.D **49**, 247 (1994).

Pion-Nucleon Analysis at Low Eenergy

Mikko E. Sainio[1], Pekko Piirola[2]

[1]*Helsinki Institute of Physics*

[2]*Department of Physical Sciences, University of Helsinki, Finland*

The motivation for performing a new phase-shift analysis of the pion-nucleon interaction is twofold. Firstly, there is a large amount of πN data from the meson factories, LAMPF, SIN/PSI and TRIUMF, which was not included in the Karlsruhe-Helsinki analysis in the 70's. Secondly, advances in chiral perturbation theory call for a careful study of the low-energy range of the pion-nucleon interaction.

Our aim is to perform a πN phase-shift analysis, with fixed-t constraints imposed, with the expansion method in the spirit of the work of the Karlsruhe-Helsinki group. There the invariant amplitudes are expressed as a sum of powers of a conformal variable and the Born term, e.g. in the case of the C^+-amplitude we have

$$C^+(\nu, t) = C_N^+(\nu, t) + H(Z, t) \sum_{n=0}^{N} c_n^+ Z^n,$$

where $C_N^+(\nu, t)$ is the Born term, the function H reflects the asymptotic behaviour of the amplitude and the coefficients c_n^+ are adjusted to the data and an existing phase-shift solution. Z is the conformal mapping

$$Z(\nu^2, t) = \frac{\alpha - \sqrt{\nu_{th}^2 - \nu^2}}{\alpha + \sqrt{\nu_{th}^2 - \nu^2}},$$

where $\nu_{th} = M_\pi + t/4m$ and α is a real parameter ($\nu = (s - u)/4m$).

In the first phase we are working in the isospin limit, where the electromagnetic corrections are handled through the Tromborg formalism. However, the P_{33} -splitting of π^+p and π^-p amplitudes, clearly observable in the total cross sections, is taken into account.

Our focus is on low energies and we intend to extract values for the subthreshold expansion coefficients, threshold parameters, the πN coupling constant and the amplitude at the Cheng-Dashen point.

Measurement of Σ^+p elastic scattering cross sections at KEK-PS

Hiroki Kanda, et al.

Department of Physics, Tohoku University

on behalf of the KEK-PS E289 collaboration.

The nuclear force have been intensely investigated and well understood in the view of the exchange of mesons mediating the force between nucleons. Theoretical models are developed to reproduce the observables of the nuclear interactions in the nucleon-nucleon (NN) sector. Some of the models are extended to calculate the nuclear interaction in the hyperon-nucleon (YN) sector, which reproduce the observables measured in 1970's using the bubble chambers. However, the predictions of the models differ in the observables which was not experimentally measured. New experimental data for the YN interactions will give information on better understanding of the nuclear force not only in the YN sector but also in the NN sector.

An experiment to measure the Σ^+p scattering cross sections was carried out with use of a scintillating fiber active target system at KEK 12 GeV proton synchrotron. The active target system consisted of a block of stacked scintillating fibers, and two sets of image intensifiers and CCD cameras. The pion beam of 1.64 GeV/c was incident on the active target and produced hyperons via p(π^+, K$^+$)Σ^+ reaction. The produced hyperon traveled through the active target and scattered on protons. The active target system recorded tracks of charged parcicles relevant to the production and scattering of hyperons as digital image data. In 420 hours of data aquisition, we have collected 1.3×10^6 hyperon production events which was selected by the off-line analysis of the spectrometer. Human scanners looked into the image data of the selected events to identify the scattering of the hyperons on the protons. After the unified analysis of the informations of image data provided by the human scanners and the informations of the spectrometer analysis, 31 events were identified as Σ^+p elastic scattering events in the momentum region of $350 \leq p_{\Sigma^+} \leq 750$ MeV/c. The efficiencies and acceptances of the analysing process, including the human scanners, were estimated using the Monte Carlo simulation with the image simulator. Some kinds of possible background processes were considered and their amount was estimated as 20.3±10.5% in the extracted events. We obtained the differential cross sections in four bins in the angular region of $-0.8 \leq \cos\theta_{CM} \leq 0.8$ and the cross sections in three bins in the above momentum region. The result was compared with theoretical predictions by the Nijmegan group (Nijmegen Soft Core 97) and the Kyoto-Niigata group (RGM-FSS and -fss2).

ϕ-meson production in pN collisions close to threshold

Yoshikazu Maeda, et al.

Institut für Kernphysik, Universität zu Köln and Institut für Kernphysik, Forschungszentrum Jülich

on behalf of the ANKE collaboration.

At the ANKE facility of COSY Jülich, the reactions pp→ppϕ and pn→dϕ have been measured by detecting K^+K^- pairs from the ϕ-meson decay in coincidence with the fast proton and deuteron, respectively. Data for the total cross section in pp-channel have been obtained at the excess energies of 76 MeV, 35 MeV and 19 MeV, being new data points below the energy of DISTO measurement. The reaction pn→dϕ has been measured using a deuterium target at a fixed beam energy 2.65 GeV. First data for the total cross section has been obtained at the excess energies range from 0 to 80 MeV making use the Fermi motion of the target neutron. The observed cross section ratio $\sigma_{d\phi}/\sigma_{pp\phi}$ amounts to about a factor of five at an excess energy around 20 MeV, whereas it is a factor of two at 80 MeV, indicating that the isospin dependence for ϕ production is weaker than for η production.

The new ϕ data combined with SPES-III, TOF-COSY and ANKE results on ω-meson production provide additionally the total cross section ratios of ϕ/ω production in pp- and pn-channel. The ratio is found to be similar for both channel, i.e. of about five times larger than the ratio based on OZI rule ($R_{OZI} = 4.2 \times 10^{-3}$). This indicates that there is no strong dependence on the initial spin state of entrance nucleons, i.e. the spin-triplet state and spin-singlet state in pp- and pn-channel, respectively. The total cross sections as well as the differential distributions for both reactions will be also presented and discussed.

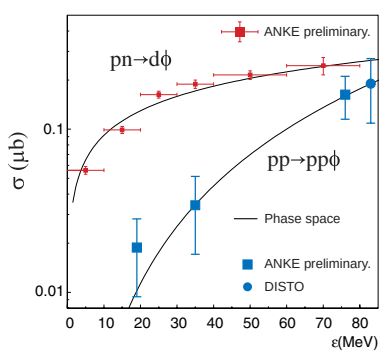

Fig. 1. Total cross section for the reaction pn→dϕ and pp→ppϕ. Lines show the phase space calculation.

The nucleon and Roper resonance in a chiral quark-diquark model

Keitaro Nagata, Atsushi Hosaka
Research Center for Nuclear Physics, Osaka University

We report the recent results on the study of the ground and first excited states of nucleons in a chiral quark-diquark model by using the path-integral hadronization method [1].

Recently, several approaches incorporating with the diquark degrees of freedom are employed to study the nuclear and hadron physics [2, 3, 4]. We include two diquarks with color anti-triplet such that the diquark and the third quark gives the quantum number of the nucleon $J^P = (1/2)^+$; one is the Lorentz scalar and iso-scalar diquark (scalar diquark) and the other is the Lorentz axial-vector and iso-vector one (axial-vector diquark). Therefore the model incorporates with two quark-diquark channels of the scalar and axial-vector types for the nucleon states. The diquark correlation violating the spin-(two-) flavor $SU(4)_{SF}$ symmetry allows to treat the two quark-diquark channels independently. Hence the two states appear as the superpositions of the two quark-diquark channels; one is the nucleon and the other is a state which does not appear in the $SU(4)_{SF}$ quark models. The masses of the two states are extracted through the quark-diquark loop diagrams and physical states are obtained so as to diagonalize the mass matrix. With a reasonable choice of model parameters, the mass of the excited state appears at around 1.5 GeV, which we identify with the Roper resonance $N(1440)$.

We discuss the mechanism of the small excitation energy of the Roper resonance and the difference between the current approach and $SU(4)_{SF}$ quark models. In a naive consideration, the mass difference of the nucleon and Roper resonance is related to that of the scalar and axial-vector diquark. Hence, the small excitation energy of the Roper resonance is basically generated by the difference of the spin-spin interaction between the scalar and axial-vector diquark, which is similar to the case of the nucleon and delta and is different from the excitation energy about $2\hbar\omega$ in $SU(4)_{SF}$ quark models with the confining potential.

References

[1] K. Nagata and A. Hosaka, arXiv:hep-ph/0506193.

[2] N. Ishii, W. Bentz and K. Yazaki, Phys. Lett. B **318**, 26 (1993).

[3] M. Oettel, G. Hellstern, R. Alkofer and H. Reinhardt, Phys. Rev. C **58**, 2459 (1998).

[4] L. J. Abu-Raddad, A. Hosaka, D. Ebert and H. Toki, Phys. Rev. C **66**, 025206 (2002).

Measurement of photoproduction of ϕ mesons near threshold by LEPS/SPring-8 Experiment

Keito Horie

Research Center for Nuclear Physics, Osaka

on behalf of the LEPS collaboration.

The LEPS (Laser Electron Photons at SPring-8, Japan) experiment generates real photon beam of maximum energy 2.4 GeV with high degree of linear polarization by backward-Compton scattering. We study the reaction mechanisms of diffractive photoproduction of ϕ mesons near threshold from liquid hydrogen and deuteron target. Simultaneous measurements of cross sections and decay asymmetry make possible disentangling the contributions of Pomeron exchange (or other) with positive-parity from those of meson (π, η) exchange with negative-parity. Furthermore, identifying the coherent interaction with the deuteron, an isoscalar target, provides an unique way of separating out the isovector π-meson exchange.

In this talk, the results of cross sections and decay angular distributions of ϕ-photoproductio will be reported and they provide a coherent picture on ϕ-photoproduction at this non-perturbative regime.

V.4 Heavy Flavor Physics - Search for New Particles: *Top Physics*

Measurement of the Top Quark Mass in the Lepton+Jets Channel at the Tevatron

Peter Renkel

Southern Methodist University

on behalf of the DZero collaboration.

The top quark mass is a key parameter of the standard model. We present measurements of the top quark mass in the lepton+jets channel from different techniques using data taken during Run II of the Fermilab Tevatron collider in $p\bar{p}$ collisions at $\sqrt{s} = 1.96$ TeV . The lepton+jets final state is characterized by four or more jets, a high transverse momentum isolated electron or muon and high missing transverse energy, resulting from the decay of one W boson into a charged lepton and a neutrino and the other W boson into a quark-antiquark pair.

Measurement of the Top Quark Mass in the Dilepton channel at CDF

Tuula Maki

University of Helsinki

on behalf of the CDF collaboration.

We report the world's best measurement in the dilepton channel of the top quark mass using 350 pb $^{-1}$ of $p\bar{p}$ collisions at $\sqrt{s} = 1.96$ TeV collected by the CDF detector. We select $t\bar{t}$ events where both W bosons decay leptonically. The top quark mass is extracted from the posterior ensemble probability distribution, which is formed by evaluating for each event the differential cross section for top quark pair production and decay as a function of the top quark mass. The differential cross sections for the background processes are treated similarly and are included in the probability evaluation. The observed top quark mass is 165.3$\pm$6.3(stat)$\pm$ 3.6 (syst) GeV/c^2. We find consistent results using a Neutrino Weighting algorithm and two other kinematic techniques, where in each case the top quark mass distributions reconstructed in data is compared to Monte Carlo expectations. We discuss future prospects for futher reducing the statistical and systematic uncertainties.

Measurement of the Top Quark Pair Production Cross Section

Robert Kehoe
Southern Methodist University

on behalf of the DZero collaboration.

The measurement of the top quark pair ($t\bar{t}$) production cross section at hadron colliders can be used to test the standard model (SM) and search for new phenomena affecting the top quark sector. Within the SM, the top quark almost always decays to a W boson and a b quark. We present measurements of the $t\bar{t}$ production cross section at $\sqrt{s} = 1.96$ TeV in $p\bar{p}$ collisions in three final states using data taken during Run II of the Fermilab Tevatron collider. The dilepton+jets final state is characterized by two or more jets, two high transverse momentum isolated charged leptons, either two electrons, one electron and one muon, or two muons, and high missing transverse energy, resulting from the leptonic decay of both W bosons in the event. The lepton+jets final state is characterized by four or more jets, a high transverse momentum isolated electron or muon and high missing transverse energy, resulting from the decay of one W boson into a charged lepton and a neutrino and the other W boson into a quark-antiquark pair. The all-jets channel is characterized by at least six jets in the final state. Tagging of b jets is used to discriminate against background.

Top Properties: W helicity, Branching Ratios, Top Charge

Charles Plager
University of California, Los Angeles

on behalf of the CDF collaboration.

Searches for Non-SM t-$\bar{t}$ Production Resonances at CDF and D0

Valentin Necula
University of Florida

Search for Single Top Quark Production at the Tevatron

Yurii Maravin

Kansas State University

on behalf of the DZero collaboration.

We report on the search for single top quark production using data taken during Run II of the Fermilab Tevatron collider in $p\bar{p}$ collisions at $\sqrt{s} = 1.96$ TeV. The standard model predicts two main modes of single top quark production: the s-channel decay of a virtual W boson and the t-channel exchange of a W boson. We set upper limits on the cross sections for these two processes.

VI.4 Fundamental Symmetries: *Rare B Decays*

Recent Results in Electroweak Penguin B Decays from the Babar Experiment

Karsten Koeneke

Massachusetts Institute of Technology

on behalf of the Babar Collaboration.

We present recent measurements of electroweak penguin decays of the B meson. In the Standard Model, such decays are flavor-changing neutral currents which proceed at lowest order through electroweak loop diagrams. The decay rates, kinematic distributions, and CP asymmetries of these rare processes could be dramatically modified by the virtual creation of new particles at the electroweak scale. The results are based on data samples comprising as many as 232 million $B\bar{B}$ pairs collected with the BaBar detector at the PEP-II asymmetric-energy B Factory at SLAC. New results include: two independent measurements of the $b \to s\gamma$ decay rate, a measurement of the time-dependent CP asymmetry of $b \to s\gamma$ in the exclusive decay $B^0 \to K^0_S\pi^0\gamma$, a search for the rare decay $B^0 \to \bar{D}^{*0}\gamma$, and measurements of the asymmetries and decay rates of the $b \to s\ell^+\ell^-$ process via the exclusive decays $B \to K\ell^+\ell^-$ and $B \to K^*\ell^+\ell^-$.

Power Corrections and CP phases

Tsung-Wen Yeh

Department of Nature Sceince Education, NTCTC

We investigate the impact of power corrections from possible known sources on the understanding of CP violation phenomenology from B decay processes. By comparing the theoretical predictions with experimental data, we also try to pindown the uncertainty related to power corrections. This may help to search for new physics beyond the standard model.

In the heavy quark mass limit, there exist perturbation theories for describing rare hadronic B decays from first principle of QCD. However, the leading order theoretical predictions may not be able to explain the experimental branching ratios and CP asymmetries in a consistent way. It was also found that the power suppressed corrections are important for understanding of some measured processes. The existence of power corrections is then one major uncertainty of perturbation theories.

The search for new physics beyond the standard model is also one main activity in studies of rare hadronic B decays. One large uncertainty is due to hadronic effects. Thus, more controls over the hadronic effects can significantly improve the search for new physics.

Charmless Hadronic B decays in the Context of Flavor Symmetries

Denis Suprun
Brookhaven National Laboratory

Hadronic B decays to a pair of charmless mesons are analyzed within the framework of flavor symmetries and the Kobayashi-Maskawa mechanism of CP violation. Updated and improved analysis of the current experimental data on PP and VP decays will be presented. Values of the weak phase γ are extracted from the fits and theoretical uncertainties related to the assumption of flavor symmetries are estimated.

Measurement of the matrix element $|V_{ub}|$ at Belle

Ilija Bizjak
Jozef Stefan Institute, Ljubljana

on behalf of the Belle collaboration.

We present the current status of inclusive and exclusive measurements of the Cabibbo-Kobayashi-Maskawa matrix element $|V_{ub}|$ at Belle. The exclusive measurements use neutrino reconstruction and the reconstruction of the accompanying B meson into a semileptonic $B \to D^* \ell \nu$ decay to increase the purity of the signal. Branching fractions and q^2 distributions to light unflavored mesons are also reported. The inclusive measurements are performed at the endpoint of the electron momentum spectrum, and in three kinematical regions: a selection using the hadronic invariant mass M_X, the combined selection using M_X and the leptonic invariant mass squared q^2, and a selection based on the variable P_+. The measurement in three kinematical regions is done on a sample where the decay chain of one of the B mesons was fully reconstructed.

Measurements of the CKM elements $|V_{ub}|$ and $|V_{cb}|$ at Babar

Romulus Godang
University of Mississippi

on behalf of the Babar Collaboration.

We report on new measurements of the CKM matrix elements $|V_{ub}|$ and $|V_{cb}|$ with inclusive and exclusive semileptonic B decays. The data sample produced at the $\Upsilon(4S)$ resonance was collected by the BaBar detector at the PEP-II collider at SLAC.

Observation of $b \to d\gamma$

Debabrata Mohapatra
Virginia Polytechnic Institute and State University

on behalf of the Belle collaboration.

We report the observation of the flavor-changing neutral current process $b \to d\gamma$ using a sample of 386 million B meson pairs accumulated by the Belle detector at KEKB. Assuming that the three exclusive decay modes $B^- \to \rho^-\gamma$, $\overline{B} \to \rho^0\gamma$ and $\overline{B} \to \omega\gamma$ are related by isospin, we find $B(B \to (\rho,\omega)\gamma) = 1.34\,^{+0.34}_{-0.31}(\text{stat.})\,^{+0.14}_{-0.10}(\text{syst.}) \times 10^{-6}$ with a significance of 5.5σ. This result is used to measure the ratio of CKM matrix elements $|V_{td}/V_{ts}| = 0.200\,^{+0.026}_{-0.025}(\text{exp.})\,^{+0.038}_{-0.029}(\text{theo.})$.

VII.2 Fundamental Interactions in Atomic and Neutron Physics:
Fundamental Measurements in Atomic and Molecular Physics

Effects of variation of fundamental constants from Big Bang to atomic clocks

Victor Flambaum
University of New South Wales,

Effects of variation of fundamental constants from Big Bang to atomic clocks

Theories unifying gravity with other interactions suggest temporal and spatial variation of the fundamental "constants" in expanding Universe. I discuss effects of variation of the fine structure constant $\alpha = e^2/\hbar c$, strong interaction, quark mass and gravitational constant. The measurements of these variations cover lifespan of the Universe from few minutes after Big Bang to the present time and give controversial results. There are some hints for the variation in Big Bang nucleosynthesis, quasar absorption spectra and Oklo natural nuclear reactor data.

A very promising method to search for the variation of the fundamental constants consists in comparison of different atomic clocks. A billion times enhancement of the variation effects happens in transition between accidentally degenerate atomic energy levels.

Precision Measurement of Parity Violation in Polarized Neutron Capture on the Proton: the NPDγ Experiment.

Bernhard Lauss

University of California, Berkeley

on behalf of the NPDGamma collaboration.

J.D. Bowman[b], R.D. Carlini[c], T.E. Chupp[d], W. Chen[e], M. Dabaghyan[f], D. Desai[g], S.J. Freedman[a], T.R. Gentile[e], M.T. Gericke[h], R.C. Gillis[h], G.L. Greene[g], F.W. Hersman[f], T. Ino[i], T. Ito[g], G.L. Jones[j], M. Kandes[d], M. Leuschner[k], B. Losowki[k], R. Mahurin[g], Y. Masuda[i], J. Mei[k], G.S. Mitchell[b], S. Muto[i], H. Nann[k], S. Page[h], S. Penttila[b], D. Ramsay[h], S. Santra[k], P.-N. Seo[l], E. Sharapov[m], T. Smith[n], W.M. Snow[k], W.S. Wilburn[b], V. Yuan[b], and H. Zhu[f]

[a] Univ. of California, Berkeley and LBNL, [b] Los Alamos National Laboratory, [c] Thomas Jefferson National Accelerator Facility, [d] Univ. of Michigan, Ann Arbor, [e] NIST, Gaithersburg, [f] Univ. of New Hampshire, [g] Univ. of Tennessee, [h] Univ. of Manitoba, [i] HEARO, Tsukuba, [j] Hamilton College, [k] Indiana University, Bloomington, [l] North Carolina State Univ., [m] JINR, Dubna, [n] Univ. of Dayton

A measurement of the parity-violating directional asymmetry A_γ of the 2.2 MeV γ-ray emitted in the radiative capture of spin-polarized cold neutrons on the proton probes the weak nucleon-nucleon interaction. A_γ is directly proportional to the weak pion-nucleon-nucleon coupling f_π^1. Effective theory predictions for A_γ are on the 10^{-8} level, yet there have been no unambiguous direct measurements to date. Experiments on anapole moments and circular γ-ray polarizations are in partial conflict and the extraction of f_π^1 is obscured by nuclear difficulties. The NPDγ experiment's goal is a result with a precision of 5×10^{-9} and, if the estimated value is correct, the first measured value for A_γ and f_π^1. We will describe the present status of the experiment and measurements from our installation at the Los Alamos Neutron Science Center.

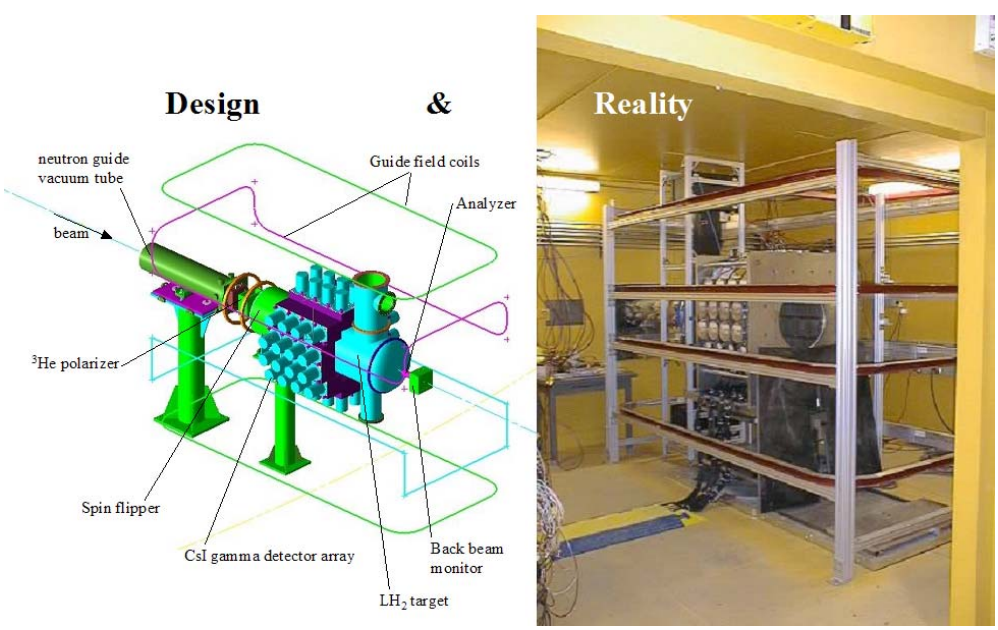

Fig. 1. View of the NPDγ apparatus: design and setup in the experimental area at the Los Alamos Neutron Science Center.

Gravitationally bound quantum states of neutrons: applications and perspectives

Valery V. Nesvizhevsky

Institut Laue-Langevin, Grenoble

on behalf of the GRANIT collaboration.

Gravitationally bound quantum states of matter were observed for the first time due to unique properties of ultracold neutrons. The neutrons were allowed to fall towards a horizontal mirror which, together with the earth's gravitational field, provided the necessary confining potential well. We discuss here actual status and possible improvements in this experiment: so-called integral and differential measuring modes; the storage and the flow-through measuring modes; resonance transitions between the quantum states in the gravitational field.

This phenomenon and related experimental techniques could be applied to various domains ranging from the physics of elementary particles and fields (for instance, the spin-independent or spin-dependent short-range fundamental forces, or search for non-zero neutron electric charge), to the surface studies related to the fundamental physics experiments (for instance, distribution of hydrogen in/above surfaces of solids or liquids, or thin films on surface) or to foundations of quantum mechanics (for instance, the quantum-mechanical localization with the longest possible travel of UCN matter waves in medium and in neutron wave-guides, or loss of the quantum coherence).

References:

1. V.V.Nesvizhevsky, H.G.Börner, A.K.Petukhov, H.Abele, S.Baeßler, F.J.Rueß, Th.Stöferle, A.Westphal, A.M.Gagarsky, G.A.Petrov, and A.V.Strelkov (2002). "Quantum states of neutrons in the Earth's gravitational field." Nature 415: 297-299.
2. V.V.Nesvizhevsky, H.G.Börner, A.M.Gagarski, A.K.Petukhov, G.A.Petrov, H.Abele, S.Baeßler, G.Divkovic, F.J.Rueß, T.Stöferle, A.Westphal, A.V.Strelkov, K.V.Protasov, A.Yu.Voronin (2003). "Measurement of quantum states of neutrons in the Earth's gravitational field." Physical Review D 67: 102002.
3. V.V.Nesvizhevsky, A.K.Petukhov, H.G.Börner, T.A.Baranova, A.M.Gagarski, G.A.Petrov, K.V.Protasov, A.Yu.Voronin, S.Bäßler, H.Abele, A.Westphal, and L.Lucovac (2005). "Study of the neutron quantum states in the gravity field." European Physical Journal C 40(4): 479-491.

The radiative potential method for calculations of QED radiative corrections to energies and E1 amplitudes in many-electron atoms; application to parity nonconservation in cesium

Jacinda Ginges, Victor Flambaum

University of New South Wales

We derive an approximate expression for a "radiative potential" that can be used to calculate QED strong Coulomb field radiative corrections to energies and electric dipole (E1) transition amplitudes in many-electron atoms with an accuracy of a few percent. The expectation value of the radiative potential gives radiative corrections to the energies. Radiative corrections to E1 amplitudes can be expressed in terms of the radiative potential and its energy derivative (the low-energy theorem): the relative magnitude of the radiative potential contribution is $\sim \alpha^3 Z^2 \ln(1/\alpha^2 Z^2)$, while the sum of other QED contributions is $\sim \alpha^3 (Z_i + 1)^2$, where Z is the nuclear charge and Z_i is the ion charge; that is, for neutral atoms ($Z_i = 0$) the radiative potential contribution exceeds other contributions $\sim Z^2$ times. The advantage of the radiative potential method is that it is very simple and can be easily incorporated into many-body theory approaches: relativistic Hartree-Fock, configuration interaction, many-body perturbation theory, etc. As an application we have calculated the radiative corrections to the energy levels and E1 amplitudes as well as their contributions (-0.34% and +0.43%, respectively) to the parity nonconserving (PNC) $6s$-$7s$ amplitude in neutral cesium (Z=55). Combining these results with the QED correction to the weak matrix elements (-0.41%) we obtain the total QED correction to the PNC $6s$-$7s$ amplitude, (-0.32 $\pm$ 0.03)%. The cesium weak charge $Q_W = -72.66(29)_{exp}(36)_{theor}$ agrees with the Standard Model value $Q_W^{SM} = -73.19(13)$, the difference is 0.53(48).

Pionic Hydrogen - Precision Measurements at PSI

Johann Marton, et al.

Stefan Meyer Institute

on behalf of the Pionic Hydrogen Collaboration.

The experimental program of the Pionic Hydrogen Collaboration at the Paul Scherrer Institut (PSI) [1] aims at a measurement of the strong interaction induced shift and width of the pionic hydrogen ground state with unprecedented precision. A sophisticated crystal spectrometer is used to measure the strong interaction shift and width with a precision of ~ 0.2 percent and ~ 1 percent respectively. The improvement in the precision of the width will amount to almost an order of magnitude compared to the most precise former experiment. From strong interaction shift and width the isospin-dependent pion-nucleon scattering lengths can be determined.

At PSI a high intensity pion beam and a cyclotron trap ensure optimal conditions for this experiment. In order to reach the envisaged high precision all features of the experimental setup have to be studied in detail, e.g. for the extraction of the strong interaction width the resolution function has to be determined with high precision. The characterization of the Bragg crystals is done by using an electron cyclotron resonance ion trap (ECRIT) as an intense X-ray source [2]. The experimental method will be presented.

Measurements of X-ray transitions in muonic hydrogen (exotic atom like pionic hydrogen but without strong interaction) were performed to study the effect of Doppler broadening due to high energetic muonic atoms after Coulomb transition within the electromagnetic cascade.

The present status of the experiment and the results on the strong interaction shift and width will be presented at this conference.

[1] http:// www.psi.ch
[2] D.F. Anagostopoulos et al., Nucl. Instr. Meth. B 205 (2003) 9.

Measurement of the Parity-Violating Neutron Spin Rotation in ^{4}He

Anna M. Micherdzinska *et al.*

Indiana University & Indiana University Cyclotron Facility

Weak interactions between *u* and *d* quarks induce weak interactions between nucleons. These weak interaction effects can be isolated using parity violation. The nucleon-nucleon (NN) weak interaction can be constrained by a meson exchange model, where the exchange of virtual mesons between the nucleons is parameterized by a set of NN weak interaction amplitudes. The strengths of these amplitudes from theoretical calculations are not well known and experimental measurement of parity-odd (PV) observables in different nuclear systems have not yet constrained their values. The natural scale for the size of PV amplitudes is set by the ratio of the amplitudes for W and Z bosons exchange to that for meson exchange between nucleons and is of the order of 10^{-7}.

We plan to measure the PV neutron spin rotation of transversely-polarized cold neutrons propagating through liquid-^{4}He. A cold neutron beam provided by the reactor at National Institute Standard and Technology (NIST) in Gaithersburg, will be polarized by a supermirror, travel through a liquid- ^{4}He target, and then be analyzed by another supermirror. The magnitude of the rotation angle of the incident neutrons depends on a parity-even (PC) component due to residual magnetic fields, which is neutron velocity dependent, as well as a PV component due to the weak interaction. The experimental design challenge is to suppress the effects of the residual longitudinal magnetic field upon which almost all of the systematic effects depend.

A similar measurement was attempted at NIST in 1996 with the (unpublished) result $(8.0 \pm 14(\text{stat}) \pm 2.2(\text{syst})) \times 10^{-7}$ rad/m and was consistent with zero. Our measurement will be conducted with an upgraded version of the previous apparatus. I will present the current status of the experiment and detail our efforts to reduce systematic effects in order to reach a sensitivity goal of 3×10^{-7} rad/m.

VIII.4 Neutrino Physics: *Neutrino Theoretical Developments*

A possible nuclear effect on the NuTeV $\sin^2\theta_W$ anomaly

S. Kumano, M. Hirai, T.-H. Nagai

IPNS, KEK, 1-1, Ooho, Tsukuba, Ibaraki, 305-0801, Japan

The NuTeV collaboration announced that their neutrino-nucleus scattering data indicate a significant deviation from the standard model. If the neutrino-nucleus scattering data are excluded, the average value is $\sin^2\theta_W = 0.2227 \pm 0.0004$ in the on-shell scheme. The NuTeV value, $\sin^2\theta_W = 0.2277 \pm 0.0013\,(\text{stat}) \pm 0.0009\,(\text{syst})$ [1], is significantly larger than the average value. This deviation is called "NuTeV anomaly".

Noting that the target of the NuTeV experiment is the iron nucleus instead of the isoscalar nucleon, we investigate a possibility to explain the NuTeV anomaly in terms of a nuclear modification difference between up-valence and down-valence quark distributions [2,3]. We determined the nuclear modification difference ($w_{u_v} - w_{d_v}$) by a χ^2 analysis so as to reproduce nuclear data on the structure function F_2 and Drell-Yan processes [3]. The modification factors w_{u_v} and w_{d_v} are defined by

$$xu_v^A = w_{u_v}\frac{Zxu_v + Nxd_v}{A}, \quad xd_v^A = w_{d_v}\frac{Zxd_v + Nxu_v}{A}, \tag{1}$$

where the distributions on the right-hand-side are the nucleonic ones.

We obtain the difference, which is shown in Fig. 1. The solid curve indicates the optimum $w_{u_v} - w_{d_v}$ distribution, and the shaded area shows its uncertainties which are estimated by the Hessian method. As we find in the figure, the difference cannot be determined from the data at this stage because the error band is large. The modification-difference effect on the NuTeV anomaly should be estimated by taking into their kinematical condition. Using the nuclear PDF definitions in Eq. (1) and the NuTeV conventions, we find that our $w_{u_v} - w_{d_v}$ distribution is related to the isospin-violating distributions in the NuTeV convention: $\delta u_v^* = u_{vp}^* - d_{vn}^* = (w_{u_v} - w_{d_v})\,x\,u_v$, $\delta d_v^* = d_{vp}^* - u_{vn}^* = -(w_{u_v} - w_{d_v})\,x\,d_v$, where the distributions with the asterisk (*) indicate the NuTeV ones. Then, taking the NuTeV kinematics into account, we calculate a contribution to the $\sin^2\theta_W$ determination and its uncertainty. Although the uncertainty becomes comparable to the NuTeV deviation, the effect is not large enough to explain the whole NuTeV $\sin^2\theta_W$ anomaly at this stage. The nuclear modification difference is difficult to be determined from the current experimental data, so that we need future efforts to find it.

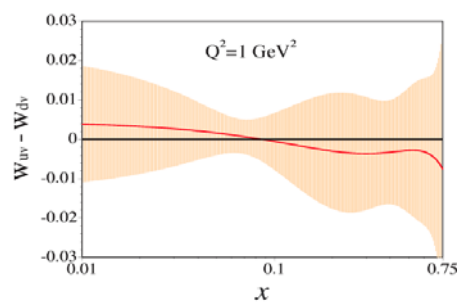

Figure 1. Nuclear modification difference between u_v and d_v distributions in the iron [3].

References

[1] G. P. Zeller *et al.*, Phys. Rev. Lett. 88 (2002) 091802.

[2] S. Kumano, Phys. Rev. D66 (2002) 111301.

[3] M. Hirai, S. Kumano, and T.-H. Nagai, Phys.Rev. D71 (2005) 113007.

Magnetic Moments of Dirac Neutrinos

Nicole Bell
Caltech

The existence of a neutrino magnetic moment implies contributions to the neutrino mass via radiative corrections. We derive model-independent, ”naturalness” upper bounds on the magnetic moments of Dirac neutrinos generated by physics above the electroweak scale. The neutrino mass receives a contribution from higher order operators, which are renormalized by operators responsible for the neutrino magnetic moment. This contribution can be calculated in a model independent way. In the absence of fine-tuning, we find that current neutrino mass limits imply that $|\mu_\nu| < 10^{-14}$ Bohr magnetons. This bound is several orders of magnitude stronger than those obtained from solar and reactor neutrino data and astrophysical observations.

Constraints on Weakly Mixed Sterile Neutrinos in the Hollanda- Smirnov Model

S. Dev Sharma

Himachal Pradseh University

The possibility of flavor transitions into sterile neutrinos (accompanying the dominant LMA transitions) in the solar boron neutrino flux has been examined in a scenario proposed by Hollanda and Smirnov to overcome some generic problems of the pure LMA scenario. There are, at least, two generic predictions of LMA indicating new physics beyond LMA. One of these is the prediction of the high argon production rate for Homestake experiment which is about 2σ above the observed rate. Another generic prediction of the LMA scenario is the 'spectral upturn' at low energies. Both these predictions of the LMA solution can, only, be tested in the forthcoming phase of high precision measurements in the solar neutrino experiments and are crucial for the final confirmation of the LMA solution. Another unresolved issue is whether the solar neutrinos oscillate into the sterile component. While the SNO charged current data excluded the maximal mixing to sterile neutrinos at 5.4σ, arbitrary active-sterile admixtures were not considered. Consequently, a significant sterile fraction in the solar neutrino flux reaching the earth is, still, possible. The discovery of the sterile neutrinos would be of great importance for particle physics, even though, it is, still, not clear how these hypothetical 'exotic' degrees of freedom would fit into elementary particle theory.

It is found that the most recent SNO salt phase solar neutrino data and the KamLAND 766.3 Ty spectral data, allow for a significant sterile presence in the solar boron neutrino flux reaching the earth. The indications for the presence of sterile component in the boron neutrino flux in the light of the latest SNO salt phase data and the 766.3 Ty KamLAND data are found to be strong enough to be taken seriously. A precise determination of the CC and NC fluxes at SNO within the present 1σ range gives a transition probability into sterile states which is non-zero at more than 4.4σ. It is found that the sterile component in the boron neutrino flux could be as large as the electron neutrino flux for the present central values of SNO CC and NC fluxes. If the future measurements at SNO yield smaller values of CC/NC flux ratio, the sterile fraction will be, further, enhanced. Thus, there are strong indications of a sterile presence in the boron neutrino flux reaching the detectors on the earth but it will require a precise determination of CC and NC fluxes to pass a final judgment.

Neutrino interactions with nucleons and nuclei at intermediate energies

Luis Alvarez Ruso, T. Leitner, U. Mosel
Institut fur Theoretische Physik, Universitat Giessen

We have developed a model to describe the interactions of neutrinos with nucleons and nuclei via neutral and charged currents, focusing on the region of the quasi-elastic and $\Delta(1232)$ peaks.

We describe neutrino nucleon collisions with a fully relativistic formalism which incorporates state-of-the-art parameterizations of the form factors for both the nucleon and the $N - \Delta$ transition. In the case of neutral current quasielastic scattering, we studied the sensitivity of the cross section to the strangeness content of the nucleon and how it is constrained by the results of the new experiments on the electric and magnetic strange form factors. It is remarkable that the contribution of the vector form factors to the cross section on the proton ($\nu\, p \rightarrow \nu\, p$) is negligible. Therefore, this cross section specially sensitive to the strange part of the proton axial form factor, related to the strange quark contribution to the spin, which could be accessed through the experimental study of proton knockout in nuclei.

The model has then been extended to finite nuclei, taking into account nuclear effects such as Fermi motion, Pauli blocking (both within the local density approximation), nuclear binding and final state interactions (FSI). The in-medium modification of the Δ resonance due to Pauli blocking and collisional broadening has been also included. FSI is implemented by means of the Boltzmann-Uehling-Uhlenbeck (BUU) coupled channel semiclassical transport model. Pions and nucleons undergo elastic and charge exchange scattering with the nucleons in the medium. Pions can also be absorbed or be created in secondary collisions. The propagation of particles between collisions is influenced by momentum dependent mean-field potentials.

Motivated by the advent of new experiments like MINERνA and FINeSSE, we have calculated inclusive double differential cross sections $d\sigma/dQ^2dE_\mu$ for charge current processes on Fe, and neutrino energies between 0.4 and 2 GeV. We have also considered exclusive channels, namely pion production and nucleon knockout. Pion production is dominated by Δ excitation; quasielastic scattering followed by pion production in NN collisions are sizable only at high Q^2. For π^0 production, we found and enhancement due to the dominant π^+ production followed by charge exchange.

In the case of neutral currents we focused our attention on two issues: the angular distributions and total cross sections of π^0 production, since they are a source of background in ν_e appearance experiments and proton knockout as a source of information on the axial strange form factor of the nucleon, provided that nuclear effects are under control.

Neutrino Oscillation Parameters in a Six-channel Reduced Rank Seesaw

G. J. Stephenson, Jr.[1], T. Goldman[2], B. H. J. McKellar[3]

[1]*University of New Mexico*
[2]*LANL*
[3]*University of Melbourne*

Recent developments have reduced the stringency of cosmological and astrophysical constraints on the number and masses of sterile neutrinos. We examine, in a seesaw model for neutrino masses with reduced rank for the sterile neutrino mass matrix, the parameters available to accomodate the data from all laboratory neutrino oscillation experiments including LSND. The effect of allowing CKM-like mixing in the Dirac basis will be presented. The difficulty of extracting reliable parameter values from sequential 2-channel fits to specific experiments will also be discussed.

Deviation from maximal mixing of atmospheric muon neutrinos via matter effects

Probir Roy

Tata Institute of Fundamrntal Research

The difference $\Delta P^{A}_{\mu\mu}$ between atmospheric muon neutrino and antineutrino survival probabilities is due to earth matter effects. For a nonzero flavor mixing angle θ_{13}, this difference probes the deviation $D \equiv 1/2 - \sin^2\theta_{23}$ of the flavor mixing angle θ_{23} from its maximal value. The magnitude and sign of such a deviation is of great interest to builders of neutrino mass and mixing models. We quantitatively investigate the feasibility of determining D in a statistically significant manner by measuring the up-down asymmetry of atmospheric muon neutrinos and antineutrinos for various relevant baselines and energy ranges from one Megaton-year of exposure with a magnetized iron calorimeter such as the proposed INO detector (www.imsc.res.in/ ino) taking various input values of θ_{13}. The sensitivity to concerned oscillation parameters is discussed in detail.

IX.2 Muon Physics: *Muon Lifetime and Capture*

Precision measurement of the positive muon lifetime at RIKEN-RAL

Dai Tomono
RIKEN

on behalf of the RIKEN-RAL R77 collaboration.

A new experiment to measure the positive muon lifetime (τ_μ^+) have been performed at the RIKEN-RAL Muon Facility in UK. The muon lifetime is directly associated with the Fermi coupling constant (G_F) which is one of the fundamental parameters in the Standard Model. The present most accurate value of τ_{μ^+} is 2.19695$\pm$ 0.00006 μs (27 ppm), given in 1984 [1]. So far, the accuracy of τ_μ^+ is limited by the statistical error rather than the systematic error due to the experiment technique which measures one muon decay in an observation time window. Strong muon beam will not help to improve the muon lifetime in this way.

A novel method by using a strong pulsed muon beam was developed and applied to the experiment. The essential features of our method are summarized as follows:

(1) The strong pulsed muon beam was used to measure a large number of muon decays in a time window.
(2) A fine segmented detector (multi-wire proportional chamber, MWPC) was used as a positron counter to reduce pile-up signals due to a dead-time of the counter. Remaining pile-up signals were corrected numerically in the off-line analysis.
(3) The para-magnetic holmium was used as a muon stopping target to reduce the polarization effect.
(4) An accurate clock system combined to the GPS signal was developed to measure the positron hit timing with good differential and integral linearity.

The latest status of data analysis and results will be presented.

References

[1] K.L. Giovanetti, *et al.*, *Phys. Rev.* **D29** (1984) 343.

Measurement of the Muon Lifetime to 1 ppm

Ronald McNabb
University of Illinois Urbana-Champaign

on behalf of the MuLan collaboration.

The MuLan experiment at PSI is designed to measure the positive muon lifetime to 1 ppm, a factor of 20 improvement over the current world average. This will result in an improved knowledge of the Fermi coupling constant, G_F. It will also be used for comparison with the results of the MuCap experiment, which will measure the negative muon lifetime in hydrogen and use the difference from the μ^+ lifetime to determine the pseudo-scalar form factor, g_p.

A DC muon beam of up to 10 MHz is directed into a target for $5\ \mu$s (accumulation period), it is then switched off for $27\ \mu$s (measurement period) by an upstream electrostatic kicker. During the measurement period, muon decay positrons are observed by 170 scintillating detector pairs around the target. A time spectrum of these decays, from a subset of the 2004 data, is shown in the figure below.

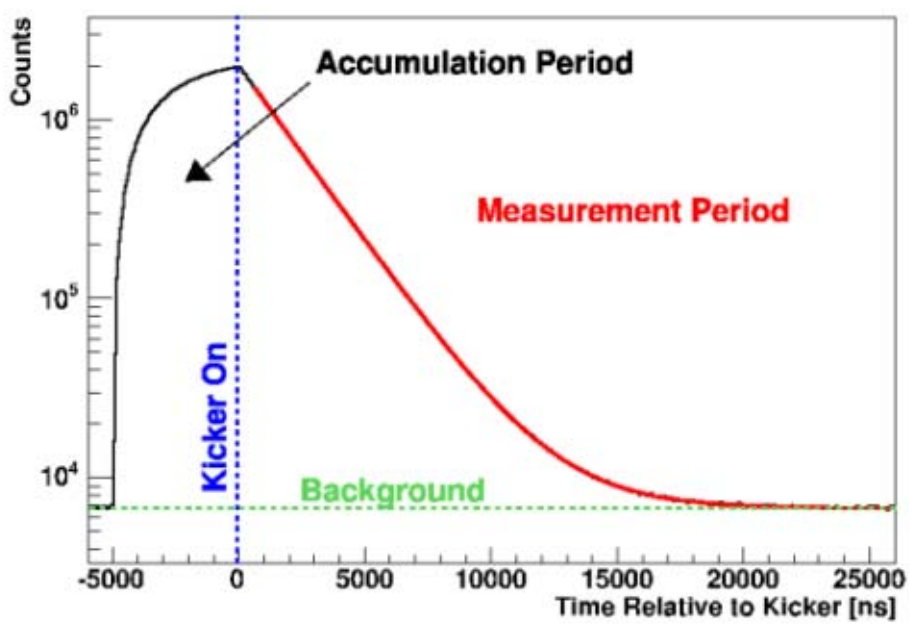

The decay spectrum is fit to an exponential plus a constant background to obtain the muon lifetime. Obtaining a result with an uncertainty of 1ppm will require observing more than 10^{12} muon decays. It will also require stringent control of systematic errors, including pileup and changes in the background rate during the measurement period.

Data from the 2004 run, which is currently being analyzed, should provide an uncertainty of less than 10 ppm. A new data set, with improved readout electronics and higher beam rates, is being taken this fall. This talk will discuss the status of the analysis, the progress of the 2005 run, and plans for the future.

Muon Capture as a Probe of the Nucleon's Axial Structure - the MuCap Experiment

Peter Kammel

University of Illinois at Urbana-Champaign

on behalf of the MuCap collaboration.

The goal of the μCap experiment is a precision measurement of the ordinary muon capture reaction on the free proton to directly determine the pseudoscalar form factor g_P. This is the least-well-known of the nucleon form factors characterizing the structure of its charged electro-weak current. By now g_P can be precisely calculated by modern effective theories based on the chiral symmetry of QCD and its breaking. In spite of efforts spanning the last 30 years, experimental results are still controversial and subject to uncertainties in their interpretation. This problem is most severe in experiments with LH_2 targets, where the relative population of ppμ molecular states is uncertain, depending on the rate λ_{OP} for ppμ ortho-para conversion. Because of the poor knowledge of λ_{OP}, g_P is currently only constrained within ~50% uncertainty (see figure).

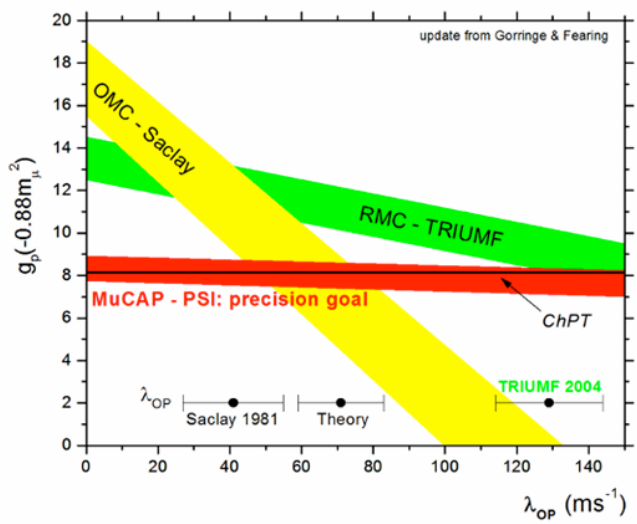

The μCap experiment is designed to avoid these uncertainties and to measure g_P to 7% precision. The method requires a combination of challenging detector techniques. A time projection chamber operating with 10 bar hydrogen gas determines the incoming muon stop position. Electrons from muon decay are reconstructed with a deadtime-free electron tracking system. A sophisticated gas system maintains and monitors the ultra-high purity deuterium depleted H_2 gas. In 2004 the detector was commissioned and a first physics run collected 25% of our final statistics goal. It surpasses all previous experiments both in statistics as well as in reduction of systematic uncertainties. The collaboration is working on a first physics publication on the μp capture rate with an uncertainty of few percent. As a possible further stage, we are planning to measure muon capture on deuterium with 1% precision, which could be compared with recent high precision calculations, provide information on the two-nucleon axial current and on fundamental neutrino reactions.

Work supported by the US NSF, DOE and CRDF, PSI and the Russian Academy of Sciences.

The Muon (g-2) Experiment: Present and Future

B Lee Roberts
Boston University

on behalf of the muon (g-2) collaborations: E821 and E969 collaboration.

The recent results of the muon $(g-2)$ experiment at Brookhaven and the plans to improve it will be discussed. The relative precision obtained for the muon anomalous magnetic moment by the E821 collaboration at Brookhaven was 0.5 parts per million . An upgraded experiment with a design goal of 0.2 ppm has scientific approval at Brookhaven.

Resolving the τ versus electroproduction discrepancy for the isovector spectral function and its implications for the SM prediction for $(g-2)_\mu$

Kim Maltman

Dept. Math and Stats, York Univ.

The largest of the non-pure-QED contributions to $a_\mu = (g-2)_\mu$ in the SM (that due to the leading order hadronic vacuum polarization contribution, $[a_\mu]^{LO}_{had}$) can be written as a weighted integral over the electromagnetic (EM) spectral function. CVC relates the isovector component thereof to the flavor ud, charged vector current spectral function measured in hadronic τ decay. Attempts to incorporate hadronic τ decay data using isospin-breaking (IB) corrected versions of the CVC relation have encountered the problem that, even after accounting for known sources of IB for the the $\pi\pi$ final state[1], the $\pi\pi$ component of the resulting τ-based isovector vector spectral function is incompatible with that obtained from the high-precision CMD2 $e^+e^- \to \pi^+\pi^-$ data[2], with surprisingly large ($\sim 10\%$) discrepancies for $\pi\pi$ invariant masses from ~ 0.85 to ~ 1 GeV[3]. This discrepancy complicates deciding whether or not the current experimental determination of a_μ[4] shows signs of possible beyond-the-SM contributions (SM predictions based solely on electroproduction data indicate $\sim 2.5\sigma$ deviations from the SM, those based on the hadronic τ decay data, in contrast, are compatibile at the $\sim 1\sigma$ level).

To resolve the above discrepancy we study sum rule constraints on the electroproduction and τ-decay data sets. The sum rules used have excellent OPE convergence, and an OPE strongly dominated by its leading $D = 0$ term. The OPE constraints are then essentially entirely determined by the single input, $\alpha_s(M_Z)$, which may be taken from high-scale determinations independent of τ decay and electroproduction data.

We find that the τ-decay-based spectral integrals are compatible with the high-scale input for a wide range of s_0 (the maximum s value appearing in the relevant spectral integrals) and non-negative weights, but that the EM data yields spectral integrals consistenly lower than the OPE predictions[5]. The s_0 dependence of the OPE and corresponding spectral integrals is also in good agreement for the τ decay data, but in significant disagreement for the electroproduction data[5].

We conclude that either (i) non-one-photon physics effects, as yet unidentified, are contaminating the EM data or (ii) there remain experimental problems with the (pre-2005) EM data. (The latter conclusion is favored by the just-released SND $e^+e^- \to \pi^+\pi^-$ data[6].) In either case it follows that determinations of $[a_\mu]^{LO}_{had}$ incorporating τ decay data are favored over those based solely on electroproduction cross-sections and hence that, at present, the SM prediction for a_μ is in good agreement with current experimental results.

[1] V. Cirigliano, G. Ecker and H. Neufeld, JHEP **0208** (2002) 002 and refs. therein

[2] R.R. Akhmetshin *et al.* (The CMD-2 Collaboration), Phys. Lett. **B578** (2004) 285

[3] M. Davier, S. Eidelman, A. Hocker and Z. Zhang, Eur. Phys. J. **C31** (2003) 503

[4] G.W. Bennett *et al.* (The Muon $g-2$ Collaboration), Phys. Rev. Lett. **92** (2004) 161802

[5] K. Maltman, hep-ph/0504201

[6]M.N. Achasov *et al.* (The SND Collaboration), hep-ex/0506076

XI.4 Nuclear and Particle Astrophysics and Cosmology: *Gamma Rays II*

High-Energy Emission from Gamma-Ray Bursts

Peter Meszaros
Pennsylvania State University

The GLAST Gamma–Ray Telescope Mission

Robert P Johnson
U.C. Santa Cruz

on behalf of the GLAST collaboration.

The Gamma–ray Large Area Space Telescope, GLAST, is an orbital mission under construction to measure the cosmic gamma–ray flux in the energy range 20 MeV to >300 GeV, with supporting measurements for gamma–ray bursts from 10 keV to 25 MeV. With its launch in 2007, GLAST will open a new and important window on a wide variety of high energy phenomena, including black holes and active galactic nuclei; gamma–ray bursts; the origin of cosmic rays and supernova remnants; and searches for hypothetical new phenomena such as supersymmetric dark–matter annihilations, Lorentz–invariance violation, and exotic relics from the Big Bang. In addition to a short review of the science opportunities, this talk will describe the high–energy gamma–ray telescope and its components and review the mission status.

Surveying the TeV Sky with Milagro

Curtis P Lansdell

University of Maryland / LANL

on behalf of the Milagro collaboration.

A wide field of view, high duty factor, TeV gamma–ray observatory is essential for studying TeV astrophysical sources, because most of these sources are either highly variable or are extended. Milagro is such a TeV detector and has performed the deepest survey of the Northern Hemisphere sky. In addition to detecting the known TeV sources of the Crab Nebula and Mrk421, Milagro has made the first detection of diffuse TeV emission from the Galactic plane. The Milagro data has been searched for unknown point sources and extended sources. Evidence for a new extended TeV source is seen and is coincident with an EGRET unidentified source. The Milagro data has also been searched for the predicted TeV emitters of gamma–ray bursts, galaxy clusters, and EGRET unidentified sources. Solar energetic particles from coronal mass ejections have been detected by Milagro. Based on the success of Milagro, a second generation water Cherenkov gamma–ray observatory is planned which will give an increase in sensitivity of more than an order of magnitude.

XII.4 Facilities and Instrumentation:

New Detector Systems - Particle ID & Trigger Detectors

The Lead Tungstate Electromagnetic Calorimeter of the CMS Detector

Quentin Ingram

PSI

on behalf of the CMS ECAL collaboration.

The Electromagnetic Calorimeter of the CMS detector at the LHC contains 75,848 lead tungstate crystals read out by avalanche photodiodes in the barrel part and by vacuum phototriodes in the end-caps. Silicon strip pre-shower detectors in front of the end-caps enhance ã/ð° discrimination. It is located within the 4 Tesla solenoid of the detector. The front end electronics, using CMOS 0.25 micron technology, consists of a preamplifier, a multistage amplifier and ADC, and circuits to build the trigger primitives and transmit the data over optical links to the upper level electronics. A laser driven system monitors the crystal transparency and the read–out gain. All these components have been specially developed for the demanding requirements of CMS including fast response and a level of radiation tolerance to allow their survival after 10 years of high luminosity at the LHC. Since it will be very difficult or impossible to service components mounted on the calorimeter, reliability is an essential requirement. Recent results from tests with high energy electron beams show that the performance will satisfy the requirements necessary to detect the Higgs via the decay to two photons within 2 - 3 years of high luminosity running of the LHC. The strategy for calibration of the calorimeter will be discussed.

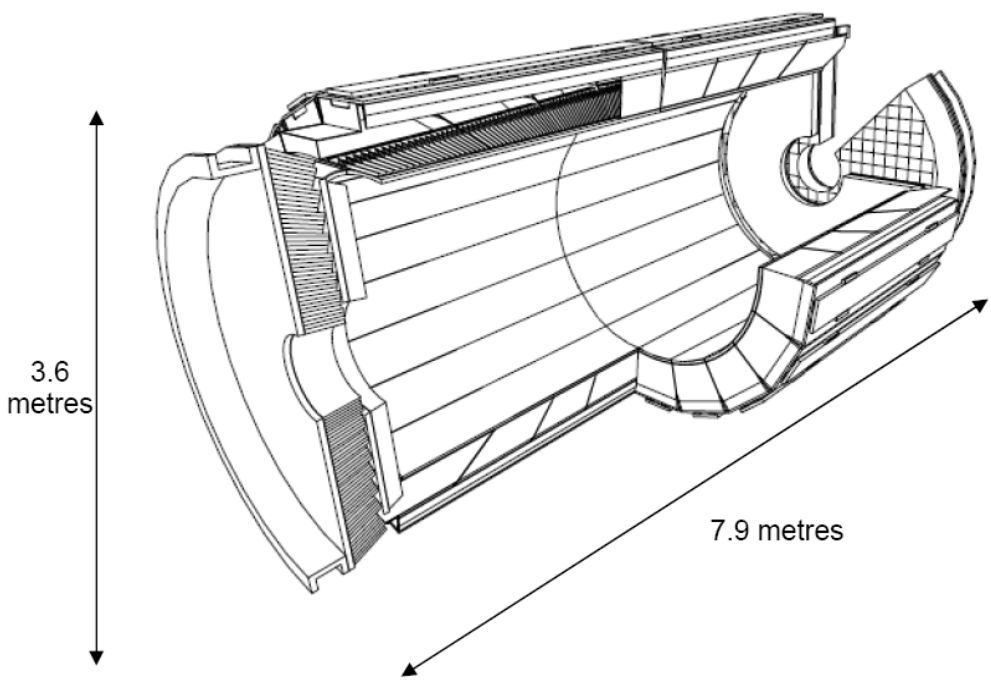

The CMS Electromagnetic Calorimeter

The PHOS Detector at ALICE

Toru Sugitate

Hiroshima University

on behalf of the PHOS/ALICE collaboration.

Many intriguing results have been obtained by the RHIC experiments operating at BNL, with the aim to study the properties of matter under extreme condition created in ultra-relativistic nucleus-nucleus collisions. The LHC at CERN will open new opportunities by extending these studies toward the characterization of strongly interacting partonic matter at much higher temperature. At LHC energies, signals from hard scattering will become predominant and the measurement of rare probes such as photons will become instrumental for such studies.

The Photon Spectrometer, PHOS, is a high-granularity, high-resolution photon detector in the ALICE experiment at the LHC accelerator. It is made of a newly developed lead-tungstate crystal ($PbWO_4$) of 2.2x2.2x18cm^3, corresponding to 20 radiation length. An array of 56 by 64 crystals is packed in a module and kept in an operational temperature of -25deg C with 1/4 deg accuracy. Five modules, 17920 crystals in total, will be installed at a distance of 4m from the interacting point, covering the pseudo-rapidity domain within ±0.12 and span 100deg in azimuth.

We are now building the first module, to be completed in fall 2005. In this talk, we will discuss the physics motivation, the apparatus including the signal readout electronics, the results from prototype tests, and present status of the construction.

Calorimetry Upgrade at Forward Rapidities for the PHENIX detector

Mickey Chiu
University of Illinois at Urbana-Champaign

on behalf of the PHENIX collaboration.

The baseline PHENIX detector at RHIC has been designed as a relatively small acceptance, high rate detector optimized for studying a variety of rare probes that are essential to characterizing the states of matter created in heavy ion collisions and selectively recording as many of the interesting processes in polarized p+p collisions which will give information on the spin structure of the proton. We report on a proposal to greatly extend the coverage and capabilities of PHENIX by adding forward calorimetry to the existing muon spectrometer, so that in addition to the existing electromagnetic calorimeters at mid-rapidity (covering two 90° patches in ϕ and $|\eta| < 0.35$), two calorimeters would be added: a Tungsten calorimeter with silicon pixel readout which would cover $0.9 < |\eta| < 3.0$, and a Lead-Tungstate ($PbWO_4$) calorimeter with APD readout which would cover $3.0 < |\eta| < 4.0$. These new calorimeters would allow PHENIX to measure π^0's, prompt photons, and jets in a new kinematic region and thus significantly expand the physics capabilities of PHENIX, such as increased acceptance for high p_T jet-photon measurements (jet tomography) in A+A, extend studies of nuclei structure down to x $\sim$ 10^{-3} in p+A collisions (thus testing the possible existence of a Color-Glass-Condensate), increase the reach and coverage of PHENIX's ΔG measurements, and study forward Single-Spin Asymmetries in transversely polarized p+p collisions. We will report on the design of these new proposed detectors along with the current status of their implementation.

Time of Flight System for the PHENIX high-pt Detector Upgrade

Julia Velkovska
Vanderbilt University

on behalf of the PHENIX collaboration.

One of the most striking experimental observations at RHIC, unpredicted by theory, is the large baryon and anti-baryon enhancement over the expectation from parton fragmentation. Particle identification (PID) out to high-p_T (¿ 8 GeV/c) is needed to better characterize this effect and differentiate between competing theoretical descriptions. The PHENIX detector is being upgraded with a high-pt PID system. A cost-effective Time-of-Flight (TOF) system based on Multi-gap Resistive Plate chambers (MRPC) is being implemented as part of this upgrade. The MPRC-TOF will provide high-resolution timing measurement in the PHENIX West arm. It will supplement the PID provided by the Aerogel and Ring Imaging Cerenkov Counters and thus allow for continuous PID for π,K, p in the range $0.2 < p_T < 9$GeV/c. Three different prototypes were installed and operated during RUN5 of RHIC. The full detector system will become available for the upcoming RUN6. The details on the MRPC design, the electronics chain and the prototype results obtained in $\sqrt{(}s_{NN} = 200$ GeV Cu+Cu collisions will be presented.

Physics with Muons in CMS - Potential and Challenges

Kerstin Hoepfner

RWTH Aachen, Phys. Inst. IIIA

on behalf of the CMS Muon collaboration.

The CMS detector is currently being constructed at the LHC proton-proton collider, which has been designed to search for the Higgs boson while being sensitive to signs of supersymmetry and other mechanisms leading to physics beyond the Standard Model. Given the extreme environment of the LHC, efficient event selection via a multi-level trigger is mandatory. Fortunately, interesting physics events often lead to final state muons, and as a result, the muon system is a key component of the detector. It is required to provide an efficient muon identification and a stand-alone momentum resolution of $\Delta p/p$ = 10% of p, to efficiently distinguish interesting physics events from the underlying background.

At the high-rate environment of the LHC collider, stand-alone tracking of muons in a magnetic field with a spatial resolution of 100 μm is aimed for, an unprecedented precision for such a large muon system, in addition to the need of fast trigger information. Along with a magnetic field, the precision tracking allows to determine the muons momentum with the desired 10% in stand-alone mode (and $\sim$1% when combined with the tracker information) and the muon charge with $\sim$99% efficiency. A redundancy within the muon system is provided by exploiting two different technologies in both the central region (drift tubes and RPC) and the forward region (cathode strip chambers and RPC).

The muon detection performance has been studied both with physics simulations and the operation of detectors in muon testbeams. Simulations include the benchmark channel of the standard model Higgs boson decaying into 4 final state muons ($H \to ZZ \to \mu\mu\mu\mu$) as well as studies for new particles such as a heavy vector boson W prime in the channel $W' \to \mu\nu_\mu$. Operational studies included tests with a beam of the 40 MHz LHC bunch structure along with LHC-like high backgrounds. The developed tracking algorithms performed with high efficiency.

It will be shown how the physics requirements have driven the system design, and first results demonstrating performance, obtained from test beam and cosmic ray events, will be presented.

A Level–1 Muon Trigger for the PHENIX Forward Spectrometer Upgrade

John G Lajoie

Iowa State University

on behalf of the PHENIX collaboration.

The PHENIX Forward Upgrade adds nosecone calorimeters and Level–1 trigger detectors to the muon forward spectrometers to allow the PHENIX experiment to pursue a rich program of spin physics at sqrt(s) = 500 GeV. The muon trigger detectors and Level–1 trigger electronics will allow the experiment to select high p_T muons from W decay and reject both beam–associated and low–momentum background, enabling the study of quark and antiquark polarization in the proton. The PHENIX Forward upgrade will add momentum and timing information to the present muon Level–1 trigger, which currently only makes use of tracking in the PHENIX muon identifier panels. Signals from 3 Resistive Plate Chambers (RPCs) will provide momentum and timing information for the Level–1 trigger. Each RPC carries a plane with coarse structure to establish a space point for timing and one with radial cathode strips for additional azimuthal resolution. A timing resolution of ~2 ns will permit rejection of beam related backgrounds while tracking information from the RPCs will be used by the trigger to minimize muons from hadron decays. The RPC hit information is sent by optical fibers to a set of Level–1 trigger processors. The layout of the upgrade, details of RPC design and tests, and simulations on background from beam scraping and hadron decays will be presented.

4:30–6:00 PM, Parallel Session #5

I.9 Quarks and Gluons in Hot/Cold and Dense Matter: *Electromagnetic Probes*

Direct photon measurement in Au+Au collisions at $\sqrt{s_{NN}}$=200GeV at RHIC

Takao Sakaguchi

Brookhaven National Laboratory

on behalf of the PHENIX collaboration.

Direct photons are a powerful probe to investigate the thermodynamical nature of states of matters during relativistic heavy ion collisions, since photons do not interact strongly once produced and thus can directly carry out information of these states of matter. They are emitted from all the states such as the initial state, the Quark-Gluon Plasma (QGP), and the final hadron-gas state. In addition, the yield of photons provides an excellent input to theoretical predictions because photons are produced only from Compton scattering of quarks and gluons, annihilation of quarks and anti-quarks, or bremsstrahlung, which have no ambiguity arising from uncertainties on hadronization process.

Recently, direct photons with high transverse momentum (p_T >4 GeV/c) were measured for the first time in Au+Au collisions at $\sqrt{s_{NN}}$=200GeV by the PHENIX experiment at RHIC. The yields are in good agreement with a NLO pQCD calculation scaled by the number of binary nucleon collisions, implying that the initial-hard-scattering probability is not suppressed, and therefore the suppression of high p_T hadrons is attributed to final state interaction.

Photons from intermediate p_T (1< p_T <4 GeV/c) contain many contribution on top of the hard scattering, such as the ones produced through the interaction of hard scattered partons with the medium, thermal radiation from the QGP and processes in the hadron-gas phase. So far, WA98 at CERN is the only experiment that showed a significant excess in this p_T region. The result can be described by a contribution from QGP state with a temperature of T=270MeV and no initial k_T broadening, a temperature of T=200MeV and initial k_T broadening. The two scenarios are indistinguishable because it was not possible to measure the pQCD contribution in the experiment.

The PHENIX experiment has measured photons in the intermediate p_T region in Au+Au collisions at $\sqrt{s_{NN}}$=200GeV using high statistics and stable data from RHIC Year-4 run. The analysis was carried out using both conventional background-subtraction method and a new method where real direct photons are measured by their virtual counterparts. An excess of the signal over background has been seen in this p_T region. In this talk, the latest result on direct photon measurement in Au+Au collisions at $\sqrt{s_{NN}}$=200GeV will be presented, and the contribution of photons from various states will be discussed.

Electromagnetic Signals at SPS and RHIC

Simon Turbide
McGill University

The production of real and virtual photons in relativistic heavy-ion collisions is studied. Low-p_T photons, dominated by hadron gas contributions, are evaluated within a massive Yang-Mills approach. Earlier calculations are reexamined with additional constraints, including new production channels and form-factors. The intermediate to high-p_T region is dominated by the physics of jets. A treatment, complete to leading-order in the strong coupling, is used to calculate energy loss in the strongly interacting medium. This approach is convolved with a physical description of the initial spatial distribution of jets and with an expansion of the emission zone. The role played by jet-plasma interactions is highlighted, showing that they dominate in the range $2 < p_T < 4$ GeV, at the Relativistic Heavy Ion Collider (RHIC). This mechanism has an important impact on both the total photon yield and the photon elliptic flow.

Dielectron production in C+C collisions with HADES

Malgorzata Sudol

GSI/ Frankfurt University

on behalf of the HADES collaboration.

The HADES spectrometer installed at GSI Darmstadt is devoted to study production of di-electron pairs from proton, pion and nucleus induced reactions at 1-2 AGeV. The main goal is to search for in-medium modifications of spectral functions of the light vector meson ρ/ω at moderate temperatures and nuclear matter densities of ρ_0 - 3*ρ_0 [1].

Spectroscopy of rare lepton pairs in reactions with abundant hadron production requires an efficient electron identification. In HADES it is achieved with a large geometrical acceptance (35% for pairs), fast electron identification in hadron blind RICH accompanied by set of Pre-Shower and TimeOfFlight counters and selective multistage trigger scheme. Particles momentum is measured by a tracking system surrounding a toroidal superconducting magnet.

The detector went into operational in 2002 and since then has taken data from $^{12}C+^{12}C$ collisions at 2AGeV (2002), 1AGeV (2004) and proton-proton (2004) reactions at 2.2 GeV. The main goal of the measurement with $^{12}C+^{12}C$ system is to investigate spectacular dielectron enhancement found in $^{12}C+^{12}C$ and $^{40}Ca+^{40}Ca$ collisions at 1 AGeV in the pioneering experiments of DLS collaboration [2]. In the pp collisions we have focused on η meson production which contributes to the invariant mass range of 140< M_{e+e-} <550 MeV/c^2. Prelimary results from this experiment have been submitted for presentation in the poster session.

In this contribution we would like to focus on the first results obtained from $^{12}C+^{12}C$ collisions at 2 AGeV. Invariant mass, rapidity and transverse momentum distributions corrected for reconstruction efficiencies will be shown and compared with calculations based on the thermal (PLUTO) and microscopic transport (QMD, HSD) models [3].

[1] P.Salabura et.al., Nucl.Phys., A749(2005)150c
[2] R. J. Porter et al., Phys. Rev., Lett. 79 (1997)1229
[3] Shekter et al., Phys. Rev C(2003)
E. Bratkovskaya, priv. communications

Pion and Quark Annihilation Mechanisms of Dilepton Production

Dmitry Vladlenovich Anchishkin
Bogolyubov Institute for Theoretical Physics

We revise the pion-pion and quark-quark annihilation mechanisms of dilepton production during relativistic heavy-ion collisions. We focus on the modifications caused by the specific features of intramedium pion states rather than by medium modification of the rho-meson spectral density. The main ingredient emerging in our approach is a form-factor of the multi-pion (multi-quark) system. Replacing the usual delta-function the form-factor plays the role of distribution which, in some sense, ”connects” the 4-momenta of the annihilating and outgoing particles. The difference between the c.m.s. velocities attributed to annihilating and outgoing particles is a particular consequence of this replacement and results in the appearance of a new factor in the formula for the dilepton production rate. We obtained that the form-factor of the multi-pion (multi-quark) system causes broadening of the rate which is most pronounced for small invariant masses, in particular, we obtain a growth of the rate for the invariant masses below two masses of the annihilating particles.

Generalized Weinberg sum rules, four-quark condensates and chiral symmetry restoration

Stefan Leupold

Institut fuer Theoretische Physik, Universitaet Giessen

In QCD, weighted averages (moments) of the difference of spectra in the vector and axial-vector channel can be identified as order parameters of chiral symmetry breaking (generalized Weinberg sum rules [1]). One of these moments is connected to a specific four-quark condensate. It is pointed out how this condensate can be evaluated for in-medium situations in the large-N_c limit, where N_c denotes the number of colors [2].
The four-quark condensate is evaluated
1. for low temperature (and vanishing baryo-chemical potential) by approximating the mediu by a pion gas;
2. for finite baryo-chemical potential (and vanishing temperature) by approximating the medium by a Fermi sphere of nucleons;
3. for sizable temperature and sizable baryo-chemical potential by approximating the mediu by a resonance gas [3].
For the first two cases it is demonstrated that the corrections to the respective large-N_c result can be expected to be small. The third case allows the determination of a transition line to the chirally restored phase as a function of temperature and baryo-chemical potential [4]. The regime of sizable temperature and sizable baryo-chemical potential is especially relevant for the Compressed Baryonic Matter (CBM) project [5] at the future Facility for Antiproton and Ion Research (FAIR) at GSI.

[1] J. I. Kapusta and E. V. Shuryak, Phys. Rev. D **49**, 4694 (1994), hep-ph/9312245.

[2] S. Leupold, “Factorization and non-factorization of in-medium four-quark condensates,” hep-ph/0502061.

[3] P. Gerber and H. Leutwyler, Nucl. Phys. B **321**, 387 (1989).

[4] S. Leupold, in preparation.

[5] http://www.gsi.de/zukunftsprojekt/experimente/CBM/

Phi meson propagation in a hot hadronic gas

Luis Alvarez Ruso[1], V. Koch[2]

[1]*Institut fur Theoretische Physik, Universitat Giessen*
[2]*Nuclear Science Division, LBNL*

The ϕ meson is a nice probe of the properties of matter created in ultra-relativistic heavy-ion collisions. It is widely accepted that the ϕ mean free path (MFP) in the hot hadronic fireball is large due to the small cross section for scattering with non-strange hadrons. This implies that ϕ spectra would retain the information about the stage of the collision at which the plasma hadronizes. However, ϕ production in $\mathrm{Pb}-\mathrm{Pb}$ collisions at SPS shows some intriguing features that are difficult to match with the picture of a ϕ weakly interacting with the hadronic medium. Both absolute yields and inverse slope parameters in the transverse mass distributions exhibit different values when measured via $\mu^+\mu^-$ or $\mathrm{K}^+\mathrm{K}^-$ decays. The inverse slope, as obtained from the hadronic measurement, suggests that the ϕ's flow together with pions, kaons and protons, while the dilepton measurement is consistent with the assumption of an early freezeout. The modification of visible ϕ spectra due to kaon rescattering inside the fireball is an important ingredient but does not fully explain the discrepancies.

We have calculated ϕ collision rates and MFP in a hot hadronic gas of pseudoscalar (π, K) and vector mesons (ρ, ω, K^*, ϕ). The reaction cross sections are obtained within the Hidden Local Symmetry Lagrangian, which includes both Goldstone bosons and vector mesons in a manner consistent with the symmetries of QCD. The use of such a realistic model allows us to take into account many mechanisms that are not present in calculations that rely only in couplings extracted from observed decays but are allowed by the symmetries.

We obtain that at hadronization, the ϕ mean free path λ is much smaller than the typical size of the hadronic system formed in the collision. Therefore, ϕ's will not scape without scattering

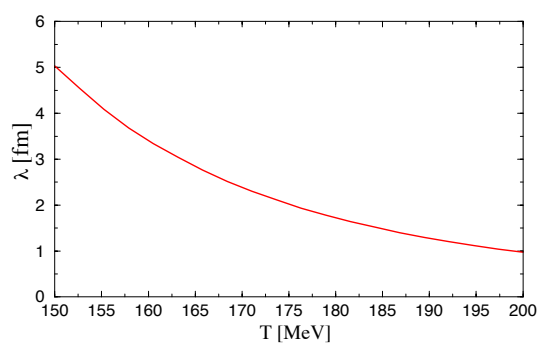

The implications of this result for the ϕ yield has been investigated by solving the rate equation for the ϕ density assuming kinetic but not chemical equilibrium. The high collision rates at the early stages of the hadronic evolution tend to maintain the equilibrium, causing a reduction of the ϕ number with respect to hadronization. This decrease ranges from 5 % to 45 % depending on hadronization temperature, freezeout temperature and flow velocity.

II.5 Quantum Chromodynamics: *Experimental Results II*

Experimental Studies on Kaonic Atoms at DAΦNE: Recent Results and Perspectives

Johann Marton

Stefan Meyer Institute for Subatomic Physics

on behalf of the DEAR / SIDDHARTA team.

A research program at the DAFNE electron-positron collider of Laboratori Nazionali di Frascati [1] is focused on experimental studies of kaonic atoms, taking advantage of the low-energy kaons produced in the phi-meson decay. The low-energy kaon-nucleon interaction in kaonic hydrogen and kaonic deuterium can be investigated under unprecedented conditions.

The DEAR (DAFNE Exotic Atom Research) experiment and its successor SIDDHARTA (Silicon Drift Detector for Hadronic Atom Research by Timing Application) are using precision X-ray spectroscopy of kaonic hydrogen and deuterium atoms to measure the strong interaction induced shift and absorption width of the ground state. From these quantities the isospin-dependent antikaon-nucleon scattering lengths can be determined. Furthermore, these precision measurements are a powerful tool to test chiral symmetry breaking in systems with strangeness.

The experimental method of the DEAR experiment and the results of the studies on kaonic atoms will be presented. The obtained values of DEAR [2] for the hadronic shift and width of the 1s state in kaonic hydrogen are

$$\text{shift}_{1s} = -193 \pm 37 \text{ (stat.)} \pm 6 \text{ (syst.) eV}$$

$$\text{width}_{1s} = 249 \pm 111 \text{ (stat.)} \pm 30 \text{ (syst.) eV.}$$

Within the SIDDHARTA project new X-ray detectors are in development. Whereas in the DEAR experiment CCDs (charge coupled devices) were used as X-ray detectors, SIDDHARTA will employ an array of large area silicon drift detectors (SDDs). The timing capability of SDDs will result in a large suppression of background events. They also exhibit excellent energy resolution comparable with CCDs. New high precision experiments on kaonic hydrogen and deuterium will be performed using SDDs in an optimized experimental setup. The status of these developments and an outlook to the future experiments will be presented.

Work supported by TARI-INFN, Contract HPRI-CT-1999-00088 and
Contract No. RII3-CT-2004-506078.

[1] http:// www.lnf.infn.it
[2] G. Beer et al. (DEAR Collaboration), Phys. Rev. Lett. 94 (2005) 212302

First measurement of inclusive jet yields in polarized p+p collisions at sqrt(s) = 200 GeV

Michael l Miller

MIT

on behalf of the STAR collaboration.

RHIC is the world's first high energy polarized proton-proton collider. Of the two large detectors, STAR is uniquely capable of full jet reconstruction in *p*+*p* collisions and is just embarking on a rich and diverse set of jet measurements in *p*+*p* collisions. The calibration of the jet energy scale and transverse energy resolution are critical to many physics analyses including, but not limited to, constraint of the gluon polarization (ΔG) via measurement of jet production in *polarized p*+*p* collisions. High statistics measurement of *unpolarized* jet cross sections at RHIC may provide significant constraints to previously measured large-*x* parton distributions, which could impact searches for new physics at the LHC. We present preliminary measurements of inclusive jet yields in the transverse energy region $5<E_T<50$ GeV from ~1 pb^{-1} of data at $\sqrt{s}$ =200 GeV. Final state hadron energies were measured using charged particle tracking in the time projection chamber and energy deposition in the electromagnetic calorimeter. Hadrons were clustered using both the k_T and midpoint-cone algorithms. The data were corrected for detector inefficiency and resolution using PYTHIA events processed through a full GEANT simulation. The measured jet yields are compared to simulation and NLO pQCD calculations. These "proof of principle" measurements pave the way for ongoing analyses of the higher statistics (~3 pb^{-1}) data sample from the 2005 RHIC run.

D0 Measurement of the Inclusive Jet Cross Section

Nirmalya Parua

SUNY, Stony Brook

on behalf of the D0 collaboration.

D0 Mesurement of the Dijet Azimuthal Decorrelations

Marek Zielinski

Univ. of Rochester

on behalf of the D0 collaboration.

Two–particle momentum correlations in jets at Tevatron

Sergo R. Jindariani[1], Andrey Korytov[1], Alexandre Pronko[2]
[1]*University of Florida*
[2]*Fermilab*

on behalf of the CDF collaboration.

Presented are the measurements of two–particle momentum correlations in jets produced in p–pbar collisions at center of mass frame energy 1.96 TeV. Studies were performed for charged particles within restricted opening angle of 0.5 rad around the jet axis and for dijet events with various dijet masses. Comparison of the experimental results to the theoretical predictions obtained for partons within the framework of the resummed perturbative QCD (Next–to_leading Log Approximation) shows that the parton momentum correlations do survive the hadronization stage of jet fragmentation, thus, giving further support to the hypothesis of Local Parton–Hadron Duality.

Heavy Flavour Production in CDF II Detector

Igor V. Gorelov
Dept. of Phys. and Astr., Univ. of New Mexico, USA

Using the data collected with the CDF Run II detector the measurements of the charm and bottom production cross-sections will be presented. The results are based both on large sample of fully reconstructed hadronic decay modes of charm and bottom states made available by the tracking triggers and on calorimeter jet triggered sample tagged by the presence of secondary vertex. The agreement with a theoretical prediction from recent NLO QCD calculations is going to be discussed.

III.7 Nucleon Structure: *Fragmentation and Transverse Spin II*

Nucleon Resonances Spin Structure - RSS: Experiment 01-006 at Jefferson Lab

Oscar A. Rondon
University of Virginia

We have measured the spin structure of the nucleon in the region of the resonances (final state mass $W <\sim 2$ GeV,) at intermediate four-momentum transfer $Q^2 \sim 1.3$ (GeV/c)^2. Double-spin inclusive asymmetries for longitudinally polarized 5.75 GeV electrons incident on longitudinal and transverse solid polarized targets were measured in Jefferson Lab's Hall C. Frozen ammonia and deuterated ammonia were used as the polarized materials. The neutron spin structure is extracted from the proton and deuteron asymmetries.

We will present new results for the proton and deuteron spin asymmetries A_1 and A_2 and spin structure functions g_1 and g_2, and preliminary results for the corresponding neutron quantities, including determinations of the moments of the SSF's at the experiment's mean Q^2. These are the first measurements of the transverse proton and deuteron spin structure in the resonances. We will also report on our measurement of the ratio of the proton electromagnetic form factors with our polarized target.

Collins function measurements at Belle

Akio Ogawa
Brookhaven National Lab

on behalf of the Belle collaboration.

The Collins fragmentation function connects the transverse quark spin with a measurable azimuthal dependence of the produced hadrons around the quark's momentum axis. Therefore, it can be used as a transverse spin analyzer in semi-inclusive DIS and proton-proton collisions. While in those measurements the Collins function appears convoluted with the so far unknown quark transversity distribution, it is directly accessible in e+e- collisions, where one measures a combination of a quark and an antiquark fragmentation function. We present measurements of azimuthal asymmetries for certain charge combinations of pions in which it is possible to minimize other systematic effects that could obscure the effect of spin-dependent fragmentation.

Collins and Sivers asymmetries on the deuteron from COMPASS

Andrea Bressan
University of Trieste & INFN

on behalf of the COMPASS collaboration.

COMPASS is a fixed target experiment presently running at CERN. In 2002, 2003, and 2004 the experiment scattered a 160 GeV positive muon beam on a polarized ^{6}LiD target. The nucleons in the target can be polarized either longitudinally or transversely with respect to the muon beam direction, and 20% of the running time was devoted to transverse polarization. Results for the Collins and Sivers asymmetries from the transverse polarization data are presented here.

Transverse Single-Spin asymmetries for $\pi^{\pm}$ production from pp collisions at

Flemming Videbaek
Brookhaven national Laboratory

on behalf of the BRAHMS collaboration.

Measurements of transverse spin asymmetries in pp collisions at forward angles may reveal information on the internal spinstructure of the proton, in particular on the orbital angular momenta of the quarks. Large asymmetries has been reported for charged pion production at $\sqrt{s_{NN}} = 19$ GeV (1), and for π^0 at 200 GeV (2). The BRAHMS data from the previous RHIC run aquiered a small sample of data at $0.15 < x_F < 0.35$ for $\pi^{\pm}$ transverse asymmetry and reported a value of $+0.05 \pm 0.02$ for π^+ and -0.08 ± 0.02 for π^- (3) The just completed RHIC run resulted in a much large data sample and allows an extension of the measurements to higher x_F and p_T with better systematic and statistical uncertainties. Preliminary results will be presented and discussed in relation to pQCD models.

1 D.L.Adams (E704) Phys.Lett B264,462(1991); Phys.ReV D53,4747 (1996).
2 J.Adams (STAR collaboration) Phys.Rev.Lett 92,171801(2004)
3 F.Videbæk (BRAHMS collaboration) DIS 2005. IOP conference series, in print.

Transverse single spin asymmetries at mid-rapidity at $\sqrt{s}$=200 GeV in p+p collisions

Kjeld O. Eyser
UC Riverside

on behalf of the PHENIX collaboration.

Single spin asymmetries (SSA) A_N of finite values have been measured in hadron production in the E704 experiment [1] at Fermilab and the Star experiment [2] at RHIC. Theoretical descriptions of inclusive hadronic processes expect these asymmetries to vanish at leading twist in massless perturbative QCD. Different mechanisms have been studied to explain the origin of SSA. In order to quantify contributions from competing mechanisms precision measurements over a wide range of p_T and x_F are needed. Previous results from the PHENIX experiment at RHIC were consistent with zero for very small x_F and 0.5 GeV/c $\leq p_T \leq$ 5.0 GeV/c [3]. Improvements in beam polarization in recent p+p collisions opened possibilities for a more precise determination of SSA in inclusive processes. The new data will be compared with previous results and might limit QCD analyses in a more decisive way.

[1] Phys. Lett. B261 (1991) 462.
[2] Phys. Rev. Lett. 92 (2004) 171801.
[3] arXiv:hep-ex/0507073.

Measurement of Lambda polarization in longitudinally polarized proton-proton collisions at $\sqrt{s}$ =200 GeV at STAR

Qinghua Xu

LBNL & Shandong University

on behalf of the STAR collaboration.

Over the past years, the Relativistic Heavy Ion Collider (RHIC) at Brookhaven National Laboratory has successfully developed the capability to collide polarized protons. This contribution reports on a preliminary measurements of longitudinal polarization of Λ and $\bar{\Lambda}$ in longitudinally polarized proton-proton collisions at $\sqrt{s}$ = 200 GeV. The data were collected in years 2003 and 2004, and amount to about 0.8 pb^{-1} with beam polarizations up to 45%. The $\Lambda(\bar{\Lambda})$ candidates are reconstructed at mid-rapidity ($|\eta| < 1$) with the Time Projection Chamber (TPC) of the Solenoid Tracker At RHIC (STAR). Their mean momentum fraction xF is about 8 $\times 10^{-3}$ and their mean transverse momentum pT is about 1.5 GeV/c. The Λ ($\bar{\Lambda}$) polarization is extracted from the asymmetry of counts in intervals of the decay angle in the $\Lambda(\bar{\Lambda})$ rest frame for different helicity states of the colliding proton beams. In this method the detector acceptance largely cancels. Preliminary results for $\Lambda(\bar{\Lambda})$ polarization will be presented and an outlook will be given for future measurements, which may give new insights into the polarized fragmentation and parton distribution functions.

IV.7 Hadrons, Nuclei, Hypernuclei - Light Quarks: *Miscellaneous Talks II*

Nature of the scalar mesons

J. Vijande, A. Valcarce, F. Fernndez
Universidad de Salamanca

Nearly all known mesons made of u, d, and s quarks fit neatly into the multiplets expected in generic constituent quark models. The single exception are the scalar mesons, i.e., $J^{PC} = 0^{++}$. The PDG reports two isovectors: $a_0(980)$ and $a_0(1450)$; five isoscalars: $f_0(600), f_0(980), f_0(1370), f_0(1500)$ and $f_0(1710)$; and three isodoublets: $K_0^*(800)$, $K_0^*(1430)$, and $K_0^*(1950)$. The latest fit of the $p\bar{p}$ data gave rather definite information on a broad state $f_0(1200-1600)$ [1]. The recent analyses by BES of $J/\Psi \to \phi\pi^+\pi^-$ and $J/\Psi \to \phi K^+K^-$ data require a state $f_0(1790)$ distinct from the $f_0(1710)$ [2].

We address the study of hadrons with zero baryon number described as clusters of quarks interacting through a realistic potential, that provides with a good description of the baryon spectra and the baryon-baryon phenomenology. Scalar mesons are strongly affected by their coupling to open hadron channels what means that virtual hadron loop contributions are important. Therefore four-quark ($qq\bar{q}\bar{q}$) states are expected to mix with conventional $q\bar{q}$ states to yield physical mesons. The interpretation of the light scalar mesons in terms of two- and four-quark components allows for an almost one-to-one correspondence between theoretical states and experiment. A dominant tetraquark component is found for the $f_0(980)$, $f_0(1500)$, $a_0(1450)$ and the $K_0^*(1430)$, and an important tetraquark component is present for the $a_0(980)$, although it has a dominant $q\bar{q}$ structure.

Recent studies on lattice QCD confirm the existence of a scalar glueball (G) with a mass around 1.6 GeV and with a significant mixing to the nearest $q\bar{q}$ states, together with associated mass shifts in the $J^{PC} = 0^{++}$ sector [3]. The preferred glueball mass falls into the range $(M_{s\bar{s}} + M_{n\bar{n}})/2 > M_G > M_{n\bar{n}}$. We have included in our calculation a scalar glueball satisfying the above mass relation and with the mixing to the nearest $2P$ $n\bar{n}$ and $s\bar{s}$ pairs [4]. A correspondence between theoretical predictions and experiment is observed. There are four isoscalar mesons that are not dominantly $q\bar{q}$ states, they are the $f_0(980)$ ($nn\bar{n}\bar{n}$), the $f_0(1500)$ ($ns\bar{n}\bar{s}$), the $f_0(1710)$ (glueball) and the $f_0(2020)$ ($ss\bar{s}\bar{s}$).

In summary, the spectroscopy and many of the decay properties of the scalar mesons can be understood under the hypothesis of the mixing between two- and four-quark components. A scalar glueball, as suggested by lattice QCD, improves the description.

[1] V.V. Anisovich and A.V. Sarantsev, Eur. Phys. J. A **16**, 229 (2003). [2] M. Ablikim *et al.*, hep-ex/0411001. [3] C. McNeile and C. Michael, Phys. Rev. D **63**, 114503 (2001). [4] W. Lee and D. Weingarten, Phys. Rev. D **61**, 014015 (2000).

Does inclusive pion DCX drop rapidly above 0.5 GeV?

Anna Krutenkova
Institute of Theoretical and Experimental Physics

on behalf of the SKS collaboration.

The inclusive pion double charge exchange (DCX) reaction, $^{16}O(\pi^-, \pi^+)X$, at $T_0 = 0.50$ and 0.75 GeV has been studied in the kinematic region $0 \leq \Delta T \leq 140$ MeV ($\Delta T = T_0 - T$, T is the kinetic energy of the outgoing pion). This condition forbids an additional pion production which represents the background to the conventional DCX mechanism of two sequential single charge exchanges (SSCX). The experiment was performed with the SKS spectrometer at KEK PS sharing the apparatus of the E438 experiment [1]. The measured integrated forward cross section $\langle d\sigma/d\Omega \rangle_{140}$ shows (see figure) relatively slow decrease with energy, in contrast with the expected fast fall in the framework of SSCX. This result strongly supports the effect of the anomalous energy dependence of the inclusive pion DCX on nuclei recently observed at ITEP [2] in the energy range of 0.6 - 1.1 GeV. In a literature there is only one interpretation of such effect, which is based on the Gribov-Glauber picture of inelastic rescatterings (IR) [6]. In this qualitative approach the contribution of the IR mechanism of DCX (with two pions in the intermediate state) dominates over SSCX one (with neutral pion in the intermediate state). The quantitative estimate within the OPE model confirms this statement at energies above ~ 1 GeV. Thus, the inclusive pion DCX is a unique process where IR appear not as a correction but as the main mechanism of the hadron-nucleus interaction.

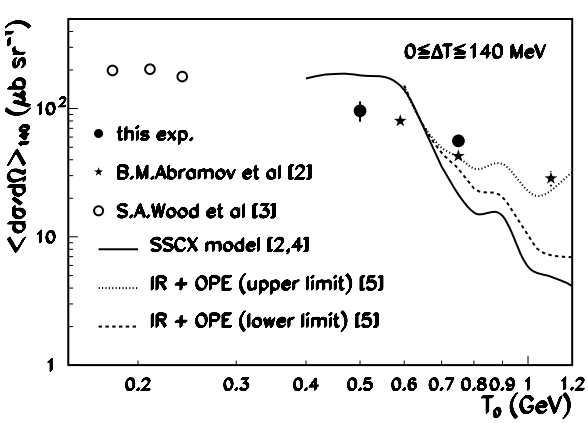

References

[1] P.K. Saha *et al.*, Phys. Rev. C **70**, 044613 (2004).

[2] B.M. Abramov *et al.*, Nucl. Phys. **A723**, 389 (2003).

[3] S.A. Wood, J.L. Matthews, E.R. Kinney, P.A.M. Gram, G.A Rebka, Jr., and D.A. Roberts, Phys. Rev. C **46**, 1903 (1992).

[4] M.J. Vicente Vacas, M.Kh. Khankhasayev, and S.G. Mashnik, nucl-th/9412023.

[5] A.B. Kaidalov, and A.P. Krutenkova, J. Phys. G: Nucl. Part. Phys. **27**, 893 (2001).

[6] A.B. Kaidalov, and A.P. Krutenkova, Phys. Atomic Nucl. **60**, 1206 (1997)).

New 8Be resonances from S-matrix poles

Philip R Page
Los Alamos National Laboratory

Partial wave analysis of four reaction channels, coupled in a unitary way, is performed to fit about 4700 data points from 69 experimental references. The data encompass integrated and differential cross-sections, and polarization data. The energies, total and partial widths, and reduced width amplitudes of the resonances are extracted by finding the complex S-matrix poles. The application is to ^{8}Be resonances up to an excitation energy of 26 MeV. The presence of an extremely broad $J^P = 2^+$ "intruder" resonance is confirmed, while a new 1^+ and very broad 4^+ resonance are discovered. A previously known 22 MeV 2^+ resonance is likely resolved into two resonances. The experimental $J^P I = 3^{(+)}$? resonance at 22 MeV is determined to be 3^-0, and the experimental 1^-? (at 19 MeV) and 4^-? resonances to be isospin 0. The presentation is based on P.R. Page, nucl-th/0506063.

Parton Distributions in Hadrons

Mary Alberg[1], Ernest M. Henley[2]

[1]*Seattle University and University of Washington*
[2]*University of Washington*

We use the statistical model of Zhang et al. [1] to calculate parton distributions in hadrons. The model does reasonably well in predicting the distributions of partons in the proton, including the $(\bar{d} - \bar{u})$ excess in the proton sea. We extend the model to calculate quark and gluon distributions in the pion, kaon, and the pentaquark. The hadrons are described in terms of quark and gluon Fock states. Detailed balance between each pair of states is assumed, from which the coefficients of the Fock state expansion are determined. The parton distribution functions are found in the hadron rest frame from a Monte Carlo calculation. The results are evolved to appropriate QCD scales for comparison with experiment. Despite its simplicity, the model is in good agreement with the experimentally measured distributions of partons in the pion and kaon. This project has included significant participation by undergraduates at Seattle University, made possible by support from the Research in Undergraduate Institutions Program of the National Science Foundation.

[1] Y.-J. Zhang, B.-S. Zou and L.-M. Yang, Phys. Lett. B 528 (2002) 228.

Dispersive e. m. Contributions to the πN scattering Amplitude at Threshold

Torleif E. O. Ericson[1], A. Ivanov[2]

[1]*Theory Division, CERN, Geneva*
[2]*Atomic Institute and SMI of Austrian Academy of Sciences, A-1040 Wien, Austria*

It was shown in Ref. [1] that the strong hadronic level shift of the ns levels of pionic hydrogen and the physical πN scattering amplitude at threshold in the presence of the iterated Coulomb field can be accurately expressed in terms of a hadronic scattering length by appropriately exploiting of the empirical knowledge of the e. m. form factors of the pion and nucleon. This raises the question of the e. m. contribution from processes for which intermediate hadron state no longer has the quantum numbers of the initial πN channel [2]. The large relative value of the imaginary amplitude due to the radiative Kroll-Ruderman process $\pi^- p \to \gamma N$ (4%) suggests that such and similar processes play a particularly important role. We investigate the corresponding dispersive contribution to the πN scattering lengths of charged pions in the heavy baryon limit, assuming them to be saturated by the radiative processes $\pi^\pm N \to N'\gamma$ and $\pi^\pm N \to \Delta\gamma$. The e. m. contributions are greatly simplified for threshold processes in this limit. We start from PCAC with minimal e. m. coupling. The experimental axial form factor of the nucleon (Δ) is used, such that there is no free parameter. The dominant term in the soft pion limit comes from the intermediate $\Delta\gamma$ states and not from the $N\gamma$ ones. However, the Δ contribution is tempered by the $N\Delta$ mass splitting, which is an important feature. The underlying physics is closely related to that of the well explored p-wave πN scattering using the Δ-isobar picture. This mechanism gives a large isospin violating contribution to the isoscalar scattering length for charged pions in the soft limit and a 6% contribution to the 1s level shift of pionic hydrogen. One can regard this result as a model calculation of the unknown chiral constant f_1 [3] with $F_\pi^2 f_1 = 23$ MeV.

In the case of a non-vanishing pion mass we find for the nucleon contribution the identical coefficient for the term proportional to $m_\pi \ln m_\pi$ as the one found in ChPt approach for the corresponding term [4]. This provides independent support for the relevance of our direct comparison with ChPt results. The model independent terms from the nucleon give a -0.9% contribution to the isovector scattering length. However, when the Δ isobar term is included on an equal level with the nucleon one, it is is of similar importance and must be included in any realistic approach. Further implications and possible other contributions will also be discussed.

References

[1] T. E. O. Ericson, B. Loiseau and S. Wycech, Phys. Lett. **B 594**, 76 (2004).

[2] T. E. O. Ericson and A. N. Ivanov, hep-ph/0503277.

[3] V. E. Lyubovitskij and A. Rusetsky, Phys. Lett. B **494**, 9 (2000).

[4] J. Gasser,*al.*, Eur. Phys. J. C **26** (2002) 13.

Coincidence Exclusive Measurement of the Non-Mesonic Weak Decay of ${}^{12}_{\Lambda}$C

Mijung Kim

Department of Physics, Seoul National University, Seoul, Korea

on behalf of the KEK-PS E462/E508 collaboration.

We have measured nucleon pairs in coincidence emitted in the non-mesonic weak decay(NMWD) of ${}^{12}_{\Lambda}$C hypernucleus produced via (π^+,K^+) reaction especially in order to determine Γ_n/Γ_p ratio unambiguously. The Γ_n/Γ_p ratio is the ratio of the decay widths of the two NMWD channels(one nucleon induced NMWD), namely neutron-induced($\Lambda n \rightarrow nn$), and proton-induced ($\Lambda p \rightarrow np$) ones. It is a very important quantity to understand the mechanism of NMWD. But, until recently this ratio has been a long standing puzzle in that experimental values have been close to unity and theoretical ones much smaller than unity. From the measured nucleon pair number ratio,N_{nn}/N_{np}, the Γ_n/Γ_p ratio of ${}^{12}_{\Lambda}$C is extracted to be 0.5$\pm$0.14(stat)$\pm$0.03(syst). N_{nn} and N_{np} are the pair number yields per NMWD for nn- and np-pairs respectively and they are obtained by requring the condition of back-to-back coincident events in their opening angle distribution($\cos\theta_{NN} < -0.7$) in order to suppress two nucleon induced ($\Lambda NN \rightarrow NNN$) NMWD events and those affected by final state interaction(FSI) which is the rescattering effects of propagating nucleons in the residual nucleus. The measured values are almost free from the two nucleon induced NMWD and FSI events and now agree well with recent theoretical values finally resolving the long standing Γ_n/Γ_p puzzle unambiguously. The obtained Γ_n/Γ_p ratio for ${}^{12}_{\Lambda}$C is close to that for ${}^{5}_{\Lambda}$He[1]. Comparing ${}^{5}_{\Lambda}$He(s-shell) and ${}^{12}_{\Lambda}$C(p-shell) hypernucleus, we can study FSI effects and mass dependence of decay mechanism of NMWD. In the talk, we will present the details of Γ_n/Γ_p extraction method from the measured nucleon pair numbers and compared results of s-shell (${}^{5}_{\Lambda}$He) and p-shell(${}^{12}_{\Lambda}$C) hypernucleus.

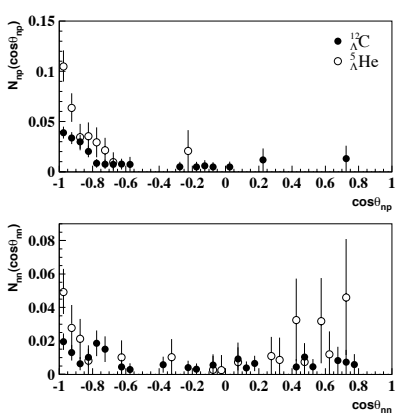

Fig. 1. The yields of np(top)- and nn(bottom)- pairs per NMWD of ${}^{5}_{\Lambda}$He(open circle) and ${}^{12}_{\Lambda}$C(filled circle) are represented as a function of their opening angle.

References

[1] B. H. Kang *et al.*, Sendai03 proceedings(2003)

V.5 Heavy Flavor Physics - Search for New Particles: *SUSY/New Physics*

Gauge Coupling Unification, SUSY Scale and Strong Coupling Running

Dimitri Bourilkov
University of Florida

The apparent unification of gauge couplings around 10^{16} GeV is one of the strong arguments in favor of Supersymmetric extensions of the Standard Model. In this contribution an analysis, using the latest experimental data and paying special attention to numerical and statistical details, is presented. The strong coupling emerges as the key factor for interpreting the results of the fits, as the experimental and theoretical uncertainties in its measurements are substantially higher than for the electromagnetic and weak couplings. The generic SUSY scale favored in this analysis is easily within LHC, and possibly even within TEVATRON reach. The implications of the results for experimental measurements of the strong coupling at hadron colliders in the next decade are discussed.

Search for the Associated Production of Charginos and Neutralinos at the Tevatron

Daniela Kaefer
RWTH Aachen, III. Physics Institute A, Aachen, Germany

on behalf of the DZero collaboration.

We report on the search for associated production of charginos and neutralinos in the trilepton final state using data taken during Run II of the Fermilab Tevatron collider in $p\bar{p}$ collisions at $\sqrt{s} = 1.96$ TeV. The results constrain the associated production of charginos and neutralinos beyond the existing limits.

Searches for Squarks and Gluinos

Xavier Portell
IFAE Barcelona

Search for the Production of Scalar Top Quarks and Scalar Bottom Quarks at the Tevatron

Shaohua Fu
Fermilab

on behalf of the DZero collaboration.

We report on the search for the production of scalar top quarks and scalar bottom quarks using data taken during Run II of the Fermilab Tevatron collider in $p\bar{p}$ collisions at $\sqrt{s} = 1.96$ TeV. We find our data to be consistent with standard model expectations and derive a 95% CL limit in the plane of stop and neutralino mass and a 95% CL limit in the plane of sbottom and neutralino mass.

Searches for Neutral Particles in Dilepton and Photon Final States

Jedong Lee
University of Rochester

SUSY Search in ATLAS

Gianluca Comune

Michigan State University

We discuss the recent studies of Super Gravirty models with the ATLAS detector. Detail studies are performed with the realistic G4 simulation. The following two new results are focused in this talk. (1) Study of the background and the limitations to the sensitivity arising from different sources of systematic uncertainties: (2) The reconstruction of the characteristic signatures of SUSY models in the stau coannihilation and Focus Point regions of parameter space, in which the predicted relic density of the Lightest Neutralino is consistent with cosmological constraints.

VI.5 Fundamental Symmetries:
CP Violation in B Decays and Constraints on New Physics

Time-Dependent CP Asymmetries in b to s Penguins

Hideki Miyake
Graduate School of Science, Osaka Univ.

on behalf of the Belle collaboration.

We present measurements of time-dependent CP asymmetry parameters in $B^0 \to \phi(1020)K$ $\eta' K^0$, $K^0_S K^0_S K^0_S$, $K^0_S \pi^0$, $f_0(980)K^0_S$, $\omega(782)K^0_S$ and $K^+K^-K^0_S$ decays based on a sample of $386 \times 10^6 B\bar{B}$ pairs collected at the $\Upsilon(4S)$ resonance with the Belle detector at the KEKB energy asymmetric e^+e^- collider. These decays are dominated by the $b \to s$ gluonic penguin transition and are sensitive to new CP-violating phases from physics beyond the standard model. One neutral meson is fully reconstructed in one of the specified decay channels, and the flavor of the accompanying B meson is identified from its decay products. CP-violation parameters are obtained from the assymetries in the distributions of the proper-time intervals between the two B decays. We also perform measurement of time-dependent CP asymmetry parameters in $B^0 \to K^0_S \gamma$ decay that is dominated by the $b \to s$ radiative penguin.

Measurements of the CP-violating parameter sin2beta at Babar

Katherine George
University of Liverpool

on behalf of the Babar Collaboration.

We present measurements of the time-dependent CP asymmetries in decays of neutral B mesons to charmonium, open-charm, and gluonic penguin-dominated charmless final states. These measurements are based on a sample of approximately 230 million $\Upsilon(4S) \to B\bar{B}$ decays collected by the BaBar detector at the PEP-II asymmetric-energy B-meson factory. The hints of physics beyond the Standard Model in penguin-dominated charmless

ϕ_1 measurements from $b \to c$ decays at Belle

Kazutaka Sumisawa
KEK

on behalf of the Belle collaboration.

We report an improved measurement of time-dependent CP asymmetries in $B^0 \to J/\psi K^0$ decays based on a sample of 386×10^6 $B\bar{B}$ pairs collected at the $\Upsilon(4S)$ resonance with the Belle detector at the KEKB energy-asymmetric e^+e^- collider. One neutral B meson is fully reconstructed in the decay $B^0 \to J/\psi K^0$, and the flavor of the accompanying B meson is identified from its decay products. CP-violation parameters are obtained from the asymmetry in the distributions of the proper-time interval between the two B decays. We obtain $\sin 2\phi_1 = +0.652 \pm 0.039(\text{stat}) \pm 0.020(\text{syst})$, and $\mathcal{A} = +0.010 \pm 0.026(\text{stat}) \pm 0.036(\text{syst})$. We also report a preliminary measurement of the ϕ_1 using time-dependent analysis of $D^0 \to K^0_S\pi^+\pi^-$ decays produced in $B^0 \to D^0h^0$. The method allows one to directly extract the value of $2\phi_1$. The ambiguity between $2\phi_1$ and $\pi - 2\phi_1$ in the measurement of $\sin 2\phi_1$ can be resolved. We obtain $\phi_1 = (16 \pm 21 \pm 11)^\circ$. The 95% CL region including systematic error is $-30^\circ < \phi_1 < 62^\circ$, thus ruling out the second solution from $\sin 2\phi_1 = 0.726 \pm 0.037$ at the 97% CL.

Measurements of the angles alpha and gamma of the CKM unitarity triangle with the Babar experiment

Julie Malcles
LPNHE

on behalf of the BaBar collaboration.

We present measurements of the CKM angle α in $B \to \rho\rho$, $\rho\pi$ and $\pi\pi$ decays and measurements of the CKM angle γ in $B^+ \to D^0K^{(*)+}$ (GLW, ADS, and GGSZ). The data were collected on the $\Upsilon(4S)$ resonance with the BABAR detector at the PEP-II asymmetric energy e^+e^- collider.

Constraint on CKM angle ϕ_2 from B decays

Akito Kusaka
Department of Physics, University of Tokyo

on behalf of the Belle collaboration.

We report a measurement of CKM angle ϕ_2 with the decay modes $B^0 \to \pi^+\pi^-$ and $B^0 \to \rho^+\rho^-$. The results are obtained from a 253fb^{-1} data sample containing 275 million $B\bar{B}$ pairs collected by the Belle detector at the KEKB asymmetric energy e^+e^- collider operating at the $\Upsilon(4S)$ resonance. We measure the CP-violating parameters: $\mathcal{A}_{\pi\pi} = +0.56 \pm 0.12(\text{stat.}) \pm 0.06(\text{syst.})$ and $\mathcal{S}_{\pi\pi} = -0.67 \pm 0.16(\text{stat.}) \pm 0.06(\text{syst.})$ for $B^0 \to \pi^+\pi^-$, and $\mathcal{A}^L_{\rho\rho} = 0.00 \pm 0.30(\text{stat.})^{+0.10}_{-0.09}(\text{syst.})$ and $\mathcal{S}^L_{\rho\rho} = 0.09 \pm 0.42(\text{stat.}) \pm 0.08(\text{syst.})$ for $B^0 \to \rho^+\rho^-$. Using an isospin analysis, we obtain the model independent constraints on the CKM angle ϕ_2 from the CP asymmetry measurements. Combining the constraints from the two decay modes, we obtain $\phi_2 = 93^{+12}_{-11}\,\text{deg.}$ as a central value and one sigma error, and $75\,\text{deg.} < \phi_2 < 113\,\text{deg.}$ as a 90% confidence interval.

Testing Standard Model and New Physics with the Unitarity Triangle Fit

Maurizio Pierini, et al.
Univeristy of Wisconsin, Madison

on behalf of the UTfit collaboration.

Starting from the latest determinations of several theoretical and experimental parameters, we use the Unitarity Triangle analysis to test the consistency of the CKM matrix in describing CP violation and flavor mixing in the Standard Model. We generalize the analysis beyond the Standard Model allowing arbitrary new physics contributions to loop-mediated $\Delta F = 2$ processes. We then consider models with Minimal Flavor Violation, and present the determination of the Universal Unitarity Triangle that can be defined in this class of extensions of the Standard Model. Finally, we perform a combined fit of the Unitarity Triangle and new physics contributions in Minimal Flavor Violation, reaching a sensitivity to a new physics scale of about 4 TeV. We also extrapolate all these analyses into a ”year 2010” scenario for experimental and theoretical inputs in the flavor sector.

VII.3 Fundamental Interactions in Atomic and Neutron Physics:
Neutron Lifetime and Beta Decay

Testing T invariance in the interaction of slow neutrons with aligned nuclei

Alexey L. Barabanov[1], Anatoly G. Beda[2]

[1]*Kurchatov Institute, Moscow 123182, Russia*

[2]*Institute for Theoretical and Experimental Physics, Moscow 117259, Russia*

The existence of T violating (TV) fundamental interactions beyond Standard Model remains one of the most intriguing questions of modern physics. This is a reason to look for T odd angular correlations in nuclear reactions caused by possible TV interactions. Among the different reactions an interaction of slow neutrons with medium and heavy nuclei has an advantage. Indeed, the capture of a neutron by the nucleus results in the formation of narrow compound resonances. The long life time of the resonances should lead to a large enhancement of T odd effects in the same way as occurs for P odd ones [1,2].

One of the possible tests of T invariance is a search for five-fold correlation $(\mathbf{s}[\mathbf{k} \times \mathbf{I}])(\mathbf{kI})$ in the total neutron-nucleus cross section (see, e.g. [3]) when neutrons are polarized and spins of target nuclei are aligned ($\mathbf{s}$ and $\mathbf{k}$ are the neutron spin and momentum, respectively, and $\mathbf{I}$ is the nucleus spin). This test is sensitive to a hypothetical P conserving T violating (PCTV) interaction. The current situation with bounds on the PCTV interactions favors the study of the five-fold correlation in neutron compound resonances [4,5].

The P even T odd five-fold correlation is enhanced in p wave resonances as well as P odd correlation ($\mathbf{sk}$). Last few years, due to studies of P violation in the neutron-nucleus interaction at LANSCE, a list of known p wave resonances for many nuclei was considerably expanded (see, e.g. [6]). Among the nuclei studied at LANSCE, ^{121}Sb, ^{123}Sb and ^{127}I are the most promising targets for five-fold correlation search. Indeed, quadrupole splitting of spin sublevels in the appropriate compoundes is rather high. Thus significant values of nuclear alignment can be obtained by the well known "brute force" method at temperatures of about 20 mK.

A new method is proposed for statistical estimation of the magnitudes of five-fold correlation in given p wave resonances. Numerical estimations are performed for known p wave resonances of ^{121}Sb, ^{123}Sb and ^{127}I nuclei. It is shown that the results of the measurements (at LANSCE) of P odd correlation in the same p wave resonances may be used to estimate the feasibility of the proposed measurement of five-fold correlation. Our conclusion is that the current bound on PCTV interaction could be improved by one-two orders of magnitude (at best, the PCTV effect would be found) at the measurement conditions realized for P violation studies at LANSCE. An improvement of measurement conditions may be possible at new high intensity spallation neutron sources – SNS (USA) and JSS (Japan).

1. O. P. Sushkov, V. V. Flambaum, JETP Lett. 32 (1980) 352.

2. V. E. Bunakov, E. D. Davis, H. A. Weidenmuller, Phys. Rev. C 42 (1990) 1718.

3. P. R. Huffman et al. Phys. Rev. C 55 (1997) 2684.

4. C. R. Gould, Astrophysics, symmetries, and applied physics at spallation neutron sources eds. P. E. Koehler, C. R. Gould, R. Haight, T. E. Valentine, World Scientific, 2002, p.209.

5. A. L. Barabanov, A. G. Beda, J. Phys. G: Nucl. Part. Phys. 31 (2005) 161.

6. G. E. Mitchell, J. D. Bowman, S.I. Penttila, E. I. Sharapov, Phys. Rep. 354 (2001) 157.

Search for the Electric Dipole Moment of the Neutron

Maurits van der Grinten, et al.

Rutherford Appleton Lab & Sussex University

on behalf of the RAL/Sussex/ILL nEDM collaboration.

The search for the electric dipole moment (EDM) of the neutron plays a prominent role in particle physics because of its direct baring on CP and T violation: a non-zero value of the neutron EDM would be evidence of CP and T violation. The neutron EDM is of particular interest because it is very sensitive to CP violation beyond the Standard Model. The region that is probed by past experiments is already putting tight constraints on models such as Supersymmetry, additional Higgs fields and Left-Right symmetric models.

The nEDM experiment at the Institut Laue Langevin (ILL) is based on a measurement of the Larmor precession frequency of polarised ultracold neutrons stored in a cell in a magnetic field. An EDM would reveal itself by a response of the Larmor precession frequency of the neutron to an electric field applied over the storage volume. The magnetic field is monitored by a cohabiting mercury magnetometer. The experiment has been taking data over a period of six years and has subsequently been running for one year devoted to systematic studies related to the experiment. These systematic studies have now been completed.

This experiment will result in an EDM measurement with a sensitivity of the order of 10^{-26} *e*cm. The experimental techniques used in the experiment will be presented as well as the systematic studies and the results of the data analysis of the experiment.

Search for Time Reversal Violation in Neutron Decay - A Measurement of the Transverse Polarization of Electrons

Kazimierz Bodek, et al.

Institute of Physics, Jagiellonian University, Cracow, Poland

on behalf of the nTRV collaboration.

The Standard Model (SM) predictions of T-violation, originating from the quark mixing scheme, for systems built up of u and d quarks, are by 7 to 10 orders of magnitude lower than the experimental accuracies available at present. It is a general presumption that time reversal phenomena are caused by a tiny admixture of exotic interaction terms. Therefore, weak decays provide a favorable testing ground in a search for such feeble forces. Physics with very slow, polarized neutrons has a great potential in this respect. Our experiment looks for small deviations from the SM in two observables that have never before been addressed experimentally in neutron decay. It aims at the simultaneous determination of both transversal polarization components of electrons emitted in the decay of free neutrons. A non-zero value of the R-correlation coefficient due to the e^- polarization component, perpendicular to the plane spanned by the spin of the decaying neutron and the electron momentum, would signal a violation of time reversal symmetry and thus physics beyond the Standard Model. The value of the N-correlation coefficient, given by the transverse e^- polarization component within that plane, is expected to be finite. The measurement of N, both, probes the SM and serves as an important systematic check of the apparatus for the R-measurement. The first phase of data taking using the polarized cold neutron beam (FUNSPIN) from the SINQ spallation source at the Paul Scherrer Institute, Villigen, has been completed. The present status of the project and the results from data analysis will be discussed.

Precision measurement of the neutron's beta asymmetry using ultra-cold neutrons

Mark F. Makela[1], Back, H. O.[2], Melconian, D.[3], Plaster, B.[4], et al.

[1]*Los Alamos National Lab*
[2]*North Carolina State University*
[3]*University of Washington*
[4]*California Institute of Technology*

on behalf of the UCNA collaboration.

A measurement of A_β, the correlation between the e^- momentum and neutron spin (the β asymmetry) in n (neutron) beta-decay, together with the n lifetime, provides a method for extracting fundamental parameters for the charged-current weak interaction of the nucleon. In particular when combined with decay measurements, one can extract the V_{ud} element of the CKM matrix, a critical element in CKM unitarity tests. By using a new SD_2 super-thermal source at LANSCE, large fluxes of UCN (ultra-cold neutrons) are expected for the UCNA project. These UCN will be 100% polarized using a 7 T field, and directed into the β spectrometer. This approach, together with an expected large reduction in backgrounds, will result in an order of magnitude reduction in the critical systematic corrections associated with current n β asymmetry measurements.

This talk will give an overview of the A_β measurement, as well as an update on the status of the experiment.

Measuring the Neutron Lifetime Using Magnetically Trapped Ultracold Neutrons

Pil-Neyo Seo, et al.

North Carolina State University

on behalf of the Neutron Lifetime collaboration.

As part of an on-going program that seeks to improve the measurement of the neutron lifetime by utilizing magnetically trapped ultracold neutrons (UCN), we are developing a technique that offers the possibility of improving the precision of the neutron lifetime by more than an order of magnitude. Some initial proof-of-principle data, along with studies of numerous systematic effects, will be presented. The experiment works by loading an Ioffe-type superconducting magnetic trap with UCNs through inelastic scattering of 0.89 nm neutrons with phonons in superfluid He-4. Trapped neutrons are detected when they decay; charged decay electrons ionize helium atoms in the superfluid resulting in scintillation light that is recorded in real time using photomultiplier tubes. At present, we are installing a larger, deeper superconducting magnetic trap into our apparatus, implementing techniques to reduce background events, and working to increase the neutron decay detection efficiency. We will report on the status of the construction of the improved apparatus and present future prospects for this measurement at neutron facilitities currently being constructed.

Neutron Lifetime Collaboration: F.H. DuBose, R. Golub, E. Korobkina, C.M. O'Shaughnessy, G.L. Palmquist, P.-N. Seo, P.R. Huffman (NC State Univ.); L. Yang, J.M. Doyle (Harvard Univ.), K.J. Coakley, H.P. Mumm, A.K. Thompson (NIST), G.L. Yang (Univ. of Maryland/NIST), S.K. Lamoreaux (LANL)

a high–accuracy measurement of the spin–dependent neutron scattering length of the deuteron

Florian M. Piegsa, et al.

Paul Scherrer Institut, CH−5232 Villigen PSI, Switzerland

on behalf of the nd–Collaboration (TU München, PSI, CE Saclay) team.

The doublet neutron–deuteron scattering length a_2, which is at present only known with an accuracy of 6%, is a crucial value for a better understanding of few–nucleon systems. These systems can be described by novel effective field theories including only nucleons, respectively nucleons and pions as explicit degrees of freedom. The value of a_2 can be obtained via a linear combination of the spin–independent nd scattering length $a_{c,d}$ and the spin–dependent one, $a_{i,d}$. The latter is limiting the total accuracy. Our aim is to measure $a_{i,d}$ with a relative accuracy of 10^{-3} using the effect of nuclear pseudomagnetic precession of neutron spins passing through a target with polarised nuclei. Due to this phenomenon the neutron spins precess around the axis of the nuclear polarisation equivalent to the precession in a normal magnetic field. The precession angle is thereby proportional to the incoherent scattering lengths a_i of the nuclear species present in the sample.
The ideal tool to measure this angle very accurately is Ramsey's technique of separated oscillating fields. In 2004 a Ramsey–apparatus for neutrons has been set up and tested at the polarised cold neutron beamline FUNSPIN at the Paul Scherrer Institut in Switzerland.

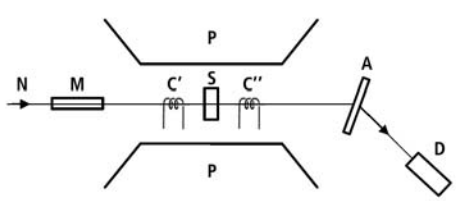

Figure 1 Scheme of the Ramsey–setup

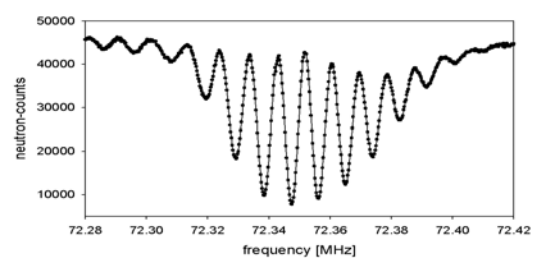

Figure 2 Ramsey resonance pattern

This setup (scheme see figure 1) consists of a monochromating NiTi–supermirror (M) which selects a small bandwidth of the cold neutron spectrum. The polarisation of the neutrons (N) is then flipped twice by 90° by two phase–stabilized high frequency coils (C' and C'') which are located between the pole pieces (P) of a normal conducting 2.5 T magnet. The sample (S) is placed in a ^{3}He–^{4}He dilution refrigerator with a base temperature of about 100 mK ensuring a very long relaxation time of the nuclear polarisation in the sample, which is achieved using the technique of dynamic nuclear polarisation (DNP). The so–called Ramsey resonance patterns (see figure 2) are then obtained by measuring the neutron count rate behind a spin–analyzing bender (A) as a function of the frequency of the high frequency coils.
In a first beamtime the behavior and stability of the Ramsey–setup has been investigated, while in this year's beamtime we implemented the dilution refrigerator with a polarised deuteron target. We successfully observed the phase shift the neutron spins experience passing the pseudomagnetic field of this polarised target.
The talk will outline the project and its experimental challenges as well as recent results.

VIII.5 Neutrino Physics: *Solar, Reactor, and Other Neutrinos*

Production of Electron Neutrinos at Nuclear Power Reactors and the Prospects for Neutrino Physics

Biao Xin

Department of Nuclear Physics, China Institute of Atomic Energy

on behalf of the TEXONO collaboration.

High flux of electron neutrinos(ν_e) is produced at nuclear power reactors through the decays of nuclei activated by neutron capture. Realistic simulation studies on the neutron transport and capture at the reactor core were performed. The production of ^{51}Cr and ^{55}Fe give rise to mono-energetic ν_e's at Q-values of 753 keV and 231 keV and fluxes of 8.3×10^{-4} and 3.0×10^{-4} ν_e/fission, respectively. Using data from a germanium detector at the Kuo-Sheng Power Plant, we derived direct limits on the ν_e magnetic moment and the radiative lifetime of $\mu_\nu < 1.3 \times 10^{-8}$ μ_B and $\tau_\nu/m_\nu > 0.11$ s/eV at 90% confidence level (CL), respectively. Indirect bounds on τ_ν/m_ν^3 were also inferred. The ν_e-flux can be enhanced by loading selected isotopes to the reactor core, and the potential applications and achievable statistical accuracies were examined. These include accurate cross-section measurements, studies of mixing angle θ_{13} and monitoring of plutonium production.

Probing fundamental neutrino properties with solar neutrinos

Alexander Friedland

Theoretical Division, LANL

One of the most important current tasks in neutrino physics is to understand the full implications of the oscillation measurements that have become available in the last five years. While much of the effort in the field has been dedicated to establishing the values of the neutrino masses and mixing, there has also been a growing realization that the same data can tell us a lot about other neutrino properties. I will discuss the sensitivity of the present and future solar neutrino experiments to fundamental neutrino properties, such as its interactions with matter or with electromagnetic fields.

Radiative Corrections to Neutrino-Deuteron Scattering Revisited

Takahiro Kubota[1], Masataka Fukugita[2]

[1]*Department of Physics, Osaka University*
[2]*Institute for Cosmic Ray Research, University of Tokyo*

The problem of QED and electroweak radiative corrections to neutrino deuteron scattering is investigated. In the calculation of Kurylov et al. the constant term in the correction for the Gamow-Teller transitions $(1+\delta_{\mathsf{in}}^{\mathsf{GT}})$ is not calculated, but is assumed implicitly to be nearly equal to that for the Fermi transition $(1+\delta_{\mathsf{in}}^{\mathsf{F}})$. This Gamow-Teller term is calculated and included in our numerical calculation. We also found an error in previous extraction of the radiative correction to the neutral current counterpart $(1+\Delta_{\mathsf{in}}^{\mathsf{GT}})$. After correcting this error we calculate the correction to the neutral current induced reaction relative to the charged current induced reaction, $(1+\Delta_{\mathsf{in}}^{\mathsf{GT}})(1+\delta_{\mathsf{in}}^{\mathsf{GT}})/(1+\delta_{\mathsf{in}}^{\mathsf{GT}}) = 1.017$ for $\mathsf{m_H} = 1.5\mathsf{m_Z}$. Although this is close to the value of Kurylov et al., it is due to an accidental cancellation of the effects mentioned above.

What fraction of Boron-8 solar neutrinos arrive at the earth as a nu-2 mass eigenstate?

Stephen Parke

Fermilab

Model Independent Analysis of 391-Day Salt Phase SNO Data Set

S. Dev Sharma
Himachal Pradesh University

We perform the most general model independent analysis of the 391-Day Salt Phase SNO Data Set and the SuperKamiokande measurement of the ^{8}B flux through the ES reaction by including the possible subdominant transitions into antineutrinos and sterile neutrinos (in addition to the dominant LMA transitions) in the analysis and obtain bounds on the antineutrino and sterile neutrino flux. If the solar boron neutrinos do not undergo transitions into antineutrinos and sterile neutrinos, the total active boron neutrino flux will be equal to the SNO NC flux. However, the presence of transitions into antineutrinos and/ or sterile neutrinos will change this situation.

The non-electronic (muon/ tauon) antineutrino component is ruled by the 391-Day Salt Phase SNO Data Set and the SuperKamiokande measurement of the ^{8}B flux through the ES reaction at 80%C.L. However, the arbitrary $\nu_x - \overline{\nu}_x$ admixtures are still allowed above this confidence level. The maximum allowed value of the muon/tauon antineutrino flux coming from the Sun is $(3.43 \pm 0.47) \times 10^6 \mathrm{cm}^{-2}\mathrm{s}^{-1}$. With the increasing accuracy in the SNO CC and NC fluxes, it will become possible in near future to obtain more precise constraints on the $\nu_x - \overline{\nu}_x$ admixture present in the solar boron neutrino flux. Combining the SuperKamiokande ES flux with the SNO CC and NC fluxes, the sterile flux is found to be non-zero at about one standard deviation. The upper bound on the sterile flux is $3.37 \times 10^6 \mathrm{cm}^{-2}\mathrm{s}^{-1}$ at 95.5%C.L.

A Large Liquid Argon TPC for Off-axis NuMI Neutrino Physics

Scott Menary
York University

The ICARUS collaboration has shown the power of the liquid argon time projection chamber (LArTPC) technique to image events with bubble-chamber-like quality. I will describe a proposed long-baseline ν_e appearance experiment utilizing a large ($\geq$ 15 ktonne) LArTPC placed off-axis of Fermilab's NuMI ν_μ beam. The complete LArTPC program as it presently stands, which includes a number of smaller R&D projects designed to examine the key design issues, will be outlined.

IX.3 Muon Physics: *Lepton Flavor Violation*

PRISM/PRIME; the Advanced Muon Beam and the Experiment Searching for μ-e Conversion with 10^{-18} Sensitivity

Masaharu Aoki

Osaka University

on behalf of the PRISM collaboration.

Lepton flavor violation (LFV) in the charged lepton sector, such as μ-e, τ-μ, τ-e transitions, are not built in the Standard Model (SM). Therefore, any experimental evidences to the LFV processes at a level much larger than 10^{-60} will immediately suggest the physics beyond SM. Actually, a model based on supersymmetry (SUSY) with a see-saw mechanism by right-handed heavy neutrino suggests muon-LFV at only a few orders of magnitudes less than the current experimental limits. SUSY Grand Unified Theory also suggests the potential observation at a few orders of magnitudes less than the current experimental limits. These predictions boosted the activity of experimental searches for muon-LFV processes in the world.

PRISM/PRIME is one of such activities. PRISM, which stands for Phase Rotated Intense Slow Muon source, aims to provide slow muon beam with high intensity, high brightness and high purity by using a phase-rotation technique. PRIME (PRIsm Muon-Electron conversion experiment) is an experiment aiming to search for μ-e conversion process down to a level of 10^{-18} by taking a full advantage of PRISM beam. The PRISM consists of 1) high power pulsed proton driver, 2) pion capture system, 3) pion-decay and muon-transport section, and 4) phase rotation system. It will use a pulsed proton beam at J-PARC 50 GeV proton synchrotron. The central momentum of muon is 70 MeV/c, and the designed intensity is 10^{11}-10^{12} muons per second for both μ^+ and μ^-, which is almost four orders of magnitude higher than the currently-available muon source at PSI. The momentum spread is only $\pm 2\%$ after the phase rotation in a ring. This narrow momentum spread is quite important in order to reduce potential backgrounds related to the thickness of muon stopping target.

Note that the $\mu \to e\gamma$ decay is only sensitive to the process in which a photon couples to the μ-e vertex, while μ-e conversion process is also sensitive to other types of processes, such as higgs mediated process. Thus on-going MEG experiment (searching for $\mu \to e\gamma$ decay) and PRISM/PRIME experiment are complementary each others.

A phase-rotation ring of PRISM is now under construction, and the other components will be built in several years. We are hoping to start the experiment at early 2010's. PRISM is also attracting the interests of world's accelerator scientists since it manipulates muon beam by using accelerator techniques. Muon acceleration is one of key technologies in the future of particle physics; a neutrino factory and muon collider. PRISM would be a good pilot project toward the realization of those advanced accelerator facilities.

Lepton Flavor Violation in Supersymmetric Models

Ryuichiro Kitano
SLAC

We calculate various lepton flavor violating processes in supersymmetric models and discuss possibility of extracting model information. Particulary, the effect of Higgs-boson exchange diagrams is studied.

Muons and Atomic Spectroscopy

Andrzej Czarnecki
University of Alberta

In the last few years, new theoretical tools have revolutionized the theory of simple atomic spectra. In this talk I will review the recent progress and stress the importance of measuring the muonic hydrogen Lamb shift and of renewing measurements of muonium hyperfine splitting.

Status and Prospects for mu -> e+gamma with the MEG Experiment

Giovanni Signorelli
Scuola Normale Superiore & INFN, Pisa

X.1 Theoretical Topics

Soft Collinear Effective Theory

Sean P Fleming
University of Arizona

In this talk I give an overview of soft collinear effective theory (SCET). SCET describes the limit of QCD where highly energetic particles move through a soft background; a configuration which is typical in high energy scattering, and in the decay of a heavy particle to light particles. After motivating SCET, I will highlight the important properties of the theory, and point out some of its novel aspects. I will then discuss some recent applications of SCET including: B-meson decays, J/ψ production, and DIS for $x \sim 1$. I will finish by speculating on future applications of SCET.

The T-Violating Effective Chiral Lagrangian

William H Hockings
University of Arizona

At quark level, there are numerous sources of T violation that generate T-odd interactions among hadrons, with the form of the interactions determined by the chiral symmetry properties of the sources. These sources include the QCD $\bar{\theta}$ term, the quark electric and chromoelectric dipole moments, and other terms that are formally of dimension six and higher. I present a method to construct the corresponding T-violating effective chiral Lagrangian, in which I eliminate by field redefinitions the terms that would lead to vacuum instability. As an illustration of the uses of this Lagrangian, I present a calculation of the electric dipole form factor of the nucleon to sub-leading order in an expansion in powers of momenta and quark masses.

Vaccum Polarization Effects in the Worldline Variational Approach to Quantum Field Theory

R. Rosenfelder

Paul Scherrer Institute

Worldline methods in Quantum Field Theory have seen a revival in recent years as an efficient technique in perturbative calculations but also as a non-perturbative method to deal with strongly-interacting systems. We have extended the variational approach used by Feynman for the polaron problem [1] to simple super-renormalizable scalar field theories [2] and to Quantum Electrodynamics [3]. In this approach fields are eliminated and replaced by (bosonic and fermionic) worldlines parametrized by the proper time. Recent progress includes more general trial actions [4], Abraham-Lorentz-like equations for the electron [5] and treatment of the relativistic bound-state problem [6].

In all these applications the "quenched approximation" was made, i.e. vacuum polarization (VP) graphs have been neglected. This allowed the functional integral over exchange fields (mesons, photons) to be performed and gave a compact worldline action for the heavy particles. Here we report on an attempt to include (part of) the VP effects while keeping the huge reduction in the number of degrees of freedom which is characteristic for the worldline representation and essential for a successful variational approximation. In a simple scalar model where the heavy particles ("nucleons") are described by an N-component field Φ coupled to a meson field χ with mass m via $g\,\Phi^2\chi$ this is achieved by expanding the functional determinant up to second order in the meson field. After integration over $\chi(x)$ the linear terms give rise to irrelevant tadpoles whereas the quadratic terms change the interaction part of the n-particle worldline action to

$$S_{int} = -\frac{g^2}{2}\sum_{i,j=1}^{n}\int_0^{T_i} dt \int_0^{T_j} dt' \int \frac{d^4p}{(2\pi)^4}\,\frac{\exp\left[-ip\cdot\left(x_i(t)-x_j(t')\right)\right]}{p^2-m^2-\pi_r(p^2)+i0}\,.$$

Here $\pi_r(p^2)$ is the renormalized one-loop VP contribution to the meson propagator. Therefore VP insertions into all meson lines are included in the present approach but not the interactions of the pair-produced heavy particles with other nucleons. These can be taken into account by using a "hybrid" trial action for *both* the meson field χ and the worldlines $x_i(t)$ as in the linear polaron model [7]. Variation then leads to non-linear coupled equations which are much more involved than in the quenched approximation. Numerical results for a single nucleon ($n = 1$) will be presented as well as for the relativistic bound state energy of two nucleons including vacuum polarization with various numbers of flavors N.

[1] R. P. Feynman, Phys. Rev. **97** (1955) 660

[2] R. Rosenfelder and A. W. Schreiber, Phys. Rev. **D 53** (1996) 3337, 3354

[3] C. Alexandrou, R. Rosenfelder and A. W. Schreiber, Phys. Rev. **D 62** (2000) 085009

[4] R. Rosenfelder and A. W. Schreiber, Eur. Phys. J. **C 25** (2002) 139

[5] R. Rosenfelder and A. W. Schreiber, Eur. Phys. J.**C 37** (2004) 161

How the alteration of a thin wall for S-S di quark pairs signifies an Einstein constant dominated cosmology and the break down of semi classical approximations for Inflation

Andrew Beckwith

TcSAM/ U of Houston physics

Previously, we used particle antiparticle pairs as a model of how nucleation of a new universe occurs. This assumes a di quark identification as for S-S' constituent parts of a scalar field. We now can construct a model showing evolution from a dark matter dark energy mix to a pure cosmological constant cosmology due to changes in the slope of a graph of the resulting scalar field. The initial potential system employed is semi classical in nature, and decays to a non-classical system at the end of chaotic inflation at the same time cosmological expansion is dominated by the Einstein cosmological constant term. This assumes that a calculation consistent with Scherrer's derivation of a sound speed being zero is appropriate during initial inflationary cosmology, and changes afterwards as the slope of the scalar field moves away from a thin wall approximation. Correspondence: A. W. Beckwith: projectbeckwith2@yahoo.com PACS numbers: 03.75.Lm, 11.27.+d, 98.65.Dx, 98.80.Cq, 98.80.-k

The Origin of Matter

Sean Tulin, Christopher Lee, Vincenzo Cirigliano, Michael J. Ramsey-Musolf

Caltech

Electroweak baryogenesis (EWB) is an exciting idea because it may answer an important question -- Where does matter come from? -- with physics testable in the next generation of collider experiments and electric dipole moment searches. We study the viability of EWB in the Minimal Supersymmetric Standard Model. The general program is as follows: we derive a set of transport equations which govern the evolution of particle number densities. We determine the unknown coefficients of these equations using the closed time path formulation of non-equilibrium quantum field theory. Finally, we solve the equations and discuss the possibility of successful baryogenesis in light of current experimental limits. Using this rigorous formalism, we find resonant enhancements for certain model parameter values which may increase the viability of this scenario.

XI.5 Nuclear and Particle Astrophysics and Cosmology: *Ultra-High-Energy Cosmic Rays*

Ultra-High Energy Cosmic Rays

Charles D. Dermer
US Naval Research Laboratory

Astrophysical solutions to the problem of cosmic ray origin is treated in this talk. In particular, a comprehensive model based on acceleration of high-energy and ultra-high energy cosmic rays (UHECRs) by gamma-ray burst (GRB) outflows is presented. This model extends the conventional hypothesis that supernovae accelerate cosmic rays to include the supernovae that collapse to black holes and make GRBs. Predictions of high-energy neutrino production, testable with IceCube, and gamma-ray production, testable with GLAST, are made. Acceleration of UHECRs in the jets of active galactic nuclei is also considered.

Anisotropy studies at EeV energies

John D Hague, John A. J. Matthews, Miguel A. Mostafa
University of New Mexico

on behalf of the Pierre Auger collaboration.

One of the main scientific goals of the Pierre Auger Observatory is the study of the arrival direction of ultra-high energy cosmic rays. We present the results of a search for an excess of events near the direction of the galactic center (in several energy ranges), a blind search of overdensities in the cosmic ray flux with respect to isotropic expectations (in different energy ranges and angular scales), and searches for excesses in target directions predefined in a set of prescriptions. Present results are compatible with an isotropic sky, and do not support previous excesses at the galactic center reported by other experiments. We set an upper bound on the flux of cosmic rays arriving within a few degrees from the galactic center.

The First Scientific Results from the Pierre Auger Observatory

Tokonatsu Yamamoto
Enrico Fermi Institute, University of Chicago

on behalf of the the Pierre Auger Collaboration collaboration.

The Pierre Auger Observatory is the world's largest detector to study Ultra-High-Energy Cosmic Rays. More than half of the Southern site has been completed. The observatory has been collecting data for over 1 year and the cumulative exposure is already similar to that of the largest forerunner experiments. A hybrid technique uses model-independent energy measurements from Fluorescence detectors to calibrate the surface detector measurements. In this talk, we report the first estimation of the energy spectrum above 3 EeV and discuss its implications.

Results from the HiRes Experiment

Pierre Sokolsky, et al.
University of Utah

on behalf of the HiRes collaboration.

We report on results concerning the spectrum, anisotropy and composition of Ultra–high energy cosmic rays. The Hires experiment is an air fluorescence experiment with sensitivity to cosmic rays with energies above 10^{17} eV. Concerning the spectrum, we present results from both the monocular and stereo analysis, showing evidence for an ankle structure and a cut–off feature consistent with the GZK cutoff. While no significant large–scale anisotropy is found, an intriguing correlation with nearby BL–Lac objects will be reported on. Results on the composition of Ultra–high energy cosmic rays using the Xmax method will be reported. The composition above 10^{18} eV appears to be light and consistent with being mainly protonic. Results on the proton–air inelastic cross–section at these energies will also be presented.

XII.5 Facilities and Instrumentation: *New Detector Systems - Underground Systems*

The Henderson Mine as an Underground Laboratory

Eric D. Zimmerman
University of Colorado

on behalf of the Henderson Underground Science and Engineering Project collaboration.

The Henderson Mine, in the Rocky Mountains west of Denver, is proposed as a site for the Deep Underground Science and Engineering Laboratory (DUSEL). Henderson is a modern molybdenum mine operated by Climax Molybdenum, a subsidiary of Phelps Dodge Corporation. The proposed DUSEL will feature several multipurpose caverns at depths ranging from 4000 to 7400 feet below the surface, and will accommodate a very large cavern suitable for proton decay, atmospheric neutrino, and long baseline neutrino oscillation studies. The details of the proposed facility as well as the scientific opportunities will be presented.

DUSEL-Homestake

Kevin T. Lesko
LBNL

The Homestake DUSEL program will be described. The Homestake mine in South Dakota is proposed to be converted into the Deep Underground Science and Engineering laboratory. The plans will be described.

SNOLAB

Andrew Hime[1], Fraser Duncan[2], David Sinclair[3]

[1]*Los Alamos National Laboratory*
[2]*SNOLAB*
[3]*Carleton University*

on behalf of the SNOLAB collaboration.

SNOLAB, an international facility for underground science, is presently under construction at the INCO Creighton mine near Sudbury, Ontario, Canada. With 6000 meters of water equivalent overburden this new facility will offer a pristine site for next generation detectors of low-energy solar neutrinos, neutrinoless double beta decay, and cosmological dark matter. We report on the status of construction, the infrastructure and facilities envisioned, and the scientific program under development.

Integral Neutron Multiplicity Measurements from Cosmic Ray Interactions in Lead

Thomas E. Ward[1], Alexander Rimski-Korsakov[2], Nikolai Kudryashev[2], Denis Beller[3]

[1]*Techsource Inc.*
[2]*V.G. Khlopin Radium Institute*
[3]*University of Nevada at Las Vegas*

A 60 element He-3 neutron multiplicity detector was designed, constructed and tested for use in cosmic ray experiments. The typical experimental setup consisted of a 30cmX30cmX30cm lead cube surrounded by polyethelyene moderator 15 cm thick, and 60 He-3 neutron counters placed in the moderator layer on all sides of the lead target. In some experiments a plastic scintillator was added on top of the assembly for coincidence measurements with incoming charged particles from above. The detector performance was tested in a variety of fast pulsed neutron beams at the Idaho accelerator center and compared with MCNPX model calculations. More importantly a series of measurements were performed for the cosmic ray configuration at ground level (3 mwe), in the St. Petersburg metro (185 mwe) and at the Pyhasamlmi mine in Finland (583 and 1185 mwe). The overall efficiency of the detector system was about 23% for a neutron multiplicity of 100 neutrons/event. Anomalous coincidence events with charged cosmic ray particles at sea level produced events with 100-120 neutrons due possibly to the total disintegration of the Pb nucleus. The peak was also observed in measurements at the 185 mwe depth but as for the particles causing such disintegration, no definite evidence exists at the moment. Preliminary data from the various measurements will be presented and future plans for underground experiments, including possible WIMP searches will be discussed.

Cosmic Ray Muon Tomography for the Detection of High-Z Objects

Richard C. Schirato

Los Alamos National Laboratory

on behalf of the Muon Tomography collaboration.

Highly penetrating cosmic ray muons shower the Earth at the rate of 105 m-2min-1 at sea level. Since muons are charged particles, they may be tracked into and out of an inspection volume. A novel muon tomography technique which exploits multiple Coulomb scattering of these particles for nonintrusive inspection without the use of artificial radiation will be presented. Approaches to measuring and utilizing the small angle scatter of the muons in the inspection volume will be discussed. Validations of candidate reconstruction and detection algorithms with both Monte Carlo simulations and experiments are on-going. Large-area muon tracking detectors, e.g. drift chambers and RPC's, are being evaluated for this application. Results from both experiments and simulations suggest that cosmic ray muon tomography may be useful for the detection of compact high-Z objects, even in the presence of medium-Z background clutter.

Friday, October 28th

9:00 AM–11:45 PM, Plenary Session #5

Progress in Top Quark Physics

Evelyn Thomas
University of Pennsylvania

String Theory: Making Contact with Hadron Physics

Matthew Strassler
University of Washington

Generalized Parton Distributions: Recent Results

Markus Diehl
DESY

I report on recent progress in studying generalized parton distributions. Key physics issues are the spatial distribution of partons in the nucleon, and the contribution of orbital angular momentum to the nucleon spin. The impact of experimental measurements and calculations in lattice QCD will be highlighted.

Lattice QCD at High Temperature and the QGP

Frithjof Karsch
Brookhaven National Laboratory

Experimental Pentaquark Searches: Current Status

Reinhard Schumacher
Carnegie Mellon University

Experimental evidence for and against the existence of pentaquarks has accumulated rapidly in the last three years. The positive evidence has been for long-lived objects displaying exotic quantum numbers, such as baryons with strangeness S = +1. If they exist, they would be dramatic examples of hadronic multiplets beyond our well-tested and successful particle models. The negative evidence for these states has in some cases come from reaction channels very different from the positive evidence, making comparisons difficult. The situation has now been largely clarified, however. The curious recent history of pentaquark searches is outlined, and the present status of the data and the conclusion to be drawn discussed.

1:30–4:30 PM, Plenary Session #6

The Physics Program at J-PARC

Tomofumi Nagae

High Energy Accelerator Research Organization (KEK)

The Japan Proton Accelerator Research Complex (J-PARC) has been under construction since 2001. Two institutions, KEK and Japan Atomic Energy Research Institute (JAERI), have been working together in the Tokai campus for the expected construction completion by the end of March, 2008. The proton accelerators are composed of a proton linac, a 3-GeV rapid-cycling proton synchrotron (25 Hz, 333 μA), and a 50-GeV proton synchrotron (15 μA). These accelerated protons are used for producing various secondary beams such as neutrons, muons, kaons, anti-proton and neutrinos, of which beam intensities are also in the world highest class. By using such high-intensity beams, a broad range of sciences, nuclear/particle physics, material science, life science, and nuclear engineering will be conducted.

In this talk, I will describe the present status of the construction, and summarize the physics program in particle and nuclear physics with kaons, neutrinos, muons, and neutrons.

Physics Opportunities at the Large Hadron Collider

Albert De Roeck

CERN

Physics at the High Energy Frontier

JoAnne L. Hewett

Stanford Linear Accelerator Center

Index of First Authors

Abuki, H., 115
Accardi, A., 164
Aguilar-Arevalo, A., 45
Ajitanand, N., 118
Akerib, D.S., 268
Akintola, O., 258
Akramov, F., 259
Alarcon, R., 23
Alberg, M., 338
Albertus, C., 87, 216
Alvarez-Ruso, L., 77, 188, 306, 327
Anchishkin, D., 325
Anzaldo-Meneses, A., 189
Aoki, M., 357
Armendariz, R., 271
Artuso, M., 267
Aschenauer, E., 130
Ashery, D., 279
Aslanyan, P., 189
Athanassopoulos, S., 241
ATLAS Collaboration, 181
Aubakar, B., 254
Averett, T., 284

Babar Collaboration, 217, 225
Bagchi, M., 242
Balitsky, I., 17
Barabanov, A., 348
Bashkanov, M., 38
Bataineh, H., 260
Beck, D.H., 267
Beckford, B., 260
Beckwith, A., 361
Bekele, S., 15
Bell, N., 304
Benbow, W., 154
Bertl, W., 285
Besson, D., 138
Betalo, B., 255
Bhagwat, M., 65
Bhang, H.., 28
Bielcikova, J., 13
Bizjak, I., 295
Blaschke, D., 8
Bodek, A., 75
Bodek, K., 350
Bolokhov, P., 143
Borghi, S., 46
Bose, T., 141
Bourilkov, D., 341
Boyle, K., 72
Brannen, C., 224
Bressan, A., 332
Buesching, H., 11

Caines, H., 275
CDF Collaboration, 218
Chandra, K., 177
Chaturvedi, A., 225
Chen, X., 85
Chen, Y.-C., 68
Chertok, M., 103
Chiu, M., 318
Chiu, T.-W., 123
Cianciolo, V., 9
Cirigliano, V., 39, 141
CLEO Collaboration, 176, 207, 220, 228, 229
Comune, G., 255, 343
Connolly, B., 243
Conrad, J., 44
Cooper, P., 42
Coppi, P., 154
Costa, P., 190, 276
Cowan, R., 139
Czarnecki, A., 358

Döring, M., 78, 192
Dainese, A., 55
Danagoulian, A., 71
Danko, I., 140
Das, Swapan, 191
Datta, S., 7
Daum, M., 107
Dawson, I., 75
De Roeck, A., 369
DeMille, D., 110
Dermer, C., 362
Desiati, P., 48
Di Giacomo, A., 64
Diehl, M., 367
Djurcic, Z., 44
Dmitriev, V., 142
Donszelmann, T., 40
Dragowsky, M., 100
Dreschler, J., 131
Dukes, E., 90

Egiyan, K., 35
El-Nagdy, M., 217
Entem, D., 193
Ericson, T., 194, 195, 339
Erwin, R., 153

Eyser, K., 333

Falter, T., 59
Fatemi, R., 51, 177
Fazio, A.R., 176
Felix, J., 178
Fernandez-Carames, T., 196
Fetscher, W., 152
Fierlinger, P., 108
Filippone, B., 110
Fischer, W., 49
Flambaum, V., 234, 297
Fleming, S., 359
Fodor, Z., 273
Freedman, W.L., 265
Friedland, A., 354
Friedman, E., 36
Friedrich, J., 82
Fu, S., 342
Fujioka, H., 197
Fukao, Y., 25
Fukushima, K., 114

Gal, A., 198
Garbarino, G., 32
Gaskell, D., 37
Gehman, V., 95
Geltenbort, P., 235
George, K., 344
Gericke, M., 226
Ginges, J., 300
Glesener, L., 261
Godang, R., 296
Gonenc, A., 256
Gorelov, I., 330
Gorham, P., 47, 268
Grigoryan, H., 262
Gunji, T., 10
Gurov, Y., 199

Haegeman, C., 249
Hague, J., 362
Harris, P., 236
Harwood, L., 49
Hasinoff, M., 90
Hasty, R., 102
Hatta, Y., 18
Heejong, K., 251, 252
Heinz, M., 277
Henner, V., 219
Heppelmann, S., 284
Hertzog, D., 152
Heuser, J., 159
Hewett, J.L., 369
Hime, A., 98, 365
Hirano, T., 269
Hirenzaki, S., 200
Hobbs, R., 283
Hockings, W., 359
Hoepfner, K., 320
Holzmann, W., 12
Homma, K., 250
Horie, K., 290
Horikawa, T., 201
Horner, M., 119
Hosaka, A., 86
Howell, D., 262
Hu, J., 153
Huang, G., 138
Hyodo, T., 201

Ilieva, Y., 33
Imai, K., 84
Ingram, Q., 316
Isaev, T., 143
Ishii, N., 136
Isobe, T., 14
Issah, M., 166

Jackson, H., 126
Jahn, H., 179
Jaikumar, P., 244
Jawahery, H., 268
Jia, J., 117
Jindariani, S., 330
Johnson, E., 270
Johnson, R., 314
Joosten, R., 283
Jungmann, K., 227

Kaefer, D., 341
Kageyama, T., 106
Kaiser, R., 162
Kamaev, O., 79
Kamat, S., 245
Kammel, P., 311
Kanda, H., 287
Karsch, F., 368
Kaskulov, M., 134
Kayser, B., 267
Kehoe, R., 292
Keppel, C., 74
Kilminster, B., 91
Kim, H., 92
Kim, M., 340
Kiryluk, J., 27
Kitano, R., 358
Klein, S., 47
Koeneke, K., 263, 294
Kohl, M., 68

Kolomeitsev, E., 219, 246
Komarov, V., 202
Kondratyuk, S., 69
Kopeliovich, V., 203, 204
Koretune, S., 180
Kosower, D.A., 5
Kosowsky, A., 103
Kovner, A., 64
Kozlov, G., 94
Krutenkova, A., 336
Kulikov, V., 205
Kumano, S., 127, 167, 303
Kunota, T., 355
Kusaka, A., 346

Lacey, R., 168
Laehde, T., 120
Lajoie, J., 321
Lansdell, C., 315
Lappi, T., 272
Lauss, B., 298
Lee, J., 343
Lee, J.H., 60
Lenti, V., 158
Lesko, K., 364
Leupold, S., 326
Lin, H., 101
Lingenfelter, R., 246
Liu, C.-P., 236
Liu, J., 21
Liu, M., 73
Lo Vetere, M., 88
Louis, W.C., 267
Lublinsky, M., 176

Maeda, Y., 288
Maezawa, Y., 206
Makela, M., 351
Maki, T., 291
Malcles, J., 345
Maltman, K., 313
Maravin, Y., 293
Marciano, W., 5
Mares, J., 208
Marton, J., 301, 328
Matevosyan, H., 22
Mazzucato, E., 41
McGaughey, P., 161
McNabb, R., 310
Mei, D., 98
Mekjian, A., 169
Melnitchouk, A., 93
Menary, S., 356
Menzemer, S., 140
Mermod, P., 209
Meszaros, P., 314
Meyer, E., 263
Micherdzinska, A., 302
Mignerey, A., 270
Miller, M., 329
Mintz, S., 151
Miyake, H., 344
Mohapatra, D., 296
Mokeev, V., 70
Montaruli, T., 150
Morfin, J., 149
Mottola, E., 104
Mukhopadhyay, D., 170
Muramatsu, H., 138
Murphree, D., 237

Nagae, T., 369
Nagahiro, H., 66
Nagata, K., 289
Nagle, J., 109
Nakamoto, C., 81
Narodetskiy, I., 135
Nassalski, J., 72
Naviliat-Cuncic, O., 238
Nayak, G., 137
Necula, V., 292
Nelson, R., 45
Nemura, H., 132
Nesvizhevsky, V., 299
Netrakanti, P.K., 274
Niclasen, R., 42
Nishida, Y., 171
Norman, E., 97
Nouicer, R., 61
Nozar, M., 76

Ogawa, A., 331
Oke, O., 257
Okiharu, F., 67
Olinto, A., 5
Omiwade, O., 253
Onderwater, C., 144
Oset, E., 80
Outa, H., 30

Page, P., 337
Paley, J., 148
Palomba, M., 31
Pandola, L., 96
Parappilly, M., 121
Paris, M., 85
Parke, S., 355
Parreno, A., 29
Parua, N., 329

Pasztor, G., 157
Pate, S., 22
Pavlunin, V., 40
Petrov, A., 89, 221
Picker, R., 238
Piegsa, F., 353
Pierini, M., 346
Piskunova, O., 182
Pivarski, J., 279
Plager, C., 292
Platchkov, S., 26
Portell, X., 342
Potter, F., 230, 247
Procura, M., 122
Protasov, K., 156, 239
Pruneau, C., 271
Ptitsyn, V., 50
Pursley, J.M., 39
Purwar, A., 183
Putschke, J., 118

Qian, X., 278
Qiang, Y., 83

Radford, S., 137
Rajagopal, K., 109
Rak, J., 119
Rakitin, A., 89
Ramsey-Musolf, M., 110
Randrup, J., 111
Raparia, D., 105
Ratti, C., 113
Reil, K., 48
Reimer, P., 128
Reinhold, J., 29
Renkel, P., 291
Richman, J., 268
Riska, D., 20
Roberts, B., 312
Rodríguez, D., 240
Rondon, O., 331
Rosenfelder, R., 360
Roy, P., 308
Rozynek, J., 172
Ruan, L., 16
Rustamov, A., 264

Sachrajda, C., 109
Saeed, M., 209
Sainio, M., 286
Saito, N., 266
Sakaguchi, T., 322
Salme, G., 34
Sandacz, A., 184
Santoso, Y., 221
Sarkar, S., 134, 210
Sato, M., 133
Savage, M., 5
Schirato, R., 366
Schmidt, C., 112
Schmitt, L., 52
Schumacher, R., 368
Scielzo, N., 145
Seele, J., 185
Seo, P.-N., 352
Seth, K., 138
Sharafiddinov, R., 230
Sharma, S., 305, 356
Sichtermann, E., 129
Signorelli, G., 358
Skorodko, T., 211
Sokolsky, P., 363
Solana, J.C., 165
Solvignon, P., 186
Stankus, P., 277
Steiner, A., 99
Stephenson, G.J., 307
Stone, S., 280
Strassler, M., 367
Strikman, M., 19, 62
Stutz, R., 145
Sudol, M., 324
Suganuma, H., 124
Sugitate, T., 317
Sugiyama, J., 212
Sumisawa, K., 345
Sun, W., 88, 139
Suprun, D., 295
Suzuki, T., 212
Syphers, M., 105
Szleper, M., 41

Takahashi, T., 125
Takai, H., 63
Takeuchi, S., 213, 222
Tan, P., 160
Tatsumi, T., 248
Thomson, E., 367
Tomono, D., 309
Topaksu, A.K., 146
Trodden, M., 268
Tsbychev, D., 39
Tsutsui, N., 43
Tulin, S., 361
Turbide, S., 323
Turchetti, P., 43
Tvaskis, V., 186
Tzanakos, G., 147
Tzeng, Y., 214

Ullrich, T., 173
Usai, G., 6

Vaandering, E., 88
van der Grinten, M., 349
van Hess, H., 56
Velasco, M., 231, 232
Velkovska, J., 319
Videbaek, F., 332
Vijande, J., 335
Vogelsang, W., 24
Vogt, R., 53, 174

Wang, C.-H., 40, 232
Wang, Q.-H., 175
Wang, X., 53
Ward, T., 233, 365
Wascko, M., 44
Webb, J., 187
Weekes, T., 155
Weigert, H., 17
Weiss, C., 19
Wiedemann, U.A., 266
Wilking, M., 264
Winter, D., 116
Witt, R., 57

Xin, B., 354
Xu, Q., 334
Xu, Z., 54

Yamagata, J., 215
Yamamoto, T., 363
Yamauchi, M., 268
Yamazaki, Y., 175, 223, 233, 278
Yeh, T.-W., 294
Yokkaichi, S., 281
Yuan, F., 282

Zahed, I., 112
Zhang, C., 61
Zielinski, M., 329
Zihlmann, B., 282
Zimmerman, E., 364
Zweber, P., 71

Notes